

# World Journal of *Gastroenterology*

*World J Gastroenterol* 2020 January 21; 26(3): 266-374



**MINIREVIEWS**

- 266 Abdominal compartment syndrome: Often overlooked conditions in medical intensive care units  
*Rajasurya V, Surani S*
- 279 Fibroblast growth factor signaling in non-alcoholic fatty liver disease and non-alcoholic steatohepatitis: Paving the way to hepatocellular carcinoma  
*Ocker M*

**ORIGINAL ARTICLE****Basic Study**

- 291 *Bacteroides fragilis* enterotoxin upregulates heme oxygenase-1 in dendritic cells *via* reactive oxygen species-, mitogen-activated protein kinase-, and Nrf2-dependent pathway  
*Ko SH, Jeon JI, Woo HA, Kim JM*

**Case Control Study**

- 307 Nucleotide excision repair pathway gene polymorphisms are associated with risk and prognosis of colorectal cancer  
*Li YK, Xu Q, Sun LP, Gong YH, Jing JJ, Xing CZ, Yuan Y*

**Retrospective Study**

- 324 Idarubicin *vs* doxorubicin in transarterial chemoembolization of intermediate stage hepatocellular carcinoma  
*Roth GS, Teyssier Y, Abousalihac M, Seigneurin A, Ghelfi J, Sengel C, Decaens T*

**Observational Study**

- 335 Metabolite profile comparisons between ascending and descending colon tissue in healthy adults  
*Baxter BA, Parker KD, Nosler MJ, Rao S, Craig R, Seiler C, Ryan EP*

**SYSTEMATIC REVIEWS**

- 353 Programmed cell death-1 inhibitor-related sclerosing cholangitis: A systematic review  
*Onoyama T, Takeda Y, Yamashita T, Hamamoto W, Sakamoto Y, Koda H, Kawata S, Matsumoto K, Isomoto H*

**CASE REPORT**

- 366 Unexpected metastasis of intraductal papillary neoplasm of the bile duct without an invasive component to the brain and lungs: A case report  
*Nam NH, Taura K, Kanai M, Fukuyama K, Uza N, Maeda H, Yutaka Y, Chen-Yoshikawa TF, Muto M, Uemoto S*



**ABOUT COVER**

Editorial board member of *World Journal of Gastroenterology*, Rakesh Kumar Tandon, FRCP (Hon), MD, PhD, Doctor, Professor, Department of Gastroenterology, Pushpawati Singhania Hospital & Research Institute, Sheikh Sarai-Phase II, New Delhi 110017, Delhi, India

**AIMS AND SCOPE**

The primary aim of *World Journal of Gastroenterology* (WJG, *World J Gastroenterol*) is to provide scholars and readers from various fields of gastroenterology and hepatology with a platform to publish high-quality basic and clinical research articles and communicate their research findings online.

WJG mainly publishes articles reporting research results and findings obtained in the field of gastroenterology and hepatology and covering a wide range of topics including gastroenterology, hepatology, gastrointestinal endoscopy, gastrointestinal surgery, gastrointestinal oncology, and pediatric gastroenterology.

**INDEXING/ABSTRACTING**

The WJG is now indexed in Current Contents®/Clinical Medicine, Science Citation Index Expanded (also known as SciSearch®), Journal Citation Reports®, Index Medicus, MEDLINE, PubMed, PubMed Central, and Scopus. The 2019 edition of Journal Citation Report® cites the 2018 impact factor for WJG as 3.411 (5-year impact factor: 3.579), ranking WJG as 35<sup>th</sup> among 84 journals in gastroenterology and hepatology (quartile in category Q2). CiteScore (2018): 3.43.

**RESPONSIBLE EDITORS FOR THIS ISSUE**

Responsible Electronic Editor: *Yu-Jie Ma*

Proofing Production Department Director: *Yun-Xiaojuan Wu*

**NAME OF JOURNAL**

*World Journal of Gastroenterology*

**ISSN**

ISSN 1007-9327 (print) ISSN 2219-2840 (online)

**LAUNCH DATE**

October 1, 1995

**FREQUENCY**

Weekly

**EDITORS-IN-CHIEF**

Subrata Ghosh, Andrzej S Tarnawski

**EDITORIAL BOARD MEMBERS**

<http://www.wjgnet.com/1007-9327/editorialboard.htm>

**EDITORIAL OFFICE**

Ze-Mao Gong, Director

**PUBLICATION DATE**

January 21, 2020

**COPYRIGHT**

© 2020 Baishideng Publishing Group Inc

**INSTRUCTIONS TO AUTHORS**

<https://www.wjgnet.com/bpg/gerinfo/204>

**GUIDELINES FOR ETHICS DOCUMENTS**

<https://www.wjgnet.com/bpg/GerInfo/287>

**GUIDELINES FOR NON-NATIVE SPEAKERS OF ENGLISH**

<https://www.wjgnet.com/bpg/gerinfo/240>

**PUBLICATION MISCONDUCT**

<https://www.wjgnet.com/bpg/gerinfo/208>

**ARTICLE PROCESSING CHARGE**

<https://www.wjgnet.com/bpg/gerinfo/242>

**STEPS FOR SUBMITTING MANUSCRIPTS**

<https://www.wjgnet.com/bpg/GerInfo/239>

**ONLINE SUBMISSION**

<https://www.f6publishing.com>



## Abdominal compartment syndrome: Often overlooked conditions in medical intensive care units

Venkat Rajasurya, Salim Surani

**ORCID number:** Venkat Rajasurya (0000-0002-9957-0382); Salim Surani (0000-0001-7105-4266).

**Author contributions:** All authors have contributed to the preparation of manuscript, literature search and review of the manuscript.

**Conflict-of-interest statement:** The authors have no conflict of interest to disclose.

**Open-Access:** This article is an open-access article that was selected by an in-house editor and fully peer-reviewed by external reviewers. It is distributed in accordance with the Creative Commons Attribution NonCommercial (CC BY-NC 4.0) license, which permits others to distribute, remix, adapt, build upon this work non-commercially, and license their derivative works on different terms, provided the original work is properly cited and the use is non-commercial. See: <http://creativecommons.org/licenses/by-nc/4.0/>

**Manuscript source:** Invited manuscript

**Received:** November 25, 2019

**Peer-review started:** November 25, 2019

**First decision:** December 4, 2019

**Revised:** December 17, 2019

**Accepted:** January 2, 2020

**Article in press:** January 2, 2020

**Published online:** January 21, 2020

**P-Reviewer:** Lee JG, Manenti A, Yeh YC, Zhang LY

**S-Editor:** Ma L

**Venkat Rajasurya**, Department of Pulmonary and Critical Care, Novant Health System, Winston-Salem, NC 27103, United States

**Salim Surani**, Department of Pulmonary Critical Care and Sleep Medicine, Texas A&M Health Science Center, Bryan, TX 77807, United States

**Corresponding author:** Salim Surani, MD, MPH, NSHM, FACP, FCCP, Adjunct Clinical Professor of Medicine, Division of Pulmonary Critical Care and Sleep Medicine, Texas A&M Health Science Center, 8441 Riverside Pkwy, Bryan, TX 77807, United States.  
[salim.surani@hcahealthcare.com](mailto:salim.surani@hcahealthcare.com)

### Abstract

Intra-abdominal hypertension (IAH) and abdominal compartment syndrome are well recognized entities among surgical patients. Nevertheless, a number of prospective and retrospective observational studies have shown that IAH is prevalent in about half of the critically ill patients in the medical intensive care units (ICU) and has been widely recognized as an independent risk factor for mortality. It is alarming to note that many members of the critical care team in medical ICU are not aware of the consequences of untreated IAH and the delay in making the diagnosis leads to increased morbidity and mortality. Frequently it is underdiagnosed and undertreated in this patient population. Elevated intra-abdominal pressure decreases the blood flow to the kidneys and other abdominal viscera and also results in reduced cardiac output and difficulties in ventilating the patient because of increased intrathoracic pressure. When intraabdominal hypertension is not promptly recognized and treated, it leads to abdominal compartment syndrome, multiorgan dysfunction syndrome and death. Large volume fluid resuscitation is very common in medical ICU patients presenting with sepsis, shock and other inflammatory conditions like pancreatitis and it is one of the major risk factors for the development of intra-abdominal hypertension. This article presents an overview of the epidemiology, definitions, risk factors, pathophysiology and management of IAH and abdominal compartment syndrome in critically ill medical ICU patients.

**Key words:** Intra-abdominal pressure; Intra-abdominal hypertension; Abdominal compartment syndrome; Acute kidney injury; Large volume resuscitation; Open abdomen; Bladder pressure; Medical intensive care unit

©The Author(s) 2020. Published by Baishideng Publishing Group Inc. All rights reserved.



L-Editor: A  
E-Editor: Qi LL



**Core tip:** Intra-abdominal hypertension and abdominal compartment syndrome are very common in medical intensive care unit. Recognizing the risk factors for the development of intra-abdominal hypertension, timely measurement of intra-abdominal pressure and promptly implementing the resuscitation strategies can significantly reduce the morbidity and mortality associated with abdominal compartment syndrome.

**Citation:** Rajasurya V, Surani S. Abdominal compartment syndrome: Often overlooked conditions in medical intensive care units. *World J Gastroenterol* 2020; 26(3): 266-278

**URL:** <https://www.wjgnet.com/1007-9327/full/v26/i3/266.htm>

**DOI:** <https://dx.doi.org/10.3748/wjg.v26.i3.266>

## INTRODUCTION

Intra-abdominal hypertension (IAH) and abdominal compartment syndrome (ACS) are frequently encountered in critically ill patients in the intensive care unit (ICU) and result in significant morbidity and mortality. The World Society of the Abdominal Compartment Syndrome has published evidence-based medicine consensus guidelines for diagnosing and managing elevated intra-abdominal pressure (IAP)<sup>[1]</sup>. IAH is a graded phenomenon or continuum of process which when not recognized leads to ACS. It is extremely important to recognize this entity in critically ill patients because of the impact of elevated intra-abdominal pressure on end organ function.

## SCOPE OF THE PROBLEM

Overall IAH and ACS are widely under-recognized in medical ICU. An Australian study conducted a survey of critical care nurses knowledge of IAH and ACS and it was found that less than 20% were able to recognize the less apparent causes of IAH and lack of education related to IAP monitoring was identified by nearly half of respondents as the primary barrier to monitor IAP<sup>[2]</sup>. Results from a clinical survey indicate less than 30% of clinicians being aware of correct definition of IAH and ACS and only few of them applied the guidelines in managing patients with IAH<sup>[3]</sup>. General lack of clinical awareness and lack of clinical application of available knowledge resulted in not measuring the intra-abdominal pressures in a number of ICUs. A multidisciplinary survey on recognition and management of IAH and ACS was performed by Kimball *et al*<sup>[4]</sup>. The results demonstrated moderate recognition and understanding of IAH and ACS among surgical specialists and significant ignorance among medical specialists.

## PREVALENCE

ACS is well described in surgical patients, but limited data is available regarding the prevalence of ACS in medical ICU patients. Study published by Malbrain *et al*<sup>[5]</sup> in 2004 showed that nearly 50% of all ICU patients were at risk for IAH and 8% were at risk for full-blown ACS and it also showed contrary to the popular belief, ACS was more prevalent in medical ICU patients than in surgical ICU patients. A prospective observational study that screened 491 ICU patients in 15 ICUs worldwide found IAH in 34% of patients on the day of admission and 48.9% of the patients developed IAH during the observational period. In this mixed ICU patient cohort, IAH occurred in almost half of the all ICU patients and was twice as prevalent in mechanically ventilated patients<sup>[6]</sup>.

## DEFINITIONS

The World Society of the Abdominal Compartment Syndrome was founded in 2004 and has published consensus definitions on IAH and ACS as listed in the [Table 1](#). IAH is defined as IAP equal to or greater than 12 mmHg and ACS is defined as sustained IAP above 20 mmHg with new onset of end organ dysfunction<sup>[7]</sup>. Normal IAP in healthy individuals ranges between 5 to 7 mmHg and obese patients tend to have

higher baseline IAP values<sup>[8]</sup>.

## ETIOLOGY

The abdomen is a closed anatomic space and increase in intraabdominal volume results in proportional increase in IAP. The abdominal compliance is largely determined by the elastic recoil of the abdominal wall and the diaphragm. It is important to recognize the risk factors and conditions that predispose to development of IAH and ACS in a timely fashion to prevent the end organ damage. The presence of these risk factors should suggest clinicians to start monitoring the IAP. The risk factors can be classified into 4 categories as mentioned in Table 2. Decreased abdominal wall compliance, increased intraluminal contents, collection of contents in the abdominal cavity, capillary leak and fluid resuscitation are the broad categories that lead to the development of IAH and ACS<sup>[9]</sup>.

## PHYSIOLOGICAL CONSEQUENCES

Increased IAP has significant impact on various organ systems and leads to physiologic derangements as shown in Figure 1. In addition, certain pre-existing comorbidities such as chronic renal failure, pulmonary disease, cardiomyopathy, morbid obesity which are frequently encountered in the medical ICU play an important role in aggravating the effects of elevated IAP.

### Cardiovascular system

When the IAP increases, the diaphragm moves cephalad and this in turn increases the intrathoracic pressure. Elevation in intrathoracic pressure reduces cardiac output by reducing the venous return. The cephalad movement of the diaphragm results in direct cardiac compression leading to reduced ventricular compliance and contractility<sup>[10]</sup>. Increased IAP compresses the aorta and pulmonary parenchyma leading to increased systemic vascular resistance and pulmonary vascular resistance respectively. IAH reduces venous return leading to peripheral edema and increased risk of development of deep venous thrombosis<sup>[11]</sup>.

### Pulmonary system

By increasing the intrathoracic pressure, IAH leads to increased peak airway pressure, reduced pulmonary compliance leading to alveolar volutrauma and ventilation perfusion mismatch respectively. The cephalad movement of diaphragm leads to atelectasis that results in intrapulmonary shunting and pneumonia<sup>[12]</sup>.

### Renal system

IAH results in significant reduction in urinary output by reducing the renal blood flow and function. The resultant reduction in renal artery blood flow, increase in the renal vein pressure and the renal vascular resistance leads to impaired glomerular and tubular function<sup>[13]</sup>. Studies have shown that oliguria can develop at an IAP of 15 mmHg and anuria at an IAP of 30 mmHg<sup>[14]</sup>. The renal filtration gradient (FG) is the difference between glomerular filtration pressure (GFP) and proximal tubular pressure (PTP). When IAH occurs PTP is same as IAP<sup>[9]</sup>.

$$FG = GFP - PTP$$

$$FG = (MAP - IAP) - IAP$$

$$FG = MAP - 2 \times IAP$$

Hence doubling of IAP results in fourfold increase in filtration gradient, which significantly affects the net urine output.

### Gastrointestinal system

Gut is very sensitive to elevations in IAP. Reduction in mesenteric flow can occur at IAP of only 10 mmHg. IAP of 40 mmHg can reduce the celiac artery blood flow by 43% and superior mesenteric artery flow by 69%<sup>[15]</sup>. This is further augmented by hypovolemia. IAH also compresses mesenteric veins resulting in intestinal edema which further increases IAP initiating a vicious cycle that results in worsening perfusion, bowel ischemia, decreased intraluminal pH, feeding intolerance, systemic metabolic acidosis and significantly increased mortality. IAH impedes the lymphatic flow by direct compression as well as by increasing the intrathoracic pressure and exacerbates intestinal edema and ascites<sup>[16]</sup>. ACS in turn leads to multiorgan dysfunction syndrome<sup>[17]</sup>.

### Abdominal wall



**Table 1 Definitions and diagnostic criteria for intra-abdominal hypertension/abdominal compartment syndrome**

1	IAP is the steady-state pressure concealed within the abdominal cavity
2	$APP = MAP - IAP$
3	$FG = GFP - PTP = MAP - 2 \times IAP$
4	IAP should be expressed in mmHg and measured at end-expiration in the complete supine position after ensuring that abdominal muscle contractions are absent and with the transducer zeroed at the level of the mid-axillary line
5	The reference standard for intermittent IAP measurement is via the bladder with a maximal instillation volume of 25 mL of sterile saline
6	Normal IAP is approximately 5-7 mm Hg in critically ill adults
7	IAH is defined by a sustained or repeated pathologic elevation of IAP $\geq 12$ mmHg
8	IAH is graded as follows: Grade I: IAP 12-15 mmHg Grade II: IAP 16-20 mmHg Grade III: IAP 21-25 mmHg Grade IV: IAP $> 25$ mmHg
9	ACS is defined as a sustained IAP $> 20$ mmHg (with or without an APP $< 60$ mmHg) that is associated with new organ dysfunction/failure
10	Primary ACS is a condition associated with injury or disease in the abdomino-pelvic region that frequently requires early surgical or interventional radiological intervention
11	Secondary ACS refers to conditions that do not originate from the abdomino-pelvic region
12	Recurrent ACS refers to the condition in which ACS redevelops following previous surgical or medical treatment of primary or secondary ACS

(Adapted with permission from Kirkpatrick *et al*<sup>[30]</sup>). ACS: Abdominal compartment syndrome; APP: Abdominal perfusion pressure; FG: Filtration gradient; GFP: Glomerular filtration pressure; IAH: Intra-abdominal hypertension; IAP: Intra-abdominal pressure; MAP: Mean arterial pressure; PTP: Proximal tubular pressure.

Increased IAP reduces abdominal wall blood flow resulting in ischemia and edema. This reduces abdominal wall compliance and exacerbates IAH<sup>[18]</sup>.

### **Hepatic function**

Elevation of IAP impairs hepatic cell function and liver perfusion. Decreased hepatic arterial and portal venous flow results in decreased lactate clearance and altered mitochondrial function<sup>[19]</sup>.

### **Central nervous system**

IAH results in elevation of intracranial pressure by decreased lumbar venous plexus blood flow, decreased cerebral venous outflow and increased cerebral blood flow secondary to increased PaCO<sub>2</sub>. This in turn significantly affects cerebral perfusion and function<sup>[20]</sup>.

## **ACUTE PANCREATITIS AND ACS**

IAH is seen in at least 50% of patients with severe pancreatitis<sup>[21]</sup>. IAH is being increasingly recognized as a point of specific intervention in patients with acute pancreatitis and timely management has shown to improve mortality in this group of patients. IAH and ACS occurs early during the first 3 to 5 days of acute pancreatitis. Significant local and visceral edema from pancreatic and peripancreatic inflammation, ascites, ileus, aggressive volume resuscitation are some of the contributing factors<sup>[22]</sup>. IAP surveillance should be routinely done in patients with acute pancreatitis receiving aggressive fluid resuscitation, high severity, renal and respiratory complications and fluid accumulation in multiple areas as observed by the CT scan.

## **LARGE VOLUME FLUID RESUSCITATION AND ACS**

Large volume resuscitation is very common in the ICU setting and is the most common cause of IAH in patients without primary abdominal pathology. During the

**Table 2 Risk factors for the development of intra-abdominal hypertension/abdominal compartment syndrome****Reduced abdominal wall compliance**

Obesity  
 Abdominal surgery  
 Prone positioning  
 Rectus sheath hematoma  
 Burns with abdominal eschars  
 Mechanical ventilation with high positive end-expiratory pressure  
 Ventilator dyssynchrony

**Increased intra-luminal contents**

Gastric distention  
 Gastroparesis  
 Colonic pseudo-obstruction  
 Volvulus  
 Abdominal tumor  
 Intra-abdominal or retroperitoneal tumor  
 Damage control laparotomy  
 Enteral feeding

**Abdominal cavity collections**

Ascites  
 Hemoperitoneum  
 Pneumoperitoneum  
 Major trauma  
 Laparoscopy with excessive inflation pressures  
 Peritoneal dialysis  
 Abdominal inflammation-peritonitis, pancreatitis  
 Abdominal abscess

**Capillary leak and fluid resuscitation**

Acidosis  
 Hypothermia  
 Coagulopathy  
 Massive transfusion  
 Trauma  
 Sepsis  
 Large volume fluid resuscitation  
 Major burns

initial period of resuscitation large volume of fluids is frequently administered in critically ill patients with septic shock, hemorrhagic shock, burns, acute pancreatitis and other conditions associated with systemic inflammation. Although fluid resuscitation remains the cornerstone in managing critically ill patients, there is enough data to suggest that, administration of more than 5 L of fluids during the initial resuscitative phase can be harmful and leads to increased mortality.

IAH is very common in major burn patients and ACS was frequently seen in patients with more than 70% body surface area burns in the study published by Ivy *et al*<sup>[23]</sup> in 2000. This study also showed a linear correlation between volume of fluid infused and development of IAH. IAH is also frequently seen in cardiac surgery patients. Out of 69 patients undergoing cardiac surgery, 31% developed IAH and positive fluid balance was a strong independent risk factor for IAH<sup>[24]</sup>.

Volume resuscitation and net fluid balance were also important risk factors for development of IAH in liver transplant recipients and major trauma patients. A prospective clinical study done in Italy found IAH in 32% of the liver transplant cases<sup>[25]</sup>. Adequate intravascular volume resuscitation is vital in management of patients with IAH and ACS as elevated intrathoracic pressure significantly reduces cardiac output by reducing the preload. Adequate fluid resuscitation has shown to improve survival by restoring end-organ perfusion and function. Excessive fluid resuscitation doubles the risk of developing IAH and ACS and organ failure



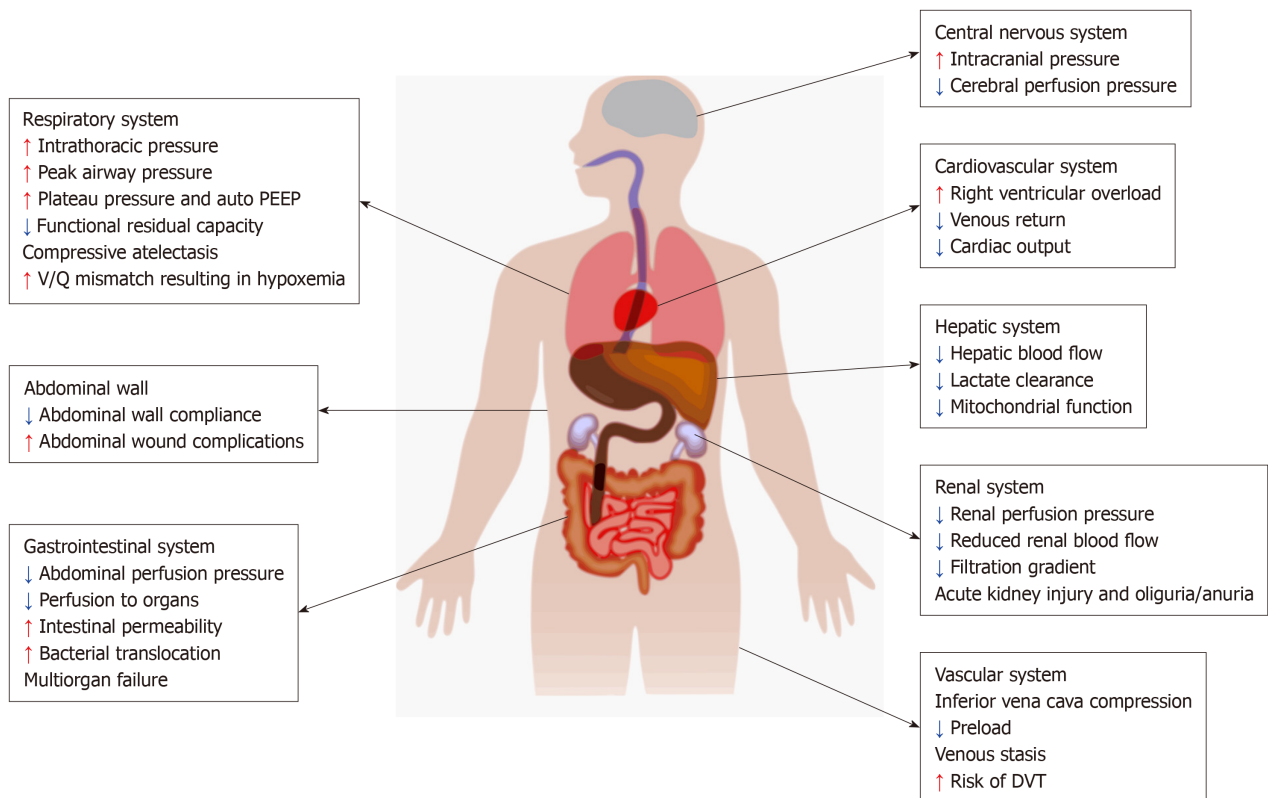


**Figure 1 Pathophysiology of intra-abdominal hypertension.** PEEP: Positive end expiratory pressure; DVT: Deep venous thrombosis.

compared to a more conservative fluid resuscitation strategy.

A prospective randomized study showed plasma resuscitated patients developed IAH less frequently than patients receiving crystalloids. Colloid and plasma resuscitation reduced fluid requirements and edema, improved cardiac parameters. Also, studies have shown that hypertonic saline during shock resuscitation in burn and trauma patients reduces the incidence of IAH. Oda *et al*<sup>[26]</sup> reported reduced risk for ACS when using hypertonic lactated saline for resuscitating burn patients and O'Mara *et al*<sup>[27]</sup> reported lower fluid requirements and lower IAP using colloids.

A prospective study screened medical ICU patients with a minimum net fluid balance of 5 L within the preceding 24 h and excluded patients with abdominal surgery, obesity. Out of the 468 medical ICU admissions screened, 40 patients met the 24-h fluid balance criteria and out of them 85% had IAH and 33% developed intra-abdominal pressure of more than 20 mmHg and 25% met the criteria for abdominal compartment syndrome. This study confirms the high incidence of IAH and ACS in medical ICU patients receiving large volume resuscitation<sup>[28]</sup>.

## MEASURING IAP IN ICU

IAP monitoring is a safe and cost-effective tool for identifying patients at risk for developing IAH and ACS. It helps in guiding resuscitative therapy and reducing mortality and morbidity associated with IAH and ACS.

Intra vesicular saline instillation is the most common technique to monitor intra-abdominal pressure. A simple closed system that can be used to measure bladder pressure in ICU is shown in Figure 2. Clinical examination by palpation has shown to have a poor sensitivity and specificity in diagnosing IAH and ACS<sup>[29]</sup>. Other less commonly used techniques to measure intra-abdominal pressures are manometry from abdominal drain, intragastric pressure measurement through a nasogastric tube, measuring pressure from the central venous catheter placed through the femoral vein into inferior vena cava *etc.* Newer modalities include abdominal wall thickness measurement using point-of-care ultrasound, wireless motility capsule, continuous IAP measurement devices and noninvasive IAP estimation using near-infrared spectroscopy.

IAP should be measured at end expiration and patient should be in a complete supine position with the transducer zeroed in mid axillary line at the level of iliac

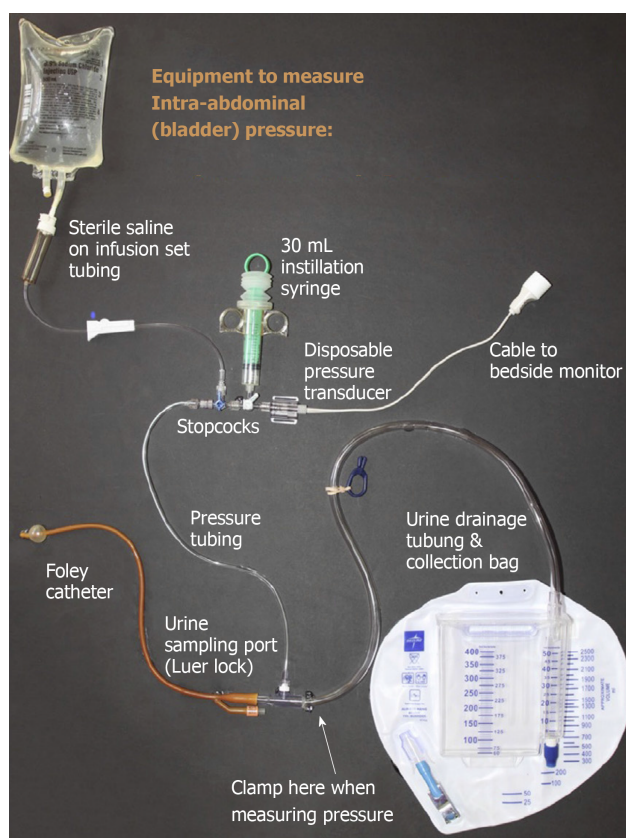


**Figure 2** Closed system to measure bladder (abdominal) pressure constructed with readily available intensive care unit equipment. (Adapted with permission from Rogers *et al*<sup>[42]</sup>).

crest. Maximal instillation volume of 25 mL of sterile saline should be used. IAP varies with BMI and obese patients tend to have a higher baseline IAP. Temperature of isotonic saline instilled can also affect IAP. Isotonic saline at room temperature significantly raises IAP due to contraction of the bladder muscle and hence it is important to wait for at least 30 to 60 s after isotonic saline instillation to allow warming of the fluid and relaxation of the detrusor muscle<sup>[30]</sup>.

Although the prevalence of IAH and ACS is high in medical ICU patients, routine monitoring in all ICU patients is not feasible and not recommended. According to WSACS guidelines, in patients with 2 or more risk factors baseline IAP must be measured and if it is elevated frequent 4 to 6-h monitoring should be done<sup>[30]</sup>.

## POLYCOMPARTMENT SYNDROME IN ICU

The term poly-compartment syndrome refers to a condition where 2 or more anatomical compartments have elevated pressures. Within the poly-compartment syndrome, abdomen plays a central role and elevated IAP that results in ACS can interact with other compartments and result in thoracic compartment syndrome, intracranial compartment syndrome and extremity compartment syndrome. Initial management of poly-compartment syndrome is focusing on primary compartment and lowering compartment pressure, supporting organ perfusion and preventing specific adverse effects<sup>[31]</sup>.

Acute bowel injury refers to a complex bowel injury caused by a first hit, either directly such as in abdominal sepsis, burns, pancreatitis, trauma or indirectly from ischemia due to shock followed by a second hit in the form of capillary leak, bowel edema and local ischemia resulting in IAH. This vicious cycle results in acute intestinal distress syndrome and abdominal compartment syndrome<sup>[9]</sup>.

## PELVIC COMPARTMENT SYNDROME

Pelvic compartment syndrome is a condition resulting from increased pressure within the true pelvis and typically follows an expanding hematoma secondary to a



traumatic fracture of the pelvis<sup>[32]</sup>. Pelvic hypertension with organ dysfunction which is characterized by reduced pelvic venous return and ureteral dilatation results in pelvic compartment syndrome. It is diagnosed by elevated bladder pressure and should be differentiated from IAH/ACS. It is important to promptly recognize this syndrome and evacuate the hematoma or fluid collection through laparotomy or percutaneous drainage to decompress the pelvis<sup>[33]</sup>.

## MANAGEMENT

### **Medical/nonsurgical**

Abdominal perfusion pressure (APP) is the difference between mean arterial pressure and intra-abdominal pressure. Targeting APP of more than 60 mmHg has been proposed as a better predictor of outcome in IAH than measuring IAP<sup>[34]</sup>. But the primary focus should be on reducing IAP rather than driving up the mean arterial pressure (MAP). The main strategies of conservative management are to improve abdominal wall compliance, evacuate intra and extraluminal contents and correct fluid balance to improve worsening IAH<sup>[35]</sup>. But when there is rapid progression to ACS, prompt surgical decompression must be undertaken.

Deep sedation, analgesia and neuromuscular blockade can improve thoracoabdominal muscle tone and abdominal wall compliance by reducing pain, agitation, ventilator dyssynchrony and accessory muscle use<sup>[36]</sup>. Ileus is very common among patients with pancreatitis, peritonitis, major trauma, abdominal surgery and after large volume fluid resuscitation. Nasogastric tube and rectal tube decompression help in reducing IAP in patients with IAH. The administration of bowel enemas and prokinetic agents also help in evacuating intraluminal contents and decrease visceral volume. Other techniques including supine positioning of patient in reducing IAP, large volume paracentesis in patients with ascites are also frequently done to reduce the risks of developing IAH. Intensivist performed percutaneous catheter decompression is an effective and less invasive modality for treating patients with IAH/ACS. Improved patient outcomes have been found in patients undergoing percutaneous drainage placement probably from early decompression when compared to open abdominal decompression<sup>[37]</sup>.

Aggressive fluid removal with diuretics or renal replacement therapy may help in reducing IAP. A review of 13 published case series suggested that an average total body fluid removal of 4.9 L resulted in reduction of IAP from  $19.3 \pm 9.1$  mmHg to  $11.5 \pm 3.9$  mmHg<sup>[38]</sup>. Because of the paucity of data on fluid removal, the focus should be more on avoiding excessive fluid administration during resuscitation phase rather than active fluid removal with diuresis in critically ill patients. The IAH/ACS management guidelines proposed by WSACS is mentioned in the Figures 3 and 4.

### **Surgical decompression**

When the nonsurgical techniques fail to reduce the IAP, surgical abdominal decompression must be promptly initiated as it is the definitive management to reduce the risk of mortality from ACS. Decompressive laparotomy when combined with negative pressure peritoneal therapy reduces the IAP, improves visceral perfusion and reduces the transmission of inflammatory mediators into the bloodstream, thereby reducing the risk of developing multiorgan dysfunction from sepsis<sup>[39]</sup>. The term open abdomen refers to surgical management strategy whereby the abdominal wall incision is temporarily left unrepaired at the end of the surgery to relieve the intra-abdominal pressure. The open abdomen technique with temporary closure using vacuum-assisted closure, patch technique, silo technique (Bagota bag) and skin-only technique using towel clips are some of the methods that reduces the risk of development of IAH and ACS. In the recent years there has been increased awareness of the deleterious effects of IAH and this has led to more open abdomen management in ICU, which also reduces the risk of recurrent ACS. A collective review of 250 patients undergoing midline laparotomy found that decompression had an overall positive effect on cardiovascular, respiratory and renal function<sup>[40]</sup>. Although surgical decompression and open abdomen can be life-saving, it can also lead to certain complications like stimulation of a hypercatabolic state and protein loss through removal of peritoneal fluid, development of fistula, large ventral hernia or life threatening hemorrhagic complications including reperfusion syndrome<sup>[41,42]</sup>. Bacterial colonization of wounds and the risk of fistulas and ventral hernias increases, the longer the abdominal cavity is left open<sup>[43]</sup>.

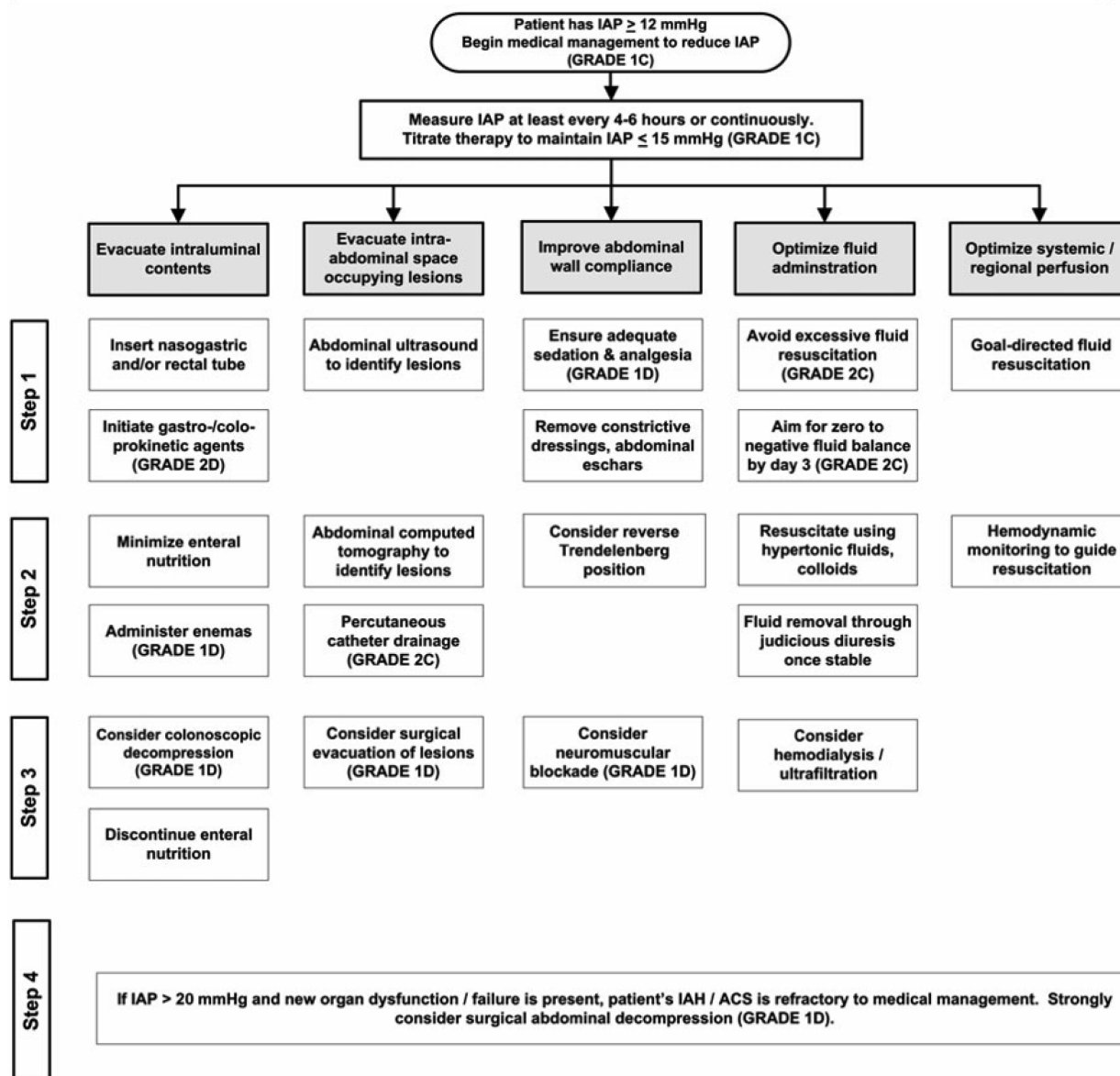
### **Differences in management of IAH/ACS among the medical and surgical intensivists**



The  
Abdominal  
Compartment  
Society

# IAH/ACS Medical Management Algorithm

- The choice (and success) of the medical management strategies listed below is strongly related to both the etiology of the patient's IAH / ACS and the patient's clinical situation. The appropriateness of each intervention should always be considered prior to implementing these interventions in any individual patient.
- The interventions should be applied in a stepwise fashion until the patient's intra-abdominal pressure (IAP) decreases.
- If there is no response to a particular intervention, therapy should be escalated to the next step in the algorithm.



Adapted from Intensive Care Med 2013 7:1190-1206

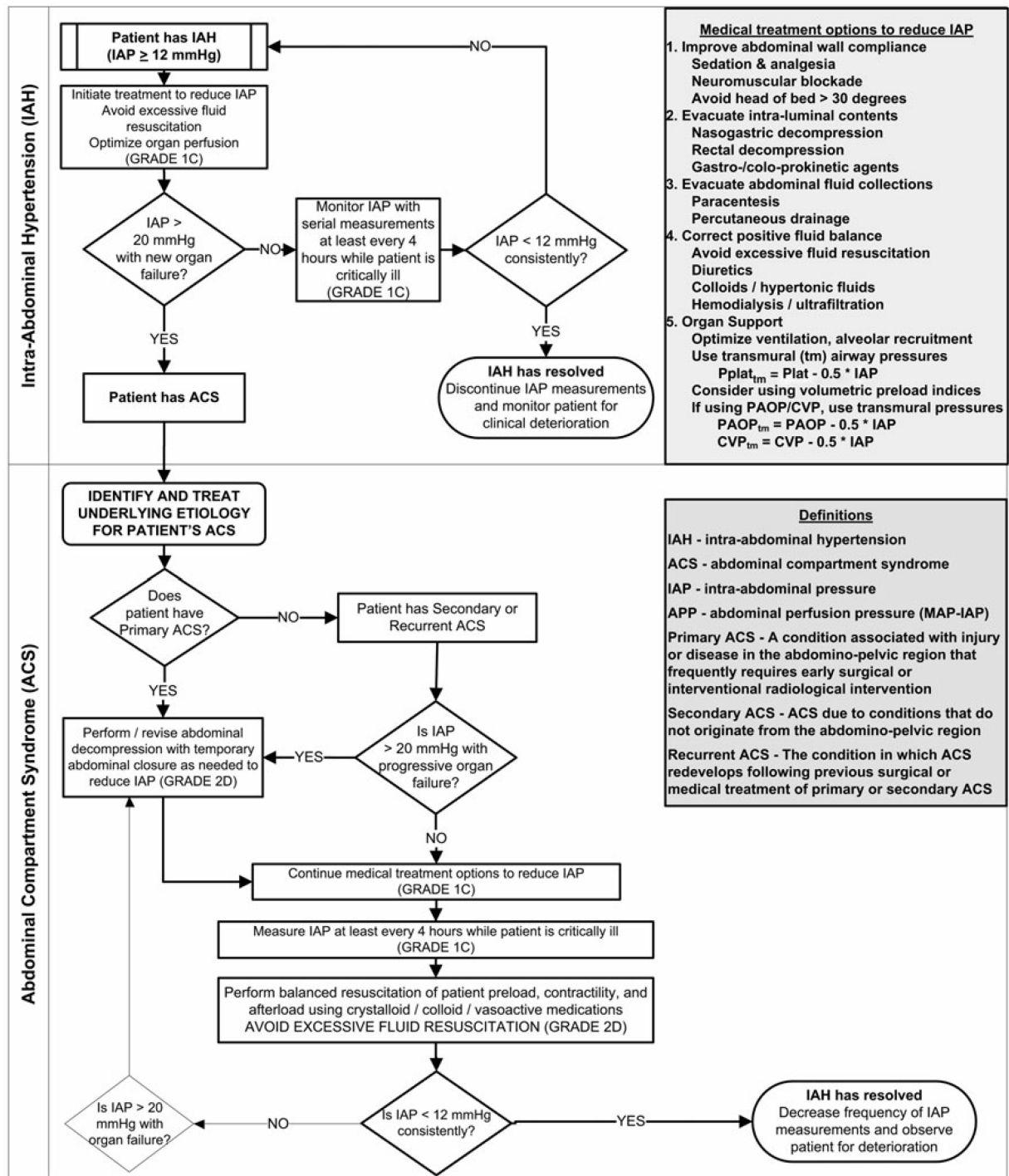
**Figure 3 Intra-abdominal hypertension/abdominal compartment syndrome management algorithm 1.** Quality of evidence for each recommendation is rated from D to A: very low (D), low (C), moderate (B) and high (A) and strength of recommendation is given by a number: strong (1) and weak (2). (Adapted with permission from Kirkpatrick *et al*<sup>[30]</sup>). IAH: Intra-abdominal hypertension; ACS: Abdominal compartment syndrome.

It is important to understand that most of the ICUs in United States have a combined model where medically trained intensivists manage both medical and surgical patients in the same ICU. As previously mentioned, the incidence of IAH/ACS is



The  
Abdominal  
Compartment  
Society

# IAH/ACS Management Algorithm



Adapted from Intensive Care Med 2013 7:1190-1206

**Figure 4** Intra-abdominal hypertension/abdominal compartment syndrome management algorithm 2. Quality of evidence for each recommendation is rated from D to A: very low (D), low (C), moderate (B) and high (A) and strength of recommendation is given by a number: strong (1) and weak (2). (Adapted with permission from Kirkpatrick *et al*<sup>[30]</sup>). IAH: Intra-abdominal hypertension; ACS: abdominal compartment syndrome.

higher in the medical intensive care unit patients. In 2001, Kimball *et al*<sup>[4]</sup> conducted a survey to assess the understanding and clinical management of IAH/ACS of 4538 physician members of Society of Critical Care Medicine with a response rate of 35.7%.

Of those surveyed 35% had a primary training in surgery and 31.5% in medicine. Nearly half (46.8%) of those surveyed worked in a combined medical/surgical ICU setting. It is interesting to note that surgeons and anesthesiologists chose intra-abdominal trauma/bleeding with large volume resuscitation as the most common cause of IAH/ACS and medical intensivists rated “third spacing of fluids” as the leading cause of IAH/ACS. Worsening oliguria, increasing ventilator pressure, decreasing cardiac output were some of the conditions that prompted both the medical and surgical intensivists to consider decompression laparotomy. Surgery trained intensivists had the most experience managing patients with IAH/ACS. The higher recognition rates of IAH/ACS among the surgical intensivists can partly be explained by the fact that the definitive treatment for this condition involves surgery. This however does lead to a component of bias and overdiagnosis. Of the medical intensivists 23% were not aware of the bladder pressure measurement procedure and 20% of them stated that they would never use decompression laparotomy to treat ACS compared with 3.6% of intensivists with surgical training. When it comes to management, it was interesting to note that 63% of surgery trained intensivists and 42% of the anesthesia trained intensivists frequently used decompression laparotomy as a management option for IAH/ACS compared to only 16% of medically trained intensivists. This survey also showed that the medical intensivists frequently considered percutaneous catheter drainage and paracentesis in managing patients with IAH/ACS, but this treatment was seldom used by the surgical intensivists<sup>[4]</sup>.

Zhou *et al*<sup>[44]</sup> did a survey of 141 intensivists with majority of them (80%) having a background in internal medicine and found that diuresis, dialysis and paracentesis were commonly chosen over decompression laparotomy and 11% of the respondents stated that their surgeons would ‘never decompress patients with ACS’.

## CONCLUSION

IAH is a continuum of pathophysiologic changes that results in ACS, which is a life-threatening condition caused by sustained acute elevation of IAP more than 20 mmHg with end organ failure. Observational studies have shown a high incidence of IAH and ACS in medical ICU patients. Large volume fluid resuscitation and inflammatory intra-abdominal conditions like acute pancreatitis are some of the frequent causes for IAH and ACS in medical ICU. Studies have shown less awareness and knowledge about IAH and ACS among clinicians and nurses working in medical ICU settings. It is very important to promptly recognize and diagnose IAH and ACS in the ICU setting because of its associated morbidity and mortality. Routine measurement of IAP in patients at risk is vital for early diagnosis and management of IAH and ACS. The gold standard, easy and cost-effective technique to measure IAP is measuring bladder pressure using intra-vesicular saline instillation. The current guidelines by WSACS on diagnosis and management of IAH and ACS should offer a roadmap for practicing intensivists in managing patients at risk. Once IAH is diagnosed, nonsurgical steps including gastric and bowel decompression, evacuation of intraluminal contents, paracentesis, diuresis, use of sedation should be promptly initiated to reduce IAP. Surgical abdominal decompression remains the mainstay of management in patients who don't respond to the medical treatment.

## REFERENCES

- Cheatham ML**, Malbrain ML, Kirkpatrick A, Sugrue M, Parr M, De Waele J, Balogh Z, Leppäniemi A, Olvera C, Ivatury R, D'Amours S, Wendon J, Hillman K, Wilmer A. Results from the International Conference of Experts on Intra-abdominal Hypertension and Abdominal Compartment Syndrome. II. Recommendations. *Intensive Care Med* 2007; **33**: 951-962 [PMID: [17377769](#) DOI: [10.1007/s00134-007-0592-4](#)]
- Hunt L**, Frost SA, Newton PJ, Salamonson Y, Davidson PM. A survey of critical care nurses' knowledge of intra-abdominal hypertension and abdominal compartment syndrome. *Aust Crit Care* 2017; **30**: 21-27 [PMID: [27036928](#) DOI: [10.1016/j.aucc.2016.02.001](#)]
- Wise R**, Roberts DJ, Vandervelden S, Debergh D, De Waele JJ, De Laet I, Kirkpatrick AW, De Keulenaer BL, Malbrain ML. Awareness and knowledge of intra-abdominal hypertension and abdominal compartment syndrome: results of an international survey. *Anaesthesiol Intensive Ther* 2015; **47**: 14-29 [PMID: [25251947](#) DOI: [10.5603/AIT.2014.0051](#)]
- Kimball EJ**, Rollins MD, Mone MC, Hansen HJ, Baraghoshi GK, Johnston C, Day ES, Jackson PR, Payne M, Barton RG. Survey of intensive care physicians on the recognition and management of intra-abdominal hypertension and abdominal compartment syndrome. *Crit Care Med* 2006; **34**: 2340-2348 [PMID: [16878034](#) DOI: [10.1097/01.CCM.0000233874.88032.1C](#)]
- Malbrain ML**, Chiumello D, Pelosi P, Wilmer A, Brienza N, Malcangi V, Bihari D, Innes R, Cohen J, Singer P, Japiassu A, Kurtop E, De Keulenaer BL, Daelemans R, Del Turco M, Cosimini P, Ranieri M, Jacquet L, Laterre PF, Gattinoni L. Prevalence of intra-abdominal hypertension in critically ill patients: a



- multicentre epidemiological study. *Intensive Care Med* 2004; **30**: 822-829 [PMID: [14758472](#) DOI: [10.1007/s00134-004-2169-9](#)]
- 6 **Reintam Blaser A**, Regli A, De Keulenaer B, Kimball EJ, Starkopf L, Davis WA, Greiffenstein P, Starkopf J; Incidence, Risk Factors, and Outcomes of Intra-Abdominal (IROI) Study Investigators. Incidence, Risk Factors, and Outcomes of Intra-Abdominal Hypertension in Critically Ill Patients-A Prospective Multicenter Study (IROI Study). *Crit Care Med* 2019; **47**: 535-542 [PMID: [30608280](#) DOI: [10.1097/CCM.0000000000003623](#)]
  - 7 **Malbrain ML**, Cheatham ML, Kirkpatrick A, Sugrue M, Parr M, De Waele J, Balogh Z, Leppäniemi A, Olvera C, Ivatury R, D'Amours S, Wendon J, Hillman K, Johansson K, Kolkman K, Wilmer A. Results from the International Conference of Experts on Intra-abdominal Hypertension and Abdominal Compartment Syndrome. I. Definitions. *Intensive Care Med* 2006; **32**: 1722-1732 [PMID: [16967294](#) DOI: [10.1007/s00134-006-0349-5](#)]
  - 8 **Sanchez NC**, Tenofsky PL, Dort JM, Shen LY, Helmer SD, Smith RS. What is normal intra-abdominal pressure? *Am Surg* 2001; **67**: 243-248 [PMID: [11270882](#)]
  - 9 **Malbrain ML**, De laet IE. Intra-abdominal hypertension: evolving concepts. *Clin Chest Med* 2009; **30**: 45-70, viii [PMID: [19186280](#) DOI: [10.1016/j.ccm.2008.09.003](#)]
  - 10 **Cullen DJ**, Coyle JP, Teplick R, Long MC. Cardiovascular, pulmonary, and renal effects of massively increased intra-abdominal pressure in critically ill patients. *Crit Care Med* 1989; **17**: 118-121 [PMID: [2914444](#) DOI: [10.1097/00003246-198902000-00002](#)]
  - 11 **Barnes GE**, Laine GA, Giam PY, Smith EE, Granger HJ. Cardiovascular responses to elevation of intra-abdominal hydrostatic pressure. *Am J Physiol* 1985; **248**: R208-R213 [PMID: [3918464](#) DOI: [10.1152/ajpregu.1985.248.2.R208](#)]
  - 12 **Pelosi P**, Quintel M, Malbrain ML. Effect of intra-abdominal pressure on respiratory mechanics. *Acta Clin Belg* 2007; **62** Suppl 1: 78-88 [PMID: [17469705](#)]
  - 13 **Kirkpatrick AW**, Colistro R, Laupland KB, Fox DL, Konkin DE, Kock V, Mayo JR, Nicolaou S. Renal arterial resistive index response to intraabdominal hypertension in a porcine model. *Crit Care Med* 2007; **35**: 207-213 [PMID: [17080005](#) DOI: [10.1097/01.CCM.0000249824.48222.B7](#)]
  - 14 **Richards WO**, Scovill W, Shin B, Reed W. Acute renal failure associated with increased intra-abdominal pressure. *Ann Surg* 1983; **197**: 183-187 [PMID: [6600601](#) DOI: [10.1097/0000658-198302000-00010](#)]
  - 15 **Friedlander MH**, Simon RJ, Ivatury R, DiRaimo R, Machiedo GW. Effect of hemorrhage on superior mesenteric artery flow during increased intra-abdominal pressures. *J Trauma* 1998; **45**: 433-489 [PMID: [9751531](#) DOI: [10.1097/00005373-199809000-00002](#)]
  - 16 **Malbrain ML**, Pelosi P, De laet I, Lattuada M, Hedenstierna G. Lymphatic drainage between thorax and abdomen: please take good care of this well-performing machinery. *Acta Clin Belg* 2007; **62** Suppl 1: 152-161 [PMID: [17469714](#)]
  - 17 **Moore FA**. The role of the gastrointestinal tract in postinjury multiple organ failure. *Am J Surg* 1999; **178**: 449-453 [PMID: [10670850](#) DOI: [10.1016/s0002-9610\(99\)00231-7](#)]
  - 18 **Diebel L**, Saxe J, Dulchavsky S. Effect of intra-abdominal pressure on abdominal wall blood flow. *Am Surg* 1992; **58**: 573-575; discussion 575-576 [PMID: [1388005](#)]
  - 19 **Luca A**, Cirera I, García-Pagán JC, Feu F, Pizcueta P, Bosch J, Rodés J. Hemodynamic effects of acute changes in intra-abdominal pressure in patients with cirrhosis. *Gastroenterology* 1993; **104**: 222-227 [PMID: [8419245](#) DOI: [10.1016/0016-5085\(93\)90855-7](#)]
  - 20 **Citerio G**, Vascotto E, Villa F, Celotti S, Pesenti A. Induced abdominal compartment syndrome increases intracranial pressure in neurotrauma patients: a prospective study. *Crit Care Med* 2001; **29**: 1466-1471 [PMID: [11445709](#) DOI: [10.1097/00003246-200107000-00027](#)]
  - 21 **Jaipuria J**, Bhandari V, Chawla AS, Singh M. Intra-abdominal pressure: Time ripe to revise management guidelines of acute pancreatitis? *World J Gastrointest Pathophysiol* 2016; **7**: 186-198 [PMID: [26909242](#) DOI: [10.4291/wjgp.v7.i1.186](#)]
  - 22 **De Waele JJ**, Leppäniemi AK. Intra-abdominal hypertension in acute pancreatitis. *World J Surg* 2009; **33**: 1128-1133 [PMID: [19350318](#) DOI: [10.1007/s00268-009-9994-5](#)]
  - 23 **Ivy ME**, Atweh NA, Palmer J, Possenti PP, Pineau M, D'Aiuto M. Intra-abdominal hypertension and abdominal compartment syndrome in burn patients. *J Trauma* 2000; **49**: 387-391 [PMID: [11003313](#) DOI: [10.1097/00005373-200009000-00001](#)]
  - 24 **Dalfino L**, Siculo A, Paparella D, Mongelli M, Rubino G, Brienza N. Intra-abdominal hypertension in cardiac surgery. *Interact Cardiovasc Thorac Surg* 2013; **17**: 644-651 [PMID: [23820668](#) DOI: [10.1093/icvts/ivt272](#)]
  - 25 **Biancofiore G**, Bindi ML, Romanelli AM, Boldrini A, Consani G, Bisà M, Filipponi F, Vagelli A, Mosca F. Intra-abdominal pressure monitoring in liver transplant recipients: a prospective study. *Intensive Care Med* 2003; **29**: 30-36 [PMID: [12528019](#) DOI: [10.1007/s00134-002-1552-7](#)]
  - 26 **Oda J**, Ueyama M, Yamashita K, Inoue T, Noborio M, Ode Y, Aoki Y, Sugimoto H. Hypertonic lactated saline resuscitation reduces the risk of abdominal compartment syndrome in severely burned patients. *J Trauma* 2006; **60**: 64-71 [PMID: [16456437](#) DOI: [10.1097/01.ta.0000199431.66938.99](#)]
  - 27 **O'Mara MS**, Slater H, Goldfarb IW, Caushaj PF. A prospective, randomized evaluation of intra-abdominal pressures with crystalloid and colloid resuscitation in burn patients. *J Trauma* 2005; **58**: 1011-1018 [PMID: [15920417](#) DOI: [10.1097/01.ta.0000162732.39083.15](#)]
  - 28 **Daugherty EL**, Hongyan Liang, Taichman D, Hansen-Flaschen J, Fuchs BD. Abdominal compartment syndrome is common in medical intensive care unit patients receiving large-volume resuscitation. *J Intensive Care Med* 2007; **22**: 294-299 [PMID: [17895487](#) DOI: [10.1177/0885066607305247](#)]
  - 29 **Sugrue M**, Bauman A, Jones F, Bishop G, Flabouris A, Parr M, Stewart A, Hillman K, Deane SA. Clinical examination is an inaccurate predictor of intraabdominal pressure. *World J Surg* 2002; **26**: 1428-1431 [PMID: [12297912](#) DOI: [10.1007/s00268-002-6411-8](#)]
  - 30 **Kirkpatrick AW**, Roberts DJ, De Waele J, Jaeschke R, Malbrain ML, De Keulenaer B, Duchesne J, Bjorck M, Leppaniemi A, Ejike JC, Sugrue M, Cheatham M, Ivatury R, Ball CG, Reintam Blaser A, Regli A, Balogh ZJ, D'Amours S, Debergh D, Kaplan M, Kimball E, Olvera C; Pediatric Guidelines Sub-Committee for the World Society of the Abdominal Compartment Syndrome. Intra-abdominal hypertension and the abdominal compartment syndrome: updated consensus definitions and clinical practice guidelines from the World Society of the Abdominal Compartment Syndrome. *Intensive Care Med* 2013; **39**: 1190-1206 [PMID: [23673399](#) DOI: [10.1007/s00134-013-2906-z](#)]
  - 31 **Malbrain ML**, Wilmer A. The polycompartment syndrome: towards an understanding of the interactions between different compartments! *Intensive Care Med* 2007; **33**: 1869-1872 [PMID: [17786404](#) DOI: [10.1007/s00134-007-0843-4](#)]

- 32 **Hessmann M**, Rommens P. Does the intrapelvic compartment syndrome exist? *Acta Chir Belg* 1998; **98**: 18-22 [PMID: [9538916](#)]
- 33 **Manenti A**, Giuliani E. The pelvic compartment syndrome. *J Am Coll Surg* 2013; **217**: 374 [PMID: [23870223](#) DOI: [10.1016/j.jamcollsurg.2013.06.011](#)]
- 34 **Cheatham ML**, White MW, Sagraves SG, Johnson JL, Block EF. Abdominal perfusion pressure: a superior parameter in the assessment of intra-abdominal hypertension. *J Trauma* 2000; **49**: 621-626; discussion 626-627 [PMID: [11038078](#) DOI: [10.1097/00005373-200010000-00008](#)]
- 35 **Cheatham ML**. Nonoperative management of intraabdominal hypertension and abdominal compartment syndrome. *World J Surg* 2009; **33**: 1116-1122 [PMID: [19363690](#) DOI: [10.1007/s00268-009-0003-9](#)]
- 36 **De Laet I**, Hoste E, Verholen E, De Waele JJ. The effect of neuromuscular blockers in patients with intra-abdominal hypertension. *Intensive Care Med* 2007; **33**: 1811-1814 [PMID: [17594072](#) DOI: [10.1007/s00134-007-0758-0](#)]
- 37 **Cheatham ML**, Safcsak K. Percutaneous catheter decompression in the treatment of elevated intraabdominal pressure. *Chest* 2011; **140**: 1428-1435 [PMID: [21903735](#) DOI: [10.1378/chest.10-2789](#)]
- 38 **Malbrain ML**, Marik PE, Witters I, Cordemans C, Kirkpatrick AW, Roberts DJ, Van Regenmortel N. Fluid overload, de-resuscitation, and outcomes in critically ill or injured patients: a systematic review with suggestions for clinical practice. *Anaesthesiol Intensive Ther* 2014; **46**: 361-380 [PMID: [25432556](#) DOI: [10.5603/AIT.2014.0060](#)]
- 39 **Kubiak BD**, Albert SP, Gatto LA, Snyder KP, Maier KG, Vieau CJ, Roy S, Nieman GF. Peritoneal negative pressure therapy prevents multiple organ injury in a chronic porcine sepsis and ischemia/reperfusion model. *Shock* 2010; **34**: 525-534 [PMID: [20823698](#) DOI: [10.1097/SHK.0b013e3181e14cd2](#)]
- 40 **De Waele JJ**, Hoste EA, Malbrain ML. Decompressive laparotomy for abdominal compartment syndrome--a critical analysis. *Crit Care* 2006; **10**: R51 [PMID: [16569255](#) DOI: [10.1186/cc4870](#)]
- 41 **Sugrue M**. Abdominal compartment syndrome and the open abdomen: any unresolved issues? *Curr Opin Crit Care* 2017; **23**: 73-78 [PMID: [27941356](#) DOI: [10.1097/MCC.0000000000000371](#)]
- 42 **Rogers WK**, Garcia L. Intraabdominal Hypertension, Abdominal Compartment Syndrome, and the Open Abdomen. *Chest* 2018; **153**: 238-250 [PMID: [28780148](#) DOI: [10.1016/j.chest.2017.07.023](#)]
- 43 **Miller PR**, Meredith JW, Johnson JC, Chang MC. Prospective evaluation of vacuum-assisted fascial closure after open abdomen: planned ventral hernia rate is substantially reduced. *Ann Surg* 2004; **239**: 608-614; discussion 614-616 [PMID: [15082964](#) DOI: [10.1097/01.sla.0000124291.09032.bf](#)]
- 44 **Zhou JC**, Zhao HC, Pan KH, Xu QP. Current recognition and management of intra-abdominal hypertension and abdominal compartment syndrome among tertiary Chinese intensive care physicians. *J Zhejiang Univ Sci B* 2011; **12**: 156-162 [PMID: [21265048](#) DOI: [10.1631/jzus.B1000185](#)]



## Fibroblast growth factor signaling in non-alcoholic fatty liver disease and non-alcoholic steatohepatitis: Paving the way to hepatocellular carcinoma

Matthias Ocker

**ORCID number:** Matthias Ocker (0000-0001-8263-6288).

**Author contributions:** Ocker M is the sole author of this publication.

**Conflict-of-interest statement:** The author declares no conflict of interest related to this publication.

**Open-Access:** This article is an open-access article that was selected by an in-house editor and fully peer-reviewed by external reviewers. It is distributed in accordance with the Creative Commons Attribution NonCommercial (CC BY-NC 4.0) license, which permits others to distribute, remix, adapt, build upon this work non-commercially, and license their derivative works on different terms, provided the original work is properly cited and the use is non-commercial. See: <http://creativecommons.org/licenses/by-nc/4.0/>

**Manuscript source:** Invited manuscript

**Received:** October 15, 2019

**Peer-review started:** October 15, 2019

**First decision:** December 4, 2019

**Revised:** December 17, 2019

**Accepted:** January 1, 2020

**Article in press:** January 1, 2020

**Published online:** January 21, 2020

**P-Reviewer:** Abenavoli L, Liu HK, Sitkin S, Tanaka N

**S-Editor:** Ma L

**L-Editor:** A

**E-Editor:** Ma YJ

**Matthias Ocker**, Department of Gastroenterology (CBF), Charité University Medicine Berlin, Berlin 10117, Germany

**Corresponding author:** Matthias Ocker, MD, Professor, Department of Gastroenterology (CBF), Charité University Medicine Berlin, Berlin 10117, Germany.  
[matthias.ocker@charite.de](mailto:matthias.ocker@charite.de)

### Abstract

Metabolic disorders are increasingly leading to non-alcoholic fatty liver disease, subsequent steatohepatitis, cirrhosis and hepatocellular carcinoma. Fibroblast growth factors and their receptors play an important role in maintaining metabolic homeostasis also in the liver and disorders in signaling have been identified to contribute to those pathophysiologic conditions leading to hepatic lipid accumulation and chronic inflammation. While specific and well tolerated inhibitors of fibroblast growth factor receptor activity are currently developed for (non-liver) cancer therapy, treatment of non-alcoholic fatty liver disease and non-alcoholic steatohepatitis is still limited. Fibroblast growth factor-mimicking or restoring approaches have recently evolved as a novel therapeutic option and the impact of such interactions with the fibroblast growth factor receptor signaling network during non-alcoholic fatty liver disease/non-alcoholic steatohepatitis development is reviewed here.

**Key words:** Fibroblast growth factor; Fibroblast growth factor receptor; Non-alcoholic fatty liver disease; Non-alcoholic steatohepatitis; Fibrosis; Cirrhosis; Hepatocellular carcinoma

©The Author(s) 2020. Published by Baishideng Publishing Group Inc. All rights reserved.

**Core tip:** Non-alcoholic fatty liver disease and non-alcoholic steatohepatitis show globally rising incidences and are expected to become the main reason for liver fibrosis, cirrhosis, liver cancer and end-stage liver disease with need for transplantation. Liver metabolism is, among other factors, regulated by fibroblast growth factors and their receptors. This review highlights the role of these signaling pathways in the context of non-alcoholic fatty liver disease and non-alcoholic steatohepatitis and discusses novel treatment options for these otherwise difficult to treat diseases.



**Citation:** Ocker M. Fibroblast growth factor signaling in non-alcoholic fatty liver disease and non-alcoholic steatohepatitis: Paving the way to hepatocellular carcinoma. *World J Gastroenterol* 2020; 26(3): 279-290

**URL:** <https://www.wjgnet.com/1007-9327/full/v26/i3/279.htm>

**DOI:** <https://dx.doi.org/10.3748/wjg.v26.i3.279>

## INTRODUCTION

Primary liver cancer, hepatocellular carcinoma (HCC) is among the most common cancer related deaths for men and women. HCC commonly develops on the background of various underlying chronic liver diseases and is often called “a disease within a disease”. Besides chronic viral infections and despite the success of vaccination campaigns, its incidence is continuously high, and even increasing, also due to the globally steep increase in metabolic liver diseases leading to non-alcoholic fatty liver disease (NAFLD) and subsequently non-alcoholic steatohepatitis (NASH), fibrosis, cirrhosis and cancer formation<sup>[1,2]</sup>. With a global prevalence of about 25%, NAFLD and NASH are a major medical burden and linked to an increasing number of patients with end-stage liver disease and transplantation need. A further increase is expected due to growing prevalence of obesity and metabolic syndrome<sup>[3]</sup>.

The pathophysiologic mechanisms underlying these processes are still not completely clear. Yet, growth factors like the fibroblast growth factor (FGF) family and fibroblast growth factor receptors (FGFRs) can contribute and drive several of these changes and have been clearly shown to possess oncogenic potential in some circumstances<sup>[4,5]</sup>. In the liver, esp. FGF19, FGF21 and FGF23 have been shown to physiologically possess endocrine functions in regulating, e.g., homeostasis of bile acids and glucose as well as regulating fasting response, lipid metabolism and other conditions<sup>[6-10]</sup>. As the dysregulation of these metabolic pathways is considered a key feature of chronic liver diseases leading to obesity, metabolic syndrome, NAFLD, NASH, fibrosis and finally HCC, FGFs and FGFRs could be interesting novel targets for diagnosis, surveillance and treatment of these conditions.

## PHYSIOLOGY OF FGFRS AND FGFs IN THE LIVER

All four FGFRs are transmembrane tyrosine kinase receptors with a single-pass transmembrane domain, an intracellular kinase domain and three extracellular immunoglobulin-like domains which are subject to alternative splicing and thus mediate ligand specificity. Binding of FGFs leads to receptor dimerization and activation of the downstream signaling cascade that mediates processes linked to cellular survival, extracellular matrix and adhesion molecule signaling but also metabolic processes, e.g., via the PI3K/AKT pathway<sup>[11,12]</sup>. While the expression of FGFR1 (predominantly mesenchymal tissues) and FGFR2 (predominantly mesenchymal and epithelial) is broad, FGFR3 is mostly found in the central nervous system, bone, skin, and to a lesser extend GI tract, kidney and male and female reproductive tissues. FGFR4 is found in endodermal tissues and the somatic myotome, including endocrine, bone marrow, pancreas, lung and liver and gallbladder tissues<sup>[5,13]</sup>. In summary, all FGFRs are expressed in the liver with higher levels of FGFR3 and FGFR4<sup>[14]</sup>.

In humans, 22 FGFs have been described so far. They can be subclustered into four intracrine (FGF11-14), fifteen paracrine (FGF1-10, 16-18, 20, 22) and three endocrine (FGF19, 21, 23) subfamilies. They consist of 150-300 amino acids and share about 30%-60% sequence homology with different N- and C-terminal parts mediating receptor specificity. Endocrine FGFs need co-receptors of the Klotho family to bind to any of the four FGFRs. Unlike paracrine FGFs, they lack the heparan sulphate binding capacity and can therefore enter circulation and act as hormones<sup>[4,15-17]</sup>. The general metabolic functions of endocrine FGFs are reviewed elsewhere<sup>[4,18]</sup> and we will here focus on their role in physiology and pathophysiology of the liver.

FGF1 is expressed in the liver and other tissues, including adipose tissue where it is upregulated upon high-fat diets<sup>[19]</sup>. It can bind to all FGFRs and can interact with integrins which are mediators of fibrogenesis, too<sup>[20,21]</sup>. FGF1 and FGF2 are upregulated in chronic liver disease, fibrogenesis and in HCC where these ligands enhance angiogenesis and invasiveness<sup>[22,23]</sup>. In addition, FGF1 and FGF2 mediate fibrogenesis by activation of hepatic stellate cells which links extracellular matrix



modulation and carcinogenesis to NAFLD/NASH<sup>[22,24]</sup>. Paracrine FGF8 and FGF10 have been shown to play important roles during embryonic liver development and during liver regeneration<sup>[25,26]</sup>. Esp. FGF10 was shown to regulate hepatoblast function, which links development and repair processes<sup>[27]</sup>. Upon hepatocyte injury, FGF7 induces progenitor cell proliferation in the liver<sup>[28]</sup>. The activation of hepatic stellate cells as a response to injury was linked to FGF9, which also induces hepatocyte proliferation in acute liver injury models<sup>[29]</sup>. Importantly, the activation of hepatic stellate cells as well as the induction of hepatocyte proliferation and recruitment of progenitor cells are key features of acute and chronic liver injury leading to fibrosis, cirrhosis and cancer formation, indicating a central role for FGFs during this process. In human HCC, upregulation of FGF8 family members (FGF8, FGF17 and FGF18) was linked to angiogenesis and enhanced cancer cell survival in 59% of the examined tissue samples. Interestingly, also different FGFRs were upregulated and overall, 82% of cases showed alterations of at least one FGFR and/or FGF<sup>[30]</sup>.

Endocrine FGFs have been shown to control several metabolic pathways in the liver *via*  $\beta$ -Klotho co-signaling. FGF19 (also called FGF15/19 due to its mouse homologue FGF15 which does not exist in humans) is a key regulator of bile acid metabolism and links gut-liver signaling. The nuclear bile acid receptor FXR induces expression of FGF19 in the ileum which in turn reduces expression of CYP7A1, the rate limiting enzyme for bile acid synthesis in hepatocytes<sup>[31]</sup>. FGF19 was also shown to control gallbladder volume<sup>[32]</sup>. Furthermore, FGF19 stimulates protein and glycogen synthesis in hepatocytes independent of insulin and is thus also involved in glucose homeostasis<sup>[33]</sup>.

FGF21 controls a plethora of metabolic pathways in hepatocytes, adipocytes and skeletal muscle<sup>[34]</sup>. Nutritional stress (*e.g.*, low carbohydrate, high fat ketogenic diets) as well as other means of hepatic injury have confirmed FGF21 as a stress response gene in the liver, *e.g.*, by inducing systemic glucocorticoid levels<sup>[35]</sup>. Interestingly, FGF21 was also identified to be a key mediator of metabolic effects mediated by gut microbiota. Several studies recently demonstrated a protective effect of probiotic microbiota like *Lactobacillus* species (*esp.* *L. rhamnosus* GG) on energy expenditure, dyslipidemia or steatosis in different animal models, which was shown to be dependent on FGF21 signaling and able to reverse NAFLD<sup>[36-39]</sup>.

Although FGF23 is linked to calcium and phosphate homeostasis in bone and kidney *via*  $\alpha$ -Klotho co-signaling and not considered to play an important role in liver pathophysiology<sup>[40]</sup>, a recent study showed that serum FGF23 was correlated with NAFLD in Chinese patients with type 2 diabetes<sup>[41]</sup>. Although the exact role of FGF23 in NAFLD pathogenesis is unclear, FGF23 mRNA was detected in the liver and is increased under metabolic stress conditions and chronic liver disease in mice<sup>[42]</sup>. Yet the observed increase could also be due to the renal pathophysiology of these conditions<sup>[43]</sup>.

## FGF SIGNALING IN NAFLD AND NASH ASSOCIATED LIVER INJURY

Deployment of extracellular matrix material, fibrosis, is the general response of the liver to chronic injury with hepatocyte damage - independent of the causing agent (viral, toxic, metabolic). Chronic hepatocyte damage and cell death leads to persistent inflammation and activation of wound healing and tissue remodeling programs to compensate the loss of functional hepatocytes and to restrict the damaged area by activation of hepatic stellate cells (Figure 1 and Table 1, for more details on general fibrosis mechanisms in the liver please see<sup>[44-46]</sup>).

Various factors have been described to contribute to NAFLD/NASH and fibrosis progression, like ROS production or inflammatory cytokine release from adipocytes but also impairment of metabolic pathways in the gut and liver like lipogenesis, cholesterol and insulin signaling<sup>[47]</sup>. Dietary factors can influence these pathways and *esp.* high dietary cholesterol, polyunsaturated fatty acids and fructose have been demonstrated to trigger NAFLD/NASH development<sup>[48,49]</sup>. In absence of insulin, fructose is subjected to liponeogenesis and thus depletes hepatocellular ATP and contributes to mitochondrial damage, ROS production and lipid accumulation, as evidenced by patients with high fructose intake (*e.g.*, soft drinks)<sup>[50,51]</sup>.

Lipid metabolism is considered a key pathogenetic driver of NAFLD progression and fibrosis development. It depends on lipolysis, liponeogenesis and triglyceride oxidation and the overload of the liver with such metabolites can trigger ER stress and autophagy responses<sup>[52,53]</sup>.

FGF21 plays a central role here. It is abundantly expressed at low levels in the liver and can be induced upon fasting<sup>[54]</sup> and seems to inhibit lipolysis under this

**Table 1 Role of fibroblast growth factors in non-alcoholic fatty liver disease, non-alcoholic steatohepatitis and hepatocellular carcinoma**

FGFs	NAFLD/NASH	HCC
FGF1	Upregulated in adipose tissue under high fat diet <sup>[19]</sup>	HSC activation, fibrogenesis, angiogenesis, invasiveness <sup>[20,21]</sup>
FGF2	No data	HSC activation, fibrogenesis, angiogenesis, invasiveness <sup>[22-24]</sup>
FGF8 family	No data	Proliferation, angiogenesis, matrix modulation <sup>[30]</sup>
FGF19	Impaired in NAFLD and by insulin resistance, contributes to lipid and bile acid dysbalance <sup>[74-76]</sup>	Proliferation, invasion, metastasis, inhibition of apoptosis <sup>[102-104]</sup>
FGF21	Induced by ketogenic diet, reduces insulin sensitivity, mediator of metabolic effects from gut microbiota <sup>[35-39,54-56]</sup>	Deficiency promotes HCC under obesity conditions <sup>[21,61]</sup>

FGF: Fibroblast growth factor; NAFLD: Non-alcoholic fatty liver disease; NASH: Non-alcoholic steatohepatitis; HCC: Hepatocellular carcinoma; HSC: Hepatic stellate cell.

condition<sup>[34]</sup>. Its expression in the liver can be induced by ketogenic (high-fat, low-carbohydrate) diets and it then negatively impacts on insulin sensitivity in adipocytes. Starvation induced hepatic FGF21 expression increases systemic glucocorticoid levels and diminishes physical activity, probably via remote effects in the central nervous system or in adipose tissues<sup>[55,56]</sup>. Hepatic FGF21 mediates various effects on energy metabolism and insulin sensitivity in the liver and the skeletal muscle via adiponectin<sup>[57,58]</sup>. In FGF21 deficient mice, a role in glucagon signaling was also described<sup>[59]</sup>. Upon hepatic injury, FGF21 serves as a protective stress-response regulator and has been shown to ameliorate various hepatotoxic conditions (viral hepatitis, alcohol)<sup>[60]</sup>.

Although high levels of FGF21 are considered to be protective against metabolic stress conditions several studies in mice and humans demonstrated also opposite effects. Deficiencies in FGF21 signaling promote HCC growth in mice on long-term obese diet and restoration of FGF21 improves hepatic steatosis<sup>[61,62]</sup>. In obese humans, increased hepatic FGF21 was described<sup>[6]</sup> and linked to prevalence and progression of NAFLD, indicating impaired FGF21 function as was seen in type II diabetes with insulin resistance<sup>[63,64]</sup>. Elevated expression of FGF21 was also established as a clinical predictive biomarker for steatosis in obese children<sup>[65]</sup> and a panel consisting of FGF21, BMI,  $\gamma$ -GT and triglycerides was proposed as a biomarker for identification of children with steatosis<sup>[66]</sup>. In adult patients with HIV, elevated FGF21 was confirmed as a risk factor for steatosis<sup>[67]</sup> and, overall, combined biomarker panels that include FGF21 have higher predictivity for steatosis also in non-obese patients<sup>[68,69]</sup>. Interestingly, no data is available on the expression levels of the main receptors for FGF21, FGFR1 and  $\beta$ -Klotho, in NAFLD and NASH.

Maintenance of chronic inflammation is required for the progression of NAFLD to NASH and for fibrosis development. Here, hepatic macrophages, so called Kupffer cells, play a central role in keeping hepatic stellate cells activated. In FGF5 deficient mice, high fat diet lead to severe steatosis and fibrosis via activation of F4/80 macrophages that were positive for CD11b and CD68 and produced TNF $\alpha$  and FasL<sup>[70,71]</sup>.

FGF19 (and its murine homologue FGF15) regulates hepatocyte proliferation. In knockout mice, liver regeneration after partial hepatectomy is impaired and toxic stimuli lead to extensive necrosis and fibrosis, the latter mediated via activation of CTGF signaling<sup>[72,73]</sup>. In human NAFLD, hepatic response to FGF19 was significantly impaired, esp. under conditions of insulin resistance, and may contribute to lipid and bile acid dysbalance in these patients<sup>[74-76]</sup>. FGF19 serum levels are reduced in pediatric and adult patients with NAFLD<sup>[77,78]</sup> while an increase in taurine and glycine metabolizing bacteria like *Escherichia* or *Bilophila* was concomitantly observed<sup>[79]</sup>. The decrease in FGF19 was proposed as a biomarker for steatosis development<sup>[77]</sup>. In mice, an FGF15-Apo A-I fusion protein (Fibapo) was shown to improve lipid accumulation and metabolic stress under high fat diet conditions in FGF15 knockouts<sup>[80]</sup>, confirming the therapeutic effect of FGF restoration. To overcome potential protumorigenic effects of FGF19 (i.e., induction of cell proliferation), recombinant molecules have been developed and are currently used in human clinical trials. Similar to FGF21, FGF19 was also evaluated as a biomarker for NAFLD and NASH. FGF19 levels were significantly reduced in children with NASH but did not show statistically significant association to the pediatric NAFLD histological score<sup>[81]</sup>. In a therapeutic study in pediatric patients, FGF19 was significantly increased by lifestyle intervention and a

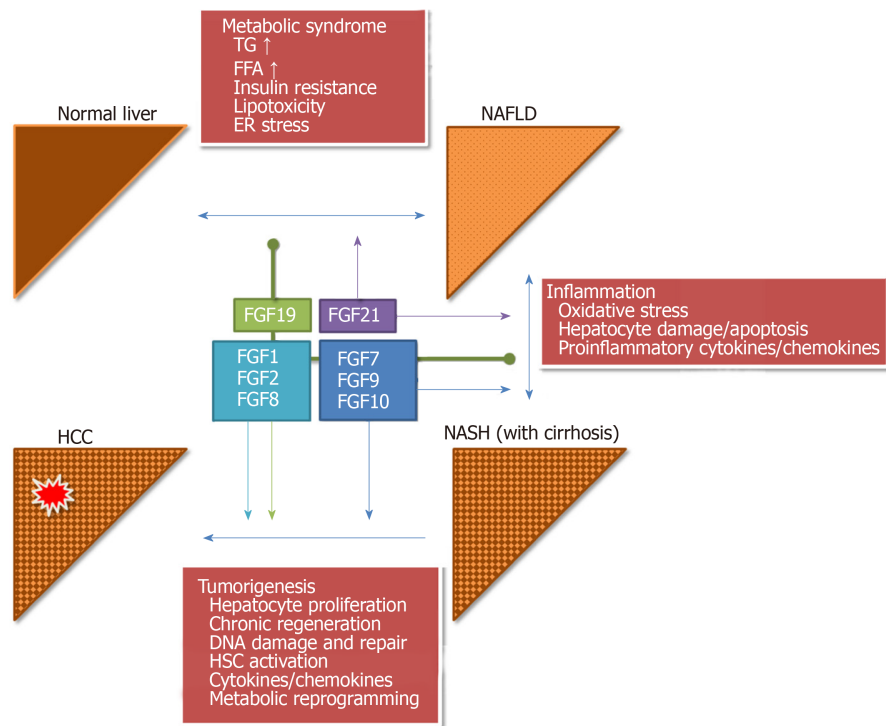


**Figure 1 Role of fibroblast growth factor signaling in non-alcoholic fatty liver disease, non-alcoholic steatohepatitis and progression to hepatocellular carcinoma.** Fibroblast growth factors (FGFs) mediate the key pathogenetic processes linked to development of non-alcoholic fatty liver disease (NAFLD) (metabolic disturbances), non-alcoholic steatohepatitis (NASH) (chronic inflammation) and hepatocellular carcinoma (HCC) (chronic regeneration). FGF21 is mostly involved in mediating metabolic effects during NAFLD and NASH progression, while paracrine FGFs (FGF7, 9, 10) activate hepatocyte proliferation and regeneration processes. FGF19 can inhibit these processes at early stages but may have pro-tumorigenic properties during later disease phases. FGF1, FGF2 and the FGF8 family (FGF8, FGF17, FGF18) mediate HCC formation by supporting angiogenesis, matrix modulation via hepatic stellate cells activation and increasing tumor cell survival. Pointed arrow heads: Activation; Rounded arrow heads: Inhibition. FGF: Fibroblast growth factor; NAFLD: Non-alcoholic fatty liver disease; NASH: Non-alcoholic steatohepatitis; HCC: Hepatocellular carcinoma; TG: Triglycerides; FA: Fatty acids; ER: Endoplasmic reticulum; HSC: Hepatic stellate cells.

mix containing docosahexaenoic acid, choline, and vitamin E and was therefore proposed as a pharmacodynamic biomarker in this setting<sup>[82]</sup>. Overall, the predictivity of FGF19 is still under debate<sup>[76]</sup>.

## FGF SIGNALING AS A NOVEL DRUG TARGET IN NAFLD AND NASH

Due to their described hepatoprotective properties and effects on inflammation, metabolism and fibrosis, restoration of FGF19 and FGF21 signaling is considered an attractive novel target for drug development against NAFLD and NASH. In the past, drug development for NAFLD and NASH has been limited by the availability of suitable (surrogate) endpoints and the debate on non-invasive measures is still ongoing<sup>[83]</sup>. While non-invasive measurements of NASH status and fibrosis have evolved as acceptable endpoints in early stage trials, Phase 3 studies may still require pre- and post-treatment biopsies. Recently, advances in patient selection were achieved that do allow timely readout of *e.g.*, changes in fibrosis, as overall survival may not be achievable pre-cirrhotic patients<sup>[53,84]</sup>.

While several agents are currently in Phase 2 and Phase 3 clinical development for treatment of NASH<sup>[53]</sup>, only few compounds are using FGF signaling as a therapeutic target.

Pegbelfermin (BMS-986036) is a recombinant PEGylated analog of human FGF21. In preclinical models, it improved diabetes, NASH and fibrosis, as demonstrated by increases in adiponectin, improved NAFLD activity score and decreased N-terminal type III collagen propeptide (Pro-C3)<sup>[85]</sup>. In a Phase 2 study in patients with obesity and type 2 diabetes, pegbelfermin achieved a significant increase in adiponectin and decrease in serum Pro-C3 after 12 wk, comparable to preclinical data. Although effects

on HbA1c were not different to placebo, the drug was overall well tolerated and it was concluded that effects on obesity-related diseases like NASH warrant further investigations<sup>[86]</sup>. This was further analyzed in a randomized, double-blind, placebo-controlled Phase 2 study in patients with confirmed NASH, fibrosis and obesity. Pegbelfermin was administered subcutaneous in a daily (10 mg/d) or a weekly (20 mg/wk) schedule for 16 wk and primary endpoints were changes in magnetic resonance imaging proton density fat fraction (MRI-PDFF), serum Pro-C3, transaminases, and liver stiffness as assessed by MR elastography. A total of 74 patients were enrolled and 68 were eligible after 16 wk of treatment. Here, a significant reduction in MRI-PDFF (-6.8% and -5.2%, respectively) and transaminases (-33.0% and -23.7% for alanine aminotransferase, -30.9% and -26.2% for aspartate aminotransferase, respectively) was detected in both treatment schedules. Furthermore, a significant proportion of patients showed improved serum Pro-C3 and reduced MR elastography liver stiffness, all paralleled by an approximate 15% increase in adiponectin versus placebo. Overall, the drug was also well tolerated in these patients and results from this study suggest clearly a beneficial effect on steatosis, liver injury and fibrosis in NASH patients<sup>[87]</sup>. Currently, additional studies are ongoing to evaluate pegbelfermin in patients with NASH associated fibrosis, cirrhosis or impaired kidney function.

NGM282 is a recombinant non-tumorigenic variant of FGF19. It was modified at the amino-terminal end to bind to FGFR4/ $\beta$ -Klotho, suppress CYP7A1 expression (the rate limiting step in bile acid synthesis) but does not activate STAT3 signaling which is considered a main driver for hepatocarcinogenesis<sup>[88]</sup>. Preclinically, NGM282 improved inflammation, hepatocyte damage and fibrosis in models of NASH and of sclerosing cholangitis in *mdr2*-deficient mice<sup>[89,90]</sup>. It was well tolerated also in humans and showed signs of reduced CYP7A1 activity, too<sup>[91]</sup>. In a randomized and placebo-controlled Phase 2 study, NGM282 lead to a rapid reduction in hepatic fat content in more than 70% of the treated patients after 12 wk, paralleled by significant reductions in transaminase and Pro-C3 levels and ELF fibrosis score and increase in low density lipoprotein cholesterol. The overall safety profile was acceptable with predominantly Grade 1 adverse events. As NGM282 is a recombinant peptide, anti-drug antibodies were observed in a small number of patients but were considered not to be neutralizing<sup>[92]</sup>. After 12 wk, NAFLD activity score was dose-dependently reduced by 2 points in up to 63% of patients without worsening of fibrosis and fibrosis was reduced by one or more stages in up to 42% of patients<sup>[93]</sup>. Due to its effects on CYP7A1, NGM282 increases low density lipoprotein cholesterol and serum cholesterol. Thus, combination with rosuvastatin was assessed to further improve the cardiovascular risk profile for NASH patients<sup>[94]</sup>.

While these approaches focus on ligands, also FGFRs could be a promising target for NAFLD and NASH drug development. Several small molecule kinase inhibitors targeting FGFRs are currently in clinical development for the treatment of various solid tumors. Yet, in none of the early clinical trials with these multi-kinase inhibitors (usually targeting FGFR1-3), metabolic effects related to FGF signaling other than phosphate increase due to renal FGFR1 inhibition were reported. BLU9931 as well as H3B-6527, two specific inhibitors of FGFR4, suppressed HCC growth in preclinical models but also induced expression of CYP7A1, although no adverse effects on lipid metabolism or steatosis were observed in the investigated rodent models<sup>[95,96]</sup>.

The protective effects of FGF19 via inhibition of endoplasmic reticulum stress, which is commonly observed in metabolic overload during NAFLD and NASH, have been shown to be mediated via the FGFR4/ $\beta$ -Klotho pathway<sup>[97]</sup>. An upregulation of FGFR4 was recently demonstrated in murine NASH models<sup>[98]</sup> and in patients developing HCC on fatty liver disease background<sup>[99]</sup>. To block FGFR4 signaling, a soluble FGFR4 extracellular domain fragment was developed that specifically inhibits FGFR4 activation *in vitro* and suppressed steatosis and fatty liver development in mice<sup>[100]</sup>, but clinical data in humans is still lacking.

Mimicking FGFR activation is currently investigated with NGM313, a humanized monoclonal antibody binding to an epitope in  $\beta$ -Klotho. It was shown that NGM313 activates FGFR1c signaling, similar to the physiologic role of FGF21. A single dose of NGM313 significantly reduced liver fat content, transaminase levels, HbA1c, triglycerides and low density lipoprotein cholesterol in obese patients with insulin resistance and NAFLD<sup>[101]</sup>.

## FGFS AND FGFRS IN HCC

The above outlined pathways of chronic inflammation and hepatocyte stress conditions commonly involve FGF signaling and various approaches in restoring FGF



physiologic conditions have been successful in preventing HCC development in preclinical models. In human HCC, several studies confirmed overexpression of different FGFs and FGFRs, which confirms the attractiveness of targeting FGF signaling also in established HCC<sup>[102,103]</sup>. FGF19 was recently proposed as a novel diagnostic biomarker with better accuracy than AFP for small HCCs<sup>[104]</sup>. As many FGFs can have different pro-tumorigenic effects (e.g., by promoting angiogenesis or chronic inflammation), FGFRs seem to be the more attractive here. While esp. inhibition of FGFR4 was shown to reduce growth of experimental HCC models<sup>[105,106]</sup> and is considered an attractive drug target<sup>[107,108]</sup>, also FGF1, FGF2 and the FGF8 subfamily as well as targeting FGFR1-3 have been shown to possess preclinical anti-HCC activity<sup>[103,109,110]</sup>. Designing specific inhibitors for FGFR4 was considered challenging and therefore initial approaches used multi-kinase or pan-FGFR inhibitors. While sorafenib was the first multi-kinase inhibitor to achieve an overall survival benefit in HCC<sup>[111]</sup>, other compounds like brivanib or lenvatinib did not achieve this endpoint<sup>[103,112]</sup>. Preclinically, the specific FGFR4 inhibitors BLU-9931, H3B-6527 or INCB062079 showed promising activities<sup>[95,96,113]</sup>.

Several clinical studies with these and other FGFR4 specific inhibitors are currently ongoing in HCC patients. Phase 1 data for fisogatinib (BLU-554) indicate good target engagement and inhibition of FGFR4 as shown by effects on bile acid and cholesterol synthesis pathways in a dose-dependent manner. With an overall good tolerability, the compound showed signs of clinical efficacy in FGF19-positive HCC patients<sup>[114]</sup>. FGF401 showed an increase in transaminases and induction of CYP7A1 in preclinical toxicology studies and co-administration of cholestyramine improved the safety profile here<sup>[115]</sup>. In humans, increase in transaminases was seen, too, but the overall safety profile is considered acceptable and no maximum tolerated dose was reached in a Phase 1/2 study. Patients had to be positive for FGFR4 and  $\beta$ -Klotho expression to be eligible to participation and the overall response rate in the Phase 1 population was about 8%<sup>[116]</sup>.

## CONCLUSION

The high global prevalence of NAFLD and NASH warrants the search for novel treatment options. FGF signaling mediates central metabolic effects in the liver (and other tissues) that are directly linked to the overload of hepatocytes with toxic metabolites and pathogenesis of lipid accumulation and chronic inflammation leading. Several approaches, e.g., FGF-mimicking peptides or receptor-specific targeting agents, have shown promising signs in preclinical and early clinical studies in humans. Yet, due to the plethora of ligands and receptors and a high tissue context dependency, further studies and esp. also long-term studies are urgently needed to fully understand how FGF and FGFR signaling pathways can be fully exploited for the benefit of affected patients.

Specific FGFR4 inhibitors are currently tested in clinical trials in HCC. The positive preclinical results are reflected in encouraging early clinical data from different Phase 1 studies. Yet, the overall efficacy of these compounds needs to be carefully investigated compared to current multi-kinase inhibitors and the emerging immune checkpoint inhibitors.

## REFERENCES

- 1 Akinyemiju T, Abera S, Ahmed M, Alam N, Alemayohu MA, Allen C, Al-Raddadi R, Alvis-Guzman N, Amoako Y, Artaman A, Ayele TA, Barac A, Bensenor I, Berhane A, Bhutta Z, Castillo-Rivas J, Chitheer A, Choi JY, Cowie B, Dandona L, Dandona R, Dey S, Dicker D, Phuc H, Ekwueme DU, Zaki MS, Fischer F, Fürst T, Hancock J, Hay SI, Hotez P, Jee SH, Kasaeian A, Khader Y, Khang YH, Kumar A, Kutz M, Larson H, Lopez A, Lunevicius R, Malekzadeh R, McAlinden C, Meier T, Mendoza W, Mokdad A, Moradi-Lakeh M, Nagel G, Nguyen Q, Nguyen G, Ogbo F, Patton G, Pereira DM, Pourmalek F, Qorbani M, Radfar A, Roshandel G, Salomon JA, Sanabria J, Sartorius B, Satpathy M, Sawhney M, Sepanlou S, Shackelford K, Shore H, Sun J, Mengistu DT, Topór-Mądry R, Tran B, Ukwaja KN, Vlassov V, Vollset SE, Vos T, Wakayo T, Weiderpass E, Werdecker A, Yonemoto N, Younis M, Yu C, Zaidi Z, Zhu L, Murray CJL, Naghavi M, Fitzmaurice C. The Burden of Primary Liver Cancer and Underlying Etiologies From 1990 to 2015 at the Global, Regional, and National Level: Results From the Global Burden of Disease Study 2015. *JAMA Oncol* 2017; **3**: 1683-1691 [PMID: 28983565 DOI: 10.1001/jamaoncol.2017.3055]
- 2 Younossi Z, Anstee QM, Marietti M, Hardy T, Henry L, Eslam M, George J, Bugianesi E. Global burden of NAFLD and NASH: trends, predictions, risk factors and prevention. *Nat Rev Gastroenterol Hepatol* 2018; **15**: 11-20 [PMID: 28930295 DOI: 10.1038/nrgastro.2017.109]
- 3 Younossi ZM, Henry L, Bush H, Mishra A. Clinical and Economic Burden of Nonalcoholic Fatty Liver Disease and Nonalcoholic Steatohepatitis. *Clin Liver Dis* 2018; **22**: 1-10 [PMID: 29128049 DOI: 10.1016/j.cld.2017.08.001]

- 4 **Beenken A**, Mohammadi M. The FGF family: biology, pathophysiology and therapy. *Nat Rev Drug Discov* 2009; **8**: 235-253 [PMID: [19247306](#) DOI: [10.1038/nrd2792](#)]
- 5 **Heroult M**, Ellinghaus P, Ince S, Ocker M. Fibroblast Growth Factor Receptor Signaling in Cancer Biology and Treatment. *Curr Sign Trans Ther* 2014; **9**: 15-25 [DOI: [10.2174/157436240901140924103836](#)]
- 6 **Fu L**, John LM, Adams SH, Yu XX, Tomlinson E, Renz M, Williams PM, Soriano R, Corpuz R, Moffat B, Vandlen R, Simmons L, Foster J, Stephan JP, Tsai SP, Stewart TA. Fibroblast growth factor 19 increases metabolic rate and reverses dietary and leptin-deficient diabetes. *Endocrinology* 2004; **145**: 2594-2603 [PMID: [14976145](#) DOI: [10.1210/en.2003-1671](#)]
- 7 **Kharitonov A**. FGFs and metabolism. *Curr Opin Pharmacol* 2009; **9**: 805-810 [PMID: [19683963](#) DOI: [10.1016/j.coph.2009.07.001](#)]
- 8 **Lundäsén T**, Gälman C, Angelin B, Rudling M. Circulating intestinal fibroblast growth factor 19 has a pronounced diurnal variation and modulates hepatic bile acid synthesis in man. *J Intern Med* 2006; **260**: 530-536 [PMID: [17116003](#) DOI: [10.1111/j.1365-2796.2006.01731.x](#)]
- 9 **Zhang X**, Yeung DC, Karpisek M, Stejskal D, Zhou ZG, Liu F, Wong RL, Chow WS, Tso AW, Lam KS, Xu A. Serum FGF21 levels are increased in obesity and are independently associated with the metabolic syndrome in humans. *Diabetes* 2008; **57**: 1246-1253 [PMID: [18252893](#) DOI: [10.2337/db07-1476](#)]
- 10 **Xu J**, Lloyd DJ, Hale C, Stanislaus S, Chen M, Sivits G, Vonderfecht S, Hecht R, Li YS, Lindberg RA, Chen JL, Jung DY, Zhang Z, Ko HJ, Kim JK, Véniant MM. Fibroblast growth factor 21 reverses hepatic steatosis, increases energy expenditure, and improves insulin sensitivity in diet-induced obese mice. *Diabetes* 2009; **58**: 250-259 [PMID: [18840786](#) DOI: [10.2337/db08-0392](#)]
- 11 **Ornitz DM**, Itoh N. The Fibroblast Growth Factor signaling pathway. *Wiley Interdiscip Rev Dev Biol* 2015; **4**: 215-266 [PMID: [25772309](#) DOI: [10.1002/wdev.176](#)]
- 12 **Lamothe B**, Yamada M, Schaeper U, Birchmeier W, Lax I, Schlessinger J. The docking protein Gab1 is an essential component of an indirect mechanism for fibroblast growth factor stimulation of the phosphatidylinositol 3-kinase/Akt antiapoptotic pathway. *Mol Cell Biol* 2004; **24**: 5657-5666 [PMID: [15199124](#) DOI: [10.1128/MCB.24.13.5657-5666.2004](#)]
- 13 **Uhlén M**, Fagerberg L, Hallström BM, Lindskog C, Oksvold P, Mardinoglu A, Sivertsson Å, Kampf C, Sjöstedt E, Asplund A, Olsson I, Edlund K, Lundberg E, Navani S, Szgyarto CA, Odeberg J, Djureinovic D, Takanen JO, Hober S, Alm T, Edqvist PH, Berling H, Tegel H, Mulder J, Rockberg J, Nilsson P, Schwenk JM, Hamsten M, von Feilitzen K, Forsberg M, Persson L, Johansson F, Zwahlen M, von Heijne G, Nielsen J, Pontén F. Proteomics. Tissue-based map of the human proteome. *Science* 2015; **347**: 1260419 [PMID: [25613900](#) DOI: [10.1126/science.1260419](#)]
- 14 **Hughes SE**. Differential expression of the fibroblast growth factor receptor (FGFR) multigene family in normal human adult tissues. *J Histochem Cytochem* 1997; **45**: 1005-1019 [PMID: [9212826](#) DOI: [10.1177/002215549704500710](#)]
- 15 **Rapraeger AC**, Krufka A, Olwin BB. Requirement of heparan sulfate for bFGF-mediated fibroblast growth and myoblast differentiation. *Science* 1991; **252**: 1705-1708 [PMID: [1646484](#) DOI: [10.1126/science.1646484](#)]
- 16 **Ding X**, Boney-Montoya J, Owen BM, Bookout AL, Coate KC, Mangelsdorf DJ, Kliewer SA.  $\beta$ Klotho is required for fibroblast growth factor 21 effects on growth and metabolism. *Cell Metab* 2012; **16**: 387-393 [PMID: [22958921](#) DOI: [10.1016/j.cmet.2012.08.002](#)]
- 17 **Kurosu H**, Kuro-O M. The Klotho gene family as a regulator of endocrine fibroblast growth factors. *Mol Cell Endocrinol* 2009; **299**: 72-78 [PMID: [19063940](#) DOI: [10.1016/j.mce.2008.10.052](#)]
- 18 **Fernandes-Freitas I**, Owen BM. Metabolic roles of endocrine fibroblast growth factors. *Curr Opin Pharmacol* 2015; **25**: 30-35 [PMID: [26531325](#) DOI: [10.1016/j.coph.2015.09.014](#)]
- 19 **Nies VJ**, Sancar G, Liu W, van Zutphen T, Struik D, Yu RT, Atkins AR, Evans RM, Jonker JW, Downes MR. Fibroblast Growth Factor Signaling in Metabolic Regulation. *Front Endocrinol (Lausanne)* 2015; **6**: 193 [PMID: [26834701](#) DOI: [10.3389/fendo.2015.00193](#)]
- 20 **Mori S**, Wu CY, Yamaji S, Saegusa J, Shi B, Ma Z, Kuwabara Y, Lam KS, Isseroff RR, Takada YK, Takada Y. Direct binding of integrin  $\alpha$ 5 $\beta$ 1 to FGF1 plays a role in FGF1 signaling. *J Biol Chem* 2008; **283**: 18066-18075 [PMID: [18441324](#) DOI: [10.1074/jbc.M801213200](#)]
- 21 **Schuppan D**, Ocker M. Integrin-mediated control of cell growth. *Hepatology* 2003; **38**: 289-291 [PMID: [12883471](#) DOI: [10.1053/jhep.2003.50338](#)]
- 22 **Yu C**, Wang F, Jin C, Huang X, Miller DL, Basilico C, McKeehan WL. Role of fibroblast growth factor type 1 and 2 in carbon tetrachloride-induced hepatic injury and fibrogenesis. *Am J Pathol* 2003; **163**: 1653-1662 [PMID: [14507672](#) DOI: [10.1016/S0002-9440\(10\)63522-5](#)]
- 23 **Jin-no K**, Tanimizu M, Hyodo I, Kurimoto F, Yamashita T. Plasma level of basic fibroblast growth factor increases with progression of chronic liver disease. *J Gastroenterol* 1997; **32**: 119-121 [PMID: [9058307](#) DOI: [10.1007/bf01213308](#)]
- 24 **Schumacher JD**, Guo GL. Regulation of Hepatic Stellate Cells and Fibrogenesis by Fibroblast Growth Factors. *Biomed Res Int* 2016; **2016**: 8323747 [PMID: [27699175](#) DOI: [10.1155/2016/8323747](#)]
- 25 **Wang J**, Rhee S, Palaria A, Tremblay KD. FGF signaling is required for anterior but not posterior specification of the murine liver bud. *Dev Dyn* 2015; **244**: 431-443 [PMID: [25302779](#) DOI: [10.1002/dvdy.24215](#)]
- 26 **Calmont A**, Wandzioch E, Tremblay KD, Minowada G, Kaestner KH, Martin GR, Zaret KS. An FGF response pathway that mediates hepatic gene induction in embryonic endoderm cells. *Dev Cell* 2006; **11**: 339-348 [PMID: [16950125](#) DOI: [10.1016/j.devcel.2006.06.015](#)]
- 27 **Berg T**, Rountree CB, Lee L, Estrada J, Sala FG, Choe A, Veltmaat JM, De Langhe S, Lee R, Tsukamoto H, Crooks GM, Bellusci S, Wang KS. Fibroblast growth factor 10 is critical for liver growth during embryogenesis and controls hepatoblast survival via beta-catenin activation. *Hepatology* 2007; **46**: 1187-1197 [PMID: [17668871](#) DOI: [10.1002/hep.21814](#)]
- 28 **Takase HM**, Itoh T, Ino S, Wang T, Koji T, Akira S, Takikawa Y, Miyajima A. FGF7 is a functional niche signal required for stimulation of adult liver progenitor cells that support liver regeneration. *Genes Dev* 2013; **27**: 169-181 [PMID: [23322300](#) DOI: [10.1101/gad.204776.112](#)]
- 29 **Antoine M**, Wirz W, Tag CG, Gressner AM, Marvituna M, Wycislo M, Hellerbrand C, Kiefer P. Expression and function of fibroblast growth factor (FGF) 9 in hepatic stellate cells and its role in toxic liver injury. *Biochem Biophys Res Commun* 2007; **361**: 335-341 [PMID: [17662249](#) DOI: [10.1016/j.bbrc.2007.06.189](#)]
- 30 **Gaughhofer C**, Sagmeister S, Schrottmaier W, Fischer C, Rodgarkia-Dara C, Mohr T, Stättner S, Bichler C, Kandioler D, Wrba F, Schulte-Hermann R, Holzmann K, Grusch M, Marian B, Berger W, Grasl-

- Kraupp B. Up-regulation of the fibroblast growth factor 8 subfamily in human hepatocellular carcinoma for cell survival and neoangiogenesis. *Hepatology* 2011; **53**: 854-864 [PMID: [21319186](#) DOI: [10.1002/hep.24099](#)]
- 31 **Inagaki T**, Choi M, Moschetta A, Peng L, Cummins CL, McDonald JG, Luo G, Jones SA, Goodwin B, Richardson JA, Gerard RD, Repa JJ, Mangelsdorf DJ, Kliewer SA. Fibroblast growth factor 15 functions as an enterohepatic signal to regulate bile acid homeostasis. *Cell Metab* 2005; **2**: 217-225 [PMID: [16213224](#) DOI: [10.1016/j.cmet.2005.09.001](#)]
  - 32 **Choi M**, Moschetta A, Bookout AL, Peng L, Umetani M, Holmstrom SR, Suino-Powell K, Xu HE, Richardson JA, Gerard RD, Mangelsdorf DJ, Kliewer SA. Identification of a hormonal basis for gallbladder filling. *Nat Med* 2006; **12**: 1253-1255 [PMID: [17072310](#) DOI: [10.1038/nm1501](#)]
  - 33 **Kir S**, Beddow SA, Samuel VT, Miller P, Previs SF, Suino-Powell K, Xu HE, Shulman GI, Kliewer SA, Mangelsdorf DJ. FGF19 as a postprandial, insulin-independent activator of hepatic protein and glycogen synthesis. *Science* 2011; **331**: 1621-1624 [PMID: [21436455](#) DOI: [10.1126/science.1198363](#)]
  - 34 **Hotta Y**, Nakamura H, Konishi M, Murata Y, Takagi H, Matsumura S, Inoue K, Fushiki T, Itoh N. Fibroblast growth factor 21 regulates lipolysis in white adipose tissue but is not required for ketogenesis and triglyceride clearance in liver. *Endocrinology* 2009; **150**: 4625-4633 [PMID: [19589869](#) DOI: [10.1210/en.2009-0119](#)]
  - 35 **Cheng X**, Vispute SG, Liu J, Cheng C, Kharitonov A, Klaassen CD. Fibroblast growth factor (Fgf) 21 is a novel target gene of the aryl hydrocarbon receptor (AhR). *Toxicol Appl Pharmacol* 2014; **278**: 65-71 [PMID: [24769090](#) DOI: [10.1016/j.taap.2014.04.013](#)]
  - 36 **Ritze Y**, Bárdos G, Claus A, Ehrmann V, Bergheim I, Schwirtz A, Bischoff SC. Lactobacillus rhamnosus GG protects against non-alcoholic fatty liver disease in mice. *PLoS One* 2014; **9**: e80169 [PMID: [24475018](#) DOI: [10.1371/journal.pone.0080169](#)]
  - 37 **Kim B**, Park KY, Ji Y, Park S, Holzapfel W, Hyun CK. Protective effects of Lactobacillus rhamnosus GG against dyslipidemia in high-fat diet-induced obese mice. *Biochem Biophys Res Commun* 2016; **473**: 530-536 [PMID: [27018382](#) DOI: [10.1016/j.bbrc.2016.03.107](#)]
  - 38 **Zhao C**, Liu L, Liu Q, Li F, Zhang L, Zhu F, Shao T, Barve S, Chen Y, Li X, McClain CJ, Feng W. Fibroblast growth factor 21 is required for the therapeutic effects of Lactobacillus rhamnosus GG against fructose-induced fatty liver in mice. *Mol Metab* 2019; **29**: 145-157 [PMID: [31668386](#) DOI: [10.1016/j.molmet.2019.08.020](#)]
  - 39 **Liu Q**, Liu Y, Li F, Gu Z, Liu M, Shao T, Zhang L, Zhou G, Pan C, He L, Cai J, Zhang X, Barve S, McClain CJ, Chen Y, Feng W. Probiotic culture supernatant improves metabolic function through FGF21-adiponectin pathway in mice. *J Nutr Biochem* 2020; **75**: 108256 [PMID: [31760308](#) DOI: [10.1016/j.jnutbio.2019.108256](#)]
  - 40 **Erben RG**. Physiological Actions of Fibroblast Growth Factor-23. *Front Endocrinol (Lausanne)* 2018; **9**: 267 [PMID: [29892265](#) DOI: [10.3389/fendo.2018.00267](#)]
  - 41 **He X**, Shen Y, Ma X, Ying L, Peng J, Pan X, Bao Y, Zhou J. The association of serum FGF23 and non-alcoholic fatty liver disease is independent of vitamin D in type 2 diabetes patients. *Clin Exp Pharmacol Physiol* 2018; **45**: 668-674 [PMID: [29574933](#) DOI: [10.1111/1440-1681.12933](#)]
  - 42 **Mirams M**, Robinson BG, Mason RS, Nelson AE. Bone as a source of FGF23: regulation by phosphate? *Bone* 2004; **35**: 1192-1199 [PMID: [15542045](#) DOI: [10.1016/j.bone.2004.06.014](#)]
  - 43 **Dokumacioglu E**, Iskender H, Musmul A. Effect of hesperidin treatment on  $\alpha$ -Klotho/FGF-23 pathway in rats with experimentally-induced diabetes. *Biomed Pharmacother* 2019; **109**: 1206-1210 [PMID: [30551370](#) DOI: [10.1016/j.biopha.2018.10.192](#)]
  - 44 **Hauff P**, Gottwald U, Ocker M. Early to Phase II drugs currently under investigation for the treatment of liver fibrosis. *Expert Opin Investig Drugs* 2015; **24**: 309-327 [PMID: [25547844](#) DOI: [10.1517/13543784.2015.997874](#)]
  - 45 **Hernandez-Gea V**, Friedman SL. Pathogenesis of liver fibrosis. *Annu Rev Pathol* 2011; **6**: 425-456 [PMID: [21073339](#) DOI: [10.1146/annurev-pathol-011110-130246](#)]
  - 46 **Schuppan D**, Afdhal NH. Liver cirrhosis. *Lancet* 2008; **371**: 838-851 [PMID: [18328931](#) DOI: [10.1016/S0140-6736\(08\)60383-9](#)]
  - 47 **Schuppan D**, Schattenberg JM. Non-alcoholic steatohepatitis: pathogenesis and novel therapeutic approaches. *J Gastroenterol Hepatol* 2013; **28** Suppl 1: 68-76 [PMID: [23855299](#) DOI: [10.1111/jgh.12212](#)]
  - 48 **Jeyapal S**, Putcha UK, Mullapudi VS, Ghosh S, Sakamuri A, Kona SR, Vadakattu SS, Madakasira C, Ibrahim A. Chronic consumption of fructose in combination with trans fatty acids but not with saturated fatty acids induces nonalcoholic steatohepatitis with fibrosis in rats. *Eur J Nutr* 2018; **57**: 2171-2187 [PMID: [28676973](#) DOI: [10.1007/s00394-017-1492-1](#)]
  - 49 **Savard C**, Tartaglione EV, Kuver R, Haigh WG, Farrell GC, Subramanian S, Chait A, Yeh MM, Quinn LS, Ioannou GN. Synergistic interaction of dietary cholesterol and dietary fat in inducing experimental steatohepatitis. *Hepatology* 2013; **57**: 81-92 [PMID: [22508243](#) DOI: [10.1002/hep.25789](#)]
  - 50 **Ter Horst KW**, Serlie MJ. Fructose Consumption, Lipogenesis, and Non-Alcoholic Fatty Liver Disease. *Nutrients* 2017; **9**: pii: E981 [PMID: [28878197](#) DOI: [10.3390/nu9090981](#)]
  - 51 **Alwahsh SM**, Gebhardt R. Dietary fructose as a risk factor for non-alcoholic fatty liver disease (NAFLD). *Arch Toxicol* 2017; **91**: 1545-1563 [PMID: [27995280](#) DOI: [10.1007/s00204-016-1892-7](#)]
  - 52 **Neuschwander-Tetri BA**. Hepatic lipotoxicity and the pathogenesis of nonalcoholic steatohepatitis: the central role of nontriglyceride fatty acid metabolites. *Hepatology* 2010; **52**: 774-788 [PMID: [20683968](#) DOI: [10.1002/hep.23719](#)]
  - 53 **Friedman SL**, Neuschwander-Tetri BA, Rinella M, Sanyal AJ. Mechanisms of NAFLD development and therapeutic strategies. *Nat Med* 2018; **24**: 908-922 [PMID: [29967350](#) DOI: [10.1038/s41591-018-0104-9](#)]
  - 54 **Murata Y**, Konishi M, Itoh N. FGF21 as an Endocrine Regulator in Lipid Metabolism: From Molecular Evolution to Physiology and Pathophysiology. *J Nutr Metab* 2011; **2011**: 981315 [PMID: [21331285](#) DOI: [10.1155/2011/981315](#)]
  - 55 **Adams AC**, Yang C, Coskun T, Cheng CC, Gimeno RE, Luo Y, Kharitonov A. The breadth of FGF21's metabolic actions are governed by FGFR1 in adipose tissue. *Mol Metab* 2012; **2**: 31-37 [PMID: [24024127](#) DOI: [10.1016/j.molmet.2012.08.007](#)]
  - 56 **Bookout AL**, de Groot MH, Owen BM, Lee S, Gautron L, Lawrence HL, Ding X, Elmquist JK, Takahashi JS, Mangelsdorf DJ, Kliewer SA. FGF21 regulates metabolism and circadian behavior by acting on the nervous system. *Nat Med* 2013; **19**: 1147-1152 [PMID: [23933984](#) DOI: [10.1038/nm.3249](#)]
  - 57 **Hui X**, Feng T, Liu Q, Gao Y, Xu A. The FGF21-adiponectin axis in controlling energy and vascular homeostasis. *J Mol Cell Biol* 2016; **8**: 110-119 [PMID: [26993043](#) DOI: [10.1093/jmcb/mjw013](#)]
  - 58 **Lin Z**, Tian H, Lam KS, Lin S, Hoo RC, Konishi M, Itoh N, Wang Y, Bornstein SR, Xu A, Li X.

- Adiponectin mediates the metabolic effects of FGF21 on glucose homeostasis and insulin sensitivity in mice. *Cell Metab* 2013; **17**: 779-789 [PMID: [23663741](#) DOI: [10.1016/j.cmet.2013.04.005](#)]
- 59 **Habegger KM**, Stemmer K, Cheng C, Müller TD, Heppner KM, Ottaway N, Holland J, Hembree JL, Smiley D, Gelfanov V, Krishna R, Arafat AM, Konkar A, Belli S, Kapps M, Woods SC, Hofmann SM, D'Alessio D, Pfluger PT, Perez-Tilve D, Seeley RJ, Konishi M, Itoh N, Kharitonov A, Spranger J, DiMarchi RD, Tschöp MH. Fibroblast growth factor 21 mediates specific glucagon actions. *Diabetes* 2013; **62**: 1453-1463 [PMID: [23305646](#) DOI: [10.2337/db12-1116](#)]
- 60 **Shan Z**, Alvarez-Sola G, Uriarte I, Arechederra M, Fernández-Barrena MG, Berasain C, Ju C, Avila MA. Fibroblast growth factors 19 and 21 in acute liver damage. *Ann Transl Med* 2018; **6**: 257 [PMID: [30069459](#) DOI: [10.21037/atm.2018.05.26](#)]
- 61 **Singhal G**, Kumar G, Chan S, Fisher FM, Ma Y, Vardeh HG, Nasser IA, Flier JS, Maratos-Flier E. Deficiency of fibroblast growth factor 21 (FGF21) promotes hepatocellular carcinoma (HCC) in mice on a long term obesogenic diet. *Mol Metab* 2018; **13**: 56-66 [PMID: [29753678](#) DOI: [10.1016/j.molmet.2018.03.002](#)]
- 62 **Bao L**, Yin J, Gao W, Wang Q, Yao W, Gao X. A long-acting FGF21 alleviates hepatic steatosis and inflammation in a mouse model of non-alcoholic steatohepatitis partly through an FGF21-adiponectin-IL17A pathway. *Br J Pharmacol* 2018; **175**: 3379-3393 [PMID: [29859019](#) DOI: [10.1111/bph.14383](#)]
- 63 **Dushay J**, Chui PC, Gopalakrishnan GS, Varela-Rey M, Crawley M, Fisher FM, Badman MK, Martinez-Chantar ML, Maratos-Flier E. Increased fibroblast growth factor 21 in obesity and nonalcoholic fatty liver disease. *Gastroenterology* 2010; **139**: 456-463 [PMID: [20451522](#) DOI: [10.1053/j.gastro.2010.04.054](#)]
- 64 **Yilmaz Y**, Eren F, Yonal O, Kurt R, Aktas B, Celikel CA, Ozdogan O, Imeryuz N, Kalayci C, Avsar E. Increased serum FGF21 levels in patients with nonalcoholic fatty liver disease. *Eur J Clin Invest* 2010; **40**: 887-892 [PMID: [20624171](#) DOI: [10.1111/j.1365-2362.2010.02338.x](#)]
- 65 **Flisiak-Jackiewicz M**, Bobrus-Chociej A, Wasilewska N, Tarasow E, Wojtkowska M, Lebensztejn DM. Can hepatokines be regarded as novel non-invasive serum biomarkers of intrahepatic lipid content in obese children? *Adv Med Sci* 2019; **64**: 280-284 [PMID: [30921653](#) DOI: [10.1016/j.advms.2019.02.005](#)]
- 66 **Hua MC**, Huang JL, Hu CC, Yao TC, Lai MW. Including Fibroblast Growth Factor-21 in Combined Biomarker Panels Improves Predictions of Liver Steatosis Severity in Children. *Front Pediatr* 2019; **7**: 420 [PMID: [31750276](#) DOI: [10.3389/fped.2019.00420](#)]
- 67 **Praktinjo M**, Djayadi N, Mohr R, Schierwagen R, Bischoff J, Dold L, Pohlmann A, Schwarze-Zander C, Wasmuth JC, Boesecke C, Rockstroh JK, Trebick J. Fibroblast growth factor 21 is independently associated with severe hepatic steatosis in non-obese HIV-infected patients. *Liver Int* 2019; **39**: 1514-1520 [PMID: [30916873](#) DOI: [10.1111/liv.14107](#)]
- 68 **He L**, Deng L, Zhang Q, Guo J, Zhou J, Song W, Yuan F. Diagnostic Value of CK-18, FGF-21, and Related Biomarker Panel in Nonalcoholic Fatty Liver Disease: A Systematic Review and Meta-Analysis. *Biomed Res Int* 2017; **2017**: 9729107 [PMID: [28326329](#) DOI: [10.1155/2017/9729107](#)]
- 69 **Yang M**, Xu D, Liu Y, Guo X, Li W, Guo C, Zhang H, Gao Y, Mao Y, Zhao J. Combined Serum Biomarkers in Non-Invasive Diagnosis of Non-Alcoholic Steatohepatitis. *PLoS One* 2015; **10**: e0131664 [PMID: [26121037](#) DOI: [10.1371/journal.pone.0131664](#)]
- 70 **Nakashima H**, Nakashima M, Kinoshita M, Ikarashi M, Miyazaki H, Hanaka H, Imaki J, Seki S. Activation and increase of radio-sensitive CD11b+ recruited Kupffer cells/macrophages in diet-induced steatohepatitis in FGF5 deficient mice. *Sci Rep* 2016; **6**: 34466 [PMID: [27708340](#) DOI: [10.1038/srep34466](#)]
- 71 **Hanaka H**, Hamada T, Ito M, Nakashima H, Tomita K, Seki S, Kobayashi Y, Imaki J. Fibroblast growth factor-5 participates in the progression of hepatic fibrosis. *Exp Anim* 2014; **63**: 85-92 [PMID: [24521867](#) DOI: [10.1538/expanim.63.85](#)]
- 72 **Uriarte I**, Fernandez-Barrena MG, Monte MJ, Latasa MU, Chang HC, Carotti S, Vespasiani-Gentilucci U, Morini S, Vicente E, Concepcion AR, Medina JF, Marin JJ, Berasain C, Prieto J, Avila MA. Identification of fibroblast growth factor 15 as a novel mediator of liver regeneration and its application in the prevention of post-resection liver failure in mice. *Gut* 2013; **62**: 899-910 [PMID: [23292666](#) DOI: [10.1136/gutjnl-2012-302945](#)]
- 73 **Uriarte I**, Latasa MU, Carotti S, Fernandez-Barrena MG, Garcia-Irigoyen O, Elizalde M, Urtasun R, Vespasiani-Gentilucci U, Morini S, de Mingo A, Mari M, Corrales FJ, Prieto J, Berasain C, Avila MA. Ileal FGF15 contributes to fibrosis-associated hepatocellular carcinoma development. *Int J Cancer* 2015; **136**: 2469-2475 [PMID: [25346390](#) DOI: [10.1002/ijc.29287](#)]
- 74 **Schreuder TC**, Marsman HA, Lenicek M, van Werven JR, Nederveen AJ, Jansen PL, Schaap FG. The hepatic response to FGF19 is impaired in patients with nonalcoholic fatty liver disease and insulin resistance. *Am J Physiol Gastrointest Liver Physiol* 2010; **298**: G440-G445 [PMID: [20093562](#) DOI: [10.1152/ajpgi.00322.2009](#)]
- 75 **Friedrich D**, Marschall HU, Lammert F. Response of fibroblast growth factor 19 and bile acid synthesis after a body weight-adjusted oral fat tolerance test in overweight and obese NAFLD patients: a non-randomized controlled pilot trial. *BMC Gastroenterol* 2018; **18**: 76 [PMID: [29866129](#) DOI: [10.1186/s12876-018-0805-z](#)]
- 76 **Liu WY**, Xie DM, Zhu GQ, Huang GQ, Lin YQ, Wang LR, Shi KQ, Hu B, Braddock M, Chen YP, Zheng MH. Targeting fibroblast growth factor 19 in liver disease: a potential biomarker and therapeutic target. *Expert Opin Ther Targets* 2015; **19**: 675-685 [PMID: [25547779](#) DOI: [10.1517/14728222.2014.997711](#)]
- 77 **Wojcik M**, Janus D, Dolezal-Oltarzewska K, Kalicka-Kasperczyk A, Poplowska K, Drozd D, Sztelfo K, Starzyk JB. A decrease in fasting FGF19 levels is associated with the development of non-alcoholic fatty liver disease in obese adolescents. *J Pediatr Endocrinol Metab* 2012; **25**: 1089-1093 [PMID: [23329754](#) DOI: [10.1515/jpem-2012-0253](#)]
- 78 **Eren F**, Kurt R, Ermiş F, Atug O, Imeryuz N, Yilmaz Y. Preliminary evidence of a reduced serum level of fibroblast growth factor 19 in patients with biopsy-proven nonalcoholic fatty liver disease. *Clin Biochem* 2012; **45**: 655-658 [PMID: [22465275](#) DOI: [10.1016/j.clinbiochem.2012.03.019](#)]
- 79 **Jiao N**, Baker SS, Chapa-Rodriguez A, Liu W, Nugent CA, Tsompana M, Mastrandrea L, Buck MJ, Baker RD, Genco RJ, Zhu R, Zhu L. Suppressed hepatic bile acid signalling despite elevated production of primary and secondary bile acids in NAFLD. *Gut* 2018; **67**: 1881-1891 [PMID: [28774887](#) DOI: [10.1136/gutjnl-2017-314307](#)]
- 80 **Alvarez-Sola G**, Uriarte I, Latasa MU, Fernandez-Barrena MG, Urtasun R, Elizalde M, Barcena-Varela M, Jiménez M, Chang HC, Barbero R, Catalán V, Rodríguez A, Frühbeck G, Gallego-Escuredo JM, Gavalda-Navarro A, Villarroya F, Rodríguez-Ortigosa CM, Corrales FJ, Prieto J, Berraondo P, Berasain C, Avila MA. Fibroblast growth factor 15/19 (FGF15/19) protects from diet-induced hepatic steatosis:



- development of an FGF19-based chimeric molecule to promote fatty liver regeneration. *Gut* 2017; **66**: 1818-1828 [PMID: [28119353](#) DOI: [10.1136/gutjnl-2016-312975](#)]
- 81 **Nobili V**, Alisi A, Mosca A, Della Corte C, Veraldi S, De Vito R, De Stefanis C, D'Oria V, Jahnel J, Zohrer E, Scorletti E, Byrne CD. Hepatic farnesoid X receptor protein level and circulating fibroblast growth factor 19 concentration in children with NAFLD. *Liver Int* 2018; **38**: 342-349 [PMID: [28746779](#) DOI: [10.1111/liv.13531](#)]
  - 82 **Zöhrer E**, Alisi A, Jahnel J, Mosca A, Della Corte C, Crudele A, Fauler G, Nobili V. Efficacy of docosahexaenoic acid-choline-vitamin E in paediatric NASH: a randomized controlled clinical trial. *Appl Physiol Nutr Metab* 2017; **42**: 948-954 [PMID: [28511023](#) DOI: [10.1139/apnm-2016-0689](#)]
  - 83 **Sanyal AJ**, Friedman SL, McCullough AJ, Dimick-Santos L; American Association for the Study of Liver Diseases; United States Food and Drug Administration. Challenges and opportunities in drug and biomarker development for nonalcoholic steatohepatitis: findings and recommendations from an American Association for the Study of Liver Diseases-U.S. Food and Drug Administration Joint Workshop. *Hepatology* 2015; **61**: 1392-1405 [PMID: [25557690](#) DOI: [10.1002/hep.27678](#)]
  - 84 **Younossi ZM**, Loomba R, Rinella ME, Bugianesi E, Marchesini G, Neuschwander-Tetri BA, Serfaty L, Negro F, Caldwell SH, Ratzu V, Corey KE, Friedman SL, Abdelmalek MF, Harrison SA, Sanyal AJ, Lavine JE, Mathurin P, Charlton MR, Chalasani NP, Anstee QM, Kowdley KV, George J, Goodman ZD, Lindor K. Current and future therapeutic regimens for nonalcoholic fatty liver disease and nonalcoholic steatohepatitis. *Hepatology* 2018; **68**: 361-371 [PMID: [29222911](#) DOI: [10.1002/hep.29724](#)]
  - 85 **Luo Y**, Krupinski J, Gao S, Charles E, Christian R. BMS-986036, a PEGylated fibroblast growth factor 21 analogue, reduces fibrosis and Pro-C3 in a mouse model of non-alcoholic steatohepatitis. *J Hepatol* 2018; **68**: S396-S397 [DOI: [10.1016/S0168-8278\(18\)31028-6](#)]
  - 86 **Charles ED**, Neuschwander-Tetri BA, Pablo Frias J, Kundu S, Luo Y, Tiruchera GS, Christian R. Pegbelfermin (BMS-986036), PEGylated FGF21, in Patients with Obesity and Type 2 Diabetes: Results from a Randomized Phase 2 Study. *Obesity (Silver Spring)* 2019; **27**: 41-49 [PMID: [30520566](#) DOI: [10.1002/oby.22344](#)]
  - 87 **Sanyal A**, Charles ED, Neuschwander-Tetri BA, Loomba R, Harrison SA, Abdelmalek MF, Lawitz EJ, Halegoua-DeMarzio D, Kundu S, Noviello S, Luo Y, Christian R. Pegbelfermin (BMS-986036), a PEGylated fibroblast growth factor 21 analogue, in patients with non-alcoholic steatohepatitis: a randomised, double-blind, placebo-controlled, phase 2a trial. *Lancet* 2019; **392**: 2705-2717 [PMID: [30554783](#) DOI: [10.1016/S0140-6736\(18\)31785-9](#)]
  - 88 **Zhou M**, Wang X, Phung V, Lindhout DA, Mondal K, Hsu JY, Yang H, Humphrey M, Ding X, Arora T, Learned RM, DePaoli AM, Tian H, Ling L. Separating Tumorigenicity from Bile Acid Regulatory Activity for Endocrine Hormone FGF19. *Cancer Res* 2014; **74**: 3306-3316 [PMID: [24728076](#) DOI: [10.1158/0008-5472.CAN-14-0208](#)]
  - 89 **Zhou M**, Learned RM, Rossi SJ, DePaoli AM, Tian H, Ling L. Engineered FGF19 eliminates bile acid toxicity and lipotoxicity leading to resolution of steatohepatitis and fibrosis in mice. *Hepatol Commun* 2017; **1**: 1024-1042 [PMID: [29404440](#) DOI: [10.1002/hep4.1108](#)]
  - 90 **Zhou M**, Learned RM, Rossi SJ, DePaoli AM, Tian H, Ling L. Engineered fibroblast growth factor 19 reduces liver injury and resolves sclerosing cholangitis in Mdr2-deficient mice. *Hepatology* 2016; **63**: 914-929 [PMID: [26418580](#) DOI: [10.1002/hep.28257](#)]
  - 91 **Luo J**, Ko B, Elliott M, Zhou M, Lindhout DA, Phung V, To C, Learned RM, Tian H, DePaoli AM, Ling L. A nontumorigenic variant of FGF19 treats cholestatic liver diseases. *Sci Transl Med* 2014; **6**: 247ra100 [PMID: [25080475](#) DOI: [10.1126/scitranslmed.3009098](#)]
  - 92 **Harrison SA**, Rinella ME, Abdelmalek MF, Trotter JF, Paredes AH, Arnold HL, Kugelmas M, Bashir MR, Jaros MJ, Ling L, Rossi SJ, DePaoli AM, Loomba R. NGM282 for treatment of non-alcoholic steatohepatitis: a multicentre, randomised, double-blind, placebo-controlled, phase 2 trial. *Lancet* 2018; **391**: 1174-1185 [PMID: [29519502](#) DOI: [10.1016/S0140-6736\(18\)30474-4](#)]
  - 93 **Harrison SA**, Rossi SJ, Paredes AH, Trotter JF, Bashir MR, Guy CD, Banerjee R, Jaros MJ, Owers S, Baxter BA, Ling L, DePaoli AM. NGM282 Improves Liver Fibrosis and Histology in 12 Weeks in Patients With Nonalcoholic Steatohepatitis. *Hepatology* 2019; Epub ahead of print [PMID: [30805949](#) DOI: [10.1002/hep.30590](#)]
  - 94 **Rinella ME**, Trotter JF, Abdelmalek MF, Paredes AH, Connelly MA, Jaros MJ, Ling L, Rossi SJ, DePaoli AM, Harrison SA. Rosuvastatin improves the FGF19 analogue NGM282-associated lipid changes in patients with non-alcoholic steatohepatitis. *J Hepatol* 2019; **70**: 735-744 [PMID: [30529590](#) DOI: [10.1016/j.jhep.2018.11.032](#)]
  - 95 **Hagel M**, Miduturu C, Sheets M, Rubin N, Weng W, Stransky N, Bifulco N, Kim JL, Hodous B, Brooijmans N, Shutes A, Winter C, Lengauer C, Kohl NE, Guzi T. First Selective Small Molecule Inhibitor of FGFR4 for the Treatment of Hepatocellular Carcinomas with an Activated FGFR4 Signaling Pathway. *Cancer Discov* 2015; **5**: 424-437 [PMID: [25776529](#) DOI: [10.1158/2159-8290.CD-14-1029](#)]
  - 96 **Joshi JJ**, Coffey H, Corcoran E, Tsai J, Huang CL, Ichikawa K, Prajapati S, Hao MH, Bailey S, Wu J, Rimkunas V, Karr C, Subramanian V, Kumar P, MacKenzie C, Hurley R, Satoh T, Yu K, Park E, Rioux N, Kim A, Lai WG, Yu L, Zhu P, Buonamici S, Larsen N, Fekkes P, Wang J, Warmuth M, Reynolds DJ, Smith PG, Selvaraj A. H3B-6527 Is a Potent and Selective Inhibitor of FGFR4 in FGF19-Driven Hepatocellular Carcinoma. *Cancer Res* 2017; **77**: 6999-7013 [PMID: [29247039](#) DOI: [10.1158/0008-5472.CAN-17-1865](#)]
  - 97 **Teng Y**, Zhao H, Gao L, Zhang W, Shull AY, Shay C. FGF19 Protects Hepatocellular Carcinoma Cells against Endoplasmic Reticulum Stress via Activation of FGFR4-GSK3 $\beta$ -Nrf2 Signaling. *Cancer Res* 2017; **77**: 6215-6225 [PMID: [28951455](#) DOI: [10.1158/0008-5472.CAN-17-2039](#)]
  - 98 **Cui G**, Martin RC, Jin H, Liu X, Pandit H, Zhao H, Cai L, Zhang P, Li W, Li Y. Up-regulation of FGF15/19 signaling promotes hepatocellular carcinoma in the background of fatty liver. *J Exp Clin Cancer Res* 2018; **37**: 136 [PMID: [29973237](#) DOI: [10.1186/s13046-018-0781-8](#)]
  - 99 **Li Y**, Zhang W, Doughtie A, Cui G, Li X, Pandit H, Yang Y, Li S, Martin R. Up-regulation of fibroblast growth factor 19 and its receptor associates with progression from fatty liver to hepatocellular carcinoma. *Oncotarget* 2016; **7**: 52329-52339 [PMID: [27447573](#) DOI: [10.18632/oncotarget.10750](#)]
  - 100 **Chen Q**, Jiang Y, An Y, Zhao N, Zhao Y, Yu C. Soluble FGFR4 extracellular domain inhibits FGF19-induced activation of FGFR4 signaling and prevents nonalcoholic fatty liver disease. *Biochem Biophys Res Commun* 2011; **409**: 651-656 [PMID: [21616061](#) DOI: [10.1016/j.bbrc.2011.05.059](#)]
  - 101 **Shankar S**, Bashir MR, Baxter BA, Phung V, Yan AZ, Rossi SJ, DePaoli AM. NGM313, a novel once-monthly activator of bkltho-FGFR1c, significantly reduces hepatic steatosis and key biomarkers of non-alcoholic steatohepatitis: results of a randomized, active-controlled clamp study in obese insulin-resistant

- patients with NAFLD. *Hepatology* 2018; **68**: LB-21 [DOI: [10.1002/hep.30256](https://doi.org/10.1002/hep.30256)]
- 102 **Cheng AL**, Shen YC, Zhu AX. Targeting fibroblast growth factor receptor signaling in hepatocellular carcinoma. *Oncology* 2011; **81**: 372-380 [PMID: [22269894](https://pubmed.ncbi.nlm.nih.gov/22269894/) DOI: [10.1159/000335472](https://doi.org/10.1159/000335472)]
  - 103 **Lee HJ**, Kang HJ, Kim KM, Yu ES, Kim KH, Kim SM, Kim TW, Shim JH, Lim YS, Lee HC, Chung YH, Lee YS. Fibroblast growth factor receptor isotype expression and its association with overall survival in patients with hepatocellular carcinoma. *Clin Mol Hepatol* 2015; **21**: 60-70 [PMID: [25834803](https://pubmed.ncbi.nlm.nih.gov/25834803/) DOI: [10.3350/cmh.2015.21.1.60](https://doi.org/10.3350/cmh.2015.21.1.60)]
  - 104 **Maeda T**, Kanzaki H, Chiba T, Ao J, Kanayama K, Maruta S, Kusakabe Y, Saito T, Kobayashi K, Kiyono S, Nakamura M, Ogasawara S, Suzuki E, Ooka Y, Nakamoto S, Nakagawa R, Muroyama R, Kanda T, Maruyama H, Kato N. Serum fibroblast growth factor 19 serves as a potential novel biomarker for hepatocellular carcinoma. *BMC Cancer* 2019; **19**: 1088 [PMID: [31718608](https://pubmed.ncbi.nlm.nih.gov/31718608/) DOI: [10.1186/s12885-019-6322-9](https://doi.org/10.1186/s12885-019-6322-9)]
  - 105 **Ho HK**, Pok S, Streit S, Ruhe JE, Hart S, Lim KS, Loo HL, Aung MO, Lim SG, Ullrich A. Fibroblast growth factor receptor 4 regulates proliferation, anti-apoptosis and alpha-fetoprotein secretion during hepatocellular carcinoma progression and represents a potential target for therapeutic intervention. *J Hepatol* 2009; **50**: 118-127 [PMID: [19008009](https://pubmed.ncbi.nlm.nih.gov/19008009/) DOI: [10.1016/j.jhep.2008.08.015](https://doi.org/10.1016/j.jhep.2008.08.015)]
  - 106 **French DM**, Lin BC, Wang M, Adams C, Shek T, Hötzel K, Bolon B, Ferrando R, Blackmore C, Schroeder K, Rodriguez LA, Hristopoulos M, Venook R, Ashkenazi A, Desnoyers LR. Targeting FGFR4 inhibits hepatocellular carcinoma in preclinical mouse models. *PLoS One* 2012; **7**: e36713 [PMID: [22615798](https://pubmed.ncbi.nlm.nih.gov/22615798/) DOI: [10.1371/journal.pone.0036713](https://doi.org/10.1371/journal.pone.0036713)]
  - 107 **Heinzel C**, Erdem Z, Paur J, Grasl-Kraupp B, Holzmann K, Grusch M, Berger W, Marian B. Is fibroblast growth factor receptor 4 a suitable target of cancer therapy? *Curr Pharm Des* 2014; **20**: 2881-2898 [PMID: [23944363](https://pubmed.ncbi.nlm.nih.gov/23944363/) DOI: [10.2174/13816128113199990594](https://doi.org/10.2174/13816128113199990594)]
  - 108 **Raja A**, Park I, Haq F, Ahn SM. FGF19-FGFR4 Signaling in Hepatocellular Carcinoma. *Cells* 2019; **8**: pii: E536 [PMID: [31167419](https://pubmed.ncbi.nlm.nih.gov/31167419/) DOI: [10.3390/cells8060536](https://doi.org/10.3390/cells8060536)]
  - 109 **Hoshi T**, Watanabe Miyano S, Watanabe H, Sonobe RMK, Seki Y, Ohta E, Nomoto K, Matsui J, Funahashi Y. Lenvatinib induces death of human hepatocellular carcinoma cells harboring an activated FGF signaling pathway through inhibition of FGFR-MAPK cascades. *Biochem Biophys Res Commun* 2019; **513**: 1-7 [PMID: [30944079](https://pubmed.ncbi.nlm.nih.gov/30944079/) DOI: [10.1016/j.bbrc.2019.02.015](https://doi.org/10.1016/j.bbrc.2019.02.015)]
  - 110 **Jo JC**, Choi EK, Shin JS, Moon JH, Hong SW, Lee HR, Kim SM, Jung SA, Lee DH, Jung SH, Lee SH, Kim JE, Kim KP, Hong YS, Suh YA, Jang SJ, Choi EK, Lee JS, Jin DH, Kim TW. Targeting FGFR Pathway in Human Hepatocellular Carcinoma: Expressing pFGFR and pMET for Antitumor Activity. *Mol Cancer Ther* 2015; **14**: 2613-2622 [PMID: [26351320](https://pubmed.ncbi.nlm.nih.gov/26351320/) DOI: [10.1158/1535-7163.MCT-14-0780](https://doi.org/10.1158/1535-7163.MCT-14-0780)]
  - 111 **Llovet JM**, Ricci S, Mazzaferro V, Hilgard P, Gane E, Blanc JF, de Oliveira AC, Santoro A, Raoul JL, Forner A, Schwartz M, Porta C, Zeuzem S, Bolondi L, Greten TF, Galle PR, Seitz JF, Borbath I, Häussinger D, Giannaris T, Shan M, Moscovici M, Voliotis D, Bruix J; SHARP Investigators Study Group. Sorafenib in advanced hepatocellular carcinoma. *N Engl J Med* 2008; **359**: 378-390 [PMID: [18650514](https://pubmed.ncbi.nlm.nih.gov/18650514/) DOI: [10.1056/NEJMoa0708857](https://doi.org/10.1056/NEJMoa0708857)]
  - 112 **Johnson PJ**, Qin S, Park JW, Poon RT, Raoul JL, Philip PA, Hsu CH, Hu TH, Heo J, Xu J, Lu L, Chao Y, Boucher E, Han KH, Paik SW, Robles-Aviña J, Kudo M, Yan L, Sobhonslidsuk A, Komov D, Decaens T, Tak WY, Jeng LB, Liu D, Ezzeddine R, Walters I, Cheng AL. Brivanib versus sorafenib as first-line therapy in patients with unresectable, advanced hepatocellular carcinoma: results from the randomized phase III BRISK-FL study. *J Clin Oncol* 2013; **31**: 3517-3524 [PMID: [23980084](https://pubmed.ncbi.nlm.nih.gov/23980084/) DOI: [10.1200/JCO.2012.48.4410](https://doi.org/10.1200/JCO.2012.48.4410)]
  - 113 **Ruggeri B**, Stubbs M, Yang Y, Juvekar A, Lu L, Condon S, DiMatteo D, Wen X, Collier P, Burn T, Wu L, Wilson D, Yeleswaram S, Roberts A, Yao W, Hollis G, Huber R, Scherle P, Liu PCC. The novel FGFR4-selective inhibitor INCB062079 is efficacious in models of hepatocellular carcinoma harboring FGF19 amplification. *Cancer Res* 2017; **77**: 1234 [DOI: [10.1158/1538-7445.AM2017-1234](https://doi.org/10.1158/1538-7445.AM2017-1234)]
  - 114 **Kim RD**, Sarker D, Meyer T, Yau T, Macarulla T, Park JW, Choo SP, Hollebecque A, Sung MW, Lim HY, Mazzaferro V, Trojan J, Zhu AX, Yoon JH, Sharma S, Lin ZZ, Chan SL, Faivre S, Feun LG, Yen CJ, Dufour JF, Palmer DH, Llovet JM, Manooogian M, Tugnait M, Stransky N, Hagel M, Kohl NE, Lengauer C, Sherwin CA, Schmidt-Kittler O, Hoeflich KP, Shi H, Wolf BB, Kang YK. First-in-Human Phase I Study of Fisogatinib (BLU-554) Validates Aberrant FGF19 Signaling as a Driver Event in Hepatocellular Carcinoma. *Cancer Discov* 2019; **9**: 1696-1707 [PMID: [31575541](https://pubmed.ncbi.nlm.nih.gov/31575541/) DOI: [10.1158/2159-8290.CD-19-0555](https://doi.org/10.1158/2159-8290.CD-19-0555)]
  - 115 **Schadt HS**, Wolf A, Mahl JA, Wuersch K, Couttet P, Schwald M, Fischer A, Lienard M, Emotte C, Teng CH, Skuba E, Richardson TA, Manenti L, Weiss A, Graus Porta D, Fairhurst RA, Kullak-Ublick GA, Chibout SD, Pognan F, Kluwe W, Kinyamu-Akunda J. Bile Acid Sequestration by Cholestyramine Mitigates FGFR4 Inhibition-Induced ALT Elevation. *Toxicol Sci* 2018; **163**: 265-278 [PMID: [29432567](https://pubmed.ncbi.nlm.nih.gov/29432567/) DOI: [10.1093/toxsci/kfy031](https://doi.org/10.1093/toxsci/kfy031)]
  - 116 **Chan SL**, Schuler M, Lin CC, Choo SP, Weiss K-H, Geier A, Okusaka T, Lim HY, Macarulla T, Zhu AX, Kakizume T, Gu Y, Porta DG, Myers AP, Delord J-P. Ph I/II study of FGF401 in adult pts with HCC or solid tumors characterized by FGFR4/KLB expression. *Cancer Res* 2017; **77**: CT106 [DOI: [10.1158/1538-7445.AM2017-CT106](https://doi.org/10.1158/1538-7445.AM2017-CT106)]

## Basic Study

# ***Bacteroides fragilis* enterotoxin upregulates heme oxygenase-1 in dendritic cells via reactive oxygen species-, mitogen-activated protein kinase-, and Nrf2-dependent pathway**

Su Hyuk Ko, Jong Ik Jeon, Hyun Ae Woo, Jung Mogg Kim

**ORCID number:** Su Hyuk Ko (0000-0002-5008-0083); Jong Ik Jeon (0000-0002-7917-0648); HA Woo (0000-0002-3483-1203); Jung Mogg Kim (0000-0002-6506-7519).

**Author contributions:** Ko SH performed the majority of experiments and analyzed the data; Jeon JI performed the molecular investigations; Woo HA participated equally in treatment of animals; Kim JM designed and coordinated the research; Ko SH and Kim JM wrote the manuscript; all authors approved the final version of the article.

**Supported by** the Basic Science Research Program through the National Research Foundation of Korea funded by the Ministry of Education, Science and Technology, South Korea, No. NRF-2018R1D1A1B07043350.

**Institutional animal care and use committee statement:** All animal experiments were performed according to protocols approved by the Institutional Animal Care and Use Committee of Hanyang University and Ewha Womans University (IACUC No. 2013-0197A and IACUC No. 17-012).

**Conflict-of-interest statement:** None of the authors of this study has any conflicts of interest.

**Data sharing statement:** No additional data are available.

**ARRIVE guidelines statement:** The authors have read the ARRIVE

**Su Hyuk Ko, Jong Ik Jeon, Jung Mogg Kim,** Department of Microbiology and Department of Biomedical Science, Hanyang University College of Medicine and Graduate School of Biomedical Science and Engineering, Seoul 04763, South Korea

**Hyun Ae Woo,** Graduate School of Pharmaceutical Sciences, Ewha Womans University, Seoul 03760, South Korea

**Corresponding author:** Jung Mogg Kim, MD, PhD, Chairman, Director, Doctor, Professor, Department of Microbiology, Hanyang University College of Medicine, 222 Wangsimni-ro, Seongdong-gu, Seoul 04763, South Korea. [jungmogg@hanyang.ac.kr](mailto:jungmogg@hanyang.ac.kr)

## Abstract

### BACKGROUND

Enterotoxigenic *Bacteroides fragilis* (ETBF) causes colitis and diarrhea, and is considered a candidate pathogen in inflammatory bowel diseases as well as colorectal cancers. These diseases are dependent on ETBF-secreted toxin (BFT). Dendritic cells (DCs) play an important role in directing the nature of adaptive immune responses to bacterial infection and heme oxygenase-1 (HO-1) is involved in the regulation of DC function.

### AIM

To investigate the role of BFT in HO-1 expression in DCs.

### METHODS

Murine DCs were generated from specific pathogen-free C57BL/6 and Nrf2<sup>-/-</sup> knockout mice. DCs were exposed to BFT, after which HO-1 expression and the related signaling factor activation were measured by quantitative RT-PCR, EMSA, fluorescent microscopy, immunoblot, and ELISA.

### RESULTS

HO-1 expression was upregulated in DCs stimulated with BFT. Although BFT activated transcription factors such as NF-κB, AP-1, and Nrf2, activation of NF-κB and AP-1 was not involved in the induction of HO-1 expression in BFT-exposed DCs. Instead, upregulation of HO-1 expression was dependent on Nrf2 activation in DCs. Moreover, HO-1 expression via Nrf2 in DCs was regulated by mitogen-activated protein kinases such as ERK and p38. Furthermore, BFT enhanced the production of reactive oxygen species (ROS) and inhibition of ROS production resulted in a significant decrease of phospho-ERK, phospho-p38, Nrf2, and HO-1

guidelines, and the manuscript was prepared and revised according to the ARRIVE guidelines.

**Open-Access:** This article is an open-access article that was selected by an in-house editor and fully peer-reviewed by external reviewers. It is distributed in accordance with the Creative Commons Attribution NonCommercial (CC BY-NC 4.0) license, which permits others to distribute, remix, adapt, build upon this work non-commercially, and license their derivative works on different terms, provided the original work is properly cited and the use is non-commercial. See: <http://creativecommons.org/licenses/by-nc/4.0/>

**Manuscript source:** Invited Manuscript

**Received:** October 28, 2019

**Peer-review started:** October 28, 2019

**First decision:** December 12, 2019

**Revised:** December 20, 2019

**Accepted:** January 11, 2020

**Article in press:** January 11, 2020

**Published online:** January 21, 2020

**P-Reviewer:** Sorio C

**S-Editor:** Gong ZM

**L-Editor:** A

**E-Editor:** Ma YJ



expression.

## CONCLUSION

These results suggest that signaling pathways involving ROS-mediated ERK and p38 mitogen-activated protein kinases-Nrf2 activation in DCs are required for HO-1 induction during exposure to ETBF-produced BFT.

**Key words:** *Bacteroides fragilis* enterotoxin; Dendritic cells; Heme oxygenase-1; Mitogen-activated protein kinases; Nrf2; Signaling

©The Author(s) 2020. Published by Baishideng Publishing Group Inc. All rights reserved.

**Core tip:** Enterotoxigenic *Bacteroides fragilis* is associated with non-invasive diarrheal diseases, inflammatory bowel diseases, and colorectal cancers. *Bacteroides fragilis* enterotoxin (BFT) is responsible for these diseases. The present study demonstrated that signaling pathways involving reactive oxygen species-mediated ERK, p38 mitogen-activated protein kinases and Nrf2 activation in dendritic cells are required for heme oxygenase-1 (HO-1) induction during exposure to BFT. This signaling pathway is different from our previous report that BFT upregulates HO-1 in intestinal epithelial cells via a p38 mitogen-activated protein kinases- and NF-κB-dependent pathway. Therefore, this is the first report concerning the effects of BFT on the HO-1 induction pathway in dendritic cells.

**Citation:** Ko SH, Jeon JI, Woo HA, Kim JM. *Bacteroides fragilis* enterotoxin upregulates heme oxygenase-1 in dendritic cells via reactive oxygen species-, mitogen-activated protein kinase-, and Nrf2-dependent pathway. *World J Gastroenterol* 2020; 26(3): 291-306

**URL:** <https://www.wjgnet.com/1007-9327/full/v26/i3/291.htm>

**DOI:** <https://dx.doi.org/10.3748/wjg.v26.i3.291>

## INTRODUCTION

Enterotoxigenic *Bacteroides fragilis* (ETBF) not only causes colitis and diarrhea but is also implicated in inflammatory bowel diseases and colorectal cancer<sup>[1-3]</sup>. ETBF secrete a single unique virulence factor called ETBF enterotoxin (*B. fragilis* toxin; BFT) that causes those diseases<sup>[1-3]</sup>. The secreted BFT first contacts the intestinal epithelial cells. Since BFT is a metalloprotease, it can destroy the tight junctions in the intestinal epithelium by cleaving E-cadherin, resulting in loss of tight junctions<sup>[3-5]</sup>. Therefore, after passing through the destroyed area of the intestinal epithelial barrier, BFT may be in direct contact with immune cells distributed in the lamina propria of the gut.

Among immune cells present in the lamina propria, dendritic cells (DCs) play an important role in mucosal immune responses to bacterial pathogens. In addition to antigen uptake through the above methods, luminal bacterial antigens such as virulence factors can enter into the mucosal tissue when lamina propria DCs extend their dendrites into the lumen<sup>[6,7]</sup>. Therefore, secreted BFT may contact DCs distributed within the intestinal mucosa. Although BFT has been reported not to directly induce maturation in bone marrow (BM)-derived DCs<sup>[8]</sup>, it is presumed that cellular responses may occur after DCs contact BFT. Nevertheless, little is known about BFT-induced DC responses.

Heme oxygenase-1 (HO-1) is an inducible enzyme that catalyzes the degradation of free heme into carbon monoxide, biliverdin, and free iron<sup>[9-11]</sup>. HO-1 plays a major protective role in various disease models through anti-inflammatory actions<sup>[12-14]</sup>. In addition, HO-1 has been associated with DC function regulation. For example, the upregulation of HO-1 endues DCs with more potent and durable immunoregulatory properties<sup>[15]</sup>. In addition, the upregulation of HO-1 in murine Kupffer cells inhibits DC migration *in vitro*<sup>[16]</sup>. HO-1-expressing DCs also promote the differentiation of Foxp3<sup>+</sup> regulatory T cells and then induce less severe airway inflammation in murine models<sup>[17]</sup>. We previously demonstrated that BFT upregulates HO-1 expression in intestinal epithelial cells, which may play a role in protection from apoptotic cell death<sup>[12]</sup>. However, there are no reports regarding BFT-induced HO-1 expression in DCs.

Several studies have demonstrated that HO-1 expression is regulated via signaling



pathways from transcription factors, including nuclear factor-kappaB (NF- $\kappa$ B), activator protein-1 (AP-1), and NF-E2-related factor 2 (Nrf2)<sup>[9,11,12]</sup>. Although BFT can activate such transcription factor signaling in intestinal epithelial cells<sup>[12]</sup>, there is no evidence that signals associated with BFT-induced transcription factors are related to HO-1 induction in DCs. In the studies reported here, we investigated HO-1 induction in response to stimulation of DCs with BFT and found that signaling pathways involving reactive oxygen species (ROS)-mediated mitogen-activated protein kinases (MAPKs)-Nrf2 in DCs are required for HO-1 induction following exposure to BFT.

## MATERIALS AND METHODS

### Reagents

GIBCO BRL (Gaithersburg, MD, USA) supplied Ca<sup>2+</sup> and Mg<sup>2+</sup>-free Hank's balanced salt solution (HBSS), antibiotics, L-glutamine, and Trizol. LPS-free fetal bovine serum (FBS) was purchased from American Type Culture Collection (ATCC, Manassas, VA, United States). RPMI 1640 media, DMEM media, N-Acetyl-L-cysteine (NAC), sodium pyruvate, non-essential amino acids, collagenase Xla, dispase, bovine serum albumin (BSA), and soybean trypsin inhibitor were obtained from Sigma Chemical Co. (St. Louis, MO, United States). Rabbit monoclonal antibodies (mAbs) against phospho-I $\kappa$ B $\alpha$  and phospho-IKK $\alpha$ / $\beta$ , and rabbit polyclonal Abs against phospho-c-jun, phospho-p65, phospho-ERK1/2, phospho-Elk1, pan-extracellular signal-regulated kinase 1/2 (ERK1/2), phospho-p38, pan-p38, phospho-JNK, pan-JNK, and were acquired from Cell Signaling Technology, Inc. (Beverly, MA, United States). Rabbit polyclonal Ab against phospho-Nrf2 was gained from Bioss Antibodies Inc. (Woburn, MA, United States). Santa Cruz Biotechnology (Santa Cruz, CA, United States) supported rabbit polyclonal Abs against Nrf2 and HO-1, and mouse mAbs against actin and lamin B, and goat anti-mouse and anti-rabbit secondary Abs conjugated to horseradish peroxidase. Thermo Fisher Scientific (Waltham, MA, United States) and AbCAM (Cambridge, MA, United States) supplied Alexa Fluor 488 and DyLight 549 secondary Abs, respectively. Chemical inhibitors such as PD98059, SP600125, SB203580, and Bay 11-7085 were acquired from Calbiochem (La Jolla, CA, United States). Tocris Bioscience (Bristol, United Kingdom) supported SR11302. Murine recombinant IL-4 and GM-CSF were gained from PeproTech (Rocky Hill, NJ, United States).

### Purification of BFT and cell culture conditions

BFT was purified from culture supernatants of a toxigenic strain of ETBF (ATCC 43858) as described previously<sup>[18-20]</sup>. An immature murine DC cell line DC2.4 cells was cultured in RPMI 1640 supplemented with 10% FBS, 1% antibiotics, L-glutamine (2 mmol/L), sodium pyruvate (1 mmol/L) and non-essential amino acids (2 mmol/L). These cells were grown at 37°C with 5% CO<sub>2</sub> as previously described<sup>[9,21]</sup>.

### Generation of primary murine bone marrow-derived DCs and colonic epithelial cells

All animal experiments were approved from the Institutional Animal Care and Use Committee of Hanyang University and Ewha Womans University. Specific pathogen-free C57BL/6 and breeding pairs of Nrf2<sup>-/-</sup> knockout mice were obtained from Orient Experimental Animals (Seoungnam, South Korea) and RIKEN BioResource Center (Tsukuba, Japan)<sup>[22]</sup>, respectively. Generation of primary murine bone marrow (BM)-derived DCs was performed as previously described<sup>[9]</sup>. Briefly, femurs, and tibias of male mice (8-12 wk of age, body mass of 20-25 g) were harvested and cells were then cultured in RPMI 1640 media supplemented with 10% FBS, 1% antibiotics, L-glutamine (2 mmol/L), 2-mercaptoethanol (55  $\mu$ mol/L), murine recombinant GM-CSF (10 ng/mL), and murine recombinant IL-4 (10 ng/mL). After six days in culture, DCs were harvested and stimulated with BFT<sup>[9]</sup>. The purity of CD11c<sup>+</sup> cells was greater than 95% as determined by flow cytometric analysis.

Primary murine colonic epithelial cells were also isolated as described previously<sup>[12]</sup>. Briefly, intestines were cut into 1-mm fragments and treated with HBSS containing an enzyme solution [dispase (0.02 mg/mL), collagenase Xla (60 units/mL), soybean trypsin inhibitor (0.2 mg/mL), and BSA (2%)]. Cells were suspended in DMEM containing FBS (10%) with antibiotics, plated on mouse fibronectin-coated dishes, and incubated in 5% CO<sub>2</sub> at 37 °C. Cells were then cultivated in medium containing equal volumes of DMEM and Ham's 12 medium supplemented with FBS (10%) and antibiotics<sup>[12]</sup>. At least 90% of primary colonic epithelial cells were viable for 2 wk in culture as determined by trypan blue exclusion. This procedure was supported by Dr. Sang Hoon Lee of the University of California, Los Angeles, CA<sup>[12,23]</sup>.

### Quantitative reverse transcriptase-PCR

Total RNA was extracted from BFT-treated cells using Trizol. Reverse transcription and PCR amplification were performed as described previously<sup>[12]</sup>. The primers and expected PCR product sizes were as follows: mouse HO-1, 5'-AAG AGG CTA AGA CCG CCT TC-3' (sense), 5'-GTC GTG GTC AGT CAA CAT GG-3' (antisense), 591 bp [NM\_010442.2 *Mus musculus* heme oxygenase (decycling) 1 (Hmox1), mRNA]<sup>[24]</sup>; mouse  $\beta$ -actin, 5'-GTG GGC CGC TCT AGG CAC CAA-3' (sense) and 5'-CTC TTT GAT GTC ACG CAC GAT TTC-3' (antisense), 540 bp [NM\_007393.4 *Mus musculus* actin, beta (Actb), mRNA]<sup>[25]</sup>. For quantifying mRNA molecules, reverse transcription and PCR amplification were performed as described previously<sup>[12]</sup>. The sizes of PCR products generated from standard RNAs for mouse HO-1 and  $\beta$ -actin are 478 bp and 746 bp, respectively<sup>[12]</sup>.

### **Electrophoretic mobility shift assays**

Cells were harvested and nuclear extracts were prepared as described previously<sup>[9,26]</sup>. The concentration of protein in extracts was determined using a Bradford assay (Bio-Rad, Hercules, CA, United States). Electrophoretic mobility shift assays were performed according to the manufacturer's instructions (Promega, Madison, WI, United States)<sup>[9]</sup>. In brief, 5  $\mu$ g of nuclear extract was incubated for 30 min at room temperature with  $\gamma^{32}$ P-labeled oligonucleotide probes (5'-AGT TGA GGG GAC TTT CCC AGG C-3' for the NF- $\kappa$ B binding site; 5'-CGC TTG ATG ACT CAG CCG GAA-3' for the AP-1 binding site; 5'-TGG GGA ACC TGT GCT GAG TCA CTG GAG-3' for the Nrf2 binding site). Oligonucleotide probes for the NF- $\kappa$ B- and AP-1-binding assays were purchased from Promega. Santa Cruz Biotechnology supplied Nrf2 oligonucleotides. Nrf2 supershift and competition assay were performed as previously described<sup>[9,12]</sup>.

### **Transfection assay**

For suppression of NF- $\kappa$ B, AP-1, Nrf2, or MAPK signals, lentiviral systems containing mammalian expression vectors were used as previously described<sup>[9,12]</sup>. Transfection assays using lentiviral systems were performed according to the manufacturer's instructions, as described previously<sup>[9,12]</sup>. Small interfering RNA (siRNA) against the NF- $\kappa$ B p65 subunit and c-jun, and negative (non-silencing) siRNA control (NS-RNA) were obtained (Qiagen, Valencia, CA, United States) as described previously<sup>[9,12]</sup>. Briefly, cells were cultured in 6-well plates to 50%-80% confluence and then transfected with siRNA using Fugene 6 (Roche, Mannheim, Germany) as a transfection reagent, as described previously<sup>[9,12]</sup>. Transfected cells were incubated for 48 h before the assay.

### **Immunoblots, ELISA, and cellular ROS assay**

For immunoblot, cells were washed with ice-cold PBS and lysed in 0.5 mL/well lysis buffer (150 mmol/L NaCl, 20 mmol/L Tris pH 7.5, 0.1% Triton X-100, 1 mmol/L PMSF, and 10  $\mu$ g/mL aprotinin). Fifteen to 50  $\mu$ g of protein per lane was size-fractionated on a polyacrylamide minigel (Mini-PROTEIN II, Bio-Rad) and electrophoretically transferred to a nitrocellulose membrane (0.1- $\mu$ m pore size). Immunoreactive proteins to which primary Abs bound were visualized using goat anti-rabbit or anti-mouse secondary Abs conjugated to horseradish peroxidase, followed by enhanced chemiluminescence (ECL system; Amersham Life Science, Buckinghamshire, United Kingdom) and exposure to X-ray film<sup>[9,12]</sup>.

The level of HO-1 proteins was measured using a commercially available kit (R&D Systems, Inc., Minneapolis, MN, United States). An ELISA kit of the TransAM Nrf2 (Active Motif, Carlsbad, CA, United States) was also used<sup>[9,25]</sup>. For detecting expression of phospho-Elk1, a p44/42 MAP kinase assay kit (Cell Signaling Technology) was used<sup>[12]</sup>. Briefly, immobilized phospho-p44/42 MAPK (Thr202/Tyr204) mAb was used to immunoprecipitate active p44/42 MAPK from cell extracts, after which an *in vitro* kinase assay was performed using Elk-1 protein as a substrate. Elk-1 phosphorylation was then detected by Western blotting using phospho-Elk-1 (Ser383) Ab. Each assay was performed according to each manufacturer's instructions.

The level of intracellular ROS was determined using a commercially available kit (Thermo Fisher Scientific). Briefly, BFT-exposed cells were washed with PBS and were then incubated with 5  $\mu$ mol/L CellROX<sup>®</sup> Reagent (Thermo Fisher Scientific) at 37 °C for 30 min. Fluorescence was measured using a Varioskan Flash spectral scanning multimode reader (Thermo Fisher Scientific). The assay was performed according to the manufacturer's protocol.

### **Immunofluorescence assay for detecting intracellular HO-1 and Nrf2**

Immunofluorescence assay was performed, as described previously<sup>[9,12,19]</sup>. Briefly, cells were cultured ( $5 \times 10^4$  cells in 0.2 mL of RPMI 1640/well) in microslides coated with poly-D-lysine (Santa Cruz). After stimulation with BFT for the indicated period, cells

were treated with goat anti-HO-1 and rabbit anti-phospho-Nrf2 Abs as primary Abs for 2 h. Cells were then treated with Alexa fluor 488-conjugated secondary Ab (green color) against goat IgG and DyLight 549-conjugated secondary Ab (red color) against rabbit IgG for 1 h. Images were captured using a fluorescence microscope (DMI4000B, Leica Microsystems GmbH, Wetzlar, Germany)<sup>[9,12,19]</sup>.

### Statistical analysis

Data from quantitative RT-PCR assays are presented as mean  $\pm$  SD and data from ELISA and ROS assay are presented as mean  $\pm$  SE. Mann-Whitney *t*-test was used for statistical analysis. *P* values < 0.05 were considered statistically significant.

## RESULTS

### BFT induces HO-1 upregulation in DCs

BFT enhanced HO-1 mRNA expression in murine BMDCs (Figure 1A). Significant increases in HO-1 mRNA expression in DC were first noted 9 h after stimulation with BFT, the expression continued to increase for 24 h before decreasing thereafter. Since BFT was known to upregulate HO-1 expression in intestinal epithelial cells<sup>[12]</sup>, we observed differences in the kinetics of HO-1 mRNA expression between DCs and intestinal epithelial cells. As shown in Figure 1B, compared with DCs, primary murine intestinal epithelial cells showed early expression of HO-1 mRNA, with peak expression approximately 6 h post-stimulation that decreased to baseline level at 24 h post-stimulation. These results suggest that the kinetics of HO-1 mRNA expression in DCs differs from that of intestinal epithelial cells. To determine whether increased levels of mRNA transcripts were parallel with protein expression, we performed immunoblot analyses. As shown in Figure 1C, BFT increased the expression of HO-1 proteins in BMDCs (top panel). Similar results were obtained in the murine DC cell line DC2.4 when stimulated with BFT (Figure 1C, middle panel). In contrast to DCs, primary murine intestinal epithelial cells first noted upregulated expression HO-1 proteins 3 h after stimulation with BFT (Figure 1C, bottom panel). In the present study, we used 100 ng/mL of BFT after previously establishing that the EC<sub>50</sub> of BFT was 99.8 ng/mL for expression of HO-1<sup>[12]</sup>.

### Activation of NF- $\kappa$ B and AP-1 is not involved in the induction of HO-1 in BFT-exposed DCs

Since there is no evidence for BFT-induced activation of NF- $\kappa$ B and AP-1 signaling in DCs, we first examined whether BFT stimulation could activate NF- $\kappa$ B and AP-1 signaling in DCs. As shown in Figure 2A, treatment of BM-derived DCs with BFT increased NF- $\kappa$ B DNA binding, as assessed by EMSA. In addition, enhanced expression of phosphorylated I $\kappa$ B $\alpha$  was observed in BFT-treated DCs. Similar results were also observed in DC 2.4 cells exposed to BFT (Figure 2B). Based on these results, we determined whether BFT-induced activation of NF- $\kappa$ B signal was related to HO-1 expression in DCs. For these experiments, we used DC2.4 cells transfected with lentivirus-I $\kappa$ B $\alpha$ -AA. As shown in Figure 2C, transfection with lentivirus-I $\kappa$ B $\alpha$ -AA suppressed NF- $\kappa$ B activity to the control level under BFT-treated condition (Figure 2C, top panel). In this experimental system, HO-1 expression induced by stimulation with BFT did not differ between untransfected and transfected cells (Figure 2C, bottom panel). Consistent with these results, transfection with lentivirus-I $\kappa$ B $\alpha$ -AA did not significantly alter HO-1 mRNA expression in DC2.4 cells under BFT exposure (Figure 2D). To confirm these results, another experiment using p65 siRNA was performed to inhibit NF- $\kappa$ B activity. As shown in Figure 2E, BFT-induced nuclear phospho-p65 protein expression was reduced in p65 siRNA-transfected cells compared with untransfected cells (Figure 2E, top panel). In contrast, no difference of BFT-induced HO-1 expression was observed between cells with p65 siRNA transfection and cells without transfection (Figure 2E, bottom panel).

BFT can activate AP-1 signaling in DCs. As shown in Figure 3, stimulation of DCs with BFT increased AP-1-DNA binding activity in murine BMDCs (Figure 3A) and DC2.4 cells (Figure 3B), as shown by EMSA. Concurrently, increased expression of phosphorylated c-jun was observed in BFT-treated murine BMDCs and DC2.4 cells. The effects of transfection with lentivirus-dn-c-jun on HO-1 expression in BFT-stimulated DC2.4 cells were assessed next. As shown in Figure 3C, transfection with lentivirus-dn-c-jun suppressed AP-1 activity to control levels in DC2.4 cells stimulated with BFT (top panel). Consistent with this, expression of nuclear phospho-c-jun was reduced in lentivirus-dn-c-jun-transfected cells compared with untransfected cells (Figure 3C, middle panel), while transfection with lentivirus-dn-c-jun did not change the BFT-induced HO-1 expression (Figure 3C, bottom panel). In addition, lentivirus-

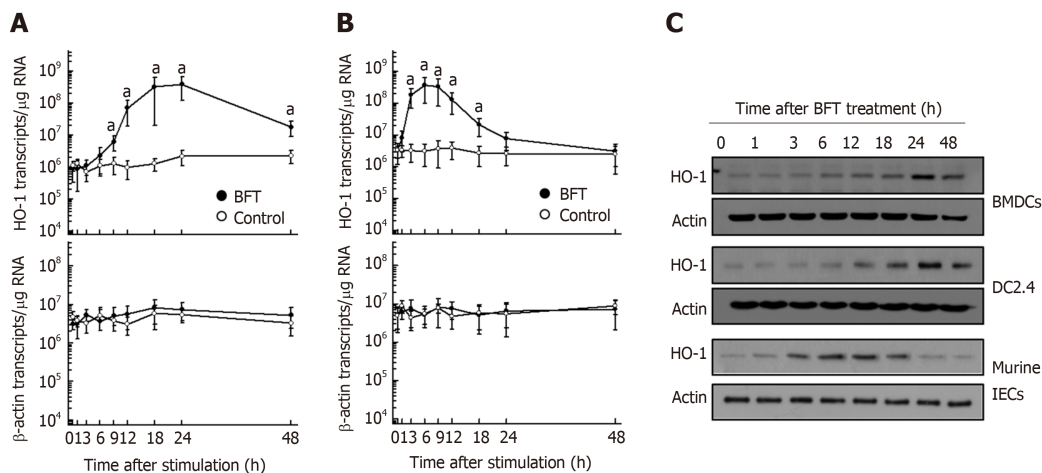


**Figure 1** Heme oxygenase-1 expression in dendritic cells stimulated with *Bacteroides fragilis* enterotoxin. A and B: Bone marrow-derived dendritic cells (DCs) (A, BMDCs) or primary murine intestinal epithelial cells (B, Murine intestinal epithelial cells, IECs) were stimulated with *Bacteroides fragilis* toxin (BFT) (100 ng/mL) for the indicated periods. Levels of heme oxygenase-1 (HO-1) and  $\beta$ -actin mRNAs were analyzed by quantitative RT-PCR using each standard RNA. The values are expressed as mean  $\pm$  SD ( $n = 5$ ).  $^aP < 0.05$  vs unstimulated controls. C: BMDCs, DC2.4 cells and murine IECs were treated with BFT (100 ng/mL) for the indicated periods. Expression of HO-1 and actin was analyzed by immunoblot. Results are representative of more than three independent experiments. IECs: Intestinal epithelial cells; HO-1: Heme oxygenase-1; BFT: *Bacteroides fragilis* toxin.

dn-c-jun-transfected cells did not significantly alter HO-1 mRNA expression compared with untransfected cells under BTT-exposed condition (Figure 3D). In another experiment, we used c-jun siRNA to suppress AP-1 activity. As shown in Figure 3E, c-jun siRNA almost completely suppressed the expression of nuclear phospho-c-jun in DC2.4 cells (top panel). However, no change was observed in BFT-induced HO-1 protein expression between AP-1-suppressed and unsuppressed cells (Figure 3E, bottom panel).

To confirm these results, BM-derived DCs were preincubated with NF- $\kappa$ B inhibitor Bay 11-7082 or AP-1 inhibitor SR11302 for 30 min, and BFT was then added to the culture system. As shown in Figure 4A, there was no significant difference between the group treated with Bay 11-7082 + BFT and the group treated with BFT alone. A similar result was observed between the group treated with SR11302 + BFT and the group treated with BFT alone. Consistent with these findings, no significant changes in BFT-induced HO-1 expression in BM-derived DCs were observed between the three groups consisting of combined treatment with Bay 11-7082 and BFT, combined treatment with SR11302 and BFT, and BFT treatment alone (Figure 3B).

#### Activation of Nrf2 is required to upregulate HO-1 expression in BFT-exposed DCs

Since there was no evidence for BFT-induced activation of Nrf2 signaling in DCs, we first examined whether BFT stimulation could activate Nrf2 signals in DCs. As shown in Figure 5A, BFT enhanced DNA-binding activity of Nrf2 in murine BM-derived DCs. Similar results were found in BFT-exposed DC2.4 cells (Figure 5B). To confirm the specificity of Nrf2-DNA binding, two assays, including a competition assay using cold Nrf2 and an inhibition assay using anti-Nrf2 Ab, were performed. In the first experiment, the addition of excess Nrf2 oligomer (cold Nrf2) markedly decreased Nrf2-DNA binding in comparison to no addition of Nrf2 oligomer (hot Nrf2) under BFT-exposed condition (Figure 5C). In the second experiment, treatment with anti-Nrf2 Ab definitely inhibited Nrf2-DNA binding in nuclear extracts from BM-derived DCs, as assessed by supershift assay (Figure 5D).

Based on these results, we next evaluated whether BFT-induced HO-1 expression was related to Nrf2 activation. For these experiments, DC2.4 cells transfected with lentivirus containing Nrf2 shRNA were used. Transfection with Nrf2 shRNA decreased BFT-induced activity of Nrf2-DNA binding in DC2.4 cells (Figure 5E, top panel). In this experimental system, enhanced expression of HO-1 protein in BFT-treated DC2.4 cells were reduced with transfection of Nrf2 shRNA compared with no transfection (Figure 5E, bottom panel). Consistent with this, transfection with Nrf2 shRNA significantly inhibited HO-1 mRNA expression in BFT-stimulated DC2.4 cells compared with no transfection (Figure 5F). An additional experiment using immunofluorescent microscopy showed that phospho-Nrf2 and HO-1 signals increased in BFT-exposed DC2.4 cells, while Nrf2 shRNA reduced the extent of phospho-Nrf2 and HO-1 signals (Figure 6A). To confirm these results, BM-derived DCs obtained from Nrf2<sup>-/-</sup> knockout mice were used. As shown in Figure 6B, there



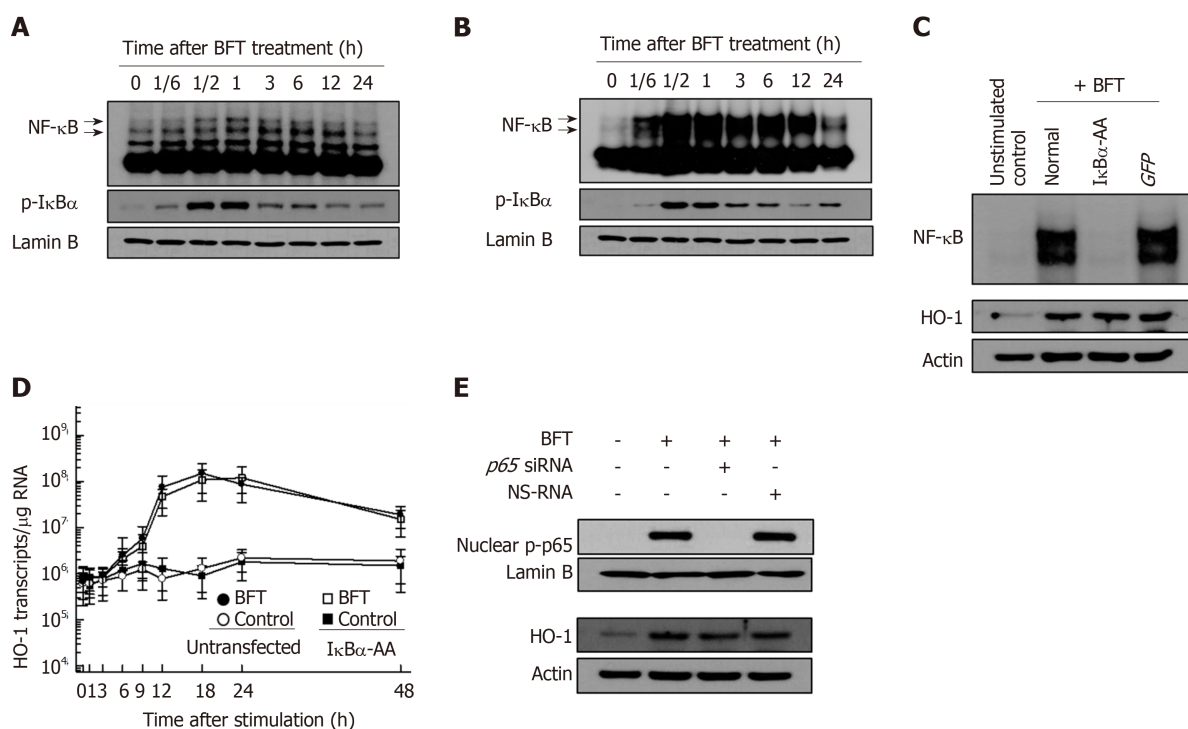


**Figure 2** Effects of NF-κB suppression on heme oxygenase-1 expression in dendritic cells treated with *Bacteroides fragilis* enterotoxin. A and B: Bone marrow-derived dendritic cells (DCs) (A) and DC2.4 cells (B) were treated with BFT (100 ng/mL) for the indicated times. NF-κB DNA binding activity was assessed by EMSA. Immunoblot results for concurrent phospho-IκBα and lamin B in nuclear extracts under the same conditions are provided beneath the EMSA. C: DC2.4 cells were transfected with either lentivirus containing IκBα-superrepressor (IκBα-AA) or control virus (GFP). Transfected cells were stimulated with BFT (100 ng/mL) for 1 h. NF-κB binding activity was assayed by EMSA (top panel). Transfected or untransfected cells were treated with BFT (100 μg/mL) for 12 h. Expression of heme oxygenase-1 (HO-1) and actin was analyzed by immunoblot (bottom panel). Results are representative of more than three independent experiments. D: Transfected DC2.4 cells were treated with BFT (100 ng/mL) for the indicated periods. The levels of HO-1 mRNA were analyzed by quantitative RT-PCR using a standard RNA. The values are expressed as mean ± SD ( $n = 5$ ). The β-actin mRNA levels in each group remained relatively constant throughout the same periods (approximately 10<sup>6</sup> transcripts/μg total RNA). \* $P < 0.05$  vs untransfected cells treated with BFT. E: DC2.4 cells were transfected with NF-κB p65-specific silencing siRNA or NS-RNA as a control for 48 h, after which cells were combined with BFT (100 ng/mL) for 1 h. Nuclear extracts were analyzed by immunoblotting with the indicated Abs (top panel). Transfected cells were stimulated with BFT (100 ng/mL) for 24 h. Expression of HO-1 and actin was analyzed by immunoblot (bottom panel). Results shown are representative of more than three independent experiments. HO-1: Heme oxygenase-1; BFT: *Bacteroides fragilis* toxin.

was a significant difference in HO-1 expression between DCs from wild-type mice and those derived from Nrf2<sup>-/-</sup> knockout mice.

### MAPKs are associated with HO-1 induction in BFT-exposed DCs

We further evaluated whether MAPK signaling could be associated with Nrf2 and HO-1 expression in DCs. As shown in Figure 7A, BFT increased phosphorylated signals of MAPKs, including phospho-ERK1/2, phospho-p38, and phospho-JNK, in BM-derived DCs. Similar results were observed in DC2.4 cells (Figure 7B). We next examined whether inhibition of MAPK activity could influence expression of HO-1 in BFT-exposed DCs. As shown in Figure 7C, pretreatment of BM-derived DCs with PD98059 ( $\geq 10$  μmol/L), SB203580 ( $\geq 10$  μmol/L), or SP600125 ( $\geq 50$  μmol/L) significantly inhibited BFT-induced expression of HO-1.

To confirm these results, lentiviral systems containing dominant-negative plasmids were used. Phosphorylation of each MAPK protein was markedly suppressed in DC2.4 cells transfected with lentiviruses containing each dominant-negative plasmid (Figure 8A). Transfection with lentivirus-dn-Erk2 and lentivirus-dn-p38 significantly decreased BFT-induced Nrf2 activation, as assessed by EMSA (Figure 8B). In these experimental systems, cells transfected with lentivirus-dn-Erk2 and lenti-dn-p38 reduced the expression of HO-1 compared with untransfected cells under BFT-treated conditions (Figure 8C). Moreover, lentivirus-dn-Erk2 and lentivirus-dn-p38 significantly inhibited the activities of both phosphorylated Nrf2 and HO-1 in BFT-stimulated cells (Figure 8D and 8E). These results suggest that exposure of DCs to BFT activates a signaling cascade involving ERK and p38 MAPKs, leading to Nrf2 activation and finally to HO-1 induction.

### HO-1 induction is dependent on ROS generation in BFT-exposed DCs

Although BFT is reported to induce the generation of ROS in T84 intestinal epithelial cells<sup>[27]</sup>, there are no reports regarding BFT-induced ROS generation in DCs. In the

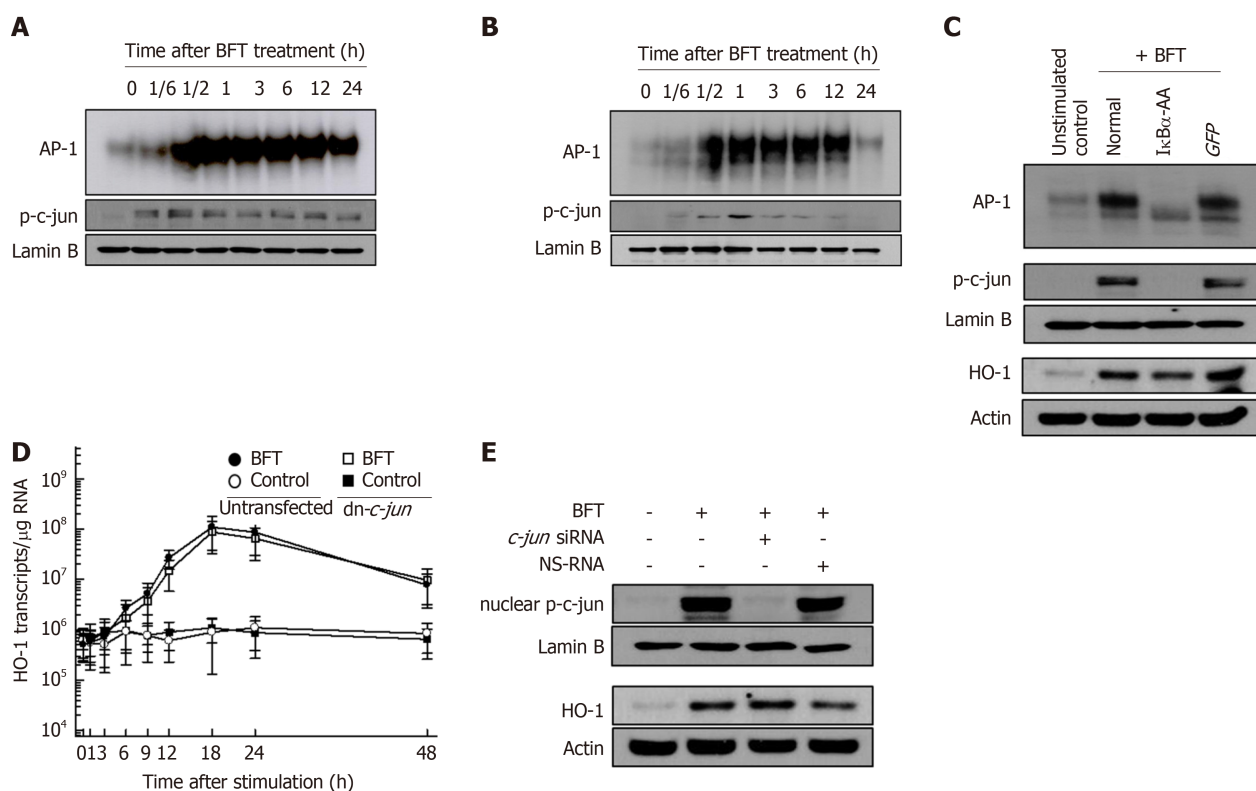


**Figure 3** Effects of AP-1 suppression on heme oxygenase-1 expression in dendritic cells stimulated with *Bacteroides fragilis* enterotoxin. A and B: Bone marrow-derived dendritic cells (DCs) (A) and DC2.4 cells (B) were treated with *Bacteroides fragilis* toxin (BFT) (100 ng/mL) for the indicated periods. AP-1 DNA binding activity was assessed by EMSA and expression of phospho-c-jun in nuclear extracts was detected using immunoblot. Results are representative of more than three independent experiments. C: DC2.4 cells were transfected with lentivirus containing dominant-negative c-jun plasmid (dn-c-jun) or control virus (GFP). Transfected cells were stimulated with BFT (100 ng/mL) for 1 h. AP-1 binding activity was assayed by EMSA (top panel). Immunoblot results for concurrent phospho-c-jun and lamin B in nuclear extracts under the same conditions are provided beneath the EMSA (middle panel). Expression of heme oxygenase-1 (HO-1) and actin proteins was analyzed by immunoblot (bottom panel). Results are representative of more than three independent experiments. D: Transfected DC2.4 cells were treated with BFT (100 ng/mL) for the indicated periods. Levels of HO-1 mRNA were analyzed by quantitative RT-PCR using a standard RNA. The values are expressed as mean  $\pm$  SD ( $n = 5$ ). The  $\beta$ -actin mRNA levels in each group remained relatively constant throughout the same periods (approximately  $10^6$  transcripts/ $\mu$ g total RNA). E: DC2.4 cells were transfected with AP-1 *c-jun*-specific silencing siRNA or NS-RNA as a control for 48 h, after which cells were combined with BFT (100 ng/mL) for 1 h. Nuclear extracts were analyzed by immunoblotting with the indicated Abs (top panel). Transfected cells were stimulated with BFT (100 ng/mL) for 24 h. Expression of HO-1 and actin was detected by immunoblot (bottom panel). Results shown are representative of more than three independent experiments. HO-1: Heme oxygenase-1; BFT: *Bacteroides fragilis* toxin.

present study, we demonstrated that BFT markedly increased intracellular ROS generation in DC2.4 cells, while antioxidant NAC significantly inhibited it (Figure 9A). In this experimental system, treatment with NAC attenuated the increased levels of phospho-ERK and phospho-p38 in DC2.4 cells exposed to BFT (Figure 9B). Upregulated expression of both phospho-Nrf2 and HO-1 were also reduced in the presence of NAC under BFT-stimulated conditions, indicating that ROS seems to regulate the overall signaling process of inducing HO-1 expression in BFT-exposed DCs.

## DISCUSSION

ETBF is a noninvasive bacterium associated with pathogenic effects in the intestine<sup>[2]</sup>. Since invasion of ETBF into the surface epithelium from the intestine has not been reported and no bacteremia has been observed in infected rabbit models<sup>[2,28]</sup>, the produced BFT seems to be primarily present in the lumen. Organized and diffuse lymphoid tissues are found in the intestinal mucosa layer and DCs are abundant in the lamina propria. DCs can extend dendritic processes between intestinal epithelial cells into the lumen to sample antigens. In addition, BFT can destroy the tight junctions in the intestinal epithelium by cleaving E-cadherin<sup>[3-5]</sup> and the secreted BFT may come into direct contact with DCs. Therefore, BFT may be exposed to DCs at the site of ETBF infection. In experiments reported here, we demonstrated that the exposure of DCs to BFT could upregulate expression of HO-1 at the mRNA and protein levels.

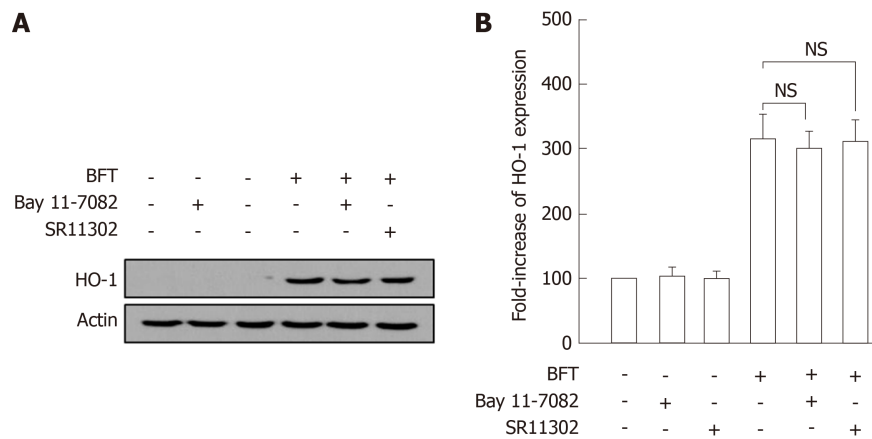


**Figure 4 Relationship between the suppression of NF- $\kappa$ B or AP-1 activity and heme oxygenase-1 expression in bone marrow-derived dendritic cells stimulated with *Bacteroides fragilis* enterotoxin.** A: Bone marrow (BM)-derived dendritic cells (DCs) were treated with *Bacteroides fragilis* toxin (BFT) (100 ng/mL) for 24 h, respectively. The expression of heme oxygenase-1 (HO-1) and actin was analyzed by immunoblot. Results are representative of more than three independent experiments. B: BM-derived DCs were preincubated with the NF- $\kappa$ B inhibitor Bay 11-7082 (50  $\mu$ mol/L) or the AP-1 inhibitor SR11302 (10  $\mu$ mol/L) for 30 min, followed by stimulation with BFT (100 ng/mL) for an additional 24 h. Expression levels of HO-1 protein were measured by ELISA (mean  $\pm$  SE,  $n = 5$ ). NS: Statistically non-significant; HO-1: Heme oxygenase-1; BFT: *Bacteroides fragilis* toxin.

Transcription factors such as NF- $\kappa$ B, AP-1, and Nrf2 regulate a variety of inflammatory responses and their promoter regions of HO-1 contain binding sites for these transcription factors<sup>[9,12,29]</sup>. We previously demonstrated that stimulation of intestinal epithelial cells with BFT activate NF- $\kappa$ B and AP-1 signaling<sup>[12]</sup>. However, there have been no reports on whether BFT may activate these transcription factors in DCs. The present study showed that signals of NF- $\kappa$ B, AP-1, and Nrf2 were activated by exposure of DCs to BFT. However, whether HO-1 induction of DCs may be regulated by NF- $\kappa$ B, AP-1 or Nrf2 remains controversial. In the present study, suppression of NF- $\kappa$ B activity either by transfection with lentivirus-I $\kappa$ B $\alpha$ -AA and p65 siRNA, or pretreatment with chemical inhibitor Bay 11-7082 did not significantly reduce BFT-induced HO-1 expression in DCs. In addition, the suppression of AP-1 signals did not result in a significant change in HO-1 expression. In contrast, the suppression of BFT-induced activation of Nrf2 led to the downregulation of HO-1 in DCs assessed by transfection with Nrf2 shRNA. These results were confirmed by experiments using DCs isolated from Nrf2<sup>-/-</sup> knockout mice. Our results differ from previous findings that LPS-induced HO-1 expression is mediated by an NF- $\kappa$ B-dependent pathway in DCs<sup>[30]</sup>. In addition, the present results are different from our previous study, in which *H. pylori* outer membrane vesicles induced HO-1 expression through both NF- $\kappa$ B- and Nrf2-dependent pathway in DCs<sup>[9]</sup>. Therefore, this Nrf2-dependent and both NF- $\kappa$ B- and AP-1-independent expression of HO-1 may be a distinctive signature of DCs exposure to BFT.

Kinetics of both NF- $\kappa$ B and AP-1 signaling in DCs resemble those in intestinal epithelial cells stimulated with BFT when comparing the present and previous results<sup>[12]</sup>. However, the kinetics of Nrf2 signals induced by BFT are different in DCs and intestinal epithelial cells. The present study showed that Nrf2 signals in DCs continued to increase over the ensuing 24 h following stimulation. In contrast, our previous study showed that the activation of Nrf2 in intestinal epithelial cells treated with BFT peaked between 1 h and 6 h after stimulation and then decreased<sup>[12]</sup>. Compared with previous results, the activation of Nrf2 in DCs was delayed compared to the response of intestinal epithelial cells to BFT stimulation. The delayed activation of Nrf2 seems to be associated with the delayed upregulation of HO-1 expression in BFT-exposed DCs.

MAPK signaling is known to be an important event underlying HO-1 expression<sup>[11,31,32]</sup>. In the present study, suppression of ERK or p38 MAPK signals in BFT-treated DCs resulted in significant inhibitions of both Nrf2 activation and HO-1 expression. Considering that suppression of p38 MAPK results in significant attenuation of BFT-induced NF- $\kappa$ B and HO-1 activities in intestinal epithelial cells<sup>[12]</sup>, two differential pathways may be involved in BFT-induced HO-1 expression. That is, the exposure of DCs to BFT can activate a signaling cascade involving ERK and p38 MAPKs, leading to Nrf2 activation and HO-1 induction. In contrast, BFT-exposed intestinal epithelial cells can activate a signaling cascade involving p38 MAPKs,

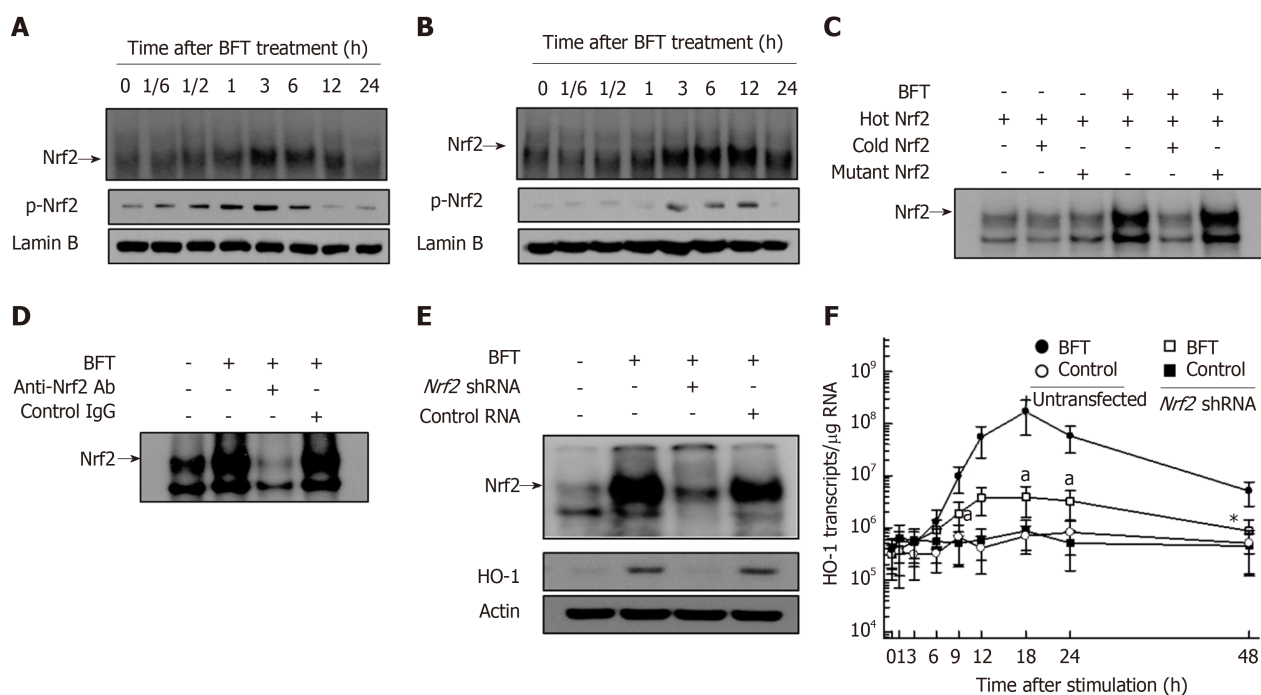


**Figure 5** Activation of Nrf2 in dendritic cells stimulated with *Bacteroides fragilis* enterotoxin. A and B: Bone marrow (BM)-derived dendritic cells (DCs) (A) and DC2.4 cells (B) were treated with BFT (100 ng/mL) for the indicated periods. Nrf2 DNA binding activity was assessed by EMSA. Immunoblot results for concurrent phospho-Nrf2 and lamin B in nuclear extracts are provided beneath the EMSA. C and D: Competition and supershift assays for Nrf2 signals. C: BM-derived DCs were treated with BFT (100 ng/mL) for 6 h and nuclear extracts were then prepared. The competition assay for Nrf2 signals was performed by adding a 100-fold excess of the unlabeled probe ("cold" probe) before the addition of the radiolabeled probe ("hot" probe) or a mutant probe to the reaction (top panel). D: Supershift assays using nuclear extracts were performed using anti-Nrf2 Ab and IgG isotype control Ab (bottom panel). Results are representative of more than three independent experiments. E: DC2.4 cells were transfected with Nrf2-specific shRNA or control RNA. Transfected cells were combined with BFT (100 ng/mL) for 12 h. Nrf2 binding activity was assayed by EMSA (top panel). Transfected cells were treated with BFT (100 ng/mL) for 24 h and the expression of heme oxygenase-1 (HO-1) and actin was analyzed by immunoblot (bottom panel). F: DC2.4 cells were treated with BFT (100 ng/mL) for the indicated periods. The levels of HO-1 mRNA were analyzed by quantitative RT-PCR using a standard RNA. The values are expressed as mean  $\pm$  SD ( $n = 5$ ).  $\beta$ -actin mRNA levels in each group remained relatively constant throughout the same periods (approximately  $10^6$  transcripts/ $\mu$ g total RNA). \* $P < 0.05$  vs untransfected cells treated with BFT. HO-1: Heme oxygenase-1; BFT: *Bacteroides fragilis* toxin.

leading to NF- $\kappa$ B activation and finally to HO-1 induction.

Since ROS production is known to be related to the activation of MAPK signaling<sup>[33]</sup> and BFT increase ROS production in intestinal epithelial cells<sup>[27]</sup>, we investigated the role of ROS in the regulation of MAPK and Nrf2 signaling. In the present study, exposure of DCs to BFT enhanced ROS production and treatment of BFT-exposed DCs with the antioxidant NAC significantly inhibited the activation of ERK and p38 MAPK signals. In addition, both Nrf2 activation and HO-1 expression were attenuated in the presence of NAC under BFT-stimulated conditions. Based on these results, increased intracellular ROS is proposed as the mechanism allowing BFT to contribute to ERK/p38 MAPK pathway-mediated Nrf2 activation and HO-1 expression in DCs.

BFT has been shown to not directly induce DC maturation<sup>[8]</sup>. Nevertheless, many papers have demonstrated that HO-1 expression is associated with inhibition of DC maturation<sup>[31,34,35]</sup>. Therefore, BFT-induced HO-1 upregulation seems to affect the maturation process of DCs and consequently inhibit maturation. Further studies are needed to clarify the role HO-1 plays in DC maturation in ETBF infection.

Upregulated HO-1 is likely to attenuate acute inflammation in ETBF infection. The rationale for this supposition is that HO-1 controls a variety of infections in mice, including *Mycobacterium avium*<sup>[36]</sup>, *Listeria monocytogenes*<sup>[37]</sup>, and *Salmonella Typhimurium*<sup>[38]</sup>. Further, HO-1 expression induces anti-inflammatory cytokine IL-10 production<sup>[34,39]</sup> and HO-1 mediates the anti-inflammatory effect of IL-10<sup>[40]</sup>. Based on these results, upregulated HO-1 may be an important mediator of the anti-inflammatory effects of DCs in acute ETBF infection. However, further studies are required to clarify the anti-inflammatory effects in BFT-stimulated DCs.

In summary, we demonstrated that exposure of DCs to BFT resulted in ROS-mediated activation of MAPK signaling, which then led to the induction of HO-1 molecules via Nrf2 signaling pathway in DCs.



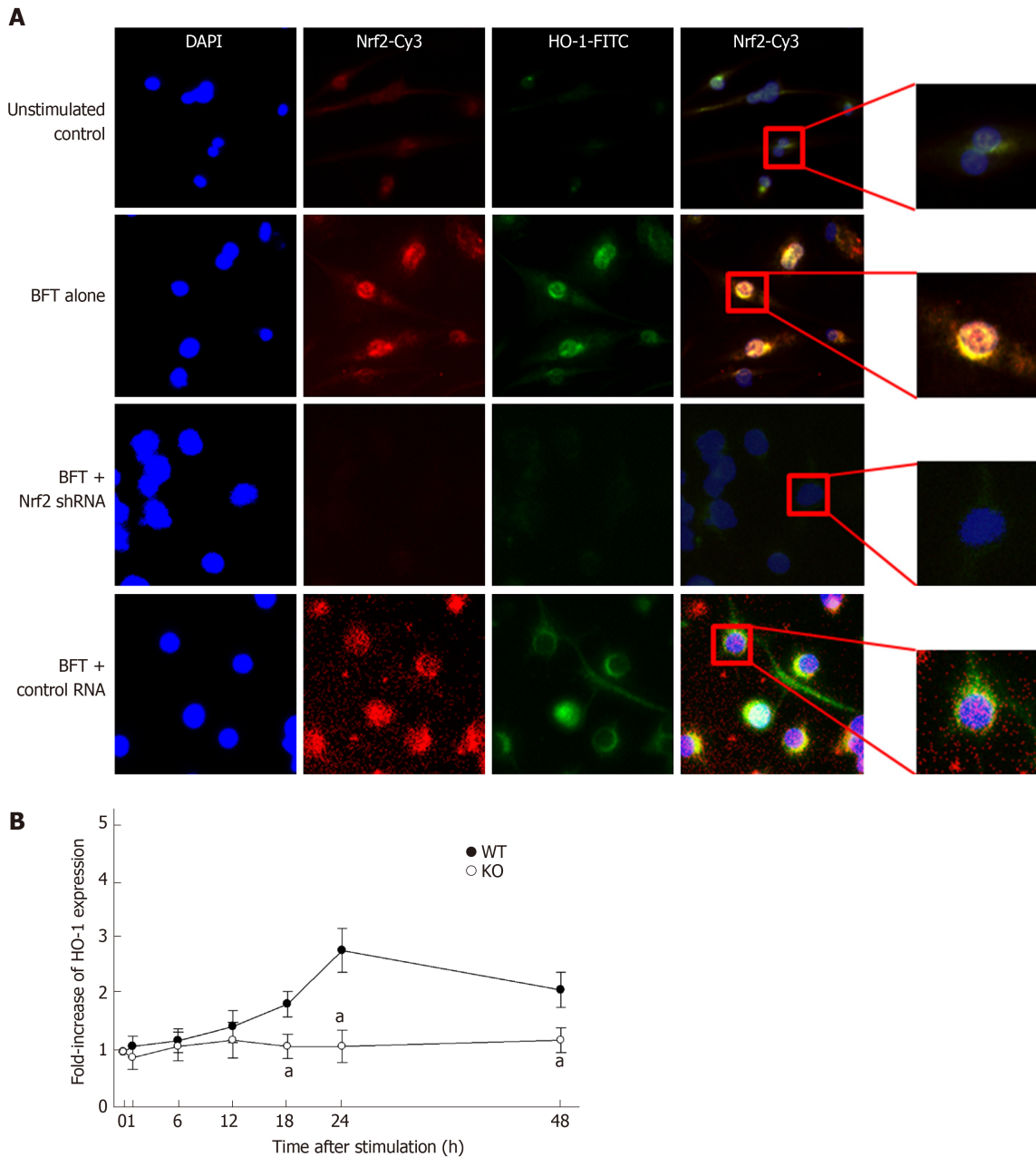


**Figure 6** Effects of Nrf2 suppression on heme oxygenase-1 expression in dendritic cells stimulated with *Bacteroides fragilis* enterotoxin. A: Nrf2 translocation and heme oxygenase-1 (HO-1) expression in *B. fragilis* enterotoxin (BFT)-stimulated dendritic cells (DCs). DC2.4 cells were transfected with Nrf2-specific shRNA or control RNA. Cells were treated with BFT (100 ng/mL) for 24 h and immunofluorescent microscopy was performed. Each group of cells was stained with the active form-specific anti-Nrf2-Cys Ab (red), anti-HO-1 Ab (green), and DAPI (blue, nucleus). The data are representative of at least five experiments. B: HO-1 expression in cells derived from wild-type and Nrf2<sup>-/-</sup> knockout mice. BMDCs derived from wild-type or Nrf2<sup>-/-</sup> knockout mice were exposed to BFT (100 ng/mL) for the indicated periods. Expression of HO-1 protein in each panel was measured by ELISA (mean  $\pm$  SE,  $n=5$ ). <sup>a</sup> $P < 0.05$  vs each group of cells derived from wild-type mice. HO-1: Heme oxygenase-1; BFT: *Bacteroides fragilis* toxin; WT: Wild-type; KO: Knockout.

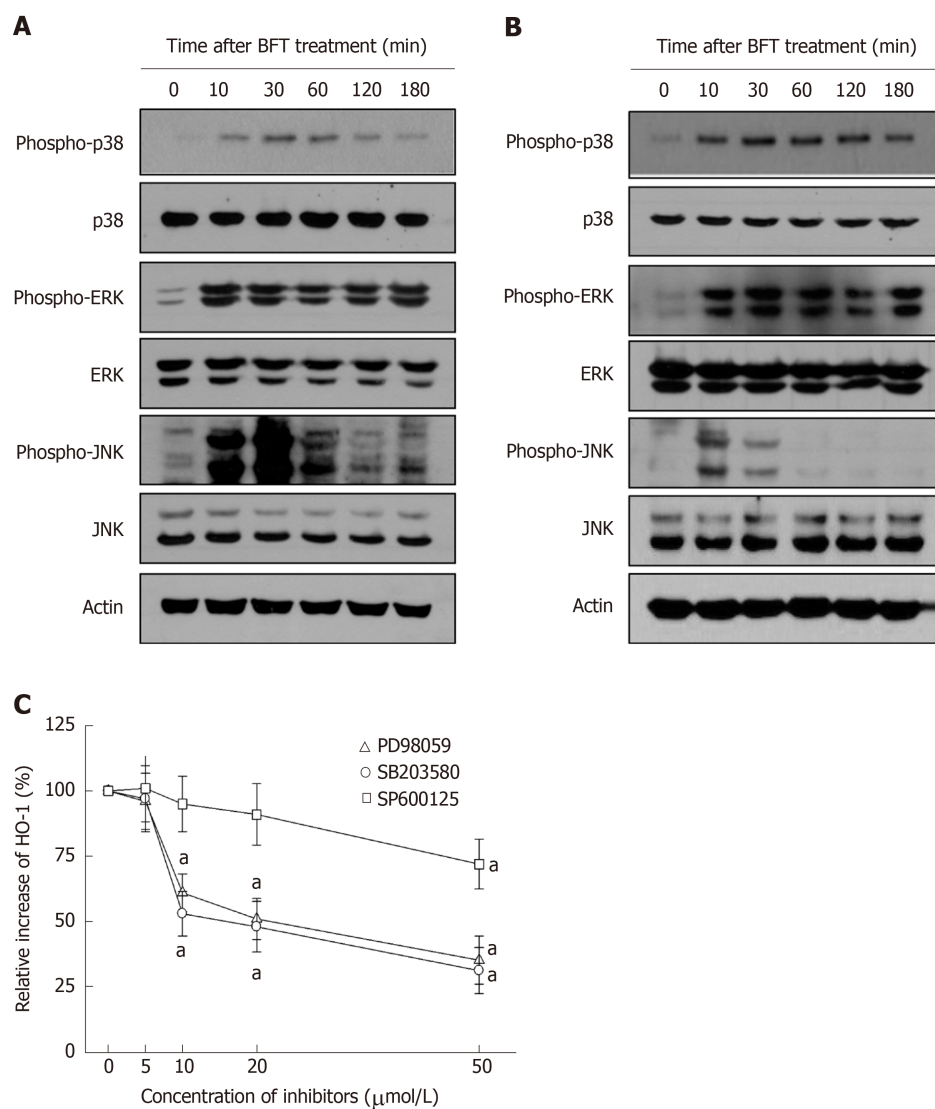


**Figure 7 Mitogen-activated protein kinases signals associated with heme oxygenase-1 expression in *Bacteroides fragilis* enterotoxin-stimulated dendritic cells.** A and B: Bone marrow (BM)-derived dendritic cells (DCs) (A) and DC2.4 cells (B) were stimulated with *Bacteroides fragilis* toxin (BFT) (100 ng/mL) for the indicated periods. ERK1/2, p38, and JNK activities were measured by immunoblot analysis. Results are representative of three independent experiments. C: BM-derived DCs were preincubated with SB203580 (open circle), PD98059 (open triangle), or SP600125 (open square) for 30 min, and then stimulated with BFT (100 ng/mL) for another 24 h. Expression levels of heme oxygenase-1 (HO-1) protein were determined by ELISA. Data are expressed as the mean % increase relative to unstimulated controls  $\pm$  SE ( $n = 5$ ).  $^aP < 0.05$  vs BFT alone. HO-1: Heme oxygenase-1.

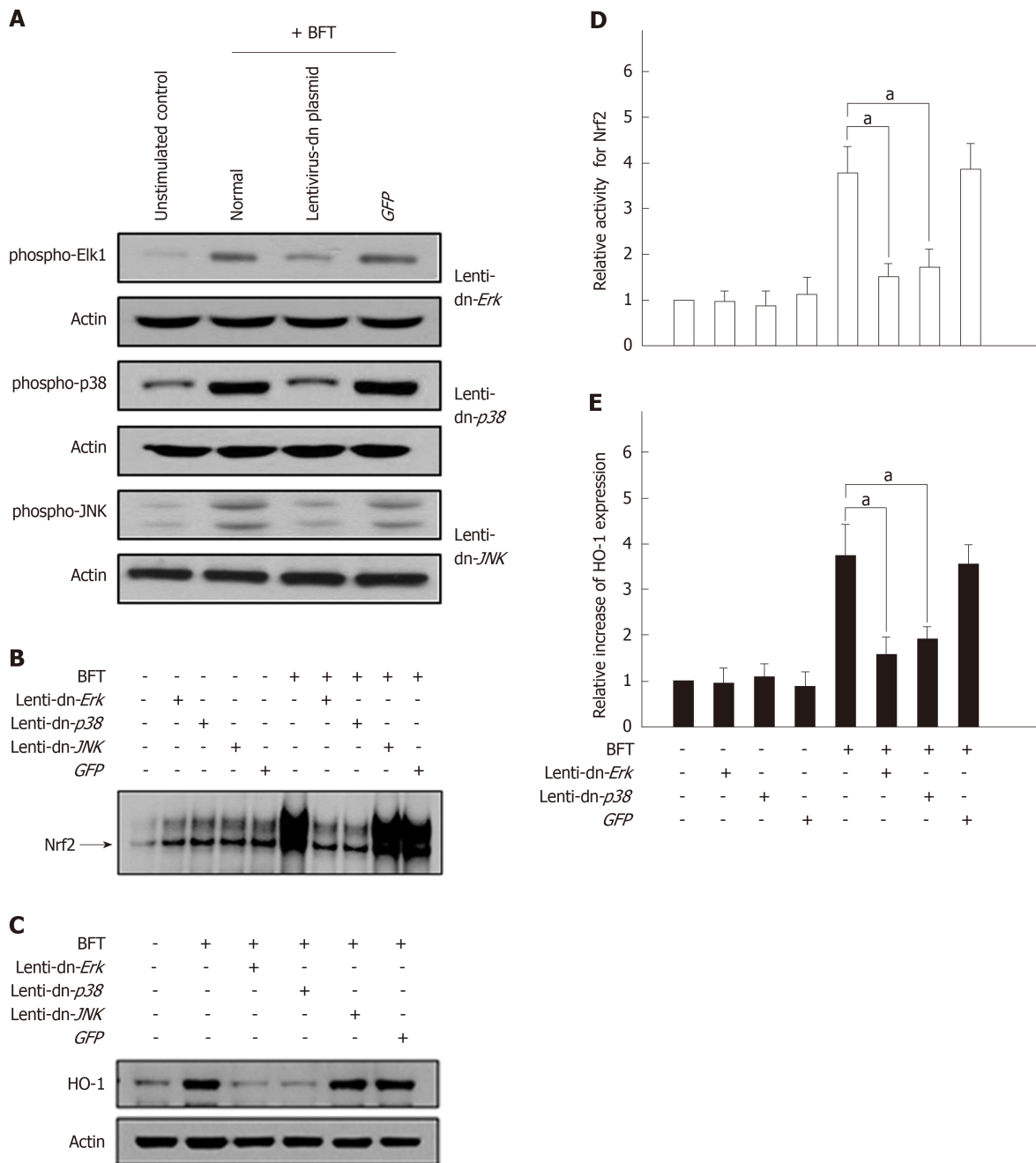


**Figure 8** Effects of mitogen-activated protein kinases suppression on heme oxygenase-1 expression in dendritic cells stimulated with *Bacteroides fragilis* enterotoxin. A: DC2.4 cells were infected with lentiviruses containing either a dominant-negative or control plasmid (GFP). Transfected cells were stimulated with BFT (100 ng/mL) for 30 min and immunoblots were then performed. Results are representative of three independent experiments. B and C: Transfected cells were stimulated with BFT (100 ng/mL) for 3 h (Nrf2) or 24 h (heme oxygenase-1, HO-1). B: DNA binding activities of Nrf2 were evaluated by EMSA. C: Expression of HO-1 and actin was analyzed by immunoblot. Results are representative of more than three independent experiments. D: Transfected cells were stimulated with BFT (100 ng/mL) for 3 h. Phospho-Nrf2 activities were measured using an ELISA kit. Data are expressed as mean fold induction  $\pm$  SE of Nrf2 relative to untreated controls ( $n = 5$ ). E: Transfected cells were stimulated with BFT (100 ng/mL) for 24 h. Transfected cells were either left untreated or stimulated with BFT (100 ng/mL) for another 6 h (Nrf2) or 24 h (HO-1). Each ELISA kit measured activities of phospho-IkB $\alpha$  and Nrf2, as well as HO-1 expression. Data are expressed as mean fold induction  $\pm$  SE (%) relative to untreated controls ( $n = 5$ ). <sup>a</sup> $P < 0.05$ . HO-1: Heme oxygenase-1; BFT: *Bacteroides fragilis* toxin.

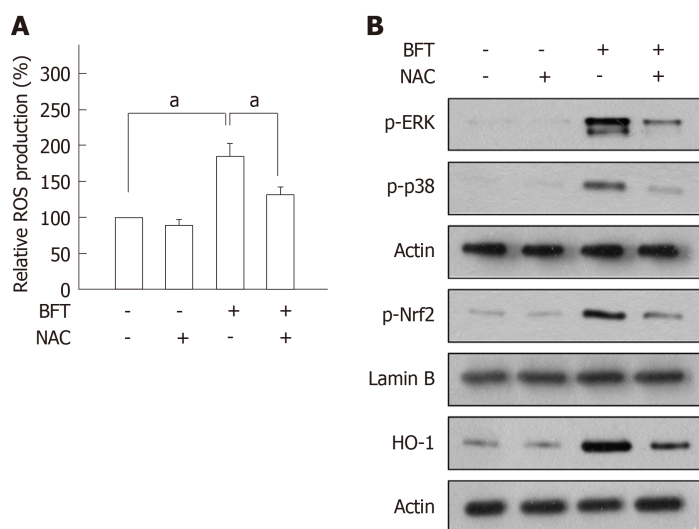


**Figure 9** Reactive oxygen species mediated *Bacteroides fragilis* enterotoxin-induced heme oxygenase-1 expression in dendritic cells. A: DC2.4 cells were stimulated with BFT (100 ng/mL) in the absence or presence of the antioxidant N-acetyl-L-cysteine (NAC, 0.5 mmol/L) for 6 h. Production of reactive oxygen species (ROS) was measured by a commercially available ROS detection kit. Data are expressed as mean fold induction  $\pm$  SE (%) relative to untreated controls ( $n = 5$ ).  $^aP < 0.05$ . B: DC2.4 cells were stimulated with BFT (100 ng/mL) in the absence or presence of NAC (0.5 mmol/L) for 30 min (phospho-ERK and phospho-p38), 3 h (phospho-Nrf2), or 24 h (heme oxygenase-1, HO-1). The effects of NAC on each protein level were determined using immunoblot. Results are representative of three independent experiments. NAC: N-acetyl-L-cysteine; HO-1: Heme oxygenase-1; BFT: *Bacteroides fragilis* toxin.

## ARTICLE HIGHLIGHTS

### Research background

Enterotoxigenic *Bacteroides fragilis* (ETBF) causes colitis and diarrhea, and is considered a candidate pathogen in inflammatory bowel diseases as well as colorectal cancers. These diseases are dependent on ETBF-secreted toxin (BFT). Dendritic cells (DCs) play an important role in directing the nature of adaptive immune responses to bacterial infection and heme oxygenase-1 (HO-1) is involved in the regulation of DC function.

### Research motivation

Although BFT can activate such transcription factor signaling in intestinal epithelial cells, there is no evidence that signals associated with BFT-induced transcription factors are related to HO-1 induction in DCs. These led us to this study.

### Research objectives

The present study aimed to investigate the role of BFT in HO-1 expression in DCs.

### Research methods

Murine DCs were generated from specific pathogen-free C57BL/6 and Nrf2<sup>-/-</sup> knockout mice. DCs were exposed to BFT, after which HO-1 expression and the related signaling factor activation were measured by quantitative RT-PCR, EMSA, fluorescent microscopy, immunoblot, and ELISA.

### Research results

HO-1 expression was upregulated in DCs stimulated with BFT. Although BFT activated transcription factors such as NF- $\kappa$ B, AP-1, and Nrf2, activation of NF- $\kappa$ B and AP-1 was not involved in the induction of HO-1 expression in BFT-exposed DCs. Instead, upregulation of HO-1 expression was dependent on Nrf2 activation in DCs. Moreover, HO-1 expression via Nrf2 in DCs was regulated by mitogen-activated protein kinases (MAPKs) such as ERK and p38. Furthermore, BFT enhanced the production of reactive oxygen species (ROS) and inhibition of ROS production resulted in a significant decrease of phospho-ERK, phospho-p38, Nrf2, and HO-1 expression.

### Research conclusions

These results suggest that signaling pathways involving ROS-mediated ERK and p38 MAPK-Nrf2 activation in DCs are required for HO-1 induction during exposure to ETBF-produced BFT.

### Research perspectives

Upregulated HO-1 expression in DCs will help explain the pathogenesis of the ETBF infection. In addition, upregulated HO-1 may be an important mediator of the anti-inflammatory effects of DCs in acute ETBF infection. However, further studies are required to clarify the anti-inflammatory effects in BFT-stimulated DCs.



## REFERENCES

- 1 **Sears CL.** The toxins of *Bacteroides fragilis*. *Toxicon* 2001; **39**: 1737-1746 [PMID: [11595636](#) DOI: [10.1016/S0041-0101\(01\)00160-X](#)]
- 2 **Sears CL.** Enterotoxigenic *Bacteroides fragilis*: a rogue among symbiotes. *Clin Microbiol Rev* 2009; **22**: 349-369, Table of Contents [PMID: [19366918](#) DOI: [10.1128/CMR.00053-08](#)]
- 3 **Sears CL, Geis AL, Housseau F.** *Bacteroides fragilis* subverts mucosal biology: from symbiont to colon carcinogenesis. *J Clin Invest* 2014; **124**: 4166-4172 [PMID: [25105360](#) DOI: [10.1172/JCI72334](#)]
- 4 **Wu S, Lim KC, Huang J, Saidi RF, Sears CL.** *Bacteroides fragilis* enterotoxin cleaves the zonula adherens protein, E-cadherin. *Proc Natl Acad Sci USA* 1998; **95**: 14979-14984 [PMID: [9844001](#) DOI: [10.1073/pnas.95.25.14979](#)]
- 5 **Wexler HM.** *Bacteroides*: the good, the bad, and the nitty-gritty. *Clin Microbiol Rev* 2007; **20**: 593-621 [PMID: [17934076](#) DOI: [10.1128/CMR.00008-07](#)]
- 6 **MacDonald TT, Monteleone I, Fantini MC, Monteleone G.** Regulation of homeostasis and inflammation in the intestine. *Gastroenterology* 2011; **140**: 1768-1775 [PMID: [21530743](#) DOI: [10.1053/j.gastro.2011.02.047](#)]
- 7 **Rescigno M, Urbano M, Valzasina B, Francolini M, Rotta G, Bonasio R, Granucci F, Kraehenbuhl JP, Ricciardi-Castagnoli P.** Dendritic cells express tight junction proteins and penetrate gut epithelial monolayers to sample bacteria. *Nat Immunol* 2001; **2**: 361-367 [PMID: [11276208](#) DOI: [10.1038/86373](#)]
- 8 **Rhee KJ, Wu S, Wu X, Huso DL, Karim B, Franco AA, Rabizadeh S, Golub JE, Mathews LE, Shin J, Sartor RB, Golenbock D, Hamad AR, Gan CM, Housseau F, Sears CL.** Induction of persistent colitis by a human commensal, enterotoxigenic *Bacteroides fragilis*, in wild-type C57BL/6 mice. *Infect Immun* 2009; **77**: 1708-1718 [PMID: [19188353](#) DOI: [10.1128/IAI.00814-08](#)]
- 9 **Ko SH, Rho DJ, Jeon JI, Kim YJ, Woo HA, Kim N, Kim JM.** Crude Preparations of *Helicobacter pylori* Outer Membrane Vesicles Induce Upregulation of Heme Oxygenase-1 via Activating Akt-Nrf2 and mTOR-I $\kappa$ B Kinase-NF- $\kappa$ B Pathways in Dendritic Cells. *Infect Immun* 2016; **84**: 2162-2174 [PMID: [27185786](#) DOI: [10.1128/IAI.00190-16](#)]
- 10 **Liu XM, Peyton KJ, Durante W.** Physiological cyclic strain promotes endothelial cell survival via the induction of heme oxygenase-1. *Am J Physiol Heart Circ Physiol* 2013; **304**: H1634-H1643 [PMID: [23604711](#) DOI: [10.1152/ajpheart.00872.2012](#)]
- 11 **Paine A, Eiz-Vesper B, Blaszczyk R, Immenschuh S.** Signaling to heme oxygenase-1 and its anti-inflammatory therapeutic potential. *Biochem Pharmacol* 2010; **80**: 1895-1903 [PMID: [20643109](#) DOI: [10.1016/j.bcp.2010.07.014](#)]
- 12 **Ko SH, Rho da J, Jeon JI, Kim YJ, Woo HA, Lee YK, Kim JM.** *Bacteroides fragilis* Enterotoxin Upregulates Heme Oxygenase-1 in Intestinal Epithelial Cells via a Mitogen-Activated Protein Kinase- and NF- $\kappa$ B-Dependent Pathway, Leading to Modulation of Apoptosis. *Infect Immun* 2016; **84**: 2541-2554 [PMID: [27324483](#) DOI: [10.1128/IAI.00191-16](#)]
- 13 **Katada K, Takagi T, Uchiyama K, Naito Y.** Therapeutic roles of carbon monoxide in intestinal ischemia-reperfusion injury. *J Gastroenterol Hepatol* 2015; **30** Suppl 1: 46-52 [PMID: [25827804](#) DOI: [10.1111/jgh.12742](#)]
- 14 **Ryter SW, Choi AM.** Targeting heme oxygenase-1 and carbon monoxide for therapeutic modulation of inflammation. *Transl Res* 2016; **167**: 7-34 [PMID: [26166253](#) DOI: [10.1016/j.trsl.2015.06.011](#)]
- 15 **Zhao Y, Jia Y, Wang L, Chen S, Huang X, Xu B, Zhao G, Xiang Y, Yang J, Chen G.** Upregulation of Heme Oxygenase-1 Endues Immature Dendritic Cells With More Potent and Durable Immunoregulatory Properties and Promotes Engraftment in a Stringent Mouse Cardiac Allotransplant Model. *Front Immunol* 2018; **9**: 1515 [PMID: [30013566](#) DOI: [10.3389/fimmu.2018.01515](#)]
- 16 **Ma YY, Yang MQ, He ZG, Fan MH, Huang M, Teng F, Wei Q, Li JY.** Upregulation of heme oxygenase-1 in Kupffer cells blocks mast cell degranulation and inhibits dendritic cell migration in vitro. *Mol Med Rep* 2017; **15**: 3796-3802 [PMID: [28393189](#) DOI: [10.3892/mmr.2017.6448](#)]
- 17 **Wong TH, Chen HA, Gau RJ, Yen JH, Suen JL.** Heme Oxygenase-1-Expressing Dendritic Cells Promote Foxp3<sup>+</sup> Regulatory T Cell Differentiation and Induce Less Severe Airway Inflammation in Murine Models. *PLoS One* 2016; **11**: e0168919 [PMID: [28033400](#) DOI: [10.1371/journal.pone.0168919](#)]
- 18 **Kim JM, Oh YK, Kim YJ, Oh HB, Cho YJ.** Polarized secretion of CXCL chemokines by human intestinal epithelial cells in response to *Bacteroides fragilis* enterotoxin: NF- $\kappa$ B plays a major role in the regulation of IL-8 expression. *Clin Exp Immunol* 2001; **123**: 421-427 [PMID: [11298129](#) DOI: [10.1046/j.1365-2249.2001.01462.x](#)]
- 19 **Ko SH, Jeon JI, Myung HS, Kim YJ, Kim JM.** *Bacteroides fragilis* Enterotoxin Induces Formation of Autophagosomes in Endothelial Cells but Interferes with Fusion with Lysosomes for Complete Autophagic Flux through a Mitogen-Activated Protein Kinase-, AP-1-, and C/EBP Homologous Protein-Dependent Pathway. *Infect Immun* 2017; **85**: pii: e00420-17 [PMID: [28694294](#) DOI: [10.1128/IAI.00420-17](#)]
- 20 **Roh HC, Yoo do Y, Ko SH, Kim YJ, Kim JM.** *Bacteroides fragilis* enterotoxin upregulates intercellular adhesion molecule-1 in endothelial cells via an aldose reductase-, MAPK-, and NF- $\kappa$ B-dependent pathway, leading to monocyte adhesion to endothelial cells. *J Immunol* 2011; **187**: 1931-1941 [PMID: [21724992](#) DOI: [10.4049/jimmunol.1101226](#)]
- 21 **Lee JY, Kim H, Cha MY, Park HG, Kim YJ, Kim IY, Kim JM.** *Clostridium difficile* toxin A promotes dendritic cell maturation and chemokine CXCL2 expression through p38, IKK, and the NF- $\kappa$ B signaling pathway. *J Mol Med (Berl)* 2009; **87**: 169-180 [PMID: [18985311](#) DOI: [10.1007/s00109-008-0415-2](#)]
- 22 **Itoh K, Chiba T, Takahashi S, Ishii T, Igarashi K, Katoh Y, Oyake T, Hayashi N, Satoh K, Hatayama I, Yamamoto M, Nabeshima Y.** An Nrf2/small Maf heterodimer mediates the induction of phase II detoxifying enzyme genes through antioxidant response elements. *Biochem Biophys Res Commun* 1997; **236**: 313-322 [PMID: [9240432](#) DOI: [10.1006/bbrc.1997.6943](#)]
- 23 **Choi YJ, Im E, Chung HK, Pothoulakis C, Rhee SH.** TRIF mediates Toll-like receptor 5-induced signaling in intestinal epithelial cells. *J Biol Chem* 2010; **285**: 37570-37578 [PMID: [20855887](#) DOI: [10.1074/jbc.M110.158394](#)]
- 24 **Khor TO, Huang MT, Kwon KH, Chan JY, Reddy BS, Kong AN.** Nrf2-deficient mice have an increased susceptibility to dextran sulfate sodium-induced colitis. *Cancer Res* 2006; **66**: 11580-11584 [PMID: [17178849](#) DOI: [10.1158/0008-5472.CAN-06-3562](#)]
- 25 **Ko SH, Jeon JI, Kim H, Kim YJ, Youn J, Kim JM.** Mitogen-activated protein kinase/I $\kappa$ B kinase/NF- $\kappa$ B-dependent and AP-1-independent CXCL1 expression in intestinal epithelial cells stimulated with

- Clostridium difficile toxin A. *J Mol Med (Berl)* 2014; **92**: 411-427 [PMID: [24362517](#) DOI: [10.1007/s00109-013-1117-y](#)]
- 26 **Yoo do Y**, Ko SH, Jung J, Kim YJ, Kim JS, Kim JM. Bacteroides fragilis enterotoxin upregulates lipocalin-2 expression in intestinal epithelial cells. *Lab Invest* 2013; **93**: 384-396 [PMID: [23381626](#) DOI: [10.1038/labinvest.2013.1](#)]
  - 27 **Goodwin AC**, Destefano Shields CE, Wu S, Huso DL, Wu X, Murray-Stewart TR, Hacker-Prietz A, Rabizadeh S, Woster PM, Sears CL, Casero RA. Polyamine catabolism contributes to enterotoxigenic Bacteroides fragilis-induced colon tumorigenesis. *Proc Natl Acad Sci USA* 2011; **108**: 15354-15359 [PMID: [21876161](#) DOI: [10.1073/pnas.1010203108](#)]
  - 28 **Myers LL**, Shoop DS, Collins JE, Bradbury WC. Diarrheal disease caused by enterotoxigenic Bacteroides fragilis in infant rabbits. *J Clin Microbiol* 1989; **27**: 2025-2030 [PMID: [2778065](#)]
  - 29 **Aw Yeang HX**, Hamdam JM, Al-Huseini LM, Sethu S, Djouhri L, Walsh J, Kitteringham N, Park BK, Goldring CE, Sathish JG. Loss of transcription factor nuclear factor-erythroid 2 (NF-E2) p45-related factor-2 (Nrf2) leads to dysregulation of immune functions, redox homeostasis, and intracellular signaling in dendritic cells. *J Biol Chem* 2012; **287**: 10556-10564 [PMID: [22311972](#) DOI: [10.1074/jbc.M111.322420](#)]
  - 30 **Jung ID**, Lee JS, Lee CM, Noh KT, Jeong YI, Park WS, Chun SH, Jeong SK, Park JW, Son KH, Heo DR, Lee MG, Shin YK, Kim HW, Yun CH, Park YM. Induction of indoleamine 2,3-dioxygenase expression via heme oxygenase-1-dependant pathway during murine dendritic cell maturation. *Biochem Pharmacol* 2010; **80**: 491-505 [PMID: [20430013](#) DOI: [10.1016/j.bcp.2010.04.025](#)]
  - 31 **Al-Huseini LM**, Aw Yeang HX, Hamdam JM, Sethu S, Alhumeed N, Wong W, Sathish JG. Heme oxygenase-1 regulates dendritic cell function through modulation of p38 MAPK-CREB/ATF1 signaling. *J Biol Chem* 2014; **289**: 16442-16451 [PMID: [24719331](#) DOI: [10.1074/jbc.M113.532069](#)]
  - 32 **Roy Chowdhury S**, Sengupta S, Biswas S, Sinha TK, Sen R, Basak RK, Adhikari B, Bhattacharyya A. Bacterial fucose-rich polysaccharide stabilizes MAPK-mediated Nrf2/Keap1 signaling by directly scavenging reactive oxygen species during hydrogen peroxide-induced apoptosis of human lung fibroblast cells. *PLoS One* 2014; **9**: e113663 [PMID: [25412177](#) DOI: [10.1016/B978-0-12-405881-1.00002-1](#)]
  - 33 **Son Y**, Kim S, Chung HT, Pae HO. Reactive oxygen species in the activation of MAP kinases. *Methods Enzymol* 2013; **528**: 27-48 [PMID: [23849857](#) DOI: [10.1371/journal.pone.0113663](#)]
  - 34 **Chauveau C**, Rémy S, Royer PJ, Hill M, Tanguy-Royer S, Hubert FX, Tesson L, Brion R, Beriou G, Gregoire M, Josien R, Cuturi MC, Anegón I. Heme oxygenase-1 expression inhibits dendritic cell maturation and proinflammatory function but conserves IL-10 expression. *Blood* 2005; **106**: 1694-1702 [PMID: [15920011](#) DOI: [10.1182/blood-2005-02-0494](#)]
  - 35 **Campbell NK**, Fitzgerald HK, Fletcher JM, Dunne A. Plant-Derived Polyphenols Modulate Human Dendritic Cell Metabolism and Immune Function via AMPK-Dependent Induction of Heme Oxygenase-1. *Front Immunol* 2019; **10**: 345 [PMID: [30881359](#) DOI: [10.3389/fimmu.2019.00345](#)]
  - 36 **Silva-Gomes S**, Appelberg R, Larsen R, Soares MP, Gomes MS. Heme catabolism by heme oxygenase-1 confers host resistance to Mycobacterium infection. *Infect Immun* 2013; **81**: 2536-2545 [PMID: [23630967](#) DOI: [10.1128/IAI.00251-13](#)]
  - 37 **Tachibana M**, Hashino M, Nishida T, Shimizu T, Watarai M. Protective role of heme oxygenase-1 in Listeria monocytogenes-induced abortion. *PLoS One* 2011; **6**: e25046 [PMID: [21949846](#) DOI: [10.1371/journal.pone.0025046](#)]
  - 38 **Onyiah JC**, Sheikh SZ, Maharshak N, Steinbach EC, Russo SM, Kobayashi T, Mackey LC, Hansen JJ, Moeser AJ, Rawls JF, Borst LB, Otterbein LE, Plevy SE. Carbon monoxide and heme oxygenase-1 prevent intestinal inflammation in mice by promoting bacterial clearance. *Gastroenterology* 2013; **144**: 789-798 [PMID: [23266559](#) DOI: [10.1053/j.gastro.2012.12.025](#)]
  - 39 **Riquelme SA**, Carreño LJ, Espinoza JA, Mackern-Oberti JP, Alvarez-Lobos MM, Riedel CA, Bueno SM, Kalergis AM. Modulation of antigen processing by haem-oxygenase 1. Implications on inflammation and tolerance. *Immunology* 2016; **149**: 1-12 [PMID: [26938875](#) DOI: [10.1111/imm.12605](#)]
  - 40 **Lee TS**, Chau LY. Heme oxygenase-1 mediates the anti-inflammatory effect of interleukin-10 in mice. *Nat Med* 2002; **8**: 240-246 [PMID: [11875494](#) DOI: [10.1038/nm0302-240](#)]



## Case Control Study

# Nucleotide excision repair pathway gene polymorphisms are associated with risk and prognosis of colorectal cancer

Yan-Ke Li, Qian Xu, Li-Ping Sun, Yue-Hua Gong, Jing-Jing Jing, Cheng-Zhong Xing, Yuan Yuan

**ORCID number:** Yan-Ke Li (0000-0003-1114-2963); Qian Xu (0000-0002-3082-7530); Li-Ping Sun (0000-0003-1993-8544); Yue-Hua Gong (0000-0002-0522-624X); Jing-Jing Jing (0000-0002-9807-8089); Cheng-Zhong Xing (0000-0001-6463-019X); Yuan Yuan (0000-0002-7394-9036).

**Author contributions:** Yuan Y designed the study and revised the manuscript; Xing CZ recruited the patients; Sun LP collected the data; Xu Q, Gong YH, and Jing JJ performed the experiments; Li YK analyzed the data and drafted the manuscript.

**Supported by** the National Key R&D Program of China, No. 2018YFC1311600.

### Institutional review board

**statement:** The study was approved by the Ethics Committee of the First Hospital of China Medical University.

**Informed consent statement:** All subjects provided written informed consent.

**Conflict-of-interest statement:** The authors declare no conflict of interest.

**Data sharing statement:** No additional data is available.

**STROBE statement:** The guidelines of STROBE Statement have been adopted.

**Open-Access:** This article is an open-access article that was selected by an in-house editor and fully peer-reviewed by external

**Yan-Ke Li, Qian Xu, Li-Ping Sun, Yue-Hua Gong, Jing-Jing Jing, Cheng-Zhong Xing, Yuan Yuan,** Tumor Etiology and Screening Department of Cancer Institute and General Surgery, Key Laboratory of Cancer Etiology and Prevention of Liaoning Education Department, Key Laboratory of GI Cancer Etiology and Prevention of Liaoning Province, the First Hospital of China Medical University, Shenyang 110001, Liaoning Province, China

**Yan-Ke Li, Cheng-Zhong Xing,** Department of Anorectal Surgery, the First Hospital of China Medical University, Shenyang 110001, Liaoning Province, China

**Corresponding author:** Yuan Yuan, MD, PhD, Professor, Tumor Etiology and Screening Department of Cancer Institute and General Surgery, the First Hospital of China Medical University, No. 155, Nanjingbei Street, Heping District, Shenyang 110001, Liaoning Province, China. [yuanyuan@cmu.edu.cn](mailto:yuanyuan@cmu.edu.cn)

## Abstract

### BACKGROUND

Single nucleotide polymorphisms (SNPs) are universally present in nucleotide excision repair (NER) pathway genes, which could make impacts on colorectal carcinogenesis and prognosis.

### AIM

To explore the association of all tagSNPs in NER pathway genes with colorectal cancer (CRC) risk and prognosis in a northern Chinese population by a two-stage case-control design composed of a discovery and validation stage.

### METHODS

Genotyping for NER SNPs was performed using kompetitive allele specific PCR. In the discovery stage, 39 tagSNPs in eight genes were genotyped in 368 subjects, including 184 CRC cases and 184 individual-matched controls. In the validation stage, 13 SNPs in six genes were analyzed in a total of 1712 subjects, including 854 CRC cases and 858 CRC-free controls.

### RESULTS

Two SNPs (XPA rs10817938 and XPC rs2607775) were associated with an increased CRC risk in overall and stratification analyses. Significant cumulative and interaction effects were also demonstrated in the studied SNPs on CRC risk. Another two SNPs (ERCC2 rs1052555 and ERCC5 rs2228959) were newly found to be associated with a poor overall survival of CRC patients.

### CONCLUSION

Our findings suggest novel SNPs in NER pathway genes that can be predictive

reviewers. It is distributed in accordance with the Creative Commons Attribution NonCommercial (CC BY-NC 4.0) license, which permits others to distribute, remix, adapt, build upon this work non-commercially, and license their derivative works on different terms, provided the original work is properly cited and the use is non-commercial. See: <http://creativecommons.org/licenses/by-nc/4.0/>

**Manuscript source:** Unsolicited manuscript

**Received:** October 12, 2019

**Peer-review started:** October 12, 2019

**First decision:** November 27, 2019

**Revised:** December 26, 2019

**Accepted:** January 1, 2020

**Article in press:** January 1, 2020

**Published online:** January 21, 2020

**P-Reviewer:** Sazci A, Yong D

**S-Editor:** Wang J

**L-Editor:** Wang TQ

**E-Editor:** Xing YX



for CRC risk and prognosis in a large-scale Chinese population. The present study has referential values for the identification of all-round NER-based genetic biomarkers in predicting the susceptibility and clinical outcome of CRC.

**Key words:** Nucleotide excision repair; Polymorphism; Colorectal cancer; Susceptibility; Prognosis

©The Author(s) 2020. Published by Baishideng Publishing Group Inc. All rights reserved.

**Core tip:** We conducted a two-stage case-control study to explore the association of all tag-single nucleotide polymorphisms (SNPs) in eight nucleotide excision repair pathway genes with colorectal cancer (CRC) risk and prognosis in a northern Chinese population, including a discovery and validation stage. We newly found that two SNPs (XPA rs10817938 and XPC rs2607775) contributed to an increased CRC risk in overall and stratification analyses. Another two SNPs (ERCC2 rs1052555 and ERCC5 rs2228959) were also first reported to be associated with a poor CRC prognosis.

**Citation:** Li YK, Xu Q, Sun LP, Gong YH, Jing JJ, Xing CZ, Yuan Y. Nucleotide excision repair pathway gene polymorphisms are associated with risk and prognosis of colorectal cancer. *World J Gastroenterol* 2020; 26(3): 307-323

**URL:** <https://www.wjgnet.com/1007-9327/full/v26/i3/307.htm>

**DOI:** <https://dx.doi.org/10.3748/wjg.v26.i3.307>

## INTRODUCTION

Colorectal cancer (CRC) is the third common malignant neoplasm and the fifth leading cause of cancer-related death in China. The incidence has been continuously rising in the past decades, which has exceeded the average levels both in developed and developing countries<sup>[1,2]</sup>. Genetic factors are thought to play a critical role in the susceptibility to CRC with hereditary factors estimated to account for 35% of the risk<sup>[3]</sup>. The identification of genetic biomarkers associated with CRC is quite crucial for its early diagnosis and treatment.

Nucleotide excision repair (NER) is one of the most versatile DNA repair pathways, which can protect cellular DNA against ultraviolet-induced cyclobutane pyrimidine dimers, DNA crosslinks, and bulky adducts<sup>[4]</sup>. It involves damage recognition, damage demarcation and unwinding, damage incision, and new strand ligation. All the stages are completed by eight key proteins, comprising DDB2, ERCC1, ERCC2, ERCC3, ERCC4, ERCC5, XPA, and XPC<sup>[5,6]</sup>, which respond to a wide range of DNA damage but are particularly important for the removal of bulky adducts caused by environmental carcinogens, such as heterocyclic amines and polycyclic aromatic hydrocarbons. They are putative environmental risk factors for colorectal neoplasia, found in tobacco smoke and red meat cooked at high temperature<sup>[7,8]</sup>. Therefore, the dysfunction of NER system may interfere with DNA damage repair from these exogenous carcinogens, and contribute to CRC development.

Genetic variation of genes can lead to the dysfunction of their encoding proteins. As the most common genetic variants in human genomes, single nucleotide polymorphisms (SNPs) are universally present in NER pathway genes. It has been suggested that NER SNPs could influence the expression or function of corresponding proteins, leading to the aberration of DNA reparative process and thus making impacts on colorectal carcinogenesis and prognosis<sup>[9,10]</sup>. Accumulating studies have investigated the association of NER SNPs with CRC risk or prognosis in various regions. For instance, Paszkowska-Szczur *et al*<sup>[11]</sup> assessed the association between SNPs in seven XP genes (XPA-XPG) and CRC risk in the Polish population, and their results confirmed that polymorphisms in XPC (rs2228000) and XPD (rs1799793 and rs238406) might be associated with CRC risk. Another study reported by Dai *et al*<sup>[12]</sup> showed that the AA genotype of ERCC1 rs2336219 had a significantly increased CRC risk and the CC genotype of ERCC1 rs735482 was associated with a lower response to oxaliplatin-based chemotherapy, shorter survival, and higher risk of relapse or metastasis. Currently, however, most researches in this field are only focused on a few SNPs in partial NER genes. A comprehensive investigation for the association of NER pathway gene polymorphisms with CRC risk and prognosis based on a large-scale



Chinese population remains lacking.

In the present study, we intend to explore the association of all tagSNPs in NER pathway genes with CRC risk and prognosis in a northern Chinese population by a two-stage case-control design composed of a discovery and validation stage. Our study aimed to identify all-round NER-based genetic biomarkers for prediction of the susceptibility to CRC and the clinical outcome of CRC patients, particularly applicable for China region.

## MATERIALS AND METHODS

### Study subjects and study design

The Ethics Committee of the First Hospital of China Medical University approved this project. All subjects provided written informed consent. A two-stage case-control study was designed. As an exploratory evaluation of selected candidate tagSNPs for disease risk, the first-stage study was carried out in a screening population of 184 CRC cases and 184 individual-matched controls (1:1) who were recruited between 2012 and 2014. Based on the initial results from these subjects, the secondary-stage study was subsequently performed in an enlarged population to validate the association of those SNPs who showed some hints in the discovery stage, consisting of 854 CRC cases and 858 frequency-matched controls in total. All the cases were selected from histopathologically confirmed CRC patients admitted to the Department of Anorectal Surgery of the First Hospital of China Medical University between September 2012 and March 2018. The controls were recruited from the healthy subjects seeking for physical examination at the hospital and the inpatients diagnosed with benign anal diseases by digital rectal examination or other approaches during the same period. The control group was matched to the case group based on gender and age ( $\pm 5$  years). Fasting venous blood sample (5 mL) was collected from each participant.

### Information collection

The epidemiological information of study participants was collected by a questionnaire survey or from the medical records of inpatients, including smoking history, drinking history, and *Helicobacter pylori* (*H. pylori*) infection status. The clinicopathological data were obtained from the pathological reports of surgical patients. Clinical staging for CRC was performed according to the UICC/AJCC TNM staging system (2002). Regular follow-up was conducted for CRC patients after radical surgery until October 2018. A total of 565 cases with available survival information were involved in the prognosis study, including survival status and overall survival (OS).

### SNP screening

A two-step strategy was adopted for SNP selection in this association study. First, we extracted all the eight NER pathway genes encompassing 5 kb of upstream and downstream flanking sequences from the HapMap Chinese Han Beijing population (<http://www.HapMap.org>)<sup>[6]</sup>. Then, the genome sequences were imported into Haploview 4.2 software to select all the tagSNPs in NER pathway genes according to the following criteria: (1) Minor allele frequency (MAF) in CHB  $> 0.05$ ; and (2) Linkage disequilibrium (LD)  $r^2 < 0.8$ . Consequently, a total of 39 candidate tagSNPs were enrolled in the discovery stage. Second, we evaluated the association between all of them and CRC risk in a small sample size. And SNP function prediction was performed using SNPinfo Web Server (<https://snpinfo.niehs.nih.gov>). Based on the analyses from the two aspects, we further screened out several SNPs for the next large-scale exploration. The screening principles were set as follows: (1) Showing a significant or borderline association with CRC risk; or (2) Having potential biological function; and (3) Having two alleles that suited for batch genotyping. Finally, 13 SNPs in six NER pathway genes were selected as research targets in the validation stage, including DDB2 rs2029298; ERCC1 rs11615 and rs735482; ERCC2 rs1052555 and rs50871; ERCC5 rs1047768, rs2094258, rs2228959, rs2296147, and rs873601; XPA rs10817938 and rs3176629; and XPC rs2607775.

### SNP genotyping

Genomic DNA was isolated from each blood sample using the phenol-chloroform method. Genotyping was conducted using kompetitive allele specific PCR with the SNPLINE platform (LGC Genomics, Hoddesdon, United Kingdom) by Shanghai Baygene Biotechnology Company Limited (China)<sup>[13]</sup>. Additionally, 10% of samples were randomly chosen to be repeatedly assayed for quality control, and the results of duplicated samples reached a 100% consistency.

### Statistical analysis

$\chi^2$  test was used to calculate the Hardy-Weinberg equilibrium (HWE) for studied SNPs in the control group and evaluate the differences in the baseline characteristics between case and control groups. The association of each SNP with CRC risk was estimated using multiple logistic regression by calculating odds ratio (OR) and 95% confidence interval (95%CI) adjusted by gender and age. Linear regression was applied to assess the cumulative effect of increasing SNP genotypes associated with CRC risk. Haplotype analysis was performed employing SHEsis online software (<http://analysis.bio-x.cn/myAnalysis.php>). Log likelihood ratio test was used to evaluate the interaction between each SNP and environmental factors on CRC risk. Kaplan-Meier method was applied to figure out median survival time (MST) and mean survival time was adopted when MST could not be calculated. Log rank test was used to judge the differences in the survival distribution between groups. The association of each SNP with CRC prognosis was estimated using Cox regression both in univariate and multivariate modes by calculating hazard ratio with 95%CI. The dominant and recessive genetic models were, respectively, defined as variant homozygote + heterozygote *vs* wild homozygote and variant homozygote *vs* heterozygote + wild homozygote. All statistical analyses mentioned above were performed with SPSS 22.0 software (Chicago, IL, United States). All the *P*-values were two-sided and statistical significance was regarded at *P* < 0.05, except the risk study in the discovery stage (*P* < 0.1).

## RESULTS

### Characteristics of study participants

In the discovery stage, 39 tagSNPs in eight NER pathway genes were genotyped in 368 subjects. The case and control groups were exactly matched (Table S1). In the validation stage, 13 SNPs in six genes were analyzed in a total of 1712 subjects, including 854 CRC cases and 858 CRC-free controls, which were also successfully matched by gender and age. Notably, the *H. pylori* infection rate was significantly higher in CRC patients than in the controls (*P* < 0.001). No significant difference was shown in the distribution of individuals with smoking or drinking history between the two groups (Table S2).

### Basic information and function prediction results of NER SNPs

The basic information and function prediction results of all tagSNPs in NER pathway genes are presented in Table 1. The assessment items for SNP function mainly contained non-synonymous SNP (nsSNP), splicing site, splicing abolish domain, exon splicing enhancer (ESE) or exon splicing silencer (ESS), stop codon, Polyphen, and transcription factor binding site.

### Association of NER SNPs with CRC risk

In the discovery stage, the association between all tagSNPs in NER pathway genes and CRC risk was initially investigated. The results showed that seven SNPs were associated with CRC risk in a screening population (*P* < 0.1, Table S3). Combined with the findings in SNP function prediction, 13 NER SNPs were chosen in the next association study with an enlarged population.

In the validation stage, we first evaluated the association between each SNP and CRC risk in overall subjects. The genotype frequency of three SNPs in the control group did not meet the HWE ( $P_{\text{HWE}} < 0.05$ ), including ERCC2 rs50871, ERCC5 rs2228959, and XPA rs3176629. On this account, they were excluded from subsequent risk study. The validated results showed that two NER SNPs were found to be associated with CRC risk. The XPA rs10817938 polymorphism conferred to an increased CRC risk in its variant homozygote and recessive model (CC *vs* TT: *P* = 0.021, OR = 1.70, 95%CI = 1.08-2.66; CC *vs* TC + TT: *P* = 0.033, OR = 1.62, 95%CI = 1.04-2.52). The variant genotypes of XPC rs2607775 polymorphism could also enhance disease risk when compared with the wild type (CG *vs* CC: *P* = 0.027, OR = 1.49, 95%CI = 1.05-2.13; CG + GG *vs* CC: *P* = 0.016, OR = 1.54, 95%CI = 1.09-2.18, Table 2).

A stratification analysis was further performed based on host characteristics, including gender and age. The associations of XPA rs10817938 and XPC rs2607775 polymorphisms with CRC risk were both demonstrated in the subgroups of male and age ≤ 60 years, while no hint was shown in the opposite groups. All related variant genotypes of them were linked to an increased CRC risk in the specific subgroups. Similar to the overall analysis, no association was observed in other NER SNPs with CRC risk either (Table S4).

**Table 1** Function prediction of nucleotide excision repair polymorphisms in the discovery stage

SNP	Chromosome	Nearby gene	Allele	Position	ns-SNP	Splicing (site)	Splicing (abolish domain)	Splicing (ESE or ESS)	Stop Codon	Polyphen	SNPs 3D (svm profile)	SNPs 3D (svm structure)	TFBS	mi-RNA (mi-Randa)	mi-RNA (Sanger)	Reg Potential	Conservation
rs2029298	11	DDB2	A/G	Promoter	--	--	--	--	--	--	--	--	Y	--	--	0	0.001
rs326222	11	DDB2	C/T	Intron	--	--	--	--	--	--	--	--	--	--	--	0	0.001
rs3781619	11	DDB2	A/G	Intron	--	--	--	--	--	--	--	--	--	--	--	NA	0
rs830083	11	DDB2	A/C/G/T	Intron	--	--	--	--	--	--	--	--	--	--	--	NA	0
rs11615	19	ERCC1	C/T	Exon	--	--	--	Y	--	--	--	--	--	--	--	0.26724	0.989
rs2298881	19	ERCC1	A/C/T	Intron	--	--	--	--	--	--	--	--	Y	--	--	0.25261	0
rs3212955	19	ERCC1	A/G	Intron	--	--	--	--	--	--	--	--	--	--	--	0.24670	0
rs3212961	19	ERCC1	A/C/T	Intron	--	--	--	--	--	--	--	--	--	--	--	0	0
rs3212986	19	ERCC1	A/C/G/T	Exon	Y	--	--	--	--	Benign	--	--	--	--	--	0.30518	0
rs735482	19	ERCC1	A/C	Exon	Y	--	--	--	--	Benign	--	--	--	--	--	0	0
rs1052555	19	ERCC2	C/T	Exon	--	--	Y	Y	--	--	--	--	--	--	--	0.47892	1
rs13181	19	ERCC2	A/G/T	Exon	Y	--	Y	Y	--	Benign	--	--	--	--	--	0.58546	0.999
rs238406	19	ERCC2	G/T	Exon	--	--	Y	Y	--	--	--	--	--	--	--	0.36557	0.996
rs238417	19	ERCC2	A/C/G	Intron	--	--	--	--	--	--	--	--	--	--	--	0.03709	0
rs50871	19	ERCC2	G/T	Intron	--	--	--	--	--	--	--	--	--	--	--	0	0.001
rs50872	19	ERCC2	A/C/T	Intron	--	--	--	--	--	--	--	--	--	--	--	0.13736	0.001
rs4150441	2	ERCC3	A/G	Intron	--	--	--	--	--	--	--	--	--	--	--	0	0
rs4150448	2	ERCC3	A/G	Intron	--	--	--	--	--	--	--	--	--	--	--	0	0
rs4150506	2	ERCC3	C/T	Intron	--	--	--	--	--	--	--	--	--	--	--	NA	0
rs1799801	16	ERCC4	C/T	Exon	--	--	--	--	--	--	--	--	--	--	--	0.20538	0.326
rs2276464	16	ERCC4	A/C/G	3'-UTR	--	--	--	--	--	--	--	--	--	Y	Y	0	0
rs254942	16	ERCC4	A/C/G/T	Intron	--	--	--	--	--	--	--	--	--	--	--	0.16803	0.005
rs1047768	13	ERCC5	C/T	Exon	--	--	Y	Y	--	--	--	--	--	--	--	0.24405	0.914
rs2094258	13	ERCC5	A/G	Promoter	--	--	--	--	--	--	--	--	Y	--	--	0	0.001
rs2228959	13	ERCC5	A/C	Exon	--	--	--	--	--	--	--	--	--	--	--	0.18140	0.509
rs2296147	13	ERCC5	C/T	Promoter	--	--	--	--	--	--	--	--	Y	--	--	0.17599	0
rs4150291	13	ERCC5	A/T	Intron	--	--	--	--	--	--	--	--	--	--	--	0	0
rs4150383	13	ERCC5	A/G	Intron	--	--	--	--	--	--	--	--	--	--	--	0	0

rs751402	13	ERCC5	C/T	Promo-ter	--	--	Y	Y	--	--	--	--	Y	--	--	0.25613	0
rs873601	13	ERCC5	A/G	Exon	--	--	Y	Y	--	--	--	--	--	Y	Y	0	0.005
rs10817938	9	XPA	C/T	Promo-ter	--	--	--	Y	--	--	--	--	--	--	--	NA	0.94
rs2808668	9	XPA	C/G/T	Intron	--	--	--	--	--	--	--	--	--	--	--	0	0.004
rs3176629	9	XPA	C/T	Promo-ter	--	--	--	--	--	--	--	--	Y	--	--	0	0
rs1870134	3	XPC	C/G/T	Exon	Y	--	--	Y	--	--	--	--	--	--	--	0.272801	0
rs2228000	3	XPC	C/T	Exon	Y	--	--	--	--	--	--	--	--	--	--	0.136701	0
rs2228001	3	XPC	A/C	Exon	Y	--	--	--	--	--	--	--	--	--	--	0.189938	1
rs2470352	3	XPC	A/G/T	Exon	--	--	--	--	--	--	--	--	--	--	--	0	0
rs2607775	3	XPC	C/G	Exon	--	--	--	Y	--	--	--	--	Y	--	--	0.282058	0

SNP: Single nucleotide polymorphism; nsSNP: Non-synonymous SNP; ESE: Exon splicing enhancer; ESS: Exon splicing silencer; TFBS: Transcription factor binding site.

### Cumulative effect of risk-related NER SNPs

Based on the findings shown in the last part, we explored the cumulative effect of NER SNPs on CRC risk. The best genetic models were identified for each polymorphism: XPA rs10817938 CC *vs* TC + TT and XPC rs2607775 CG + GG *vs* CC. According to the number of risk genotypes that individuals carried with, all the subjects were categorized into three groups (0, 1, and 2). Then, we analyzed the linear trend in CRC risk. The disease risk was found to be significantly enhanced with the increasing number of risk genotypes of studied SNPs ( $P_{\text{trend}} = 0.001$ , Table 3).

### Association of NER SNP haplotypes with CRC risk

A haplotype analysis was conducted for the SNPs in the same NER pathway gene, including ERCC1 rs11615-rs735482 and ERCC5 rs1047768-rs2094258-rs2296147-rs873601. The association between each haplotype and CRC risk was evaluated. It was suggested that one haplotype of ERCC5, C-G-C-G, demonstrated borderline significance in the association with CRC risk ( $P = 0.051$ , OR = 1.47, 95%CI = 1.00-2.17, Table S5).

### Interaction of NER SNPs with environmental factors

We further investigated the interaction effects of NER SNPs with environmental factors on CRC risk, including smoking, drinking, and *H. pylori* infection. The DDB2 rs2029298 polymorphism could be negatively interacted with drinking. Its GG genotype could reduce CRC risk by 0.52-fold in the population with drinking history when compared with GA + AA genotype ( $P_{\text{interaction}} = 0.019$ , OR = 0.52, 95%CI = 0.30-0.90). No interaction was shown between NER SNPs and smoking or *H. pylori* infection (Table 4).

### Association of NER SNPs with CRC prognosis

Before the prognosis study, an assessment was made at first for the association between host factors and the OS of CRC patients, including all the epidemiological and clinicopathological characteristics. We found the OS could be affected by TNM stage, macroscopic type, histological type, depth of invasion, growth mode, and lymphatic metastasis ( $P < 0.001$ ). Therefore, these factors were treated as adjustment parameters in the subsequent multivariate survival analysis (Table 5).

The association between NER SNPs and CRC prognosis was evaluated next. Two SNPs showed a significant association with prognosis in both univariate and multivariate analyses. The variant homozygote of ERCC2 rs1052555 polymorphism suggested a worse OS in CRC patients (TT *vs* CC:  $P = 0.010$ , OR = 14.99, 95%CI = 1.90-118.10; TT *vs* CT + CC:  $P = 0.009$ , OR = 15.89, 95%CI = 2.20-125.16). A similar trend was also indicated in the ERCC5 rs2228959 polymorphism, which conferred to a poor CRC prognosis as well (AA *vs* CC:  $P = 0.046$ , OR = 4.32, 95%CI = 1.03-18.17; AA *vs* CA + CC:  $P = 0.049$ , OR = 4.20, 95%CI = 1.00-17.60, Table 6).



**Table 2 Association between nucleotide excision repair polymorphisms and colorectal cancer risk in the validation stage<sup>1</sup>, *n* (%)**

SNP genotype	NCBI Ref	CRC	CON	P value	OR (95%CI)
<b>DDB2</b>					
rs2029298		<i>n</i> = 849	<i>n</i> = 849		
GG	32 (37.2)	393 (46.3)	385 (45.3)		1 (Ref)
GA	38 (44.2)	359 (42.3)	368 (43.3)	0.650	0.95 (0.78-1.17)
AA	16 (18.6)	97 (11.4)	96 (11.3)	0.919	0.98 (0.72-1.35)
GA + AA <i>vs</i> GG				0.677	0.96 (0.79-1.16)
AA <i>vs</i> GA + GG				0.980	1.00 (0.74-1.36)
<i>P</i> <sub>HWE</sub>	0.584		0.570		
<b>ERCC1</b>					
rs11615		<i>n</i> = 850	<i>n</i> = 847		
CC	54 (62.8)	518 (60.9)	494 (58.3)		1 (Ref)
CT	24 (27.9)	293 (34.5)	305 (36.0)	0.355	0.91 (0.74-1.11)
TT	8 (9.3)	39 (4.6)	48 (5.7)	0.248	0.77 (0.50-1.20)
CT + TT <i>vs</i> CC				0.244	0.89 (0.73-1.08)
TT <i>vs</i> CT + CC				0.321	0.80 (0.52-1.24)
<i>P</i> <sub>HWE</sub>	0.200		0.919		
rs735482		<i>n</i> = 836	<i>n</i> = 838		
CC	18 (20.9)	169 (20.2)	168 (20.0)		1 (Ref)
CA	40 (46.5)	405 (48.4)	403 (48.1)	0.966	1.00 (0.77-1.28)
AA	28 (32.6)	262 (31.3)	267 (31.9)	0.856	0.98 (0.74-1.28)
CA + AA <i>vs</i> CC				0.920	0.99 (0.78-1.26)
AA <i>vs</i> CA + CC				0.812	0.98 (0.79-1.20)
<i>P</i> <sub>HWE</sub>	0.752		0.477		
<b>ERCC2</b>					
rs1052555		<i>n</i> = 852	<i>n</i> = 851		
CC	NA	767 (90.0)	759 (89.2)		1 (Ref)
CT	NA	84 (9.9)	91 (10.7)	0.605	0.92 (0.67-1.26)
TT	NA	1 (0.1)	1 (0.1)	0.970	0.95 (0.06-15.21)
CT + TT <i>vs</i> CC				0.602	0.92 (0.67-1.26)
TT <i>vs</i> CT + CC				0.971	0.95 (0.06-15.22)
<i>P</i> <sub>HWE</sub>	NA		0.307		
rs50871		<i>n</i> = 838	<i>n</i> = 845		
TT	40 (46.5)	429 (51.2)	451 (53.4)		1 (Ref)
TG	36 (41.9)	337 (40.2)	358 (42.4)	0.922	0.99 (0.81-1.21)
GG	10 (11.6)	72 (8.6)	36 (4.3)	0.001	2.09 (1.37-3.19)
TG + GG <i>vs</i> TT				0.374	1.09 (0.90-1.32)
GG <i>vs</i> TG + TT				< 0.001	2.08 (1.38-3.15)
<i>P</i> <sub>HWE</sub>	1.000		0.001		
<b>ERCC5</b>					
rs1047768		<i>n</i> = 839	<i>n</i> = 845		
CC	8 (9.3)	75 (8.9)	71 (8.4)		1 (Ref)
CT	30 (34.9)	348 (41.5)	351 (41.5)	0.735	0.94 (0.66-1.35)
TT	48 (55.8)	416 (49.6)	423 (50.1)	0.708	0.94 (0.66-1.33)
CT + TT <i>vs</i> CC				0.717	0.94 (0.67-1.32)
TT <i>vs</i> CT + CC				0.822	0.98 (0.81-1.19)
<i>P</i> <sub>HWE</sub>	0.480		0.880		
rs2094258		<i>n</i> = 843	<i>n</i> = 841		
GG	38 (44.2)	307 (36.4)	326 (38.8)		1 (Ref)
GA	42 (48.8)	409 (48.5)	392 (46.6)	0.389	1.10 (0.89-1.35)
AA	6 (7.0)	127 (15.1)	123 (14.6)	0.615	1.08 (0.80-1.45)
GA + AA <i>vs</i> GG				0.370	1.10 (0.90-1.33)
AA <i>vs</i> GA + GG				0.837	1.03 (0.79-1.35)

$P_{HWE}$	0.403		0.770		
rs2228959		<i>n</i> = 841	<i>n</i> = 851		
CC	74 (86.0)	754 (89.7)	782 (91.9)		1 (Ref)
CA	12 (14.0)	83 (9.9)	62 (7.3)	0.051	1.41 (1.00-1.99)
AA	0 (0.0)	4 (0.5)	7 (0.8)	0.408	0.59 (0.17-2.04)
CA + AA <i>vs</i> CC				0.095	1.33 (0.95-1.85)
AA <i>vs</i> CA + CC				0.383	0.58 (0.17-1.98)
$P_{HWE}$	1.000		< 0.001		
rs2296147		<i>n</i> = 844	<i>n</i> = 847		
TT	52 (60.5)	508 (60.2)	517 (61.0)		1 (Ref)
TC	32 (37.2)	294 (34.8)	289 (34.1)	0.684	1.04 (0.85-1.28)
CC	2 (2.3)	42 (5.0)	41 (4.8)	0.904	1.03 (0.66-1.61)
TC + CC <i>vs</i> TT				0.679	1.04 (0.86-1.27)
CC <i>vs</i> TC + TT				0.952	1.01 (0.65-1.58)
$P_{HWE}$	0.439		0.940		
rs873601		<i>n</i> = 842	<i>n</i> = 837		
GG	16 (18.6)	230 (27.3)	223 (26.6)		1 (Ref)
GA	48 (55.8)	435 (51.7)	413 (49.3)	0.807	1.03 (0.82-1.29)
AA	22 (25.6)	177 (21.0)	201 (24.0)	0.310	0.87 (0.66-1.14)
GA + AA <i>vs</i> GG				0.849	0.98 (0.79-1.22)
AA <i>vs</i> GA + GG				0.155	0.85 (0.67-1.07)
$P_{HWE}$	0.439		0.719		
XPA					
rs10817938		<i>n</i> = 823	<i>n</i> = 822		
TT	58 (67.4)	511 (62.1)	547 (66.5)		1 (Ref)
TC	24 (27.9)	259 (31.5)	241 (29.3)	0.231	1.14 (0.92-1.41)
CC	4 (4.7)	53 (6.4)	34 (4.1)	0.021	1.70 (1.08-2.66)
TC + CC <i>vs</i> TT				0.071	1.21 (0.98-1.48)
CC <i>vs</i> TC + TT				0.033	1.62 (1.04-2.52)
$P_{HWE}$	0.655		0.257		
rs3176629		<i>n</i> = 847	<i>n</i> = 852		
CC	68 (79.1)	689 (81.3)	706 (82.9)		1 (Ref)
CT	18 (20.9)	151 (17.8)	133 (15.6)	0.240	1.17 (0.90-1.51)
TT	0 (0.0)	7 (0.8)	13 (1.5)	0.225	0.56 (0.22-1.42)
CT + TT <i>vs</i> CC				0.399	1.11 (0.87-1.43)
TT <i>vs</i> CT + CC				0.205	0.55 (0.22-1.39)
$P_{HWE}$	0.752		0.024		
XPC					
rs2607775		<i>n</i> = 840	<i>n</i> = 850		
CC	76 (84.5)	755 (89.9)	792 (93.2)		1 (Ref)
CG	12 (13.3)	80 (9.5)	56 (6.6)	0.027	1.49 (1.05-2.13)
GG	2 (2.2)	5 (0.6)	2 (0.2)	0.219	2.81 (0.54-14.56)
CG + GG <i>vs</i> CC				0.016	1.54 (1.09-2.18)
GG <i>vs</i> CG + CC				0.238	2.69 (0.52-13.95)
$P_{HWE}$	0.251		0.343		

<sup>1</sup>*P* was adjusted by gender and age. Statistically significant associations are in bold (*P* < 0.05). SNP: Single nucleotide polymorphism; NCBI Ref: Reference frequency of the SNPs in healthy controls (Beijing Han, China, NCBI database); CRC: Colorectal cancer; CON: Control; OR: Odds ratio; CI: Confidence interval;  $P_{HWE}$ : Hardy-Weinberg Equilibrium in control group; NA: Not available.

## DISCUSSION

In the present study, we explored the association of all tagSNPs in eight NER pathway genes with CRC risk and prognosis in a total of 1712 northern Chinese. In the discovery stage, 39 tagSNPs were analyzed for their association and potential biological function, and 13 SNPs were enrolled in the validation stage. Among them,

**Table 3 Cumulative effect of nucleotide excision repair polymorphisms associated with colorectal cancer risk<sup>1</sup>, n (%)**

Number of SNP risk genotypes	CRC	CON	P value	OR (95%CI)
	n = 841	n = 847		
0	706 (83.9)	755 (89.1)		1 (Ref)
1	131 (15.6)	92 (10.9)	0.004	1.53 (1.15-2.04)
2	4 (0.5)	0 (0.0)	NA	NA
			<i>P</i> <sub>trend</sub> = 0.001	

<sup>1</sup>*P* was adjusted by gender and age. Statistically significant associations are in bold (*P* < 0.05). SNP: Single nucleotide polymorphism; CRC: Colorectal cancer; CON: Control; OR: Odds ratio; CI: Confidence interval; NA: Not available.

the XPA rs10817938 and XPC rs2607775 polymorphisms were found to be associated with CRC risk both in overall and stratified analyses. They also demonstrated cumulative effects on disease risk with the increasing number of risk genotypes. Moreover, the DDB2 rs2029298 polymorphism had a negative interaction effect with drinking on CRC risk. In the prognosis study, the ERCC2 rs1052555 and ERCC5 rs2228959 polymorphisms were associated with the OS of CRC cases. To our knowledge, this is the first comprehensive report on the association of NER SNPs with CRC risk and prognosis based on a large-scale Chinese population.

In our research, the XPA rs10817938 and XPC rs2607775 polymorphisms showed a significant association with an increased CRC risk. The XPA (xeroderma pigmentosum group A) gene, located in chromosome 9q22.3 containing 9 exons and 8 introns, encodes a zinc finger DNA-binding protein involved in NER to maintain genomic integrity<sup>[14]</sup>. It was suggested that the XPA protein was significantly decreased in CRC tissue than in adjacent non-tumor tissue, and its high expression showed an association with better survival of CRC cases<sup>[15]</sup>. Therefore, XPA is a CRC-related protein marker. The gene polymorphisms in XPA were also revealed to be associated with CRC risk, such as 23Gly/Ala (rs1800975)<sup>[16-19]</sup>. However, rare studies have focused on the rs10817938 polymorphism, which has been only reported by Hu *et al*<sup>[20]</sup> that rs10817938 CT/TT genotype retains a significant association with a longer OS (*P* = 0.008) in CRC patients receiving oxaliplatin-based chemotherapy. Thus, our study first referred to it as a CRC risk-related SNP. Similar to XPA, the XPC (xeroderma pigmentosum group C) gene is also a well-accepted marker related to CRC, which is located in chromosome 3p25 with 16 exons and 15 introns<sup>[21]</sup>. It encodes a 940-amino acid protein involved in DNA damage recognition and DNA repair initiation in the NER pathway, and the binding of XPC to damaged DNA is the rate-limiting step for NER<sup>[22-24]</sup>. The XPC gene is highly polymorphic and its SNPs have been foci of interest for the association with CRC risk, such as 939Lys/Gln (rs2228001) and 499Ala/Val (rs2228000)<sup>[25-29]</sup>. In our study, we newly found that the rs2607775 polymorphism could modulate CRC risk. In a word, the XPA rs10817938 and XPC rs2607775 polymorphisms could be potential genetic markers applicable for the prediction of CRC susceptibility in the future.

In the stratified analysis, it was noteworthy that the two meaningful SNPs for CRC risk in the overall population only demonstrated their association in the male and age ≤ 60 years subgroups, while no significance was found in the female and age > 60 years subgroups. The risk effects of NER SNPs seemed to change with gender and age. The morbidity and mortality of CRC are higher in men than in women both in China and worldwide<sup>[1,30]</sup>. That could be attributed to a subset of X-chromosome genes escaping X-inactivation, named “escape from X-inactivation tumor-suppressor” (EXITS) genes, which would protect females from complete functional loss by a single mutation and thus result in sex bias in a variety of tumor types<sup>[31]</sup>. In addition, it is well acknowledged that CRC incidence strongly increases with age, probably due to the weakened immunity and accumulated carcinogens with people aging<sup>[30,32]</sup>. As a result, the association of NER SNPs could be masked by gender and age but manifested when the two factors are considered as stratification items to eliminate their effects on CRC risk. These findings suggested the XPA rs10817938 and XPC rs2607775 polymorphisms might also be predictive biomarkers for the susceptibility to CRC in some specific populations like males or youngsters.

Owing to the multiple elements involved in carcinogenesis, the efficacy of single polymorphism for risk detection is relatively limited. And the combination of multi-variants usually has more advantages<sup>[33,34]</sup>. In our study, a significant cumulative trend was shown in NER SNPs for the association with CRC risk, which could be enhanced

**Table 4** Effect of interaction between nucleotide excision repair polymorphisms and environmental factors on colorectal cancer risk<sup>1</sup>

SNP genotype	Smoking		Drinking		<i>Helicobacter pylori</i> infection	
	No	Yes	No	Yes	Negative	Positive
DDB2						
rs2029298	<i>n</i> = 981	<i>n</i> = 468	<i>n</i> = 1190	<i>n</i> = 257	<i>n</i> = 810	<i>n</i> = 443
GA + AA						
Case/Control	312/220	142/104	367/274	87/49	164/286	189/44
OR (95%CI)	1 (Ref)	0.96 (0.71-1.31)	1 (Ref)	1.33 (0.90-1.95)	1 (Ref)	7.49 (5.12-10.96)
GG						
Case/Control	267/182	124/98	330/219	61/60	140/220	158/52
OR (95%CI)	1.03 (0.80-1.34)	0.89 (0.65-1.22)	1.13 (0.89-1.42)	0.76 (0.51-1.12)	1.11 (0.83-1.48)	5.30 (3.67-7.65)
	<i>P</i> <sub>interaction</sub> = 0.618		<i>P</i> <sub>interaction</sub> = 0.019 OR (95%CI) = 0.52 (0.30-0.90)		<i>P</i> <sub>interaction</sub> = 0.095	
ERCC1						
rs11615	<i>n</i> = 982	<i>n</i> = 467	<i>n</i> = 1190	<i>n</i> = 257	<i>n</i> = 812	<i>n</i> = 444
CT + TT						
Case/Control	231/160	101/88	278/205	54/40	110/210	146/42
OR (95%CI)	1 (Ref)	0.80 (0.56-1.13)	1 (Ref)	1.00 (0.64-1.56)	1 (Ref)	6.64 (4.39-10.04)
CC						
Case/Control	349/242	165/113	421/286	93/70	194/298	203/53
OR (95%CI)	1.00 (0.77-1.30)	1.01 (0.74-1.38)	1.09 (0.86-1.37)	0.98 (0.68-1.40)	1.24 (0.93-1.67)	7.31 (5.00-10.70)
	<i>P</i> <sub>interaction</sub> = 0.309		<i>P</i> <sub>interaction</sub> = 0.749		<i>P</i> <sub>interaction</sub> = 0.642	
rs735482	<i>n</i> = 968	<i>n</i> = 461	<i>n</i> = 1171	<i>n</i> = 256	<i>n</i> = 803	<i>n</i> = 434
AA						
Case/Control	175/124	87/64	213/148	49/40	89/161	115/24
OR (95%CI)	1 (Ref)	0.96 (0.65-1.43)	1 (Ref)	0.85 (0.53-1.36)	1 (Ref)	8.67 (5.20-14.44)
CA + CC						
Case/Control	396/273	174/136	471/339	99/68	212/341	224/71
OR (95%CI)	1.03 (0.78-1.36)	0.91 (0.66-1.25)	0.97 (0.75-1.24)	1.01 (0.70-1.47)	1.13 (0.82-1.53)	5.71 (3.94-8.28)
	<i>P</i> <sub>interaction</sub> = 0.638		<i>P</i> <sub>interaction</sub> = 0.446		<i>P</i> <sub>interaction</sub> = 0.082	
ERCC2						
rs1052555	<i>n</i> = 986	<i>n</i> = 468	<i>n</i> = 1193	<i>n</i> = 259	<i>n</i> = 811	<i>n</i> = 447
CT + TT						
Case/Control	55/39	30/27	68/56	17/10	27/54	39/11
OR (95%CI)	1 (Ref)	0.79 (0.41-1.53)	1 (Ref)	1.40 (0.59-3.30)	1 (Ref)	7.09 (3.15-15.99)
CC						
Case/Control	527/365	236/175	632/437	131/101	277/453	312/85
OR (95%CI)	1.02 (0.67-1.58)	0.96 (0.61-1.51)	1.19 (0.82-1.73)	1.07 (0.69-1.66)	1.22 (0.75-1.99)	7.34 (4.36-12.35)
	<i>P</i> <sub>interaction</sub> = 0.624		<i>P</i> <sub>interaction</sub> = 0.319		<i>P</i> <sub>interaction</sub> = 0.712	
ERCC5						
rs1047768	<i>n</i> = 973	<i>n</i> = 464	<i>n</i> = 1177	<i>n</i> = 258	<i>n</i> = 808	<i>n</i> = 437
CT + TT						
Case/Control	524/368	236/190	622/452	138/103	272/460	317/88
OR (95%CI)	1 (Ref)	0.87 (0.69-1.10)	1 (Ref)	0.97 (0.73-1.29)	1 (Ref)	6.09 (4.61-8.06)
CC						
Case/Control	49/32	26/12	66/37	9/8	29/47	26/6
OR (95%CI)	1.08 (0.68-1.71)	1.52 (0.76-3.06)	1.30 (0.85-1.97)	0.82 (0.31-2.14)	1.04 (0.64-1.70)	7.33 (2.98-18.03)
	<i>P</i> <sub>interaction</sub> = 0.241		<i>P</i> <sub>interaction</sub> = 0.491		<i>P</i> <sub>interaction</sub> = 0.843	
rs2094258	<i>n</i> = 973	<i>n</i> = 464	<i>n</i> = 1180	<i>n</i> = 255	<i>n</i> = 805	<i>n</i> = 443
GG						
Case/Control	209/150	97/70	251/180	55/40	119/203	116/38
OR (95%CI)	1 (Ref)	1.00 (0.69-1.44)	1 (Ref)	0.99 (0.63-1.55)	1 (Ref)	5.21 (3.39-8.01)
GA + AA						
Case/Control	364/250	169/128	442/307	91/69	181/302	233/56



OR (95%CI)	1.05 (0.80-1.36)	0.95 (0.69-1.29)	1.03 (0.81-1.31)	0.95 (0.66-1.37)	1.02 (0.76-1.37)	7.10 (4.91-10.27)
	$P_{\text{interaction}} = 0.587$		$P_{\text{interaction}} = 0.685$		$P_{\text{interaction}} = 0.314$	
rs2296147	$n = 979$	$n = 466$	$n = 1185$	$n = 258$	$n = 807$	$n = 440$
TT						
Case/Control	356/251	151/126	426/301	81/75	184/298	207/59
OR (95%CI)	1 (Ref)	0.85 (0.64-1.13)	1 (Ref)	0.76 (0.54-1.08)	1 (Ref)	5.68 (4.03-8.01)
TC+CC						
Case/Control	221/151	112/77	268/190	65/37	118/207	138/36
OR (95%CI)	1.03 (0.79-1.34)	1.03 (0.74-1.43)	1.00 (0.79-1.26)	1.24 (0.81-1.91)	0.92 (0.69-1.24)	6.21 (4.12-9.36)
	$P_{\text{interaction}} = 0.506$		$P_{\text{interaction}} = 0.089$		$P_{\text{interaction}} = 0.562$	
rs873601	$n = 974$	$n = 462$	$n = 1179$	$n = 255$	$n = 798$	$n = 439$
AA						
Case/Control	130/94	47/51	148/116	29/28	69/126	75/25
OR (95%CI)	1 (Ref)	0.67 (0.41-1.07)	1 (Ref)	0.81 (0.46-1.44)	1 (Ref)	5.48 (3.19-9.40)
GA + GG						
Case/Control	446/304	215/149	543/372	118/80	234/369	269/70
OR (95%CI)	1.06 (0.78-1.44)	1.04 (0.74-1.46)	1.14 (0.87-1.51)	1.16 (0.80-1.68)	1.16 (0.83-1.62)	7.02 (4.73-10.41)
	$P_{\text{interaction}} = 0.202$		$P_{\text{interaction}} = 0.550$		$P_{\text{interaction}} = 0.764$	
XPA						
rs10817938	$n = 952$	$n = 453$	$n = 1152$	$n = 252$	$n = 785$	$n = 429$
TC + TT						
Case/Control	527/380	239/183	631/459	135/103	281/470	311/88
OR (95%CI)	1 (Ref)	0.94 (0.75-1.19)	1 (Ref)	0.95 (0.72-1.27)	1 (Ref)	5.91 (4.47-7.81)
CC						
Case/Control	33/12	20/11	45/17	8/6	14/20	25/5
OR (95%CI)	1.98 (1.01-3.89)	1.31 (0.62-2.77)	1.93 (1.09-3.41)	0.97 (0.33-2.81)	1.17 (0.58-2.36)	8.36 (3.17-22.09)
	$P_{\text{interaction}} = 0.516$		$P_{\text{interaction}} = 0.299$		$P_{\text{interaction}} = 0.738$	
XPC						
rs2607775	$n = 979$	$n = 463$	$n = 1184$	$n = 256$	$n = 809$	$n = 439$
CC						
Case/Control	513/369	238/195	617/458	134/103	273/475	314/88
OR (95%CI)	1 (Ref)	0.88 (0.70-1.11)	1 (Ref)	0.97 (0.73-1.28)	1 (Ref)	6.21 (4.70-8.21)
CG + GG						
Case/Control	61/36	24/6	73/36	12/7	28/33	30/7
OR (95%CI)	1.22 (0.79-1.88)	2.88 (1.16-7.11)	1.51 (0.99-2.28)	1.27 (0.50-3.26)	1.48 (0.87-2.50)	7.46 (3.23-17.21)
	$P_{\text{interaction}} = 0.066$		$P_{\text{interaction}} = 0.728$		$P_{\text{interaction}} = 0.766$	

<sup>1</sup> $P$  for interaction was adjusted by gender and age. Statistically significant associations are in bold ( $P < 0.05$ ). SNP: Single nucleotide polymorphism; CRC: Colorectal cancer; CON: Control; OR: Odds ratio; CI: Confidence interval.

with the increasing number of risk genotypes (XPA rs10817938 CC and XPC rs2607775 CG + GG). That indicated a dosage effect of risk-related NER SNPs that an individual carried with. Moreover, borderline significance linked to CRC risk was observed in a haplotype of ERCC5 rs1047768-rs2094258-rs2296147-rs873601 (C-G-C-G). Therefore, better diagnostic capacity for the susceptibility to CRC could be obtained when combining multiple SNPs in NER pathway genes.

Except for genetic factors, environmental factors also play a vital role in CRC development such as tobacco smoking, alcohol consumption, and dietary constituents especially red meat<sup>[35-37]</sup>. Knowledge of gene-environment interactions may help to elucidate substantial hidden heritability within the architecture of cancer initiation<sup>[38]</sup>. The effects of interaction between SNPs in NER pathway genes and environmental factors on CRC risk has been preliminarily explored<sup>[39]</sup>. Here, we newly found that the DDB2 rs2029298 polymorphism could be negatively interacted with drinking-related CRC risk. In contrast to this, no association was found in any DDB2 SNP in the main effect analysis. Alcohol consumption is a well-recognized carcinogen of CRC due to DNA lesion caused by the exposure of DNA to acetaldehyde produced by ethanol<sup>[40]</sup>. However, the effect of DDB2 rs2029298 polymorphism was modified in the population with drinking history and its GG genotype decreased CRC risk by 0.52-fold, suggesting that an antagonism existed between DDB2 SNPs with drinking.

**Table 5 Association between host factors and the overall survival of colorectal cancer patients**

Factor	CRC patients	Death	MST (M)	P value
Total	n = 565	n = 95		
Gender				0.862
Male	384	63	46.6 <sup>1</sup>	
Female	181	32	47.1 <sup>1</sup>	
Age (yr)				0.127
≤ 60	322	46	47.9 <sup>1</sup>	
> 60	243	49	44.7 <sup>1</sup>	
Smoking				0.111
Ever Smoker	180	23	48.7 <sup>1</sup>	
Never Smoker	383	72	45.9 <sup>1</sup>	
Drinking				0.157
Drinker	107	14	49.3 <sup>1</sup>	
Non-drinker	456	81	46.1 <sup>1</sup>	
TNM stage				< 0.001
I + II	336	23	52.1 <sup>1</sup>	
III + IV	223	69	48	
Macroscopic type				< 0.001
Protrude type	104	5	53.4 <sup>1</sup>	
Ulcerative/Invasive type	458	90	45.2 <sup>1</sup>	
Histological type				< 0.001
High/Middle differentiation	367	40	50.2 <sup>1</sup>	
Low differentiation	196	55	39.3 <sup>1</sup>	
Depth of invasion				< 0.001
T1 + T2	114	6	53.4 <sup>1</sup>	
T3 + T4	450	89	44.9 <sup>1</sup>	
Growth mode				< 0.001
Nest	236	18	52.1 <sup>1</sup>	
Invasion	326	77	42.6 <sup>1</sup>	
Lymphatic metastasis				< 0.001
Positive	217	68	47	
Negative	342	24	52.0 <sup>1</sup>	

CRC: Colorectal cancer; MST (M): Median survival time (mo).

<sup>1</sup>Mean survival time was provided when MST could not be calculated. Statistically significant associations are in bold ( $P < 0.05$ ).

Hence, the interactions between NER SNPs and environmental factors may also benefit the risk prediction of CRC. The possible mechanism concerned with our findings needs to be clarified by further researches.

In addition to CRC susceptibility, the influence of SNPs in NER pathway genes on CRC prognosis cannot be ignored either. The present study showed that the ERCC2 rs1052555 and ERCC5 rs2228959 polymorphisms were associated with a poor OS in CRC patients. The ERCC2 (excision repair cross-complementing group 2) gene, also known as XPD (xeroderma pigmentosum group D) with 24 exons and 23 introns, encodes a helicase, which is a component of transcription factor TFIIH participating in the opening of damaged DNA during NER<sup>[41]</sup>. Mounting evidence has demonstrated that the SNPs in ERCC2 have predictive values for the clinical outcome of CRC patients treated with various chemotherapy, such as 751Lys/Gln (13181)<sup>[42-46]</sup>. However, no report has referred to the rs1052555 polymorphism yet, which is located in exon 24 of ERCC2. According to the SNP function prediction, it may affect the splicing pattern of mRNA after transcription as a result of the formation of splicing abolish domain or ESE/ESS. And both the RegPotential and Conservation scores were relatively high, suggesting that it might be a highly conserved variant in the course of evolution with regulatory roles. Therefore, the ERCC2 rs1052555 polymorphism is very likely to be a functional SNP and should be paid more attention in the future. The other highly polymorphic NER gene, ERCC5 (excision repair cross-

**Table 6 Association between nucleotide excision repair polymorphisms and colorectal cancer prognosis**

SNP genotype	CRC patients	Death	MST (M)	Univariate		Multivariate	
				P value	HR (95%CI)	P value	HR (95%CI)
DDB2							
rs2029298	n = 560	n = 94					
GG	262	50	44.4 <sup>1</sup>		1(Ref)		1 (Ref)
GA	230	35	47.4 <sup>1</sup>	0.368	0.82 (0.53-1.26)	0.393	0.82 (0.53-1.29)
AA	68	9	48.6 <sup>1</sup>	0.265	0.67 (0.33-1.36)	0.467	0.77 (0.37-1.57)
GA + AA vs GG				0.235	0.78 (0.52-1.17)	0.307	0.81 (0.53-1.22)
AA vs GA + GG				0.370	0.73 (0.37-1.45)	0.581	0.82 (0.41-1.65)
ERCC1							
rs11615	n = 561	n = 95					
CC	345	62	46.4 <sup>1</sup>		1 (Ref)		1 (Ref)
CT	188	29	47.2 <sup>1</sup>	0.647	0.90 (0.58-1.40)	0.947	1.02 (0.65-1.59)
TT	28	4	45.8 <sup>1</sup>	0.955	0.97 (0.35-2.67)	0.975	0.98 (0.35-2.76)
CT + TT vs CC				0.662	0.91 (0.60-1.39)	0.974	0.99 (0.65-1.53)
TT vs CT + CC				0.999	1.00 (0.37-2.73)	0.911	0.94 (0.34-2.60)
rs735482	n = 552	n = 91					
CC	123	23	46.8 <sup>1</sup>		1 (Ref)		1 (Ref)
CA	258	38	47.3 <sup>1</sup>	0.982	0.99 (0.59-1.67)	0.582	1.16 (0.69-1.96)
AA	171	30	45.5 <sup>1</sup>	0.603	1.16 (0.67-1.99)	0.774	0.92 (0.53-1.61)
CA + AA vs CC				0.829	1.05 (0.66-1.69)	0.923	1.02 (0.64-1.65)
AA vs CA + CC				0.517	1.16 (0.75-1.79)	0.521	0.86 (0.55-1.35)
ERCC2							
rs1052555	n = 563	n = 95					
CC	506	86	46.6 <sup>1</sup>		1 (Ref)		1 (Ref)
CT	56	8	48.3 <sup>1</sup>	0.377	0.72 (0.35-1.49)	0.998	1.00 (0.48-2.09)
TT	1	1	2	< 0.001	49.73 (6.37-388.47)	0.010	14.99 (1.90-118.10)
CT + TT vs CC				0.551	0.81 (0.41-1.61)	0.744	1.12 (0.56-2.26)
TT vs CT + CC				< 0.001	55.22 (7.07-431.35)	0.009	15.89 (2.02-125.16)
rs50871	n = 551	n = 92					
TT	294	43	47.0 <sup>1</sup>		1 (Ref)		1 (Ref)
TG	210	40	45.7 <sup>1</sup>	0.256	1.28 (0.83-1.98)	0.446	1.19 (0.77-1.84)
GG	47	9	45.8 <sup>1</sup>	0.541	1.25 (0.61-2.57)	0.576	0.80 (0.37-1.74)
TG + GG vs TT				0.239	1.28 (0.85-1.93)	0.646	1.10 (0.73-1.68)
GG vs TG + TT				0.749	1.12 (0.56-2.23)	0.354	0.71 (0.34-1.47)
ERCC5							
rs1047768	n = 553	n = 92					
CC	55	9	46.7 <sup>1</sup>		1 (Ref)		1 (Ref)
CT	233	44	46.5 <sup>1</sup>	0.785	1.11 (0.54-2.26)	0.945	0.97 (0.45-2.09)
TT	265	39	47.0 <sup>1</sup>	0.933	1.03 (0.50-2.13)	0.542	0.78 (0.36-1.72)
CT + TT vs CC				0.851	1.07 (0.54-2.13)	0.768	0.90 (0.43-1.87)
TT vs CT + CC				0.799	0.95 (0.63-1.43)	0.387	0.83 (0.54-1.27)
rs2094258	n = 555	n = 93					
GG	207	38	46.6 <sup>1</sup>		1 (Ref)		1 (Ref)
GA	269	42	47.0 <sup>1</sup>	0.721	0.92 (0.60-1.43)	0.400	0.82 (0.53-1.29)
AA	79	13	44.3 <sup>1</sup>	0.973	0.99 (0.53-1.86)	0.588	0.84 (0.44-1.59)
GA + AA vs GG				0.773	0.94 (0.62-1.42)	0.424	0.84 (0.55-1.29)
AA vs GA + GG				0.869	1.05 (0.59-1.89)	0.916	1.03 (0.57-1.87)
rs2228959	n = 558	n = 93					
CC	501	82	47.1 <sup>1</sup>		1 (Ref)		1 (Ref)
CA	53	9	45.4 <sup>1</sup>	0.768	1.11 (0.56-2.21)	0.811	0.92 (0.46-1.85)
AA	4	2	13.8 <sup>1</sup>	0.006	7.18 (1.75-29.50)	0.046	4.32 (1.03-18.17)
CA + AA vs CC				0.402	1.31 (0.70-2.46)	0.847	1.07 (0.56-2.02)

AA <i>vs</i> CA + CC				0.006	7.16 (1.75-29.32)	0.049	4.20 (1.00-17.60)
rs2296147	<i>n</i> = 556	<i>n</i> = 92					
TT	318	46	47.4 <sup>1</sup>		1 (Ref)		1 (Ref)
TC	207	42	45.4 <sup>1</sup>	0.384	1.21 (0.79-1.83)	0.194	1.32 (0.87-2.02)
CC	31	4	48.1 <sup>1</sup>	0.691	0.81 (0.29-2.26)	0.658	1.32 (0.38-4.57)
TC + CC <i>vs</i> TT				0.484	1.16 (0.77-1.74)	0.184	1.33 (0.87-2.02)
CC <i>vs</i> TC + TT				0.573	0.75 (0.28-2.04)	0.978	1.02 (0.31-3.32)
rs873601	<i>n</i> = 558	<i>n</i> = 95					
GG	140	21	47.5 <sup>1</sup>		1 (Ref)		1 (Ref)
GA	301	49	46.9 <sup>1</sup>	0.745	1.09 (0.65-1.82)	0.923	0.98 (0.58-1.64)
AA	117	25	44.5 <sup>1</sup>	0.293	1.37 (0.76-2.44)	0.713	1.12 (0.62-2.03)
GA + AA <i>vs</i> GG				0.526	1.17 (0.72-1.90)	0.951	1.02 (0.62-1.66)
AA <i>vs</i> GA + GG				0.275	1.29 (0.82-2.04)	0.473	1.19 (0.74-1.90)
XPA							
rs10817938	<i>n</i> = 545	<i>n</i> = 93					
TT	351	61	46.6 <sup>1</sup>		1 (Ref)		1 (Ref)
TC	163	29	46.2 <sup>1</sup>	0.815	1.05 (0.68-1.64)	0.472	1.18 (0.75-1.88)
CC	31	3	49.5 <sup>1</sup>	0.429	0.63 (0.20-2.00)	0.903	0.93 (0.29-3.02)
TC + CC <i>vs</i> TT				0.968	0.99 (0.65-1.52)	0.489	1.17 (0.75-1.83)
CC <i>vs</i> TC+TT				0.414	0.62 (0.20-1.96)	0.863	0.90 (0.28-2.89)
rs3176629	<i>n</i> = 558	<i>n</i> = 94					
CC	450	74	47.0 <sup>1</sup>		1 (Ref)		1 (Ref)
CT	103	19	44.8 <sup>1</sup>	0.470	1.20 (0.73-1.99)	0.420	0.81 (0.48-1.36)
TT	5	1	49.3 <sup>1</sup>	0.824	0.80 (0.11-5.76)	0.660	0.64 (0.09-4.64)
CT + TT <i>vs</i> CC				0.521	1.18 (0.72-1.93)	0.375	0.79 (0.47-1.33)
TT <i>vs</i> CT + CC				0.787	0.76 (0.11-5.47)	0.690	0.67 (0.09-4.82)
XPC							
rs2607775	<i>n</i> = 556	<i>n</i> = 92					
CC	494	84	46.8 <sup>1</sup>		1 (Ref)		1 (Ref)
CG	57	8	46.3 <sup>1</sup>	0.739	0.88 (0.43-1.83)	0.842	0.93 (0.44-1.94)
GG	5	0	NA	0.525	NA	0.969	NA
CG + GG <i>vs</i> CC				0.555	0.80 (0.39-1.66)	0.604	0.82 (0.40-1.72)
GG <i>vs</i> CG + CC				0.528	NA	0.970	NA

SNP: Single nucleotide polymorphism; CRC: Colorectal cancer; MST (M): Median survival time (mo); HR: Hazard ratio; CI: Confidence interval; NA: Not available.

<sup>1</sup>mean survival time was provided when MST could not be calculated. Statistically significant associations are in bold ( $P < 0.05$ ).

complementing group 5) or XPG (xeroderma pigmentosum group G), is located in chromosome 13q22-123, consisting of 15 exons and 14 introns<sup>[47]</sup>. The protein of 1186 amino acids encoded by ERCC5 is a member of the flap structure-specific endonuclease (FEN1) family and plays an essential role in the two incision steps of NER<sup>[48,49]</sup>. A few SNPs in ERCC5 have been reported to be associated with CRC prognosis although the rs2228959 polymorphism is not covered, which belongs to exon 8 of the gene<sup>[50-53]</sup>. Interestingly, the SNP function prediction showed no special hint for its potential biological function. A reasonable interpretation for the phenomenon could be that the observation on CRC prognosis might not result from the focused polymorphism rs2228959, instead, another undiscovered variant in strong LD with it located in ERCC5 or neighbor genes<sup>[54]</sup>. Anyway, the ERCC2 rs1052555 and ERCC5 rs2228959 polymorphisms could be novel genetic biomarkers with predictive values for the clinical outcome of CRC patients. Further investigations are needed to validate all the assumptions.

Some limitations in our study should be acknowledged. First, the design of a retrospective case-control study had its inherent limitations. Second, a small percentage of data missing may influence the statistical efficacy to some extent. Additionally, only association study was emphasized in our research. All involved mechanisms need to be investigated by in-depth molecular experiments in the future.

In summary, a two-stage case-control study was performed to explore the association of all tagSNPs in eight NER pathway genes with CRC risk and prognosis in a northern Chinese population, including a discovery and validation stage. Two



SNPs (XPA rs10817938 and XPC rs2607775) were found to contribute to an increased CRC risk in overall and stratification analyses. Another two SNPs (ERCC2 rs1052555 and ERCC5 rs2228959) were found to be associated with a poor CRC prognosis. The present study has referential values for the identification of NER-based genetic biomarkers in predicting the susceptibility and clinical outcome of CRC, and may also provide clues for the access to individualized early diagnosis and therapy of CRC patients.

## ARTICLE HIGHLIGHTS

### Research background

Single nucleotide polymorphisms (SNPs) are universally present in nucleotide excision repair (NER) pathway genes. Previous studies have suggested that NER SNPs could make impacts on colorectal cancer (CRC) risk and prognosis.

### Research motivation

Currently, most researches in this field are only focused on a few SNPs in partial NER genes. A comprehensive investigation based on a large-scale Chinese population remains lacking.

### Research objectives

The study aimed to explore the association of all tagSNPs in NER pathway genes with CRC risk and prognosis in a northern Chinese population by a two-stage case-control design composed of a discovery and validation stage.

### Research methods

Genotyping for NER SNPs was performed using kompetitive allele specific PCR. In the discovery stage, 39 tagSNPs in eight genes were genotyped in 368 subjects, including 184 CRC cases and 184 individual-matched controls. In the validation stage, 13 SNPs in six genes were analyzed in a total of 1712 subjects, including 854 CRC cases and 858 CRC-free controls.

### Research results

We found that two SNPs (XPA rs10817938 and XPC rs2607775) were associated with an increased CRC risk in overall and stratification analyses. Significant cumulative and interaction effects were also demonstrated in the studied SNPs on CRC risk. Another two SNPs (ERCC2 rs1052555 and ERCC5 rs2228959) were newly found to be associated with a poor overall survival in CRC patients.

### Research conclusions

Our findings suggested novel predictive SNPs in NER pathway genes for CRC risk and prognosis in a large-scale Chinese population.

### Research perspectives

The present study has referential values for the identification of NER-based genetic biomarkers in predicting the susceptibility and clinical outcome of CRC, and may also provide clues for the access to individualized early diagnosis and therapy of CRC patients.

## REFERENCES

- 1 Fang JY, Dong HL, Sang XJ, Xie B, Wu KS, Du PL, Xu ZX, Jia XY, Lin K. Colorectal Cancer Mortality Characteristics and Predictions in China, 1991-2011. *Asian Pac J Cancer Prev* 2015; **16**: 7991-7995 [PMID: 26625831 DOI: 10.7314/apjcp.2015.16.17.7991]
- 2 Zhang L, Cao F, Zhang G, Shi L, Chen S, Zhang Z, Zhi W, Ma T. Trends in and Predictions of Colorectal Cancer Incidence and Mortality in China From 1990 to 2025. *Front Oncol* 2019; **9**: 98 [PMID: 30847304 DOI: 10.3389/fonc.2019.00098]
- 3 Lichtenstein P, Holm NV, Verkasalo PK, Iliadou A, Kaprio J, Koskenvuo M, Pukkala E, Skytthe A, Hemminki K. Environmental and heritable factors in the causation of cancer--analyses of cohorts of twins from Sweden, Denmark, and Finland. *N Engl J Med* 2000; **343**: 78-85 [PMID: 10891514 DOI: 10.1056/NEJM200007133430201]
- 4 Petrusheva IO, Evdokimov AN, Lavrik OI. Molecular mechanism of global genome nucleotide excision repair. *Acta Naturae* 2014; **6**: 23-34 [PMID: 24772324]
- 5 Nospikel T. DNA repair in mammalian cells: Nucleotide excision repair: variations on versatility. *Cell Mol Life Sci* 2009; **66**: 994-1009 [PMID: 19153657 DOI: 10.1007/s00018-009-8737-y]
- 6 Liu J, Sun L, Xu Q, Tu H, He C, Xing C, Yuan Y. Association of nucleotide excision repair pathway gene polymorphisms with gastric cancer and atrophic gastritis risks. *Oncotarget* 2016; **7**: 6972-6983 [PMID: 26760766 DOI: 10.18632/oncotarget.6853]
- 7 Giovannucci E. An updated review of the epidemiological evidence that cigarette smoking increases risk of colorectal cancer. *Cancer Epidemiol Biomarkers Prev* 2001; **10**: 725-731 [PMID: 11440957]
- 8 Sandhu MS, White IR, McPherson K. Systematic review of the prospective cohort studies on meat consumption and colorectal cancer risk: a meta-analytical approach. *Cancer Epidemiol Biomarkers Prev* 2001; **10**: 439-446 [PMID: 11352852]
- 9 Berndt SI, Platz EA, Fallin MD, Thuita LW, Hoffman SC, Helzlsouer KJ. Genetic variation in the nucleotide excision repair pathway and colorectal cancer risk. *Cancer Epidemiol Biomarkers Prev* 2006;

- 15: 2263-2269 [PMID: [17119055](#) DOI: [10.1158/1055-9965.EPI-06-0449](#)]
- 30 **Moreno V**, Gemignani F, Landi S, Gioia-Patricola L, Chabrier A, Blanco I, González S, Guino E, Capellà G, Canzian F. Polymorphisms in genes of nucleotide and base excision repair: risk and prognosis of colorectal cancer. *Clin Cancer Res* 2006; **12**: 2101-2108 [PMID: [16609022](#) DOI: [10.1158/1078-0432.CCR-05-1363](#)]
- 31 **Paszkowska-Szczur K**, Scott RJ, Górski B, Cybulski C, Kurzawski G, Dymerska D, Gupta S, van de Wetering T, Masojć B, Kashyap A, Gapska P, Gromowski T, Kładny J, Lubiński J, Dębniak T. Polymorphisms in nucleotide excision repair genes and susceptibility to colorectal cancer in the Polish population. *Mol Biol Rep* 2015; **42**: 755-764 [PMID: [25391773](#) DOI: [10.1007/s11033-014-3824-z](#)]
- 32 **Dai Q**, Luo H, Li XP, Huang J, Zhou TJ, Yang ZH. XRCC1 and ERCC1 polymorphisms are related to susceptibility and survival of colorectal cancer in the Chinese population. *Mutagenesis* 2015; **30**: 441-449 [PMID: [25690281](#) DOI: [10.1093/mutage/geu088](#)]
- 33 **Lv Z**, Xu Q, Sun L, Wen J, Fang X, Xing C, Yuan Y. Four novel polymorphisms in long non-coding RNA HOTTIP are associated with the risk and prognosis of colorectal cancer. *Biosci Rep* 2019; **39** [PMID: [30940774](#) DOI: [10.1042/BSR20180573](#)]
- 34 **Asahina H**, Kuraoka I, Shirakawa M, Morita EH, Miura N, Miyamoto I, Ohtsuka E, Okada Y, Tanaka K. The XPA protein is a zinc metalloprotein with an ability to recognize various kinds of DNA damage. *Mutat Res* 1994; **315**: 229-237 [PMID: [7526200](#) DOI: [10.1016/0921-8777\(94\)90034-5](#)]
- 35 **Feng X**, Liu J, Gong Y, Gou K, Yang H, Yuan Y, Xing C. DNA repair protein XPA is differentially expressed in colorectal cancer and predicts better prognosis. *Cancer Med* 2018; **7**: 2339-2349 [PMID: [29675892](#) DOI: [10.1002/cam4.1480](#)]
- 36 **Liu J**, Zhang Z, Cao XL, Lei DP, Wang ZQ, Jin T, Pan XL. XPA A23G polymorphism and susceptibility to cancer: a meta-analysis. *Mol Biol Rep* 2012; **39**: 6791-6799 [PMID: [22314912](#) DOI: [10.1007/s11033-012-1504-4](#)]
- 37 **Dziki L**, Dziki A, Mik M, Majsterek I, Kabzinski J. Modulation of Colorectal Cancer Risk by Polymorphisms in 51Gln/His, 64Ile/Val, and 148Asp/Glu of APEX Gene; 23Gly/Ala of XPA Gene; and 689Ser/Arg of ERCC4 Gene. *Gastroenterol Res Pract* 2017; **2017**: 3840243 [PMID: [28386271](#) DOI: [10.1155/2017/3840243](#)]
- 38 **He L**, Deng T, Luo H. XPA A23G polymorphism and risk of digestive system cancers: a meta-analysis. *Onco Targets Ther* 2015; **8**: 385-394 [PMID: [25709470](#) DOI: [10.2147/OTT.S75767](#)]
- 39 **Monzo M**, Moreno I, Navarro A, Ibeas R, Artells R, Gel B, Martinez F, Moreno J, Hernandez R, Navarro-Vigo M. Single nucleotide polymorphisms in nucleotide excision repair genes XPA, XPD, XPG and ERCC1 in advanced colorectal cancer patients treated with first-line oxaliplatin/fluoropyrimidine. *Oncology* 2007; **72**: 364-370 [PMID: [18204222](#) DOI: [10.1159/000113534](#)]
- 40 **Hu X**, Qin W, Li S, He M, Wang Y, Guan S, Zhao H, Yao W, Wei M, Liu M, Wu H. Polymorphisms in DNA repair pathway genes and *ABCG2* gene in advanced colorectal cancer: correlation with tumor characteristics and clinical outcome in oxaliplatin-based chemotherapy. *Cancer Manag Res* 2019; **11**: 285-297 [PMID: [30643454](#) DOI: [10.2147/CMAR.S181922](#)]
- 41 **Li L**, Peterson C, Legerski R. Sequence of the mouse XPC cDNA and genomic structure of the human XPC gene. *Nucleic Acids Res* 1996; **24**: 1026-1028 [PMID: [8604333](#) DOI: [10.1093/nar/24.6.1026](#)]
- 42 **Leibel D**, Laspe P, Emmert S. Nucleotide excision repair and cancer. *J Mol Histol* 2006; **37**: 225-238 [PMID: [16855787](#) DOI: [10.1007/s10735-006-9041-x](#)]
- 43 **Tapias A**, Auriol J, Forget D, Enzlin JH, Schärer OD, Coin F, Coulombe B, Egly JM. Ordered conformational changes in damaged DNA induced by nucleotide excision repair factors. *J Biol Chem* 2004; **279**: 19074-19083 [PMID: [14981083](#) DOI: [10.1074/jbc.M312611200](#)]
- 44 **Thoma BS**, Vasquez KM. Critical DNA damage recognition functions of XPC-hHR23B and XPA-RPA in nucleotide excision repair. *Mol Carcinog* 2003; **38**: 1-13 [PMID: [12949838](#) DOI: [10.1002/mc.10143](#)]
- 45 **Ahmad Aizat AA**, Siti Nurfatimah MS, Aminudin MM, Ankathil R. XPC Lys939Gln polymorphism, smoking and risk of sporadic colorectal cancer among Malaysians. *World J Gastroenterol* 2013; **19**: 3623-3628 [PMID: [23801864](#) DOI: [10.3748/wjg.v19.i23.3623](#)]
- 46 **Mucha B**, Pytel D, Markiewicz L, Cuchra M, Szymczak I, Przybyłowska-Sygut K, Dziki A, Majsterek I, Dziki L. Nucleotide Excision Repair Capacity and XPC and XPD Gene Polymorphism Modulate Colorectal Cancer Risk. *Clin Colorectal Cancer* 2018; **17**: e435-e441 [PMID: [29793654](#) DOI: [10.1016/j.clcc.2016.10.001](#)]
- 47 **Steck SE**, Butler LM, Keku T, Antwi S, Galanko J, Sandler RS, Hu JJ. Nucleotide excision repair gene polymorphisms, meat intake and colon cancer risk. *Mutat Res* 2014; **762**: 24-31 [PMID: [24607854](#) DOI: [10.1016/j.mrfmm.2014.02.004](#)]
- 48 **Hua RX**, Zhu J, Jiang DH, Zhang SD, Zhang JB, Xue WQ, Li XZ, Zhang PF, He J, Jia WH. Association of XPC Gene Polymorphisms with Colorectal Cancer Risk in a Southern Chinese Population: A Case-Control Study and Meta-Analysis. *Genes (Basel)* 2016; **7**: 73 [PMID: [27669310](#) DOI: [10.3390/genes7100073](#)]
- 49 **Peng Q**, Lao X, Tang W, Chen Z, Li R, Qin X, Li S. XPC Lys939Gln polymorphism contributes to colorectal cancer susceptibility: evidence from a meta-analysis. *Diagn Pathol* 2014; **9**: 120 [PMID: [24947936](#) DOI: [10.1186/1746-1596-9-120](#)]
- 50 **Brenner H**, Kloor M, Pox CP. Colorectal cancer. *Lancet* 2014; **383**: 1490-1502 [PMID: [24225001](#) DOI: [10.1016/S0140-6736\(13\)61649-9](#)]
- 51 **Dunford A**, Weinstock DM, Savova V, Schumacher SE, Cleary JP, Yoda A, Sullivan TJ, Hess JM, Gimelbrant AA, Beroukhim R, Lawrence MS, Getz G, Lane AA. Tumor-suppressor genes that escape from X-inactivation contribute to cancer sex bias. *Nat Genet* 2017; **49**: 10-16 [PMID: [27869828](#) DOI: [10.1038/ng.3726](#)]
- 52 **Torre LA**, Bray F, Siegel RL, Ferlay J, Lortet-Tieulent J, Jemal A. Global cancer statistics, 2012. *CA Cancer J Clin* 2015; **65**: 87-108 [PMID: [25651787](#) DOI: [10.3322/caac.21262](#)]
- 53 **Hu X**, Yuan P, Yan J, Feng F, Li X, Liu W, Yang Y. Gene Polymorphisms of ADIPOQ +45T>G, UCP2 -866G>A, and FABP2 Ala54Thr on the Risk of Colorectal Cancer: A Matched Case-Control Study. *PLoS One* 2013; **8**: e67275 [PMID: [23826253](#) DOI: [10.1371/journal.pone.0067275](#)]
- 54 **Li X**, Liu W, Feng F, Hu X, Yuan P, Yan J, Yang Y. [Association between adiponectin rs2241766, rs1501299 polymorphisms and the risk of colorectal cancer]. *Zhonghua Liu Xing Bing Xue Za Zhi* 2014; **35**: 195-199 [PMID: [24739564](#)]
- 55 **Hecht SS**, Hoffmann D. Tobacco-specific nitrosamines, an important group of carcinogens in tobacco and tobacco smoke. *Carcinogenesis* 1988; **9**: 875-884 [PMID: [3286030](#) DOI: [10.1093/carcin/9.6.875](#)]
- 56 **Sinha R**, Peters U, Cross AJ, Kulldorff M, Weissfeld JL, Pinsky PF, Rothman N, Hayes RB. Meat, meat

- cooking methods and preservation, and risk for colorectal adenoma. *Cancer Res* 2005; **65**: 8034-8041 [PMID: 16140978 DOI: 10.1158/0008-5472.CAN-04-3429]
- 37 **Fang JL**, Vaca CE. Detection of DNA adducts of acetaldehyde in peripheral white blood cells of alcohol abusers. *Carcinogenesis* 1997; **18**: 627-632 [PMID: 9111191 DOI: 10.1093/carcin/18.4.627]
- 38 **Lv Z**, Sun L, Xu Q, Gong Y, Jing J, Dong N, Xing C, Yuan Y. SNP interactions of PGC with its neighbor lncRNAs enhance the susceptibility to gastric cancer/atrophic gastritis and influence the expression of involved molecules. *Cancer Med* 2018; **7**: 5252-5271 [PMID: 30155999 DOI: 10.1002/cam4.1743]
- 39 **Hansen RD**, Sørensen M, Tjønneland A, Overvad K, Wallin H, Raaschou-Nielsen O, Vogel U. XPA A23G, XPC Lys939Gln, XPD Lys751Gln and XPD Asp312Asn polymorphisms, interactions with smoking, alcohol and dietary factors, and risk of colorectal cancer. *Mutat Res* 2007; **619**: 68-80 [PMID: 17363013 DOI: 10.1016/j.mrfimm.2007.02.002]
- 40 **Brooks PJ**, Theruvathu JA. DNA adducts from acetaldehyde: implications for alcohol-related carcinogenesis. *Alcohol* 2005; **35**: 187-193 [PMID: 16054980 DOI: 10.1016/j.alcohol.2005.03.009]
- 41 **Fuss JO**, Tainer JA. XPB and XPD helicases in TFIIH orchestrate DNA duplex opening and damage verification to coordinate repair with transcription and cell cycle via CAK kinase. *DNA Repair (Amst)* 2011; **10**: 697-713 [PMID: 21571596 DOI: 10.1016/j.dnarep.2011.04.028]
- 42 **Kjersem JB**, Thomsen M, Guren T, Hamfjord J, Carlsson G, Gustavsson B, Ikdahl T, Indrebø G, Pfeiffer P, Lingjærde O, Tveit KM, Wettergren Y, Kure EH. AGXT and ERCC2 polymorphisms are associated with clinical outcome in metastatic colorectal cancer patients treated with 5-FU/oxaliplatin. *Pharmacogenomics J* 2016; **16**: 272-279 [PMID: 26261061 DOI: 10.1038/tpj.2015.54]
- 43 **Kumamoto K**, Ishibashi K, Okada N, Tajima Y, Kuwabara K, Kumagai Y, Baba H, Haga N, Ishida H. Polymorphisms of *GSTP1*, *ERCC2* and *TS-3'UTR* are associated with the clinical outcome of mFOLFOX6 in colorectal cancer patients. *Oncol Lett* 2013; **6**: 648-654 [PMID: 24137384 DOI: 10.3892/ol.2013.1467]
- 44 **Chen YM**, Wu XL, Zhang LW, Xu X, Liu JW. [Relationship between single nucleotide polymorphism in repair gene XPD751 and prognosis in colorectal carcinoma patients]. *Zhonghua Zhong Liu Za Zhi* 2012; **34**: 501-505 [PMID: 22967467 DOI: 10.3760/cma.j.issn.0253-3766.2012.07.006]
- 45 **Dong Y**, Liu JW, Gao YJ, Zhou T, Chen YM. Relationship between DNA repair gene XPD751 single-nucleotide polymorphisms and prognosis of colorectal cancer. *Genet Mol Res* 2015; **14**: 5390-5398 [PMID: 26125734 DOI: 10.4238/2015.May.22.8]
- 46 **Gan Y**, Li XR, Chen DJ, Wu JH. Association between polymorphisms of XRCC1 Arg399Gln and XPD Lys751Gln genes and prognosis of colorectal cancer in a Chinese population. *Asian Pac J Cancer Prev* 2012; **13**: 5721-5724 [PMID: 23317245 DOI: 10.7314/apjcp.2012.13.11.5721]
- 47 **Emmert S**, Schneider TD, Khan SG, Kraemer KH. The human XPG gene: gene architecture, alternative splicing and single nucleotide polymorphisms. *Nucleic Acids Res* 2001; **29**: 1443-1452 [PMID: 11266544 DOI: 10.1093/nar/29.7.1443]
- 48 **Kiyohara C**, Yoshimasu K. Genetic polymorphisms in the nucleotide excision repair pathway and lung cancer risk: a meta-analysis. *Int J Med Sci* 2007; **4**: 59-71 [PMID: 17299578 DOI: 10.7150/ijms.4.59]
- 49 **Wood RD**, Mitchell M, Lindahl T. Human DNA repair genes, 2005. *Mutat Res* 2005; **577**: 275-283 [PMID: 15922366 DOI: 10.1016/j.mrfimm.2005.03.007]
- 50 **Chen J**, Luo X, Xie G, Chen K, Jiang H, Pan F, Li J, Ruan Z, Pang X, Liang H. Functional Analysis of SNPs in the ERCC5 Promoter in Advanced Colorectal Cancer Patients Treated With Oxaliplatin-Based Chemotherapy. *Medicine (Baltimore)* 2016; **95**: e3652 [PMID: 27175691 DOI: 10.1097/MD.0000000000003652]
- 51 **Kong J**, Liu Z, Cai F, Xu X, Liul J. Relationship between the Asp1104His polymorphism of the nucleotide excision repair gene ERCC5 and treatment sensitivity to oxaliplatin in patients with advanced colorectal cancer in China. *Clinics (Sao Paulo)* 2018; **73**: e455 [PMID: 30517302 DOI: 10.6061/clinics/2017/e455]
- 52 **Sun K**, Gong A, Liang P. Predictive impact of genetic polymorphisms in DNA repair genes on susceptibility and therapeutic outcomes to colorectal cancer patients. *Tumour Biol* 2015; **36**: 1549-1559 [PMID: 25355595 DOI: 10.1007/s13277-014-2721-3]
- 53 **Wang F**, Zhang SD, Xu HM, Zhu JH, Hua RX, Xue WQ, Li XZ, Wang TM, He J, Jia WH. XPG rs2296147 T>C polymorphism predicted clinical outcome in colorectal cancer. *Oncotarget* 2016; **7**: 11724-11732 [PMID: 26887052 DOI: 10.18632/oncotarget.7352]
- 54 **Li Y**, Zhang F, Yang D. Comprehensive assessment and meta-analysis of the association between CTNNB1 polymorphisms and cancer risk. *Biosci Rep* 2017; **37** [PMID: 28963373 DOI: 10.1042/BSR20171121]



## Retrospective Study

# Idarubicin vs doxorubicin in transarterial chemoembolization of intermediate stage hepatocellular carcinoma

Gaël Stéphane Roth, Yann Teyssier, Mélodie Abousalihac, Arnaud Seigneurin, Julien Ghelfi, Christian Sengel, Thomas Decaens

**ORCID number:** Gaël Stéphane Roth (0000-0001-5822-4320); Yann Teyssier (0000-0002-9785-8729); Mélodie Abousalihac (0000-0002-0661-1684); Arnaud Seigneurin (0000-0002-2168-1672); Julien Ghelfi (0000-0002-9039-6488); Christian Sengel (0000-0001-9004-256X); Thomas Decaens (0000-0003-0928-0048).

**Author contributions:** Roth GS and Decaens T contributed to study design, data collection, analyses, writing, and revision; Teyssier Y contributed to data collection and radiological independent analyses; Abousalihac A and Sengel C contributed to data collection; Seigneurin A contributed to statistics analyses; Ghelfi J contributed to writing and revision; Teyssier Y and Abousalihac M equally contributed to this work.

### Institutional review board

**statement:** Study ethics were approved by an independent institutional review board of CECIC Rhône-Alpes-Auvergne, Clermont-Ferrand.

### Informed consent statement:

Patients gave their written consent before TACE procedures. No specific consent statement was required regarding the retrospective analysis of data as they were anonymously used.

### Conflict-of-interest statement:

Authors did not declare any conflicts of interest.

### Data sharing statement:

No

**Gaël Stéphane Roth, Mélodie Abousalihac, Thomas Decaens,** Clinique Universitaire d'Hépatogastroentérologie et Oncologie Digestive, CHU Grenoble-Alpes, Grenoble 38043, France

**Gaël Stéphane Roth, Yann Teyssier, Arnaud Seigneurin, Thomas Decaens,** Faculté de Médecine, Université Grenoble-Alpes, Domaine de la Merci, La Tronche 38700, France

**Gaël Stéphane Roth, Thomas Decaens,** Institute for Advanced Biosciences - INSERM U1209/CNRS UMR 5309/Université Grenoble-Alpes, Site Santé - Allée des Alpes, La Tronche 38700, France

**Yann Teyssier, Julien Ghelfi, Christian Sengel,** Clinique Universitaire de Radiologie et Imagerie Médicale, CHU Grenoble-Alpes, Grenoble 38043, France

**Arnaud Seigneurin,** Département de Santé Publique - CHU Grenoble-Alpes, Grenoble 38043, France

**Thomas Decaens,** Department of Hepatology and Gastroenterology, Grenoble-Alpes University Hospital, Grenoble 38043, France

**Corresponding author:** Thomas Decaens, MD, PhD, Full Professor, Department of Hepatology and Gastroenterology, Grenoble-Alpes University Hospital, BP 217, Cedex 09, Grenoble 38043, France. [tdecaens@chu-grenoble.fr](mailto:tdecaens@chu-grenoble.fr)

## Abstract

### BACKGROUND

Liver cancer is the fifth most common cancer and the second cause of cancer-related deaths worldwide. Transarterial chemoembolization (TACE) is the best treatment of intermediate hepatocellular carcinoma (HCC). Doxorubicin is the most commonly used drug despite a low level of evidence.

### AIM

To compare the objective response rate of idarubicin-based TACE (Ida-TACE) against doxorubicin-based TACE (Dox-TACE) in intermediate stage HCC.

### METHODS

Between January 2012 and December 2014, all patients treated with TACE at our academic hospital were screened. Inclusion criteria were patients with Child-Pugh score A or B, a performance status below or equal to 1, and no prior TACE. Either lipiodol TACE or drug-eluting beads TACE could be performed with 10 mg of idarubicin or 50 mg of doxorubicin. Each patient treated with idarubicin



additional data are available.

**Open-Access:** This article is an open-access article that was selected by an in-house editor and fully peer-reviewed by external reviewers. It is distributed in accordance with the Creative Commons Attribution NonCommercial (CC BY-NC 4.0) license, which permits others to distribute, remix, adapt, build upon this work non-commercially, and license their derivative works on different terms, provided the original work is properly cited and the use is non-commercial. See: <http://creativecommons.org/licenses/by-nc/4.0/>

**Manuscript source:** Unsolicited manuscript

**Received:** October 7, 2019

**Peer-review started:** October 7, 2019

**First decision:** November 10, 2019

**Revised:** December 13, 2019

**Accepted:** December 21, 2019

**Article in press:** December 21, 2019

**Published online:** January 21, 2020

**P-Reviewer:** Qi XS, Yang L, Yao DF

**S-Editor:** Tang JZ

**L-Editor:** Filipodia

**E-Editor:** Li X



was matched with two doxorubicin-treated patients. The TACE response was assessed by independent radiologists according to the mRECIST criteria.

## RESULTS

Sixty patients were treated with doxorubicin and thirty with idarubicin. There were 93% and 87% of cirrhotic patients and 87% and 70% of Child-Pugh A in the doxorubicin and idarubicin groups, respectively. The median number of HCC per patient was two in both groups with 31% and 26% of single nodules in doxorubicin and idarubicin groups, respectively. Objective response rate after first TACE was 76.7% and 73.3% ( $P = 0.797$ ) with 41.7% and 40.0% complete response in doxorubicin and idarubicin groups, respectively. Progression-free survival was 7.7 mo in both groups, and liver transplant-free survival was 24.9 mo and 21.9 mo in doxorubicin and idarubicin groups, respectively. Safety profiles were similar in both groups, with grade 3-4 adverse events in 35% of Dox-TACE and 43% of Ida-TACEs.

## CONCLUSION

Ida-TACE and Dox-TACE showed comparable results in terms of efficacy and safety. Ida-TACE may represent an interesting alternative to Dox-TACE in the management of patients with intermediate stage HCC.

**Key words:** Hepatocellular carcinoma; Transarterial chemoembolization; Idarubicin; Doxorubicin; Intermediate stage

©The Author(s) 2020. Published by Baishideng Publishing Group Inc. All rights reserved.

**Core tip:** Transarterial chemoembolization in the treatment of choice for intermediate stage hepatocellular carcinoma. Doxorubicin is the most used drug without any satisfying evidence of its superiority compared with other drugs. An increasing number of preclinical and early phase clinical studies suggest the superiority of idarubicin anti-tumor efficacy in transarterial chemoembolization. With the limits relative to retrospective analysis, this study shows that idarubicin represents an alternative to doxorubicin in the treatment of hepatocellular carcinoma with comparable efficacy and safety. It needs to be confirmed by randomized clinical trials.

**Citation:** Roth GS, Teyssier Y, Abousalihac M, Seigneurin A, Ghelfi J, Sengel C, Decaens T. Idarubicin vs doxorubicin in transarterial chemoembolization of intermediate stage hepatocellular carcinoma. *World J Gastroenterol* 2020; 26(3): 324-334

**URL:** <https://www.wjgnet.com/1007-9327/full/v26/i3/324.htm>

**DOI:** <https://dx.doi.org/10.3748/wjg.v26.i3.324>

## INTRODUCTION

Liver cancer is the fifth most common cancer and the second cause of cancer-related deaths worldwide<sup>[1]</sup>. Hepatocellular carcinoma (HCC) represents 90% of liver cancer. Only 30% of HCC patients can have access to surgical resection, percutaneous ablation, or liver transplantation (LT). Among the recommended treatments for intermediate HCC, classified as Barcelona Clinic of Liver Cancer (BCLC) B, transarterial chemoembolization (TACE) is the best treatment based upon randomized controlled trial and meta-analysis<sup>[2,3]</sup>.

In these studies, local control is obtained in 5%-55% of patients but with a short time-to-progression (6 mo to 12 mo), due to a high rate of recurrence. A recent systematic review including 10108 patients, showed a tumor response rate of 52.5%, and a median overall survival (OS) of 19.4 mo<sup>[4]</sup>. Chemotherapeutic agents can be delivered either through lipiodol emulsion [the conventional method (cTACE)] or loaded on drug-eluting microbeads (DEB-TACE), even though the latter method did not show any superiority in anti-tumor efficacy as well as no clear benefit in terms of safety<sup>[5,6]</sup>. Several methods were explored to improve results of TACE, such as the combination of systemic chemotherapies, without success<sup>[7,8]</sup>. Surprisingly, the choice of the drug used in TACE is still debated. Doxorubicin is commonly used, but no solid data confirmed its superiority compared to other drugs such as epirubicin, cisplatin,

or idarubicin. *In vitro* data have shown superiority of idarubicin to doxorubicin, especially in the SNU-449 cell line<sup>[9]</sup>. Besides, two phase 1 trials studying idarubicin in HCC showed promising results either by using drug-eluting beads or lipiodol emulsion<sup>[10,11]</sup>. An open label and single arm phase 2 trial is currently ongoing to assess the anti-tumor efficacy of idarubicin-loaded beads in HCC (NCT02185768).

This study aims to compare idarubicin-based TACE (Ida-TACE) with doxorubicin-based TACE (Dox-TACE) in the treatment of intermediate HCC.

## MATERIALS AND METHODS

### Overview

We retrospectively reviewed the medical files and imaging examinations of all consecutive patients undergoing TACE for HCC at our University hospital from 2012 to 2014. During this period, due to local drug supply constraints, patients were treated either by Dox-TACE or Ida-TACE.

### TACE procedure

Patients were treated with TACE following standard local protocol. Each indication of TACE was validated during multidisciplinary tumor board including a hepatologist, an interventional radiologist, and a liver surgeon. Procedures were realized in an interventional radiology suite (Allura Integris, Philips Medical Systems, Eindhoven, Netherlands). The contrast media used was Xenetix 350 (Xenetix®, Guerbet, Roissy, France). First, diagnostic arteriography was performed under local anesthesia, through the right femoral artery, using a 4-French introducer sheath. Portal vein patency and arterial vascular anatomy were appreciated due to the catheterization of the superior mesenteric artery and the coeliac trunk (Figure 1). Chemoembolization was as selective as possible according to tumor localization and number. The use of a microcatheter was left to the radiologist's discretion. cTACE or DEB-TACE could be performed. During cTACE, 50 mg of injectable lyophilized doxorubicin (Adriblastina®, Pfizer Pharma, United States) or 10 mg of injectable lyophilized idarubicin (Zavedos®, Pfizer Pharma, United States) were manually emulsified with 5-10 mL of iodized oil (Lipiodol® Ultra Fluide, Guerbet, France) before infusion. Drug-eluting beads (100 µm; Embozene Tandem® microspheres, Celonova Biosciences, Germany) were used for DEB-TACE procedures. Lipiodol emulsion or DEB were injected until saturation of tumor feeding arteries. In the case of cTACE, drug administration was immediately followed by embolization using absorbable gelatine sponge (Curaspon®; Curamedical, Netherlands) to obtain an arterial flow stop during 10 min. As recommended by European guidelines and as routinely done in our department, TACE could be repeated 2 mo after the first treatment in case of partial response (PR) on postoperative scan<sup>[12]</sup>.

### Patient selection

Inclusion criteria were patients treated with TACE for HCC, with Child-Pugh score A or B, with a performance status below or equal to 1, and with no prior TACE. TACE as a bridge to transplantation was not an exclusion criterion.

### Ethical approval

Every patient gave his written consent before TACE, and study ethics were approved by an independent institutional review board (CECIC Rhône-Alpes-Auvergne, Clermont-Ferrand, IRB 5891).

### Study objectives

The primary aim of this study was to compare the objective response rate (ORR) after first TACE between doxorubicin and idarubicin treated patients. Secondary objectives were to compare disease control rate (DCR), progression-free survival (PFS), OS, liver transplant-free survival (LTFS), and adverse events (AEs) between doxorubicin and idarubicin groups. A safety analysis was also performed with collection of early AEs occurring within the 1<sup>st</sup> month. Grading of AEs was done based on Common Terminology Criteria for Adverse Events V5.0. Chronic liver toxicity considered as liver function deterioration between 30 d and 90 d after TACE was also analyzed.

### Data collection

All imaging examinations were archived in a picture archiving and communication system and were reviewed. Medical parameters were extracted from the patient's electronic medical records by one of the authors who independently reviewed the entire medical record. Thus, radiological analyses were realized blindly to treatment type and clinical data.

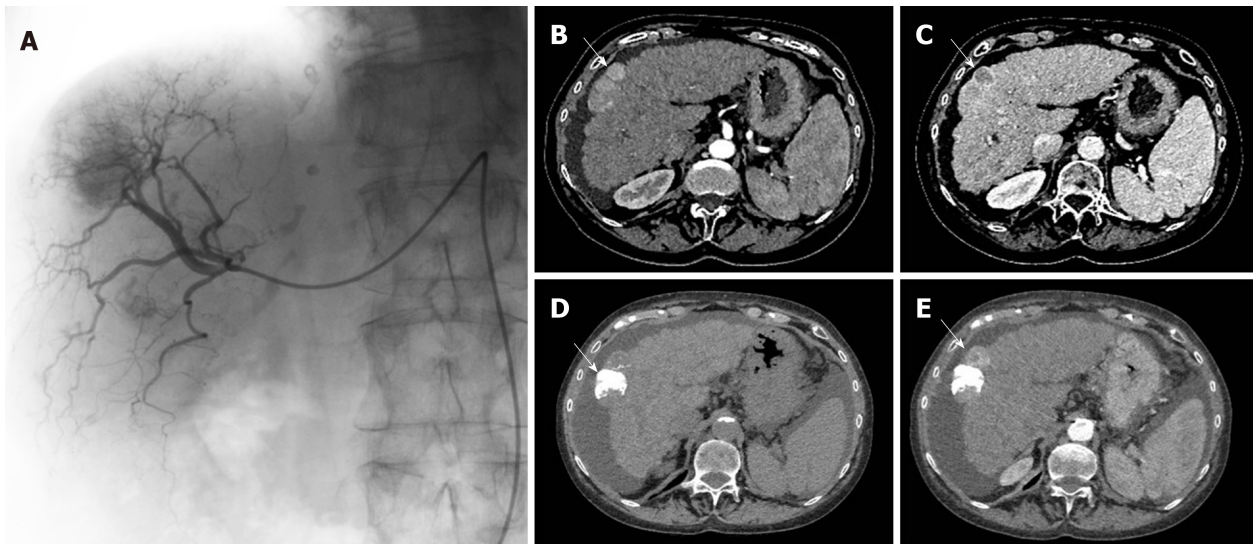


**Figure 1** Example of transarterial chemoembolization on the right liver with pre-operative and after transarterial chemoembolization computed tomography scans. A: Transarterial chemoembolization (TACE) of the right liver with presence of a tumor blush; B: Computed tomography (CT) scan before TACE showing a typical HCC nodule of the hepatic segment V with a "wash-in" corresponding to contrast enhancement during arterial phase; C: A wash out during portal phase; D: Post-TACE CT-scan unenhanced phase showing a spontaneous hyperdensity corresponding to lipiodol intake; E: Post-TACE CT-scan arterial phase showing the persistence of a contrast enhancement near the lipiodol intake, typical of a partial response.

The following patient characteristics were collected: Sex, age, World Health Organization (WHO) performance status, body mass index, etiology of chronic liver disease, and cirrhosis status.

Every patient had pre-operative imaging and post-operative imaging within 3 mo after TACE as recommended<sup>[12]</sup>, to assess tumor response and determine the need to perform an additional TACE or not. Radiological examination was performed with a computed tomography scan (Figure 1) or magnetic resonance scan. Imaging data collected were tumor number and largest nodules measurements on preoperative imaging. Tumor response was assessed according to the mRECIST criteria<sup>[12]</sup> with complete response, PR, stable disease, and progressive disease.

During the post-embolization period, AEs were monitored on clinical examinations, systematic biological follow-up (renal and hepatic functions), and classical imaging follow-up.

### Statistical analysis

Patients were matched as follows: Doxorubicin:idarubicin (2:1) based on tumor number, sum of the two largest tumors, Child-Pugh score, platelet count, WHO performance status level, cTACE, or DEB-TACE. Matching was performed blindly to tumor response data of TACE.

The ORR and DCR were compared using exact Fischer tests. The PFS and LTFS were computed by clinical characteristics using the Kaplan-Meier method. In LTFS, events corresponded to liver transplant or death. Log-rank tests were used to compare survival rates. Liver transplant events were censored in OS analyses. Analyses were performed using Stata version 13.0 (Stata Corporation, College Station, TX, United States).

## RESULTS

### Patients' characteristics

Between 2012 and 2014, 90 patients who benefited from TACE for HCC were included in this study. Thirty patients treated with Ida-TACE were matched with sixty patients treated with Dox-TACE. Both groups were comparable concerning demographics data (Table 1).

Considering tumor characteristics, median tumor number was two in both groups with a single nodule in 28.3% and 23.3% of cases, and a median tumor size (sum of the two largest tumors) of 49.5 mm [interquartile range (IQR): 32.8-62.0] and 40.5 mm (IQR: 30.5-58.8) in Dox-TACE and Ida-TACE patients, respectively.

Cirrhosis was present in 93.3% and 86.7% of patients with 86.7% and 70.0% of Child-Pugh A and a median Model for End-stage Liver Disease of 9.22 and 8.19 in

**Table 1 Patient baseline characteristics: Clinical and biological characteristics, portal hypertension evidence, and anthropometric analyses, *n* (%)**

Characteristics	Doxorubicin, <i>n</i> = 60	Idarubicin, <i>n</i> = 30
Clinical and biological data		
Sex, male/female	54 (90.0)/6 (10.0)	28 (93.3)/2 (6.7)
Age in yr, mean $\pm$ SD	62.9 $\pm$ 9.0	61.9 $\pm$ 9.8
WHO performance status 0/1	51 (85.0)/9 (15.0)	25 (83.3)/5 (16.6)
BMI, median (IQR)	27.6 (24.7-32.1)	25.2 (22.9-27.2)
< 20	2 (3.3)	2 (6.9)
20-24.9	15 (25.0)	12 (41.4)
$\geq$ 25	43 (71.7)	15 (51.7)
Tumor characteristics		
Tumor number, median (IQR)	2 (1-3)	2 (2-3.75)
1 nodule	17 (28.3)	7 (23.3)
2-3 nodules	31 (51.7)	15 (50.0)
> 3 nodules	12 (20.0)	8 (26.7)
2 largest nodules sum in mm, median (IQR)	49.5 (32.8-62.0)	40.5 (30.5-58.8)
Partial portal vein thrombosis	8 (13)	3 (10)
Underlying cirrhosis		
Yes/no	56 (93.3)/4 (6.7)	26 (86.7)/4 (13.3)
Child-Pugh class A/B	52 (86.7)/8 (13.3)	21 (70.0)/9 (30.0)
MELD, median (IQR)	9.22 (8.13-10.57)	8.19 (7.34-9.86)
Etiology		
Alcohol	18 (30.0)	6 (20.0)
HBV/HCV infection	11 (18.3)	4 (13.3)
Metabolic	7 (11.7)	1 (3.3)
Alcohol + HBV/HCV	3 (5.0)	8 (26.7)
Alcohol + Metabolic	16 (26.7)	5 (16.7)
Hemochromatosis	3 (5.0)	2 (6.7)
Biological parameters		
Platelet count in G/L, median (IQR)	112.5 (82.8-171.5)	106.5 (86.3-135.3)
Albumin in g/dL, median (IQR)	3.7 (3.4-3.9)	3.5 (3.1-3.9)
Total bilirubin in mg/dL, median (IQR)	0.94 (0.58-1.18)	0.73 (0.48-1.04)
AST in IU/L, median (IQR)	46 (33-65)	55 (34-68)
ALT in IU/L, median (IQR)	44 (34-70)	40 (29-60)
GGT in IU/L, median (IQR)	152 (92-261)	185 (141-332)
ALP in IU/L, median (IQR)	105 (88-133)	115 (88-139)
PT as %, median (IQR)	79.5 (67.0-85.8)	79.5 (63.3-89.3)
AFP in ng/mL, median (IQR)	12.7 (4.6-109.3)	16.0 (5.2-35.0)
Drug administration method		
Conventional TACE/beads	48 (80)/12 (20.0)	24 (80)/6 (20.0)
Drug dose in mg, median (IQR)	50 (50-50)	10 (10-10)
TACE territory: Global/lobar/segmental	34 (56.7)/20 (33.3)/6 (10.0)	15 (50)/14(46.7)/1(3.3)
Portal hypertension evidence		
Ascites on preoperative scan: No/yes	49 (76.6)/15 (23.4)	21 (65.6)/11 (34.4)
Splenomegaly on preoperative scan: No/yes	27 (45.0)/33 (55.0)	7 (23.3)/23 (76.7)
Esophageal varices		
None	28 (46.7)	17 (56.7)
Grade 1/2/3	14 (23.3)/17 (28.3)/1 (1.7)	2 (6.7)/9 (30.0)/2 (6.7)
Low platelet count as < 100 000/mm <sup>3</sup> : No/yes	37 (61.6)/23 (38.3)	18 (60.0)/12 (40.0)

AFP: Alpha-fetoprotein; ALP: Alkaline phosphatase; ALT: Alanine aminotransferase; AST: Aspartate aminotransferase; BCLC: Barcelona Clinic Liver Cancer; BMI: Body mass index; GGT: Gamma-glutamyltranspeptidase; HBV: Hepatitis B virus; HCV: Hepatitis C virus; PT: Prothrombin time; IQR: Interquartile range; WHO: World Health Organization; TACE: Transarterial chemoembolization; MELD: Model for end-stage liver disease; SD: Standard deviation.



Dox-TACE and Ida-TACE patients, respectively.

Considering portal hypertension, Dox-TACE and Ida-TACE patients respectively presented a splenomegaly in 55% and 76.7% of cases, a platelets count under 100000/mm<sup>3</sup> in 38.3% and 40.0 % of cases, ascites on preoperative radiological exam in 23.4% and 34.4% of cases, and grade 2-3 esophageal varices of 30.0% and 36.7% of cases (Table 1).

Considering treatment characteristics, doxorubicin and idarubicin were administered with cTACE in 80% of the cases and DEB-TACE in 20% of cases in both groups. TACE was global in 56.7% and 50% of doxorubicin and idarubicin-treated patients, respectively. Median number of TACE per patient was two (IQR: 1-3) in the doxorubicin group and two (IQR: 2-3) in the idarubicin group. Sixteen patients (27%) were transplanted in the doxorubicin group and ten (33%) in the idarubicin group.

### Anti-tumor efficacy: Comparison of Dox-TACE and Ida-TACE

Tumor response evaluation within 3 mo post-TACE, according to mRECIST criteria, showed an ORR of 76% and 73% ( $P = 0.797$ ) with 41% and 40% of complete response, and 36% and 33% of PR in Dox-TACE and Ida-TACE groups, respectively. DCR was 90% and 87%, respectively ( $P = 0.726$ ) (Figure 2).

The median follow-up was 19.8 *vs* 21.8 mo in doxorubicin *vs* idarubicin patients with a PFS of 7.71 *vs* 7.68 mo ( $P = 0.586$ ), and LTFS was 24.9 *vs* 21.9 mo in doxorubicin- *vs* idarubicin-treated patients, respectively ( $P = 0.434$ ) (Figure 2).

### Safety

Safety data is detailed in Table 2. Tolerance profiles were similar with AEs of any grade in 97% of patients in both arms. The most frequent AEs were post-embolization syndrome (Dox-TACE: 45%; Ida-TACE: 63%), pain, elevated transaminases, cholestasis, hyperbilirubinemia, and fatigue. At least one grade 3-4 AEs was found in 21 patients (35%) treated with doxorubicin and 13 patients (43%) treated with idarubicin. The most frequent grade 3-4 AEs were elevated aspartate aminotransferase (Dox-TACE: 33%; Ida-TACE: 43%), elevated alanine aminotransferase (23% in both arms), pain (Dox-TACE: 12%; Ida-TACE: 13%), fatigue (Dox-TACE: 11%; Ida-TACE: 10%), and liver failure (7% in both groups). One Dox-TACE patient died 23 d after TACE due to cardiac rhythm disturbances. The median duration of hospitalization was 3 d in both groups.

Considering chronic toxicity, mild changes of bilirubin, albumin, and prothrombin time were observed in both arms (Figure 3A), and median Child-Pugh score was 6 in both arms after TACE, compared with 5 and 6 before TACE in Dox-TACE and Ida-TACE patients, respectively. Consequences on changes in repartition of Child-Pugh grade A, B, or C are illustrated in Figure 3B.

## DISCUSSION

The aim of this study was to report our single-center experience comparing TACE with idarubicin *vs* TACE with doxorubicin. We did not report a significant difference concerning our primary objective that was tumor response within 3 mo after TACE ( $P = 0.797$ ). There was no differences between groups in terms of DCR, PFS, and LTFS.

Safety analyses revealed that idarubicin did not increase the occurrence of early AEs and chronic deterioration of liver function compared with doxorubicin. Safety profiles of both arms were comparable with TACE trials in the literature<sup>[2,13]</sup>. Interestingly, more severe biliary AEs were reported in the Dox-TACE group ( $n = 4$ ) compared to Ida-TACE group ( $n = 0$ ), but the difference was not statistically significant ( $P = 0.65$ ).

To our knowledge, this study represents the largest cohort comparing TACE using idarubicin to TACE with doxorubicin. To avoid major biases, analysis of the primary objective was blindly performed, and Dox-TACE and Ida-TACE patients were matched with stratification on essential clinical characteristics such as tumor number, tumor size, liver function level, platelet count, WHO performance status, and TACE technique.

Nonetheless, this study presents several limitations. First, it is a retrospective and monocentric study. TACE techniques are very heterogeneous from one center to another. For example, ORR and DCR obtained in both groups were superior to tumor response available in the literature, which confirms that TACE results are strongly influenced by center experience<sup>[2,14]</sup>. A larger prospective multicenter trial is needed to confirm these results.

Both patients receiving TACE in a palliative setting or as a bridge to liver transplant were included. However, the proportions of patients on LT waiting list was well balanced between the groups with approximately 30% of patients in each group. To

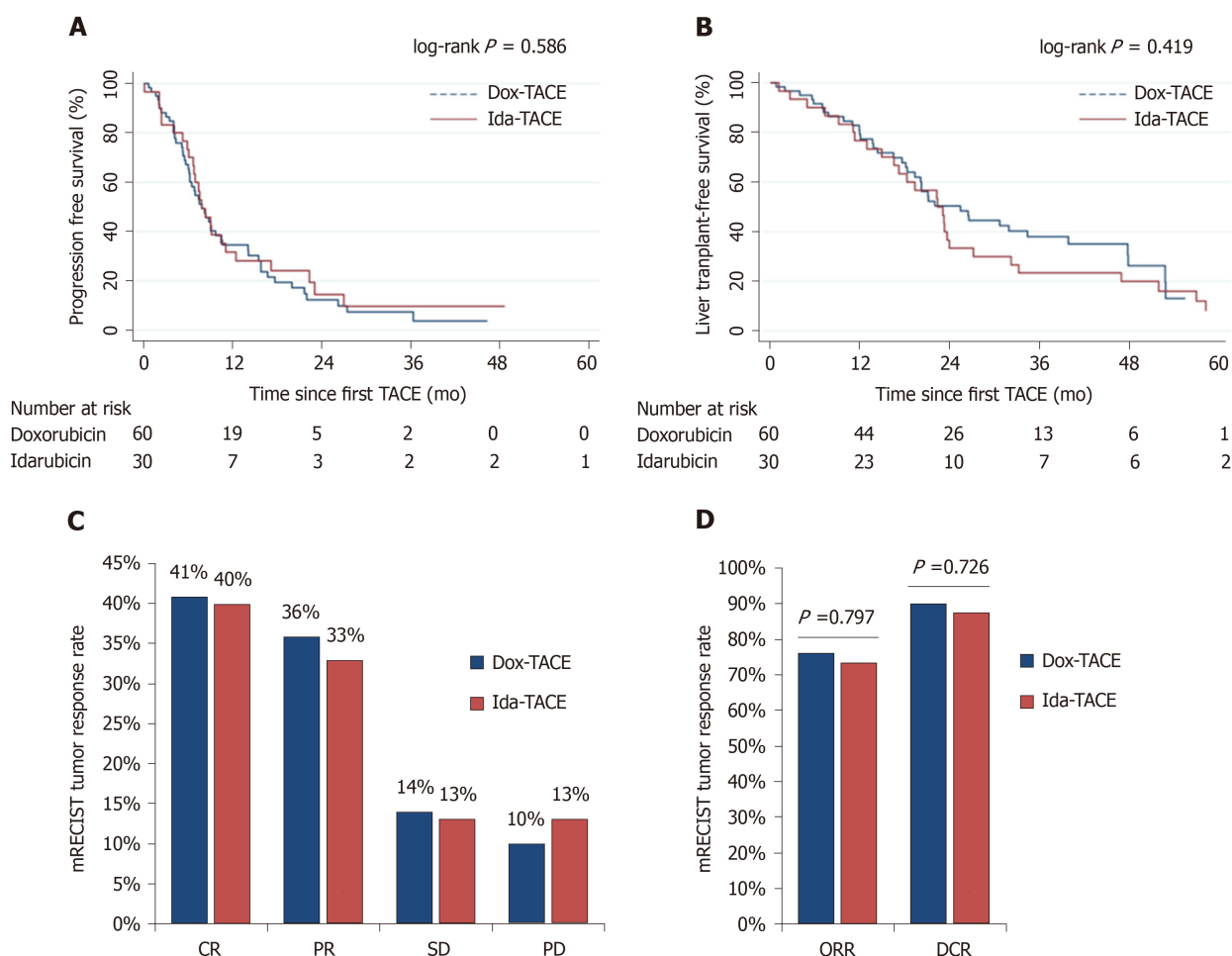


**Figure 2** Comparison of tumor response and survival in doxorubicin (doxorubicin-based transarterial chemoembolization) vs idarubicin (idarubicin-based transarterial chemoembolization) patients. A: Progression-free survival; B: Liver transplant-free survival; C: Objective response; D: Disease control rate. TACE: Transarterial chemoembolization; Dox-TACE: Doxorubicin-based transarterial chemoembolization; Ida-TACE: Idarubicin-based transarterial chemoembolization.

avoid impact on OS analysis of LT, LTFS was analyzed rather than OS to consider both death and liver transplant as events. This offers a better illustration of survival due to TACE.

Even though TACE is largely used in the treatment of intermediate HCC, several essential issues are still debated. Four meta-analyses<sup>[14-17]</sup> and a recent randomized trial including 101 patients<sup>[18]</sup> suggested that transarterial embolization, also called bland embolization, offers comparable outcomes to TACE. These studies suffer from methodological issues, and TACE is still the standard of care in BCLC B HCC.

The choice of the administered drug, its administration, and its dosage are also debated<sup>[14]</sup>. Different studies tried to optimize TACE efficacy through technical improvements, notably by using drug-eluting beads, but without success<sup>[5,19]</sup>. The use of doxorubicin is the most widespread, but it is only based on a low level of evidence<sup>[14]</sup>. *In vitro* studies showed that idarubicin has a toxicity index on HCC cell-lines 57-fold higher than doxorubicin<sup>[9]</sup>. While doxorubicin has a low lipophilicity binding, idarubicin is highly hydrophobic suggesting better cell penetrance<sup>[20]</sup> and allows more stable lipiodol-drug emulsion<sup>[21]</sup>. The 10 mg dose was chosen based on preliminary data of the IDASPHIRE phase 1 trial that included 31 patients between 2010 and 2012 treated with beads loaded with idarubicin<sup>[10]</sup>. This dose was confirmed in two prospective single-arm trials including IDASPHIRE II phase 2 trials published in 2019<sup>[22,23]</sup>. However, as 80% of patients were treated with cTACE in our study, the optimal dose may differ from DEB-TACE. Indeed, a phase 1 trial published in 2018 evaluating idarubicin dose in cTACE showed interesting results in terms of efficacy and safety with a maximum tolerated dose of idarubicin at 20 mg<sup>[11]</sup>, suggesting that further studies at a higher dose such as 15 mg or 20 mg are required. Another explanation, is that the impact of drug type is probably mild in TACE as illustrated by the controversy around chemoembolization *vs* bland embolization with conflicting results in literature<sup>[14-18,24]</sup>. Thus, a higher number of patients is probably needed to prove superiority of idarubicin.

**Table 2 Early adverse events according to treatment group occurring within the month after transarterial chemoembolization, *n* (%)**

Adverse events	Doxorubicin, <i>n</i> = 60		Idarubicin, <i>n</i> = 30	
	Any grade	Grade 3-4	Any grade	Grade 3-4
Any adverse event	58 (97)	21 (35)	29 (97)	13 (43)
Treatment-related death	1 (2)	1 (2)	0	0
Post embolization syndrome	27 (45)	NA	19 (63)	NA
Fatigue	27 (45)	7 (11)	19 (63)	3 (10)
Pain	9 (15)	7 (12)	5 (17)	4 (13)
Gastrointestinal disorders				
Biliary complications	5 (8)	4 (7)	1 (3)	0
Liver failure	6 (10)	4 (7)	4 (13)	2 (7)
Paralytic ileus	1 (2)	0	0	0
Portal thrombosis	0	0	1 (2)	1 (2)
Liver biological parameters				
Elevated AST	55 (92)	20 (33)	26 (87)	13 (43)
Elevated ALT	51 (85)	14 (23)	24 (80)	7 (23)
Elevated GGT	21 (35)	0	12 (40)	0
Elevated ALP	16 (27)	0	5 (17)	0
Hyperbilirubinemia	34 (57)	0	22 (73)	0
Decreased prothrombin time	28 (48)	0	9 (32)	0
Neurological disorders				
Stroke	1 (2)	0	0	0
Respiratory disorders				
Lung failure	1 (2)	0	1 (3)	1 (3)
Lung infection	0	0	2 (7)	2 (7)
Urinary tract disorders				
Acute kidney failure	1 (2)	0	0	0
Acute urine retention	3 (5)	0	1 (3)	0
Urinary tract infection	1 (2)	1 (2)	0	0

Biological adverse events are expressed based on their comparison with normal values or with patient's baseline value in case of abnormal baseline as recommended by Common Terminology Criteria for Adverse Events Version 5.0. ALP: Alkaline phosphatase; ALT: Alanine aminotransferase; AST: Aspartate aminotransferase; GGT: Gamma-glutamyltranspeptidase; NA: Not applicable.

Finally, idarubicin was randomly assigned to patients in the setting of routine care due to the temporary shortage of doxorubicin, but as it is retrospective, we cannot control this aspect.

During the last decade, realization of Dox-TACE in BCLC B patients has become complex due to discontinuation of production of lyophilized doxorubicin by many pharmaceutical groups. For technical reasons, use of the lyophilized form is essential to obtain a mix with sufficient viscosity. This will induce tumor ischemia and increase the exposure time of the tumor to the drug, leading to a higher cytotoxicity, whereas liquid forms seem to be rapidly washed out in the blood flow. Nowadays, only Pfizer continues to produce lyophilized doxorubicin, with recurring shortage periods. Thus, finding alternatives to doxorubicin becomes a challenge to allow clinicians to perform TACE in optimal conditions.

Idarubicin showed comparable efficacy and safety to doxorubicin in this indication and may represent a new option in the management of patients with BCLC B HCC.

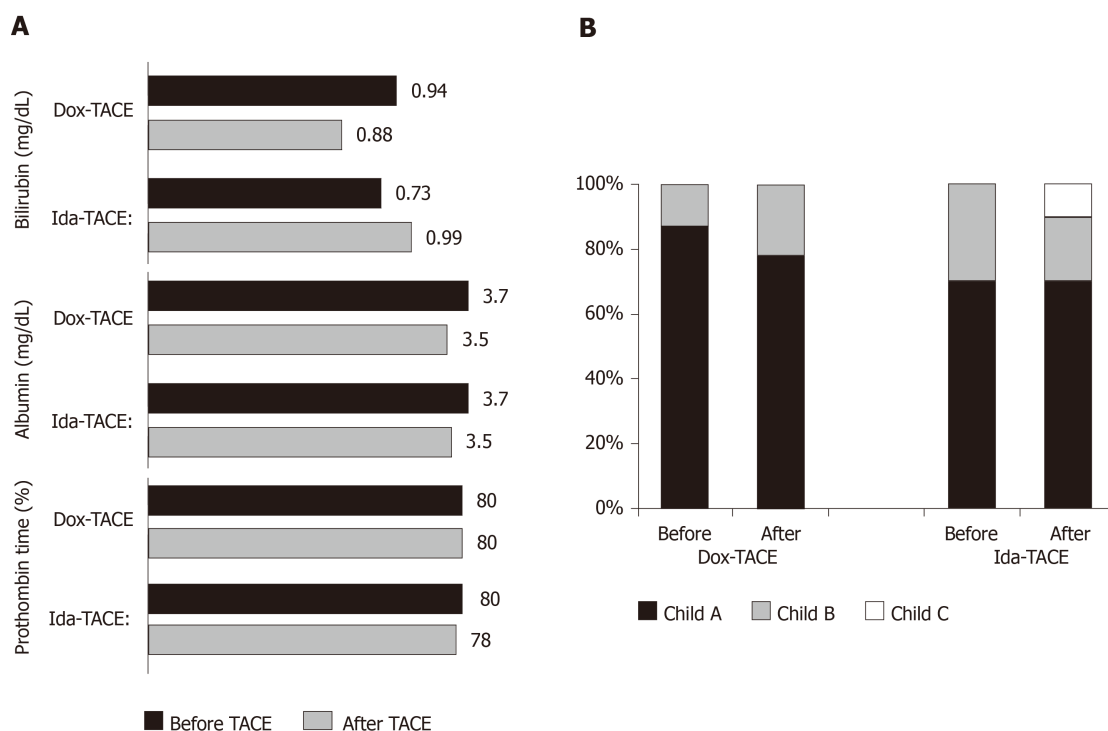


**Figure 3** Chronic liver toxicity after transarterial chemoembolization. A: Bilirubin, albumin, and prothrombin time changes; B: Child-Pugh class repartition changes between pre-transarterial chemoembolization and after transarterial chemoembolization (30-90 d) clinical and biological evaluation. Dox-TACE: Doxorubicin-based transarterial chemoembolization; Ida-TACE: Idarubicin-based transarterial chemoembolization.

## ARTICLE HIGHLIGHTS

### Research background

Transarterial chemoembolization (TACE) is the treatment of choice in intermediate hepatocellular carcinoma (HCC). Doxorubicin is largely used but without solid evidence in literature.

### Research motivation

Growing research suggests that idarubicin is a serious candidate for use in TACE with one phase 1 clinical trial using lipiodol emulsion and a phase 1 as well as two phase 2 trials using drug-eluting beads. Idarubicin was never compared to doxorubicin in this setting. Because of multiple worldwide doxorubicin shortages, realization of TACE in patients with Barcelona Clinic Liver Cancer B becomes challenging and finding new alternatives to doxorubicin seems essential.

### Research objectives

The objective of this study was to compare idarubicin-based TACE (Ida-TACE) with doxorubicin-based TACE (Dox-TACE) in the treatment of intermediate HCC in terms of anti-tumor efficacy and safety.

### Research methods

All patients undergoing TACE between January 2012 and December 2014 were screened and included with the following inclusion criteria: Child-Pugh score A or B, a performance status below or equal to 1, and no prior TACE. Lipiodol emulsion or drug-eluting beads TACE could be performed with 10 mg of idarubicin or 50 mg of doxorubicin. Each patient treated with idarubicin was matched with two doxorubicin-treated patients. Objective tumor response of TACE was assessed based on mRECIST criteria by independent radiologists. Progression-free survival and liver-transplant free survival were compared between groups using log-rank tests.

### Research results

Both treatment group showed comparable characteristics. There were no differences in objective tumor response, progression-free survival, and liver-transplant free survival between Dox- and Ida-TACE. No additional toxicity was observed with idarubicin-TACE.

### Research conclusions

Idarubicin showed comparable efficacy and safety to doxorubicin in TACE and may represent a new option in the management of patients with Barcelona Clinic of Liver Cancer B HCC. In this study, due to the vast majority of patients treated by TACE using lipiodol, this constitutes the largest cohort of patients treated with idarubicin during TACE with delivery through lipiodol-emulsion.

### Research perspectives

Idarubicin represents a serious alternative to doxorubicin without complicating the procedure or increasing its toxicity. As lipiodol TACE is the most widespread technique to deliver chemotherapy, these results should easily help to improve HCC patient care worldwide. These results need to be confirmed by further clinical studies, and a phase II trial is scheduled.

## ACKNOWLEDGEMENTS

Thank you to Marine Faure for her help in the safety analysis process.

## REFERENCES

- 1 **Jemal A**, Bray F, Center MM, Ferlay J, Ward E, Forman D. Global cancer statistics. *CA Cancer J Clin* 2011; **61**: 69-90 [PMID: [21296855](#) DOI: [10.3322/caac.20107](#)]
- 2 **Llovet JM**, Bruix J. Systematic review of randomized trials for unresectable hepatocellular carcinoma: Chemoembolization improves survival. *Hepatology* 2003; **37**: 429-442 [PMID: [12540794](#) DOI: [10.1053/jhep.2003.50047](#)]
- 3 **Sieghart W**, Huckle F, Peck-Radosavljevic M. Transarterial chemoembolization: modalities, indication, and patient selection. *J Hepatol* 2015; **62**: 1187-1195 [PMID: [25681552](#) DOI: [10.1016/j.jhep.2015.02.010](#)]
- 4 **Lencioni R**, de Baere T, Soulen MC, Rilling WS, Geschwind JF. Lipiodol transarterial chemoembolization for hepatocellular carcinoma: A systematic review of efficacy and safety data. *Hepatology* 2016; **64**: 106-116 [PMID: [26765068](#) DOI: [10.1002/hep.28453](#)]
- 5 **Lammer J**, Malagari K, Vogl T, Pilleul F, Denys A, Watkinson A, Pitton M, Sergent G, Pfammatter T, Terraz S, Benhamou Y, Avajon Y, Gruenberger T, Pomoni M, Langenberger H, Schuchmann M, Dumortier J, Mueller C, Chevallier P, Lencioni R; PRECISION V Investigators. Prospective randomized study of doxorubicin-eluting-bead embolization in the treatment of hepatocellular carcinoma: results of the PRECISION V study. *Cardiovasc Intervent Radiol* 2010; **33**: 41-52 [PMID: [19908093](#) DOI: [10.1007/s00270-009-9711-7](#)]
- 6 **Varela M**, Real MI, Burrel M, Forner A, Sala M, Brunet M, Ayuso C, Castells L, Montañá X, Llovet JM, Bruix J. Chemoembolization of hepatocellular carcinoma with drug eluting beads: efficacy and doxorubicin pharmacokinetics. *J Hepatol* 2007; **46**: 474-481 [PMID: [17239480](#) DOI: [10.1016/j.jhep.2006.10.020](#)]
- 7 **Lencioni R**, Llovet JM, Han G, Tak WY, Yang J, Guglielmi A, Paik SW, Reig M, Kim DY, Chau GY, Luca A, Del Arbol LR, Leberre MA, Niu W, Nicholson K, Meinhardt G, Bruix J. Sorafenib or placebo plus TACE with doxorubicin-eluting beads for intermediate stage HCC: The SPACE trial. *J Hepatol* 2016; **64**: 1090-1098 [PMID: [26809111](#) DOI: [10.1016/j.jhep.2016.01.012](#)]
- 8 **Pinter M**, Ulbrich G, Sieghart W, Kölblinger C, Reiberger T, Li S, Ferlitsch A, Müller C, Lammer J, Peck-Radosavljevic M. Hepatocellular Carcinoma: A Phase II Randomized Controlled Double-Blind Trial of Transarterial Chemoembolization in Combination with Biweekly Intravenous Administration of Bevacizumab or a Placebo. *Radiology* 2015; **277**: 903-912 [PMID: [26131911](#) DOI: [10.1148/radiol.2015142140](#)]
- 9 **Boulin M**, Guiu S, Chaffert B, Aho S, Cercueil JP, Ghiringhelli F, Krause D, Fagnoni P, Hillon P, Bedenne L, Guiu B. Screening of anticancer drugs for chemoembolization of hepatocellular carcinoma. *Anticancer Drugs* 2011; **22**: 741-748 [PMID: [21487286](#) DOI: [10.1097/CAD.0b013e328346a0c5](#)]
- 10 **Boulin M**, Hillon P, Cercueil JP, Bonnetain F, Dabakuyo S, Minello A, Jouve JL, Lepage C, Bardou M, Wendremaire M, Guerard P, Denys A, Grandvillain A, Chaffert B, Bedenne L, Guiu B. Idarubicin-loaded beads for chemoembolization of hepatocellular carcinoma: results of the IDASPHERE phase I trial. *Aliment Pharmacol Ther* 2014; **39**: 1301-1313 [PMID: [24738629](#) DOI: [10.1111/apt.12746](#)]
- 11 **Guiu B**, Jouve JL, Schmitt A, Minello A, Bonnetain F, Cassinotto C, Piron L, Cercueil JP, Loffroy R, Latournerie M, Wendremaire M, Lepage C, Boulin M. Intra-arterial idarubicin\_lipiodol without embolisation in hepatocellular carcinoma: The LIDA-B phase I trial. *J Hepatol* 2018; **68**: 1163-1171 [PMID: [29427728](#) DOI: [10.1016/j.jhep.2018.01.022](#)]
- 12 **European Association for the Study of the Liver**. EASL Clinical Practice Guidelines: Management of hepatocellular carcinoma. *J Hepatol* 2018; **69**: 182-236 [PMID: [29628281](#) DOI: [10.1016/j.jhep.2018.03.019](#)]
- 13 **Monier A**, Guiu B, Duran R, Aho S, Bize P, Deltenre P, Dunet V, Denys A. Liver and biliary damages following transarterial chemoembolization of hepatocellular carcinoma: comparison between drug-eluting beads and lipiodol emulsion. *Eur Radiol* 2017; **27**: 1431-1439 [PMID: [27436016](#) DOI: [10.1007/s00330-016-4488-y](#)]
- 14 **Marelli L**, Stigliano R, Triantos C, Senzolo M, Cholongitas E, Davies N, Tibballs J, Meyer T, Patch DW, Burroughs AK. Transarterial therapy for hepatocellular carcinoma: which technique is more effective? A systematic review of cohort and randomized studies. *Cardiovasc Intervent Radiol* 2007; **30**: 6-25 [PMID: [17103105](#) DOI: [10.1007/s00270-006-0062-3](#)]
- 15 **Xie ZB**, Ma L, Wang XB, Bai T, Ye JZ, Zhong JH, Li LQ. Transarterial embolization with or without chemotherapy for advanced hepatocellular carcinoma: a systematic review. *Tumour Biol* 2014; **35**: 8451-8459 [PMID: [25038916](#) DOI: [10.1007/s13277-014-2340-z](#)]
- 16 **Cammà C**, Schepis F, Orlando A, Albanese M, Shahied L, Trevisani F, Andreone P, Craxi A, Cottone M. Transarterial chemoembolization for unresectable hepatocellular carcinoma: meta-analysis of randomized controlled trials. *Radiology* 2002; **224**: 47-54 [PMID: [12091661](#) DOI: [10.1148/radiol.2241011262](#)]
- 17 **Facciorusso A**, Bellanti F, Villani R, Salvatore V, Muscatiello N, Piscaglia F, Vendemiale G, Serviddio G. Transarterial chemoembolization vs bland embolization in hepatocellular carcinoma: A meta-analysis of randomized trials. *United European Gastroenterol J* 2017; **5**: 511-518 [PMID: [28588882](#) DOI: [10.1177/2050640616673516](#)]
- 18 **Brown KT**, Do RK, Gonen M, Covey AM, Getrajdman GI, Sofocleous CT, Jarnagin WR, D'Angelica MI, Allen PJ, Erinjeri JP, Brody LA, O'Neill GP, Johnson KN, Garcia AR, Beattie C, Zhao B, Solomon SB, Schwartz LH, DeMatteo R, Abou-Alfa GK. Randomized Trial of Hepatic Artery Embolization for



- Hepatocellular Carcinoma Using Doxorubicin-Eluting Microspheres Compared With Embolization With Microspheres Alone. *J Clin Oncol* 2016; **34**: 2046-2053 [PMID: [26834067](#) DOI: [10.1200/JCO.2015.64.0821](#)]
- 19 **Golfieri R**, Giampalma E, Renzulli M, Cioni R, Bargellini I, Bartolozzi C, Breatta AD, Gandini G, Nani R, Gasparini D, Cucchetti A, Bolondi L, Trevisani F, PRECISION ITALIA STUDY GROUP. Randomised controlled trial of doxorubicin-eluting beads vs conventional chemoembolisation for hepatocellular carcinoma. *Br J Cancer* 2014; **111**: 255-264 [PMID: [24937669](#) DOI: [10.1038/bjc.2014.199](#)]
- 20 **Gallois L**, Fiallo M, Garnier-Suillerot A. Comparison of the interaction of doxorubicin, daunorubicin, idarubicin and idarubicinol with large unilamellar vesicles: Circular dichroism study. *Biochim Biophys Acta* 1998; **1370**: 31-40 [PMID: [9518541](#) DOI: [10.1016/S0005-2736\(97\)00241-1](#)]
- 21 **Boulin M**, Schmitt A, Delhom E, Cercueil JP, Wendremaire M, Imbs DC, Fohlen A, Panaro F, Herrero A, Denys A, Guiu B. Improved stability of lipiodol-drug emulsion for transarterial chemoembolisation of hepatocellular carcinoma results in improved pharmacokinetic profile: Proof of concept using idarubicin. *Eur Radiol* 2016; **26**: 601-609 [PMID: [26060065](#) DOI: [10.1007/s00330-015-3855-4](#)]
- 22 **Guiu B**, Chevallier P, Assenat E, Barbier E, Merle P, Bouvier A, Dumortier J, Nguyen-Khac E, Gugenheim J, Rode A, Oberti F, Valette PJ, Yzet T, Chevallier O, Barbare JC, Latournerie M, Boulin M. Idarubicin-loaded Beads for Chemoembolization of Hepatocellular Carcinoma: The IDASPHERE II Single-Arm Phase II Trial. *Radiology* 2019; **291**: 801-808 [PMID: [31038408](#) DOI: [10.1148/radiol.2019182399](#)]
- 23 **Guiu B**, Colombat S, Piron L, Hermida M, Allimant C, Pierredon-Foulongne MA, Belgour A, Escal L, Cassinotto C, Boulin M. Transarterial Chemoembolization of Hepatocellular Carcinoma with Idarubicin-Loaded Tandem Drug-Eluting Embolics. *Cancers (Basel)* 2019; **11** [PMID: [31311170](#) DOI: [10.3390/cancers11070987](#)]
- 24 **Qi X**, Zhao Y, Li H, Guo X, Han G. Management of hepatocellular carcinoma: an overview of major findings from meta-analyses. *Oncotarget* 2016; **7**: 34703-34751 [PMID: [27167195](#) DOI: [10.18632/oncotarget.9157](#)]



## Observational Study

# Metabolite profile comparisons between ascending and descending colon tissue in healthy adults

Bridget A Baxter, Kristopher D Parker, Michael J Nosler, Sangeeta Rao, Rebecca Craig, Catherine Seiler, Elizabeth P Ryan

**ORCID number:** Bridget A Baxter (0000-0001-9549-1989); Kristopher D Parker (0000-0002-6872-1547); Michael J Nosler (0000-0001-9174-0538); Sangeeta Rao (0000-0002-9234-0082); Rebecca Craig (0000-0001-6503-746X); Catherine Seiler (0000-0001-8357-818X); Elizabeth P Ryan (0000-0002-1577-0919).

**Author contributions:** Ryan EP and Nosler MJ designed research and maintained study oversight; Nosler MJ, Craig R and Seiler C conducted human tissue sample collections; Baxter BA and Parker KD analyzed the metabolite profile and microbiome data collected from stool and colon; Parker KD and Rao S performed statistical analysis; Baxter BA, Parker KD, and Ryan EP wrote the manuscript; Ryan EP had primary responsibility and all authors approved the final product.

**Supported by** the CancerCure Foundation and the University of Colorado Cancer Center Support Grant, Division of Cancer Control and Prevention (Aurora, CO), No. P30CA046934.

**Institutional review board statement:** Colorado State University Institutional Review Board No. 15-6051, and University Colorado Health-North Institutional Review Board No. 0010144.

**Informed consent statement:** Participants provided written informed consent.

**Bridget A Baxter, Kristopher D Parker, Elizabeth P Ryan,** Department of Environmental and Radiological Health Sciences, Colorado State University, Fort Collins, Fort Collins, CO 80523, United States

**Michael J Nosler,** University of Colorado Health Gastroenterology Clinic, Fort Collins, CO 80524, United States

**Sangeeta Rao,** Department of Clinical Sciences, Colorado State University, Fort Collins, CO 80523, United States

**Rebecca Craig,** Harmony Surgery Center, Fort Collins, CO 80528, United States

**Catherine Seiler,** Director of Clinical Operations, Harmony Surgery Center, Fort Collins, CO 80523, United States

**Corresponding author:** Elizabeth P Ryan, PhD, Associate Professor, Department of Environmental and Radiological Health Sciences, Colorado State University, 1617 Campus Delivery, Fort Collins, CO 80523, United States. [e.p.ryan@colostate.edu](mailto:e.p.ryan@colostate.edu)

## Abstract

### BACKGROUND

Obesity is a risk factor for colorectal cancer, yet metabolic distinctions between healthy right and left colon tissue, before cancer is diagnosed, remains largely unknown. This study compared right-ascending and left-descending colon tissue metabolomes to identify differences from the stool metabolome in normal weight, overweight, and obese adults.

### AIM

To examine right and left colon tissue metabolites according to body mass index that may serve as mechanistic targets for interventions and biomarkers for colon cancer risk.

### METHODS

Global, non-targeted metabolomics was applied to assess right-ascending and left-descending colon tissue collected from healthy adults undergoing screening colonoscopies to test the hypothesis that BMI differentially impacts colon tissue metabolite profiles. The colon tissue and stool metabolome of healthy adults ( $n = 24$ ) was analyzed for metabolite signatures and metabolic pathway networks implicated in progression of colorectal cancer.

**Conflict-of-interest statement:**

Authors have nothing to disclose.

**Data sharing statement:**

Metatransomics sequence data are available *via* NCBI SRA BioProject Accession PRJNA594611 and on this project's GitHub repository [github.com/kdprkr/ConjurersBre](https://github.com/kdprkr/ConjurersBre).

**STROBE statement:** The authors have read the STROBE guidelines, and the manuscript was prepared and revised according to the STROBE guidelines.

**Open-Access:** This article is an open-access article that was selected by an in-house editor and fully peer-reviewed by external reviewers. It is distributed in accordance with the Creative Commons Attribution NonCommercial (CC BY-NC 4.0) license, which permits others to distribute, remix, adapt, build upon this work non-commercially, and license their derivative works on different terms, provided the original work is properly cited and the use is non-commercial. See: <http://creativecommons.org/licenses/by-nc/4.0/>

**Manuscript source:** Unsolicited Manuscript

**Received:** October 22, 2019

**Peer-review started:** October 15, 2019

**First decision:** November 13, 2019

**Revised:** December 11, 2019

**Accepted:** December 21, 2019

**Article in press:** December 21, 2019

**Published online:** January 21, 2020

**P-Reviewer:** Hidaka E, Manenti A, Zheng YW

**S-Editor:** Ma YJ

**L-Editor:** A

**E-Editor:** Ma YJ

**RESULTS**

Ascending and descending colon contained 504 host, food, and microbiota-derived metabolites from normal weight, overweight and obese adults grouped according to body mass index. Amino acids, lipids, and nucleotides were among the chemical types that further differentiated from the stool metabolite profiles. Normal weight adults had 46 significantly different metabolites between ascending and descending colon tissue locations, whereas there were 37 metabolite differences in overweight and 28 metabolite differences for obese adults ( $P < 0.05$ ). Obese adults had trimethylamine N-oxide, endocannabinoids and monoacylglycerols with different relative abundances identified between ascending and descending colon. Primary and secondary bile acids, vitamins, and fatty acids also showed marked relative abundance differences in colon tissue from overweight/obese adults.

**CONCLUSION**

There were metabolite profile differences between right-ascending and left-descending colon tissue in healthy adults. Colon lipids and other metabolites in obese and overweight adults were distinguished from normal weight participants and associated with gut inflammation, nutrient absorption, and products of microbiota metabolism.

**Key words:** Colon; Ascending; Descending; Metabolomics; Obesity; Stool

©The Author(s) 2020. Published by Baishideng Publishing Group Inc. All rights reserved.

**Core tip:** This study identified metabolite profile differences between right-ascending and left-descending colon from normal, overweight or obese adults. We also show that stool metabolite composition does not accurately reflect the right-ascending colon. There is limited knowledge of human colon small molecules and metabolite signatures that may impact colon cancer risk. Colon cancer of the right-ascending colon has a poorer prognosis and reduced survival outcome when compared to colon cancer on the left-descending colon. Diet and lifestyle are additional factors of overweight and obesity that may influence colon tissue metabolite composition with respect to inflammation. Right and left colon metabolite profiles may be helpful to evaluate after interventions that seek to prevent or mitigate cancer risk.

**Citation:** Baxter BA, Parker KD, Nosler MJ, Rao S, Craig R, Seiler C, Ryan EP. Metabolite profile comparisons between ascending and descending colon tissue in healthy adults. *World J Gastroenterol* 2020; 26(3): 335-352

**URL:** <https://www.wjgnet.com/1007-9327/full/v26/i3/335.htm>

**DOI:** <https://dx.doi.org/10.3748/wjg.v26.i3.335>

**INTRODUCTION**

Body mass index (BMI) of 30% or greater is an established risk factor for colon cancer in men and women<sup>[1,2]</sup>. Obesity is a complex lipid-storage disease with metabolic aberrations locally in the gut and systemically in the host that increase risk for multiple chronic diseases<sup>[3]</sup>. Similar relationships occur for obesity and the incidence of larger (*vs* smaller) colon adenomas<sup>[3,4]</sup>. Weight gain from early to middle adulthood increases risk<sup>[5]</sup>, whereby middle-aged obese adults had a 60% increase risk of right-side colon cancer compared to the left-side<sup>[6]</sup>. We and others have previously shown that stool reveals changes in microbial communities<sup>[7]</sup>, and modulation by diet<sup>[8]</sup>, yet this may not accurately reflect metabolic differences between the right and left side colon tissue<sup>[9]</sup>.

Right-cancer patients have a worse prognosis with a median survival of 76.6 mo while left-sided have median survival of 101 mo<sup>[10]</sup> and right-sided tumors are significantly larger in size with a higher tumor grade when compared to left side colon cancer<sup>[11,12]</sup>. African American and non-Hispanic blacks have 24% greater odds of right-sided colon cancer<sup>[13]</sup>. Physical inactivity, excess body weight, alcohol, smoking, and a central deposition of adiposity are consistent risk factors for colorectal cancer.

High consumption of red meat more than 3 times/wk has been associated with 2-fold increased risk for colon cancer and these food components merit attention in the tissue of healthy adults<sup>[14]</sup>.

Metabolomics is a high-throughput screening methodology that is sensitive for detection of exogenous and endogenous (microbial, host and food) products of metabolism<sup>[15]</sup> and can aid in identification of disease risk biomarkers<sup>[16]</sup>. Metabolite profiling analysis of ascending and descending colon tissue was conducted herein to assess metabolic differences between colon locations that differ from stool. This study utilized normal weight, overweight and obese adults for investigation of colonic compounds that may impact colon cancer risk<sup>[17]</sup>. Metataxonomics of colon tissue by location has varied results<sup>[18,19]</sup> and provided rationale for using metabolomics. The major objective of this study was to identify metabolic pathways that distinguished ascending and descending colon tissue and to reveal metabolites altered by overweight and obesity that may pose elevated risks for developing cancer. We hypothesized that lipids (*e.g.*, fatty acids, bile acids, phospholipids, monoacylglycerol, and endocannabinoids) are distinct in type and abundance between the ascending and descending colon, and that colon tissue metabolomes will differ according to BMI when compared to stool in overweight and obese adults.

## MATERIALS AND METHODS

### *Study design- participant recruitment*

Ninety-three healthy adults were contacted prior to a scheduled colonoscopy in Fort Collins CO. Forty adult males and females provided written informed consent to collect a stool sample and an ascending and descending colon tissue biopsy. Twenty-four individuals (colon and stool) were assessed for non-targeted metabolomics. Eligible participants were provided a stool kit and study instructions. The gastroenterology clinical nurses and research staff confirmed study code number assignments and ensured the completed de-identification at the site of colonoscopy procedure. Colorado State University study personnel were contacted by clinic staff for sample retrieval immediately following procedure. Three study groups were BMI 20-24.9 for normal weight ( $n = 9$ ), BMI 25-29.9 for overweight ( $n = 9$ ) and BMI 30+ for obese ( $n = 6$ ) adults. One normal weight female (BMI 24) had the right and left colon and stool sample applied for metataxonomic analysis (16S rRNA gene sequencing). Participant's inclusion criteria for this study were at least 18 years of age, a scheduled routine colonoscopy, no prior history of colorectal cancer diagnosis, non-smoker, and not having taken antibiotics for at least one month prior to the standard of care, routine screening colonoscopy.

The colon tissue collected for this study was visually determined by the gastroenterologist performing the procedure to be normal, healthy tissue without polyps. Each participant had an about 5 mm biopsy of ascending (right) and descending (left) colon tissue and a self-collected stool sample prior to bowel preparation. Colonoscopy was completed by Centers for Gastroenterology-Fort Collins and University of Colorado-Health North Gastroenterology Clinic (Fort Collins, CO, United States). Samples were de-identified for personal information and study ID coded before storage and metabolite processing at Colorado State University. The number of polyps removed by the doctor with the respective location was provided following the procedure. This study received IRB approval, and include protocol number; Colorado State University IRB No. 15-6051, and University of Colorado Health IRB No. 0010144. Participants in this study had no history of diseases related to the liver or biliary tract and they did not have previous procedures such as cholecystectomy or ileal resections. This study did not collect information regarding the family history of colorectal cancer and did not perform hereditary genetic or epigenetic screening history on the patients. **Table 1** shows the study participant characteristics.

### *Colon tissue and stool sample collection*

Stool samples were self-collected by participants in a pre-labeled study coded container and frozen at -80 °C. Approximately 5 mm of normal healthy colon tissue were stored immediately at -80 °C following collection. Samples were shipped on dry ice to Metabolon, Inc. (Durham, NC, United States) and a single participant sample underwent DNA extraction for metataxonomics.

### *Sample accessioning and preparation*

Tissue and stool metabolite extraction was completed using 80% methanol as previously described<sup>[7]</sup>, prior to ultrahigh performance liquid chromatography-

**Table 1** Characteristics of the study participants (*n* = 24)

Characteristics	Total ( <i>n</i> = 24)	Normal ( <i>n</i> = 9)	Overweight ( <i>n</i> = 9)	Obese ( <i>n</i> = 6)
Sex				
Males	5	0	4	1
Females	19	9	5	5
BMI (mean $\pm$ SD, kg/m <sup>2</sup> )	27.6 $\pm$ 5.8	22 $\pm$ 1	26.7 $\pm$ 1.3	35 $\pm$ 5
Total number of people with polyps removes	14	6	4	4
Total number polyps removed	-	14	13	22
Polyp Location				
Cecum	-	1	0	3
Ascending	-	6	2	10
Transverse	-	2	1	1
Sigmoid	-	2	4	6
Rectum	-	0	6	0
Descending	-	3	0	2
History of hypertension				
Yes	6	2	3	2
No	18	7	6	4
History of type 2 diabetes				
Yes	3	0	2	1
No	21	9	7	5
Taking dietary supplements				
Yes	14	4	8	2
No	10	5	1	4
Smoking history				
Past smoker	9	2	6	1
Never	15	6	4	5

No participants had cancer detected from the screening exam. BMI: Body mass index.

tandem mass spectroscopy (UPLC-MS/MS) as completed by Metabolon, Inc. Positive and negative ion modes were chosen to provide broad, non-targeted detection of metabolites.

Samples were extracted using the automated MicroLab STAR® system from Hamilton Company. A set of recovery standards were added prior to the first step in the extraction process for quality control purposes. To remove protein, dissociate small molecules bound to protein or trapped in the precipitated protein matrix, and to recover chemically diverse metabolites, proteins were precipitated with methanol under vigorous shaking for 2 min (Glen Mills GenoGrinder 2000) followed by centrifugation. The resulting extract was divided into five fractions: two for analysis by two separate reverse phase (RP)/UPLC-MS/MS methods with positive ion mode electrospray ionization (ESI), one for analysis by RP/UPLC-MS/MS with negative ion mode ESI, one for analysis by HILIC/UPLC-MS/MS with negative ion mode ESI, and one sample was reserved for backup. Samples were placed briefly on a TurboVap® (Zymark) to remove the organic solvent. The sample extracts were stored overnight under nitrogen before preparation for analysis.

#### **UPLC-MS/MS analysis**

The UPLC-MS/MS portion of the platform was based on a Waters ACQUITY ultra-performance liquid chromatography (UPLC) and a Thermo Scientific Q-Exactive high resolution/accurate mass spectrometer interfaced with a heated electrospray ionization (HESI-II) source and Orbitrap mass analyzer operated at 35000 mass resolution. The protocol has been previously described by our lab<sup>[7]</sup>.

#### **Data extraction and compound identification**

Raw data were extracted, peak-identified, and processed using Metabolon's hardware and software. Compounds were identified by comparison to library entries of purified standards or recurrent unknown entities as previously described<sup>[7]</sup>.

#### **Statistical analysis**



Healthy colon tissue or stool metabolite profiles were semi-quantified in terms of relative abundance and median scaled to 1. Fold differences were calculated for normal weight, overweight and obese (colon tissue and stool) and for colon tissue between ascending and descending sites. A matched-pairs 2-way ANOVA was completed using the scaled relative abundance of each metabolite, experimental groups in ArrayStudio on log transformed data, were used for normal weight, overweight and obese. Metabolite profile distinctions between ascending and descending colon tissue were evaluated using  $P < 0.05$  for statistical significance with matched pair *t*-test. An estimate of the false discovery rate (*Q* value) was calculated to account the multiple comparisons across metabolites that are typical of metabolomics-based studies with a *Q* value  $\geq 0.01$ . A linear regression analyses for colon metabolites were performed to compare the groups with polyp removal to no polyp removal, after adjusting for the effect of weight category of the subjects.

Principal component analysis and hierarchical clustering were applied to understand the similarities and differences between samples and/or groups of samples in a complex dataset. Unsupervised clustering was performed using the ward D2 method<sup>[20]</sup>. Random forest (RF) analysis, a supervised classification technique, was applied for identifying candidate biomarkers. To determine which variables (biochemicals) make the largest contribution to the classification of BMI, a “variable importance” measure was computed. We used the “Mean Decrease Accuracy” as this metric prediction accuracy<sup>[21]</sup>.

### **Metataxonomics: Sample handling and DNA extraction, sequence read processing, and feature table analyses**

DNA was extracted from colon tissue and stool with the MoBio PowerSoil Kit according to manufacturer protocols. Amplification of the V4 region of the 16S rRNA gene and amplicon sequencing followed the standards outlined by the Earth Microbiome Project. Raw FASTQ-formatted forward reads were imported into the Quantitative Insights Into Microbial Ecology 2 (QIIME 2) platform<sup>[22]</sup>. A feature table comprised of amplicon sequence variants (ASVs) was inferred from reads using the DADA2 algorithm<sup>[23]</sup>. Taxonomy was assigned to each representative ASV sequence using Naïve Bayes classifiers trained against 99% OTU reference collections from Greengenes 13\_8 or SILVA 132. The raw feature table, representative sequences, and taxonomy tables were exported from QIIME 2 for further processing using R<sup>[24]</sup>. Following import, a master table comprised of ASV IDs with corresponding representative sequences, full and truncated Green-Genes and SILVA taxonomic lineages, and absolute abundances for all ASVs within each sample was constructed. This master table served as the entry point for all downstream processing and analysis. Comparisons of microbiota composition proceeded from the compositional data analysis paradigm with count zero multiplicative replacement prior to applying the centred log-ratio (clr) transformation<sup>[25]</sup>. Taxon abundance are depicted as proportions (*i.e.*, relative abundances). Supplemental Methods for additional details regarding amplification conditions, library preparation, sequencing, and a comprehensive account of analytical approaches.

### **Data availability**

Metataxonomics sequence data supporting the conclusions of this manuscript are available via NCBI SRA BioProject Accession PRJNA594611 and on this project’s GitHub repository located at [github.com/kdprkr/ConjurersBrew](https://github.com/kdprkr/ConjurersBrew), along with each of the materials needed to reproduce the analysis.

## **RESULTS**

### **Colon tissue and stool metabolomes of normal weight, overweight and obese adults**

The stool metabolome of healthy adults classified according to BMI as normal weight, overweight or obese had a total of 842 named compounds (Supplemental Table 1). The 842 stool metabolites consisted of 175 amino acids, 26 peptides, 33 carbohydrates, 11 energy, 345 lipids, 46 nucleotides, 47 cofactors and vitamins, and 159 were classified as exogenous and referred to as xenobiotics. There were 98 stool metabolites that significantly differ according to BMI were 22 amino acids, 1 peptide, 8 nucleotides, 2 cofactors and vitamins, 9 xenobiotics and 56 lipids. Principal component analyses (PCA) for the stool metabolome (Supplemental Figure 1A) and hierarchical clustering (Supplemental Figure 1B) did not clearly separate participants by BMI groups. The 504 colon metabolites with known identity and 44 unnamed/unknown compounds from 24 male and female participants are provided

in **Supplemental Table 2**. The colon metabolome contained 93 amino acids, 13 peptides, 35 carbohydrates, 10 metabolites were classified under TCA cycle and oxidative phosphorylation and there were 20 cofactors and vitamins. The largest portion of the colon tissue metabolome were lipids (about 50%, 262 lipid metabolites) that span 40 sub-metabolic pathways. Other notable small molecules from colon were 38 nucleotides and 32 exogenous, xenobiotic metabolites. Fourteen out of twenty-four healthy participants had 1-14 polyps removed during screening colonoscopy. A regression analysis for colon metabolites adjusting for the effect of weight was done, revealing 17 colon metabolites that had lower expression correlated with polyps removed (**Supplemental Table 3**). **Figure 1A**, shows 2-arachidonoylglycerol, 3-phosphoglycerate, and 6-phosphogluconate had a lower relative abundance in ascending and descending tissue from participants with polyps removed. **Figure 1B-C**, shows 1-dihomo-linolenylglycerol, aspartate, and glycerophosphorycholine (GPC) with lower expression in ascending colon tissue, while glutarate (C5-DC), and 2-hydroxyarachidate had lower expression in descending tissue from participants with polyps removed (**Figures 1B and C**).

Random forest analysis of colon tissue comparing normal weight *vs* overweight/obese yielded 30 metabolites with a predictive accuracy of 56% for the overweight/obese phenotype (**Supplemental Figure 2A**). BMI associated colon metabolites were bile acids and cofactors/vitamins (*e.g.*, biliverdin, alpha-tocopherol, and pyridoxate). The predictive accuracy for metabolites in ascending versus descending colon was 73%, and 24 of the top 30 metabolites were classified as lipids (**Supplemental Figure 2B**). **Table 2** further shows the 12 metabolites with statistically significant fold difference identified in right/left colon tissue and in stool by BMI comparisons. **Figure 2** shows lipids that are significantly different between weight groups for colon tissue and stool ( $P < 0.05$ ). The phospholipid, trimethylamine N-oxide (TMAO), was 2.80-fold difference from ascending in obese adults, and 6.23-fold difference from stool in overweight adults when compared to normal weight adults (**Figure 2A**). Endocannabinoids, linoleylethanolamide (2.11-fold) and oleylethanolamide (1.60-fold) difference from ascending in normal weight adults and decrease in stool of obese adults (**Figure 2B**). Furthermore, the median scaled relative abundance of primary and secondary bile acids (chenodeoxycholate 2.89-fold and 0.41-fold, cholate 0.55-fold, and taurodeoxycholate 1.49-fold) had significant differences by colon location and stool (**Figure 2C**). The primary bile acid, chenodeoxycholate is 2.89-fold difference from ascending in normal weight and 0.41-fold difference from descending in overweight adults, while 21.80-fold difference in stool of overweight adults when compared to normal weight. Cholate is 0.55-fold difference from obese descending colon and 61.06-fold difference from overweight stool when compared to normal weight (**Figure 2C**). The secondary bile acid, taurodeoxycholate, had 1.49-fold difference from ascending colon in overweight adults and 9.32-fold difference in stool of overweight adults compared to normal weight (**Table 2** and **Figure 2C**).

### **BMI differentiates ascending and descending colon lipids**

We next utilized metabolomics to distinguish ascending and descending colon tissue. There were 87 metabolites with statistically significant fold differences between ascending *vs* descending colon by BMI. These included, 46 metabolites in normal weight, 37 metabolites in overweight, and 28 metabolites in obese. Notably, the number of metabolites distinguishing ascending and descending colon decreased as BMI increased. We found that 62% of the metabolites distinguishing ascending and descending colon were lipids. **Table 3** shows 54 colon tissue lipids with statistically significant fold difference between ascending and descending colon. In normal weight adults there were 29 colon lipids, 24 of which were fatty acids and lysophospholipid (1.48-fold – 2.16-fold difference) from ascending, and 5 that were from descending colon. Overweight adults had 24 significantly different colon lipids; 11 metabolites from ascending, (8 derived from monoacylglycerols 1.67-fold – 2.61-fold), and 13 metabolites with higher abundance from descending tissue (**Table 3**). Obese adults had the fewest significant differences in colon lipids between ascending and descending tissue (15 identified metabolites). **Table 3** shows 4 metabolites increased in ascending tissue and 11 increased in descending tissue that were primarily fatty acids. **Figure 3** shows median scaled relative abundance of right and left colon tissue lipids, including those that are food derived long chain fatty acids and microbiome-products. The long chain fatty acids; palmitate 1.35-fold, arachidate 1.35-fold, and stearate 1.39-fold from ascending tissue in normal weight, and palmitate 0.73-fold, arachidate 0.69-fold, and stearate 0.68-fold from descending tissue in obese adults (**Figure 3A**). **Figure 3B** shows microbiome-derived metabolites that show significant fold difference in colon; 15-HETE from ascending tissue is 1.69-fold in normal weight and 1.93-fold in obese while, 3-hydroxybutyrate is 0.48-fold from descending in normal weight, and 2-

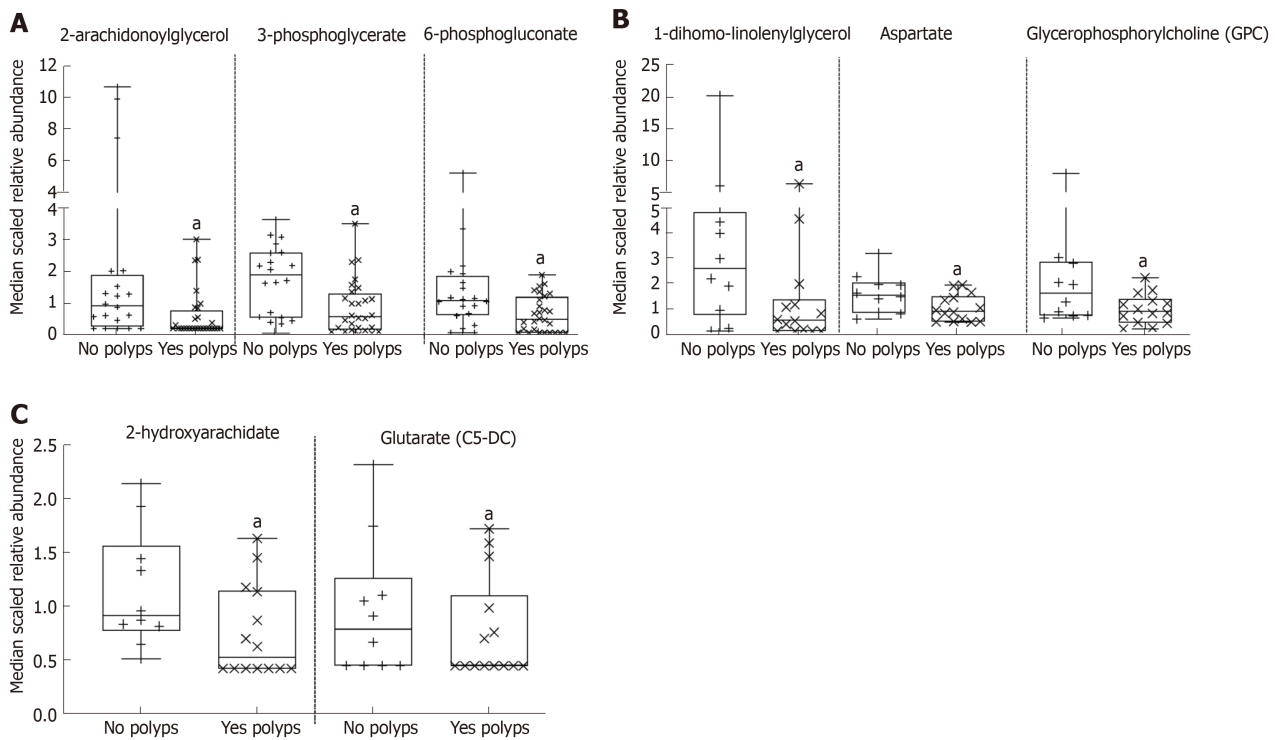


**Figure 1 Comparison of colon tissue metabolites between adults with and without polyps.** A: Colon metabolite abundance differences from both ascending and descending colon; B: Metabolite abundance in ascending colon; C: Metabolite abundance in descending colon. Statistical significance was examined using linear regression analysis ( $^aP < 0.05$ ).

archidonoylglycerol is 1.68-fold from ascending tissue in overweight adults (Figure 3B). This study suggests as BMI increases lipid diversity decrease in the colon and primarily in the ascending colon.

#### Ascending and descending colon tissue and stool microbiota composition

To explore associations of taxonomic groups with ascending colon, descending colon, and stool in a healthy weight adult female, we constructed a compositional PCA biplot from centred log-ratio transformed relative abundances. We observed marked separation across all three sample types at the phylum-, family-, and genus-levels. (Figure 4, Supplementary Table 4). Differences between ascending and descending colon were driven by increased abundance for several taxa in the Firmicutes phylum, including *Anaerostipes*, *Blautia*, *Dorea*, and *Fusicatenibacter* (all members of the *Lachnospiraceae* family), as well as *Streptococcus* and *Romboutsia* (members of the *Streptococcaceae* and *Peptostreptococcaceae* families, respectively). Stool samples were also differentiated by the genus *Bifidobacterium* (a member of the phylum Actinobacteria). Comparisons of the composition between colon samples (ascending versus descending) indicated enrichments for *Bacteroides*, *Ruminiclostridium* 9, *Ruminococcus gnavus*, and *Tyzzrella* in the ascending colon, while the descending colon harbored more *Barnesiella*, *Faecalibacterium*, *Parabacteroides*, *Parasutterella*, and *Roseburia* (Figure 4C and Supplemental Table 4).

## DISCUSSION

This study demonstrated colon tissue metabolite profile differences between normal weight, overweight and obese adults, and metabolic distinctions between ascending and descending colon within each of the BMI groups. A healthy human colon tissue metabolome had not previously been established across multiple metabolic pathways and revealed 504 known metabolites in both ascending and descending colon locations. Metabolomics has been widely employed for understanding changes that may result from colon metabolism, but the actual metabolite measurements for association with gut health have been from plasma<sup>[26]</sup>, urine<sup>[27]</sup>, stool<sup>[7,9]</sup>, and from cancerous tissue<sup>[28]</sup> or other digestive disease conditions<sup>[29]</sup>.

Our findings support that a healthy normal weight colon tissue metabolome involves complex lipid metabolism and that differences in lipid metabolite abundance between the right and left colon is associated with regulation of body weight.

**Table 2** Fold-differences of colon and stool metabolites

Sub pathway	Biochemical name	Fold difference colon ascending/descending					Fold difference stool BMI comparisons						
		NW	P value	OW	P value	OB	P value	Ow NW	P value	OB NW	P value	OB OW	P value
Methionine, Cysteine, SAM and taurine metabolism	N-acetylglutamine	<b>1.47</b>	<b>0.027</b>	1.15	0.412	1.13	0.534	1.20	0.711	<b>3.44</b>	<b>0.029</b>	0.35	0.096
Endocannabinoid	Oleoyl-ethanolamide	<b>1.6</b>	<b>0.038</b>	1.06	0.790	1.55	0.109	0.23	0.261	1.94	0.174	<b>0.12</b>	<b>0.026</b>
	Linoleoyl-ethanolamide	<b>2.11</b>	<b>0.005</b>	1.26	0.351	1.52	0.171	0.21	0.172	2.49	0.146	<b>0.08</b>	<b>0.012</b>
Phospholipid metabolism	Trimethylamine N-oxide	0.92	0.832	1.02	0.969	<b>2.8</b>	<b>0.049</b>	1.47	0.494	<b>6.23</b>	<b>0.025</b>	0.24	0.149
Phosphatidylethanolamine	1-palmitoyl-2-oleoyl-GPE (16:0/18:1)	0.77	0.145	<b>0.66</b>	<b>0.029</b>	0.7	0.113	<b>2.63</b>	<b>0.044</b>	2.57	0.244	1.02	0.322
Lysophospholipid	2-palmitoyl-GPC (16:0) <sup>1</sup>	<b>1.52</b>	<b>0.019</b>	1.18	0.317	0.93	0.709	0.84	0.667	2.81	0.061	<b>0.30</b>	<b>0.039</b>
	1-linoleoyl-GPG (18:2) <sup>1</sup>	<b>1.55</b>	<b>0.030</b>	1.26	0.239	1.05	0.819	1.25	0.335	<b>3.45</b>	<b>0.001</b>	<b>0.36</b>	<b>0.010</b>
Primary bile acid metabolism	Cholate	1.12	0.612	<b>0.84</b>	<b>0.447</b>	<b>0.55</b>	<b>0.041</b>	3.13	0.512	<b>61.06</b>	<b>0.019</b>	0.05	0.114
	Chenodeoxycholate	<b>2.89</b>	<b>0.049</b>	0.41	0.094	0.9	0.872	0.76	0.697	<b>21.80</b>	<b>0.005</b>	<b>0.03</b>	<b>0.004</b>
Secondary bile acid metabolism	Taurodeoxycholate	1.13	0.482	<b>1.49</b>	<b>0.027</b>	0.78	0.249	0.43	0.434	9.32	0.080	<b>0.05</b>	<b>0.024</b>
Purine metabolism, cytidine containing	Cytidine	<b>1.93</b>	<b>0.036</b>	1.46	0.216	1.12	0.748	1.25	0.469	<b>2.06</b>	<b>0.047</b>	0.61	0.249

<sup>1</sup>Not officially confirmed, but confident. Values presented are fold-change of the mean relative abundance within ascending versus descending colon tissue and BMI comparisons from stool. Bold indicates *P* value < 0.05. NW: Normal weight; OW: overweight; OB: Obese; BMI: Body mass index.

Differences were identified for right and left colon metabolites from the endocannabinoid pathway that may signify control over energy metabolism, which regulates appetite, lipolysis, and energy expenditure. The endocannabinoid pathway is implicated in both homeostatic and hedonic food intakes that result in increased hunger<sup>[30]</sup>. Specific endocannabinoids, such as the monounsaturated oleoylethanolamide, saturated palmitoylethanolamide and polyunsaturated linoleoylethanolamide showed higher relative abundance in normal weight adults from ascending colon compared to descending colon, and relative higher abundance from stool in overweight adult compared to normal weight. These lipids are also important for regulating metabolism in immune and neuronal cells<sup>[31]</sup>. Oleoylethanolamide levels in the mucosal layer of the proximal small intestine was shown to increase with nutrient availability and may be another factor in the

**Table 3** Colon lipid metabolites with fold-differences by colon location and body mass index

Sub pathway	Biochemical name	Fold difference ascending/descending					
		NW	P value	OW	P value	OB	P value
Long chain fatty acids	Palmitate (16:0)	1.3	0.02	1.0	0.75	0.7	0.04
		5	1	4	4	3	4
	Margarate (17:0)	1.2	0.13	0.8	0.33	0.7	0.03
		1	1	8		1	7
	Stearate (18:0)	1.3	0.01	0.9	0.61	0.6	0.01
		9	3	4	5	8	6
	Oleate/vaccenate (18:1)	1.5	0.04	1.2	0.36	0.9	0.80
			8		5	4	0
	Nonadecanoate (19:0)	1.1	0.29	0.8	0.26	0.6	0.01
		2		8	5	9	1
	Arachidate (20:0)	1.3	0.02	0.9	0.56	0.6	0.02
		5	5	3	4	9	5
Polyunsaturated fatty acid	Dihomo-linolenate (20:3n3 or n6)	1.4	0.04	1.1	0.56	1.0	0.88
		8	1	1	2	3	3
	Erucate (22:1n9)	1.5	0.03	1.0	0.81	1.1	0.47
		2	1	4	1	8	2
	Dihomo-linoleate (20:2n6)	1.5	0.04	1.2	0.28	1.1	0.56
		9	1	6	5	6	7
Fatty acid, dicarboxylate	Dodecadienoate (12:2) <sup>1</sup>	1.6	0.01	1.1	0.41	1.2	0.46
		8	7	8	7		3
		0.9	0.64	0.8	0.26	0.7	0.03
Ketone bodies	3-hydroxybutyrate (BHBA)	5	5	7	1	1	2
		0.4	0.00	0.9	0.90	1.0	0.82
		8	5	7	4	7	5
Fatty acid, metabolism (Acyl choline)	Linoleoylcholine <sup>1</sup>	1.2	0.34	1.1	0.62	2.0	0.02
		6	4	3		6	1
		1.3	0.04	0.9	0.67	0.7	0.13
Fatty acid, monohydroxy	2-hydroxystearate	2		5	7	9	5
		1.6	0.04	1.1	0.51	1.9	0.03
		9	5	8	5	3	9
Eicosanoid	15-hete	1.6	0.03	2.2	0.79	1.5	0.10
			8	3		5	9
		1.3	0.02	1.0	0.56	1.1	0.42
Endocannabinoid	Oleoyl ethanolamide	7	4	8	1	4	1
		2.1	0.00	1.2	0.35	1.5	0.17
		1	5	6	1	2	1
	Palmitoyl ethanolamide	0.8	0.28	0.6	0.01	0.7	0.15
		1	4		6		6
		0.9	0.87	0.6	0.04	0.6	0.09
Phosphatidylethanolamine	1-stearoyl-2-oleoyl-GPE (18:0/18:1)	7	5	5	3	5	7
		0.6	0.07	0.6	0.03	0.7	0.19
		9		5	8	3	
	1-oleoyl-2-docosahexaenoyl-GPE (18:1/22:6) <sup>1</sup>	0.6	0.01	0.7	0.08	0.4	0.00
		2		3	1	3	1
		1.5	0.03	1.3	0.20	1.2	0.33
Lysophospholipid	1-palmitoleoyl-GPC (16:1) <sup>1</sup>	9	6	1	2	8	3
		1.6	0.00	1.5	0.01	1.4	0.08
			8	7	1	3	5
	1-linoleoyl-GPC (18:2)	1.74	0.035	1.55	0.092	1.39	0.285
		1.8	0.00	1.4	0.07	1.2	0.31
		9	2	1	7	6	4



Plasmalogen	1-palmitoyl-GPG (16:0) <sup>1</sup>	2.1	0.00	1.3	0.18	0.8	0.51
		1	5	8	3	3	5
	1-stearoyl-GPG (18:0)	2.1	0.00	1.3	0.16	0.8	0.66
		6	2	6		9	5
	1-oleoyl-GPG (18:1) <sup>1</sup>	1.6	0.01	1.0	0.66	1.1	0.47
				7	8	6	6
	1-palmitoyl-GPI (16:0)	1.5	0.04	1.1	0.55	0.7	0.31
		8	1	3	4	7	8
	1-stearoyl-GPI (18:0)	1.4	0.03	1.0	0.66	0.8	0.50
		9	4	8	3	7	7
	1-oleoyl-GPI (18:1)	1.6	0.02	1.2	0.24	0.9	0.81
		4	7	8	7	4	8
	1-linoleoyl-GPI (18:2) <sup>1</sup>	1.4	0.01	1.1	0.48	1.2	0.22
		8	7	1	8	6	5
	1-(1-enyl-palmitoyl)-2-oleoyl-GPE (P-16:0/18:1) <sup>1</sup>	0.7	0.08	0.6	0.02	0.6	0.13
		1	9	2	2	9	8
Monoacylglycerol	1-(1-enyl-palmitoyl)-2-oleoyl-GPC (P-16:0/18:1) <sup>1</sup>	0.7	0.10	0.6	0.01	0.7	0.16
		4	5	3	9	3	
	1-(1-enyl-stearoyl)-2-oleoyl-GPE (P-18:0/18:1)	0.7	0.23	0.6	0.03	0.7	0.31
		9	4	4	3	8	1
	1-palmitoylglycerol (16:0)	1.3	0.25	2.6	0.00	1.2	0.53
		5	3	1	1	2	7
	1-palmitoleoylglycerol (16:1) <sup>1</sup>	1.6	0.09	2.2	0.00	1.1	0.62
			2	3	7	8	3
	1-oleoylglycerol (18:1)	1.6	0.20	2.2	0.03	0.7	0.50
			5	5	6	4	7
	1-linolenoylglycerol (18:3)	1.5	0.07	2.0	0.00	1.0	0.82
		4	4	7	5	7	3
	1-dihomo-linolenoylglycerol (20:3)	1.5	0.25	2.2	0.04	0.7	0.57
		5	1	6		7	4
	1-arachidonoylglycerol (20:4)	1.5	0.21	2.3	0.01	1.1	0.78
		1	8	4	7	2	3
Diacylglycerol	2-palmitoleoylglycerol (16:1) <sup>1</sup>	1.3	0.25	1.7	0.03	0.9	0.89
		4	7	7	4	6	8
	2-arachidonoylglycerol (20:4)	1.3	0.25	1.6	0.03	0.9	0.75
		1	3	8	5	1	2
	Linoleoyl-linolenoyl-glycerol (18:2/18:3) (2) <sup>1</sup>	1.3	0.51	1.6	0.29	3.3	0.03
		4	7	1	6	2	9
Ceramides	N-palmitoyl-sphingosine (d18:1/16:0)	0.9	0.73	0.6	0.00	0.7	0.04
		6	1	9	8	3	9
	N-stearoyl-sphingosine (d18:1/18:0) <sup>1</sup>	1.0	0.57	0.7	0.03	0.8	0.33
		9	8		1	3	9
	N-palmitoyl-heptadecasphingosine (d17:1/16:0) <sup>1</sup>	0.9	0.95	0.7	0.04	0.8	0.20
		9	7	4	2		0
Hexosylceramides (HCER)	Glycosyl-N-palmitoyl-sphingosine (d18:1/16:0)	0.7	0.04	0.6	0.00	0.6	0.02
		4	8	2	3	7	9
Primary bile acid	Glycochenodeoxycholate	0.9	0.75	1.8	0.00	0.8	0.54
			8	6	3	7	0
Secondary bile acid	Taurochenodeoxycholate	1.0	0.98	1.6	0.45	0.8	1
		4	7	2	6	6	
	Glycolithocholate sulfate	0.9	0.70	1.4	0.01	1	1
		5	3		2		
	Deoxycholate	0.9	0.79	0.6	0.12	0.7	0.00
			7	8	3	3	9

<sup>1</sup>Not officially confirmed, but confident. Values presented are fold-difference of the mean relative abundance between ascending/descending colon, by

weight class. Bold indicates *P* value < 0.05. BMI: Body mass index; NW: Normal weight; OW: Overweight; OB: Obese.

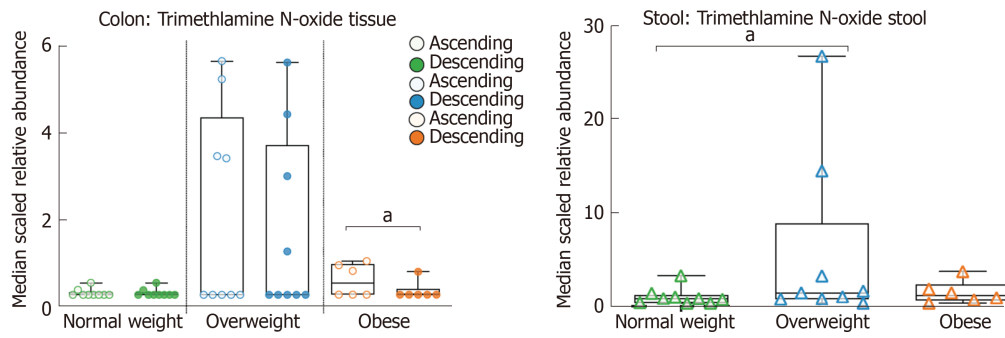
regulation of satiety<sup>[32]</sup>. Palmitoylethanolamide has supportive roles for reducing inflammation and eliciting neuroprotective effects<sup>[33]</sup>, while linoleoylethanolamide has reported anti-inflammatory functions<sup>[34]</sup>.

Bile acids are important signaling molecules which contribute to regulation of whole-body glucose, lipid metabolism, and body weight<sup>[35]</sup>. Primary and secondary bile acids were also identified for distinctions in abundance by colon location and from stool between overweight/obese and normal weight adults. Primary bile acids produced in the liver and increased bile acids in colon tissue may indicate altered reabsorption of bile acid by the liver and that results in subsequent alteration to metabolism by intestinal microbiota<sup>[36]</sup>. Primary bile acids, cholic acid and chenodeoxycholic acid, are derived from cholesterol by an enzymatic reaction occurring mainly in the liver<sup>[37]</sup>. Chenodeoxycholate has shown to increase colonic transit and improves bowel function<sup>[38]</sup>. Dietary cholic acid supplementation in rats caused a significant increase in colon tumors<sup>[39]</sup>. Interestingly, this study showed that primary bile acids; glycocholate, glycochenodeoxycholate, and taurochenodeoxycholate had 1.26-fold – 1.86-fold difference in overweight colon and merit attention as a mechanism with alongside other lipid classes to increase cancer risk in people. Concentrations of bile salts was shown to be higher in the proximal colon and bile-acid profiles were hypothesized to increase the risk of proximal cancer<sup>[40]</sup>.

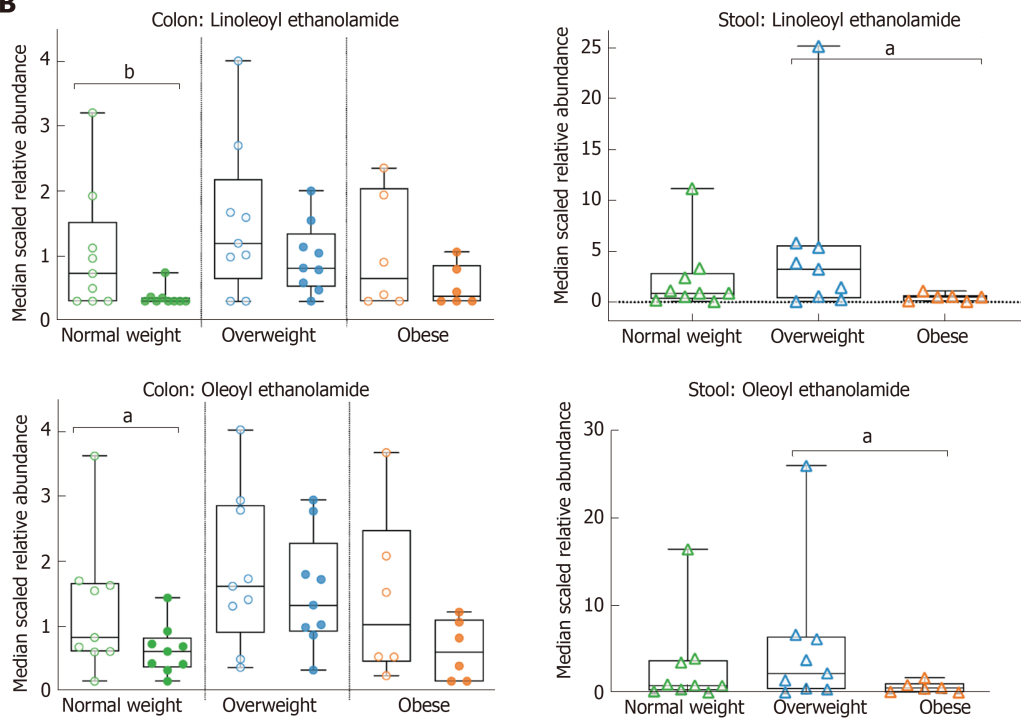
Population- based studies have shown that individuals who consume high-fat and high-beef foods display elevated levels of fecal secondary bile acids, as do patients diagnosed with colonic carcinomas<sup>[3,41]</sup>. Secondary bile acid, taurodeoxycholate are generated from primary bile acids and were shown to be increased in obese children plasma with insulin resistance when compared with their non-insulin resistant counterparts, unveiling the influence of the gut microbiota on the host metabolism<sup>[42]</sup>. Glycochenodeoxycholate a secondary bile acid produced by microbial flora in the large intestine was associated with colorectal cancer in women<sup>[43]</sup>, and high levels of deoxycholate in blood, bile feces, and mucosa were increased in colorectal cancer<sup>[7,37]</sup>. This study showed elevated glycochenodeoxycholate from descending colon in overweight adults, and elevated deoxycholate from descending colon in obese adults. Impaired bile acid signaling and dysbiosis may contribute to type 2 diabetes and other metabolic disease associated with obesity and colorectal cancer risk<sup>[44]</sup>. This study had limitations in the total sample size for each BMI group and did not control for different dietary intake patterns. The lack of gender balance in each BMI subgroup was also a potential source of bias for sex-based differences that may exist in colon tissue metabolite profiles. Future studies that control these variables merit attention because the colon tissue metabolite signatures that emerged herein did demonstrate metabolic relevance to the high risk of overweight and obesity in the progression of proximal and distal colon cancers.

Colonic TMAO abundance in obesity was a major finding from this study with respect to risk for cancer and supports a role for phospholipids from choline metabolism and produced by gut microbiota. TMAO was identified herein for increased abundance in ascending colon of obese adults and in stool of overweight adults. Deng *et al*<sup>[26]</sup> showed increased plasma levels of TMAO in patients with right sided colon cancer when compared to left sided colon cancer patients. High urine concentration of TMAO also directly correlated to the consumption of a high meat containing diet<sup>[45]</sup> and higher total milk and dairy consumption in plasma<sup>[46]</sup>. The increased levels in serum and urine were also shown to be associated with predisposition to impaired glucose homeostasis in high fat diet-fed mice<sup>[47]</sup>. Links between colorectal cancer and TMAO was detected in a genome-wide systems analysis<sup>[48]</sup> and in the development of colorectal cancer<sup>[26]</sup>. Our findings also revealed microbiome-derived metabolites in the colon tissue that were not in the stool, such as the ketone body, 3-hydroxybutyrate, an eicosanoid; 15-Hydroxyeicosatetraenoic acid (15-HETE), and the monoacylglycerol; 2-arachidonoylglycerol. Ketone bodies are strongly affected by obesity-related metabolic disorders and are utilized in the body as an energy source<sup>[49]</sup>. In visceral adipose tissue from obese subjects, 15-HETE was higher than in healthy subjects<sup>[50]</sup>. These aforementioned metabolic changes support the differences in microbiota between stool and colon and between colon locations (ascending *vs* descending). Right and left colon microbiota analysis for differences in healthy adults has been limited<sup>[19]</sup>. We observed an increased abundance of *Bacteroides* in the ascending colon and Proteobacteria in the descending colon that were consistent with Flynn *et al*<sup>[19]</sup>. Given that stool did not recapitulate the composition of the colonic mucosa-associated microbiota and metabolites, additional investigations with larger cohorts of each BMI group is warranted that will assess impacts of

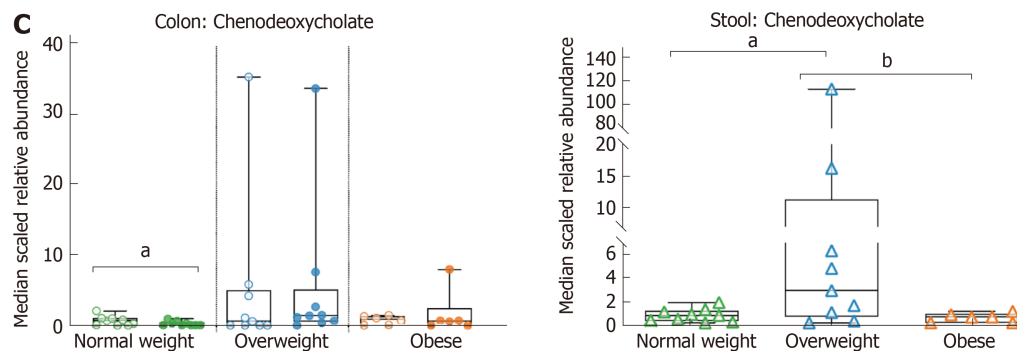
**A**



**B**



**C**



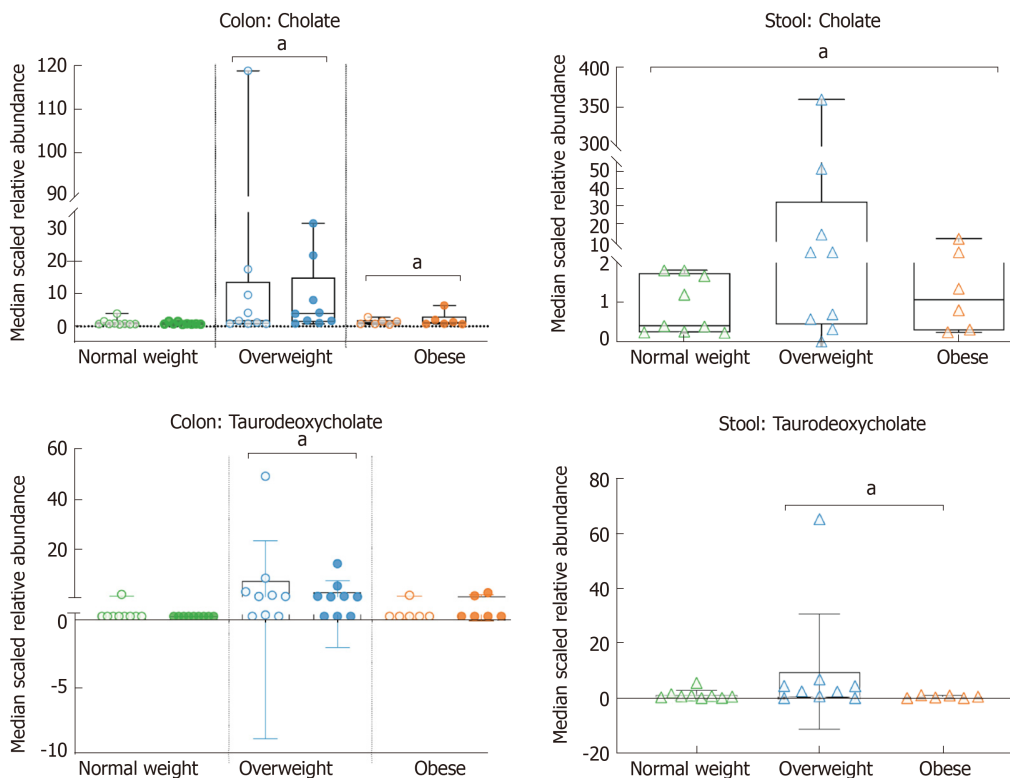


**Figure 2** Fold-differences of colon and stool metabolites according to body mass index. Metabolites were A: Phospholipid; Trimethylamine N-oxide; B: Endocannabinoids; linoleoyl ethanolamide, and oleoyl ethanolamide; C: Primary and secondary bile acids; chenodeoxycholate, cholate, and taurodeoxycholate. Left side panel colon, right side panel stool. Open circles represent ascending colon, closed circles represent descending colon, triangles represent stool (<sup>a</sup> $P < 0.05$ , <sup>b</sup> $P < 0.01$ ).

intervention strategies to reduce disease risk.

Fatty acids were also statistically supported in abundance by right and left location, and alongside BMI. Food-derived long chain fatty acids are found in dairy fat, coconut oil, palm kernel oil, peanut oil and vegetable oils. Monounsaturated long-chain fats such as oleic acid, and palmitoleic acid are found in animal fats, olive, canola and safflower oil. Oleic acid enhances insulin action and inhibits glucose production<sup>[51]</sup>, but also demonstrates cardiovascular benefits when it replaces heart-damaging saturated fat<sup>[52]</sup>. Palmitic acid is the first fatty acid produced during fatty acid synthesis, and is the precursor to longer fatty acids, while excess carbohydrates in the body may also be converted to palmitic acid. This analysis revealed major differences in long chain fatty acids as relevant to normal weight ascending colon and were also significantly different in the opposite direction of obese adults, namely increased in descending colon. Polyunsaturated long chain fats include linoleic acid, alpha-linolenic acid (seeds and nuts), arachidonic acid (meat, eggs, and algae) and eicosapentaenoic acid (fish oil)<sup>[53]</sup>. Margarate, also known as heptadecanoic acid is a biomarker of long-term milk fat intake<sup>[54]</sup>, and was elevated in the obese adults for descending colon. Stearate fed to mice showed 70% reduction of visceral fat<sup>[55]</sup>, and reduced metastasis tumor burden in a breast cancer mouse model<sup>[56]</sup>. Arachidate is necessary for the function of all cells, especially in the nervous system, skeletal muscle and immune systems<sup>[57]</sup>.

In conclusion, our study identified important metabolic differences between the right and left colon tissue of healthy adults and highlighted a wide range of lipids from normal weight, overweight and obese adults. The magnitude and abundance of a metabolite difference between ascending and descending colon tissue has not been previously evaluated and warrants further investigation for screening risk of proximal versus distal colon cancers.

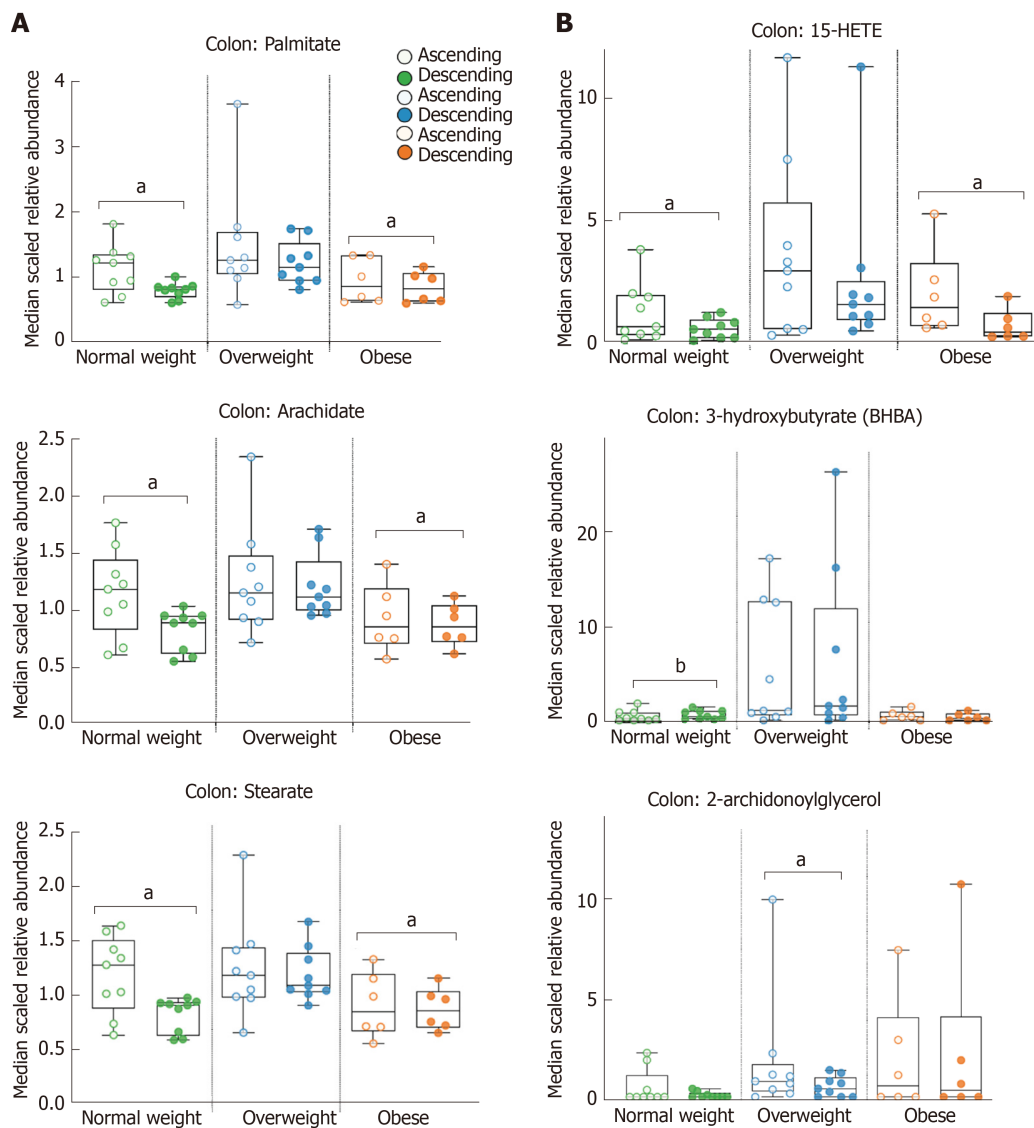


**Figure 3** Fold-differences of ascending vs descending lipid metabolites in normal weight, overweight and obese adults. A: Long chain fatty acids; palmitate, arachidate, and stearate; B: Microbiome derived metabolites; 15-HETE, 3-hydroxybutyrate (BHBA), and 2-archidonoylglycerol. Open circles represent ascending colon, closed circles represent descending colon (<sup>a</sup> $P < 0.05$ , <sup>b</sup> $P < 0.01$ ).



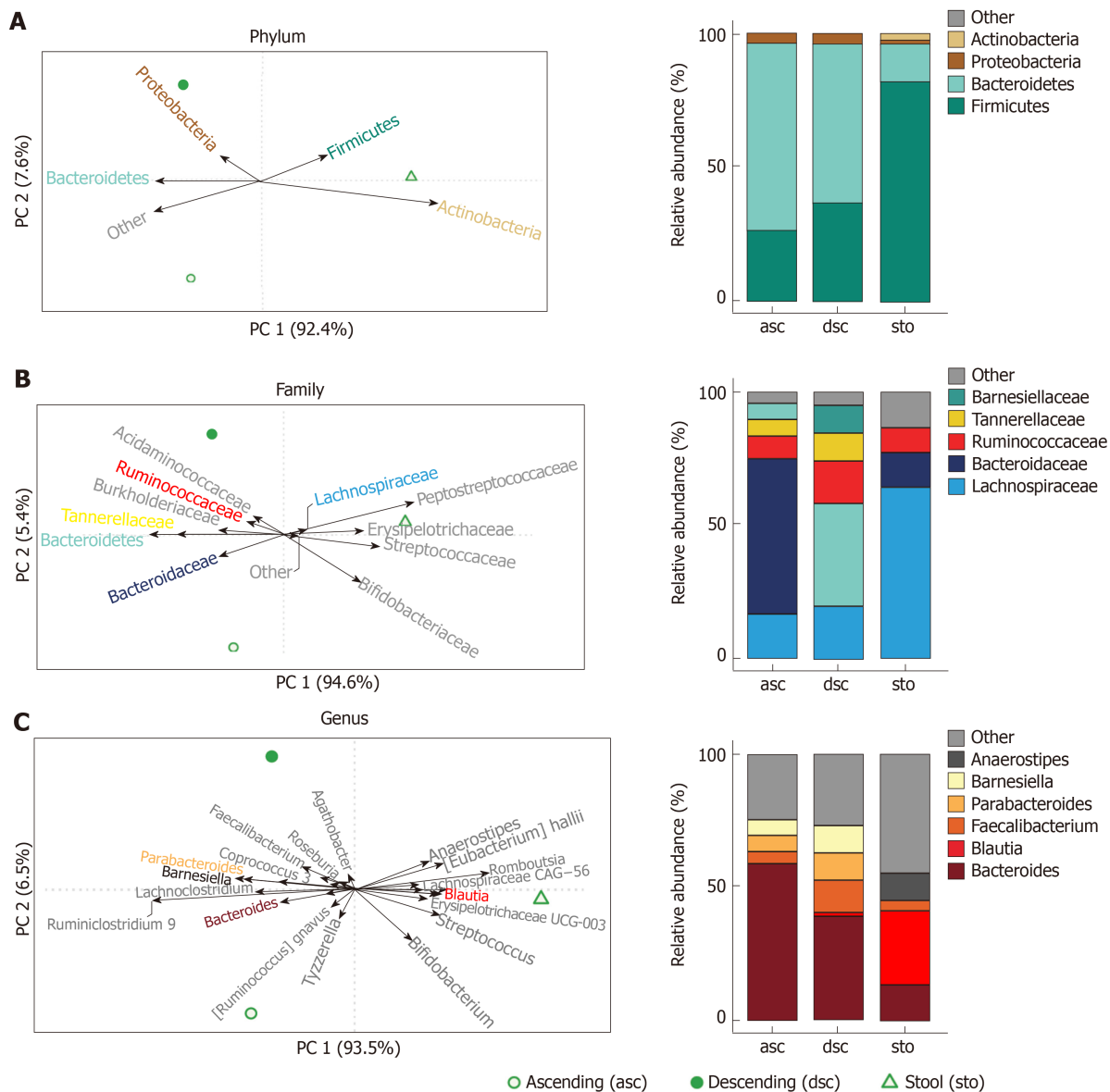


**Figure 4** Composition of microbiota from stool, ascending and descending colon in a healthy, normal weight adult. Left side shows principal components analysis biplots of centred log-ratio transformed relative abundances at the phylum; A: Family; B: Genus; C: Levels. Lines with arrows represent individual taxa. Right side shows relative abundance bar charts for the most abundant taxa at the respective taxonomic level across stool and colon location sample types.

## ARTICLE HIGHLIGHTS

### Research background

Obesity is a risk factor for colorectal cancer, yet metabolic distinctions between healthy right and left colon tissue, before cancer is diagnosed, remains largely unknown.

### Research motivation

Colon cancer of the ascending colon has a poorer prognosis and survival when compared to colon cancer on the descending colon. Stool metabolite composition does not accurately reflect proximal/ascending/right sided colon. Development of healthy colon tissue small molecule signatures for ascending and descending colon will aid in our understanding of how to improve gut metabolism and may help prevent or mitigate colorectal cancer risk.

### Research objectives

This study compared right-ascending and left-descending colon tissue metabolomes and sought to identify differences from the stool metabolome in normal weight, overweight, and obese adults.

### Research methods

Global, non-targeted metabolomics was applied to assess right-ascending and left-descending colon tissue collected from healthy adults undergoing screening colonoscopies to test the

hypothesis that body mass index (BMI) differentially impacts colon tissue metabolite profiles. The colon tissue and stool metabolome of healthy adults was analyzed for metabolite signatures and metabolic pathway networks implicated in progression and prevention of colorectal cancer.

### Research results

This is the first report using metabolomics to compare the right-ascending *vs* left--descending colon tissue of healthy adults. Our findings show that BMI was associated with metabolite profile differences between the ascending and descending colon. Disturbances in multiple metabolic pathways of the right and left colon from being overweight/obese may have important implications for increasing colorectal cancer risk.

### Research conclusions

There were metabolite profile differences between right-ascending and left-descending colon tissue in healthy adults receiving routine, screening colonoscopies. BMI impacts the number, type and magnitude of metabolite differences between the ascending and descending colon. Colon lipids and other metabolites in obese and overweight adults were distinguished from normal weight participants and associated with gut inflammation, nutrient absorption, and products of microbiota metabolism.

### Research perspectives

Right and left colon tissue metabolites that differ in relative abundance between normal weight, overweight, obese adults may be sensitive biomarkers for colon cancer risk. Diet and lifestyle influence right and left sided colon tissue metabolite composition that shape inflammation and cancer risk in overweight and obese adults. Development of healthy colon tissue small molecule signatures for ascending and descending colon will aid in our understanding of how to improve gut metabolism and may help prevent or mitigate colorectal cancer risk.

## ACKNOWLEDGEMENTS

We would like to thank the study participants, Erica Borresen, Renee Oppel and Luke Schwerdtfeger for assisting with recruitment, consent, and sample procurement from participating gastroenterology/endoscopy clinics and transporting samples to Colorado State University. We also thank Dr. Daniel Hampton, Dr. Rebecca Dunphy and Dr. Nicole Kershner for tissue biopsy collections from screening colonoscopies.

## REFERENCES

- 1 **Zeng H**, Lazarova DL. Obesity-related colon cancer: dietary factors and their mechanisms of anticancer action. *Clin Exp Pharmacol Physiol* 2012; **39**: 161-167 [PMID: [21418088](#) DOI: [10.1111/j.1440-1681.2011.05518.x](#)]
  - 2 **Tarasiuk A**, Mosińska P, Fichna J. The mechanisms linking obesity to colon cancer: An overview. *Obes Res Clin Pract* 2018; **12**: 251-259 [PMID: [29428365](#) DOI: [10.1016/j.orcp.2018.01.005](#)]
  - 3 **Lee GH**, Malietzis G, Askari A, Bernardo D, Al-Hassi HO, Clark SK. Is right-sided colon cancer different to left-sided colorectal cancer? - a systematic review. *Eur J Surg Oncol* 2015; **41**: 300-308 [PMID: [25468456](#) DOI: [10.1016/j.ejso.2014.11.001](#)]
  - 4 **Giovannucci E**, Colditz GA, Stampfer MJ, Willett WC. Physical activity, obesity, and risk of colorectal adenoma in women (United States). *Cancer Causes Control* 1996; **7**: 253-263 [PMID: [8740738](#) DOI: [10.1007/bf00051301](#)]
  - 5 **Song M**, Hu FB, Spiegelman D, Chan AT, Wu K, Ogino S, Fuchs CS, Willett WC, Giovannucci EL. Adulthood Weight Change and Risk of Colorectal Cancer in the Nurses' Health Study and Health Professionals Follow-up Study. *Cancer Prev Res (Phila)* 2015; **8**: 620-627 [PMID: [25930050](#) DOI: [10.1158/1940-6207.CAPR-15-0061](#)]
  - 6 **Moore LL**, Bradlee ML, Singer MR, Splansky GL, Proctor MH, Ellison RC, Kreger BE. BMI and waist circumference as predictors of lifetime colon cancer risk in Framingham Study adults. *Int J Obes Relat Metab Disord* 2004; **28**: 559-567 [PMID: [14770200](#) DOI: [10.1038/sj.ijo.0802606](#)]
  - 7 **Brown DG**, Rao S, Weir TL, O'Malia J, Bazan M, Brown RJ, Ryan EP. Metabolomics and metabolic pathway networks from human colorectal cancers, adjacent mucosa, and stool. *Cancer Metab* 2016; **4**: 11 [PMID: [27275383](#) DOI: [10.1186/s40170-016-0151-y](#)]
  - 8 **Hullar MA**, Fu BC. Diet, the gut microbiome, and epigenetics. *Cancer J* 2014; **20**: 170-175 [PMID: [24855003](#) DOI: [10.1097/PP0.0000000000000053](#)]
  - 9 **Weir TL**, Manter DK, Sheflin AM, Barnett BA, Heuberger AL, Ryan EP. Stool microbiome and metabolome differences between colorectal cancer patients and healthy adults. *PLoS One* 2013; **8**: e70803 [PMID: [23940645](#) DOI: [10.1371/journal.pone.0070803](#)]
  - 10 **Wang CB**, Shahjehan F, Merchea A, Li Z, Bekaii-Saab TS, Grothey A, Colibaseanu DT, Kasi PM. Impact of Tumor Location and Variables Associated With Overall Survival in Patients With Colorectal Cancer: A Mayo Clinic Colon and Rectal Cancer Registry Study. *Front Oncol* 2019; **9**: 76 [PMID: [30838175](#) DOI: [10.3389/fonc.2019.00076](#)]
  - 11 **Meguid RA**, Slidell MB, Wolfgang CL, Chang DC, Ahuja N. Is there a difference in survival between right- versus left-sided colon cancers? *Ann Surg Oncol* 2008; **15**: 2388-2394 [PMID: [18622647](#) DOI: [10.1245/s10434-008-0015-y](#)]
  - 12 **Lim DR**, Kuk JK, Kim T, Shin EJ. Comparison of oncological outcomes of right-sided colon cancer versus left-sided colon cancer after curative resection: Which side is better outcome? *Medicine (Baltimore)* 2017; **96**: e8241 [PMID: [29049212](#) DOI: [10.1097/MD.00000000000008241](#)]
- Gonzalez EC**, Roetzheim RG, Ferrante JM, Campbell R. Predictors of proximal vs. distal colorectal

- 13 cancers. *Dis Colon Rectum* 2001; **44**: 251-258 [PMID: [11227943](#) DOI: [10.1007/bf02234301](#)]
- 14 **Bernstein AM**, Song M, Zhang X, Pan A, Wang M, Fuchs CS, Le N, Chan AT, Willett WC, Ogino S, Giovannucci EL, Wu K. Processed and Unprocessed Red Meat and Risk of Colorectal Cancer: Analysis by Tumor Location and Modification by Time. *PLoS One* 2015; **10**: e0135959 [PMID: [26305323](#) DOI: [10.1371/journal.pone.0135959](#)]
- 15 **Kim S**, Kim J, Yun EJ, Kim KH. Food metabolomics: from farm to human. *Curr Opin Biotechnol* 2016; **37**: 16-23 [PMID: [26426959](#) DOI: [10.1016/j.copbio.2015.09.004](#)]
- 16 **Hale VL**, Jeraldo P, Mundy M, Yao J, Keeney G, Scott N, Cheek EH, Davidson J, Greene M, Martinez C, Lehman J, Pettry C, Reed E, Lyke K, White BA, Diener C, Resendis-Antonio O, Gransee J, Dutta T, Petterson XM, Boardman L, Larson D, Nelson H, Chia N. Synthesis of multi-omic data and community metabolic models reveals insights into the role of hydrogen sulfide in colon cancer. *Methods* 2018; **149**: 59-68 [PMID: [29704665](#) DOI: [10.1016/j.ymeth.2018.04.024](#)]
- 17 **Montrose DC**, Zhou XK, Kopelovich L, Yantiss RK, Karoly ED, Subbaramaiah K, Dannenberg AJ. Metabolic profiling, a noninvasive approach for the detection of experimental colorectal neoplasia. *Cancer Prev Res (Phila)* 2012; **5**: 1358-1367 [PMID: [22961778](#) DOI: [10.1158/1940-6207.CAPR-12-0160](#)]
- 18 **Donaldson GP**, Lee SM, Mazmanian SK. Gut biogeography of the bacterial microbiota. *Nat Rev Microbiol* 2016; **14**: 20-32 [PMID: [26499895](#) DOI: [10.1038/nrmicro3552](#)]
- 19 **Flynn KJ**, Ruffin MT 4th, Turgeon DK, Schloss PD. Spatial Variation of the Native Colon Microbiota in Healthy Adults. *Cancer Prev Res (Phila)* 2018; **11**: 393-402 [PMID: [29636352](#) DOI: [10.1158/1940-6207.Capr-17-0370](#)]
- 20 **Ward JH**. Hierarchical Grouping to Optimize an Objective Function. *J Am Stat Assoc* 1963; **58**: 236-244 [DOI: [10.1080/01621459.1963.10500845](#)]
- 21 **Breiman L**. Random Forests. *Mach Learn* 2001; **45**: 5-32 [DOI: [10.1023/a:1010933404324](#)]
- 22 **Bolyen E**, Rideout JR, Dillon MR, Bokulich NA, Abnet CC, Al-Ghalith GA, Alexander H, Alm EJ, Arumugam M, Asnicar F, Bai Y, Bisanz JE, Bittinger K, Brejnrod A, Brislawn CJ, Brown CT, Callahan BJ, Caraballo-Rodríguez AM, Chase J, Cope EK, Da Silva R, Diener C, Dorrestein PC, Douglas GM, Durall DM, Duvallet C, Edwardson CF, Ernst M, Estaki M, Fouquier J, Gaultier JM, Gibbons SM, Gibson DL, Gonzalez A, Gorlick K, Guo J, Hillmann B, Holmes S, Holste H, Huttenhower C, Huttley GA, Janssen S, Jarmusch AK, Jiang L, Kaehler BD, Kang KB, Keefe CR, Keim P, Kelley ST, Knights D, Koester I, Kosciorek T, Kreps J, Langille MGI, Lee J, Ley R, Liu YX, Loftfield E, Lozupone C, Maher M, Marotz C, Martin BD, McDonald D, McIver LJ, Melnik AV, Metcalf JL, Morgan SC, Morton JT, Naimey AT, Navas-Molina JA, Nothias LF, Orchanian SB, Pearson T, Peoples SL, Petras D, Preuss ML, Priesse E, Rasmussen LB, Rivers A, Robeson MS 2nd, Rosenthal P, Segata N, Shaffer M, Shiffer A, Sinha R, Song SJ, Spear JR, Swafford AD, Thompson LR, Torres PJ, Trinh P, Tripathi A, Turnbaugh PJ, Ull-Hasan S, van der Hooft JJJ, Vargas F, Vázquez-Baeza Y, Vogtmann E, von Hippel M, Walters W, Wan Y, Wang M, Warren J, Weber KC, Williamson CHD, Willis AD, Xu ZZ, Zaneveld JR, Zhang Y, Zhu Q, Knight R, Caporaso JG. Reproducible, interactive, scalable and extensible microbiome data science using QIIME 2. *Nat Biotechnol* 2019; **37**: 852-857 [PMID: [31341288](#) DOI: [10.1038/s41587-019-0209-9](#)]
- 23 **Callahan BJ**, McMurdie PJ, Rosen MJ, Han AW, Johnson AJ, Holmes SP. DADA2: High-resolution sample inference from Illumina amplicon data. *Nat Methods* 2016; **13**: 581-583 [PMID: [27214047](#) DOI: [10.1038/nmeth.3869](#)]
- 24 **R-Core-Team**. R: A language and environment for statistical computing. 3.5.2 ed. Vienna: R Foundation for Statistical Computing, 2019.
- 25 **Gloor GB**, Macklaim JM, Pawlowsky-Glahn V, Egozcue JJ. Microbiome Datasets Are Compositional: And This Is Not Optional. *Front Microbiol* 2017; **8**: 2224 [PMID: [29187837](#) DOI: [10.3389/fmicb.2017.02224](#)]
- 26 **Deng K**, Han P, Song W, Wang Z, Zhang F, Xie H, Zhao W, Xu H, Cai Y, Rong Z, Yu X, Cui BB, Li K. Plasma metabolomic profiling distinguishes right-sided from left-sided colon cancer. *Clin Chim Acta* 2018; **487**: 357-362 [PMID: [30296444](#) DOI: [10.1016/j.cca.2018.10.010](#)]
- 27 **Wang H**, Tso V, Wong C, Sadowski D, Fedorak RN. Development and validation of a highly sensitive urine-based test to identify patients with colonic adenomatous polyps. *Clin Transl Gastroenterol* 2014; **5**: e54 [PMID: [24646506](#) DOI: [10.1038/ctg.2014.2](#)]
- 28 **Griffin JL**, Shockcor JP. Metabolic profiles of cancer cells. *Nat Rev Cancer* 2004; **4**: 551-561 [PMID: [15229480](#) DOI: [10.1038/nrc1390](#)]
- 29 **Scoville EA**, Allaman MM, Brown CT, Motley AK, Horst SN, Williams CS, Koyama T, Zhao Z, Adams DW, Beaulieu DB, Schwartz DA, Wilson KT, Coburn LA. Alterations in Lipid, Amino Acid, and Energy Metabolism Distinguish Crohn's Disease from Ulcerative Colitis and Control Subjects by Serum Metabolomic Profiling. *Metabolomics* 2018; **14**: 17 [PMID: [29681789](#) DOI: [10.1007/s11306-017-1311-y](#)]
- 30 **Naughton SS**, Mathai ML, Hryciw DH, McAinch AJ. Fatty Acid modulation of the endocannabinoid system and the effect on food intake and metabolism. *Int J Endocrinol* 2013; **2013**: 361895 [PMID: [23762050](#) DOI: [10.1155/2013/361895](#)]
- 31 **Matias I**, Bisogno T, Di Marzo V. Endogenous cannabinoids in the brain and peripheral tissues: regulation of their levels and control of food intake. *Int J Obes (Lond)* 2006; **30** Suppl 1: S7-S12 [PMID: [16570107](#) DOI: [10.1038/sj.ijo.0803271](#)]
- 32 **Fu J**, Astarita G, Gaetani S, Kim J, Cravatt BF, Mackie K, Piomelli D. Food intake regulates oleoylethanolamide formation and degradation in the proximal small intestine. *J Biol Chem* 2007; **282**: 1518-1528 [PMID: [17121838](#) DOI: [10.1074/jbc.M607809200](#)]
- 33 **Andresen SR**, Bing J, Hansen RM, Biering-Sørensen F, Johannesen IL, Hagen EM, Rice AS, Nielsen JF, Bach FW, Finnerup NB. Ultramicronized palmitoylethanolamide in spinal cord injury neuropathic pain: a randomized, double-blind, placebo-controlled trial. *Pain* 2016; **157**: 2097-2103 [PMID: [27227691](#) DOI: [10.1097/j.pain.0000000000000623](#)]
- 34 **Ishida T**, Nishiumi S, Tanahashi T, Yamasaki A, Yamazaki A, Akashi T, Miki I, Kondo Y, Inoue J, Kawauchi S, Azuma T, Yoshida M, Mizuno S. Linoleoyl ethanolamide reduces lipopolysaccharide-induced inflammation in macrophages and ameliorates 2,4-dinitrofluorobenzene-induced contact dermatitis in mice. *Eur J Pharmacol* 2013; **699**: 6-13 [PMID: [23201070](#) DOI: [10.1016/j.ejphar.2012.11.030](#)]
- 35 **Hasenour CM**, Ridley DE, Hughey CC, James FD, Donahue EP, Shearer J, Viollet B, Foretz M, Wasserman DH. 5-Aminoimidazole-4-carboxamide-1-β-D-ribofuranoside (AICAR) effect on glucose production, but not energy metabolism, is independent of hepatic AMPK in vivo. *J Biol Chem* 2014; **289**: 5950-5959 [PMID: [24403081](#) DOI: [10.1074/jbc.M113.528232](#)]
- 36 **Li T**, Chiang JY. Bile acids as metabolic regulators. *Curr Opin Gastroenterol* 2015; **31**: 159-165 [PMID: [25704665](#) DOI: [10.1016/j.copbio.2015.09.004](#)]

- 25584736 DOI: [10.1097/MOG.0000000000000156](https://doi.org/10.1097/MOG.0000000000000156)]
- 37 **Ajouz H**, Mukherji D, Shamseddine A. Secondary bile acids: an underrecognized cause of colon cancer. *World J Surg Oncol* 2014; **12**: 164 [PMID: [24884764](https://pubmed.ncbi.nlm.nih.gov/24884764/) DOI: [10.1186/1477-7819-12-164](https://doi.org/10.1186/1477-7819-12-164)]
  - 38 **Rao AS**, Wong BS, Camilleri M, Odunsi-Shiyanbade ST, McKinzie S, Ryks M, Burton D, Carlson P, Lamsam J, Singh R, Zinsmeister AR. Chenodeoxycholate in females with irritable bowel syndrome-constipation: a pharmacodynamic and pharmacogenetic analysis. *Gastroenterology* 2010; **139**: 1549-1558, 1558.e1 [PMID: [20691689](https://pubmed.ncbi.nlm.nih.gov/20691689/) DOI: [10.1053/j.gastro.2010.07.052](https://doi.org/10.1053/j.gastro.2010.07.052)]
  - 39 **McSherry CK**, Cohen BI, Bokkenheuser VD, Mosbach EH, Winter J, Matoba N, Scholes J. Effects of calcium and bile acid feeding on colon tumors in the rat. *Cancer Res* 1989; **49**: 6039-6043 [PMID: [2790818](https://pubmed.ncbi.nlm.nih.gov/2790818/)]
  - 40 **Gervaz P**, Bucher P, Morel P. Two colons-two cancers: paradigm shift and clinical implications. *J Surg Oncol* 2004; **88**: 261-266 [PMID: [15565587](https://pubmed.ncbi.nlm.nih.gov/15565587/) DOI: [10.1002/jso.20156](https://doi.org/10.1002/jso.20156)]
  - 41 **Nagengast FM**, Grubben MJ, van Munster IP. Role of bile acids in colorectal carcinogenesis. *Eur J Cancer* 1995; **31A**: 1067-1070 [PMID: [7576993](https://pubmed.ncbi.nlm.nih.gov/7576993/) DOI: [10.1016/0959-8049\(95\)00216-6](https://doi.org/10.1016/0959-8049(95)00216-6)]
  - 42 **Mastrangelo A**, Martos-Moreno GÁ, García A, Barrios V, Rupérez FJ, Chowen JA, Barbas C, Argente J. Insulin resistance in prepubertal obese children correlates with sex-dependent early onset metabolomic alterations. *Int J Obes (Lond)* 2016; **40**: 1494-1502 [PMID: [27163744](https://pubmed.ncbi.nlm.nih.gov/27163744/) DOI: [10.1038/ijo.2016.92](https://doi.org/10.1038/ijo.2016.92)]
  - 43 **Cross AJ**, Moore SC, Boca S, Huang WY, Xiong X, Stolzenberg-Solomon R, Sinha R, Sampson JN. A prospective study of serum metabolites and colorectal cancer risk. *Cancer* 2014; **120**: 3049-3057 [PMID: [24894841](https://pubmed.ncbi.nlm.nih.gov/24894841/) DOI: [10.1002/cncr.28799](https://doi.org/10.1002/cncr.28799)]
  - 44 **Shapiro H**, Kolodziejczyk AA, Halstuch D, Elinav E. Bile acids in glucose metabolism in health and disease. *J Exp Med* 2018; **215**: 383-396 [PMID: [29339445](https://pubmed.ncbi.nlm.nih.gov/29339445/) DOI: [10.1084/jem.20171965](https://doi.org/10.1084/jem.20171965)]
  - 45 **Stella C**, Beckwith-Hall B, Cloarec O, Holmes E, Lindon JC, Powell J, van der Ouderaa F, Bingham S, Cross AJ, Nicholson JK. Susceptibility of human metabolic phenotypes to dietary modulation. *J Proteome Res* 2006; **5**: 2780-2788 [PMID: [17022649](https://pubmed.ncbi.nlm.nih.gov/17022649/) DOI: [10.1021/pr060265y](https://doi.org/10.1021/pr060265y)]
  - 46 **Rohrmann S**, Linseisen J, Allenspach M, von Eckardstein A, Müller D. Plasma Concentrations of Trimethylamine-N-oxide Are Directly Associated with Dairy Food Consumption and Low-Grade Inflammation in a German Adult Population. *J Nutr* 2016; **146**: 283-289 [PMID: [26674761](https://pubmed.ncbi.nlm.nih.gov/26674761/) DOI: [10.3945/jn.115.220103](https://doi.org/10.3945/jn.115.220103)]
  - 47 **Gao X**, Liu X, Xu J, Xue C, Xue Y, Wang Y. Dietary trimethylamine N-oxide exacerbates impaired glucose tolerance in mice fed a high fat diet. *J Biosci Bioeng* 2014; **118**: 476-481 [PMID: [24721123](https://pubmed.ncbi.nlm.nih.gov/24721123/) DOI: [10.1016/j.jbiosc.2014.03.001](https://doi.org/10.1016/j.jbiosc.2014.03.001)]
  - 48 **Xu R**, Wang Q, Li L. A genome-wide systems analysis reveals strong link between colorectal cancer and trimethylamine N-oxide (TMAO), a gut microbial metabolite of dietary meat and fat. *BMC Genomics* 2015; **16** Suppl 7: S4 [PMID: [26100814](https://pubmed.ncbi.nlm.nih.gov/26100814/) DOI: [10.1186/1471-2164-16-s7-s4](https://doi.org/10.1186/1471-2164-16-s7-s4)]
  - 49 **Giesbertz P**, Padberg I, Rein D, Ecker J, Höfle AS, Spanier B, Daniel H. Metabolite profiling in plasma and tissues of ob/ob and db/db mice identifies novel markers of obesity and type 2 diabetes. *Diabetologia* 2015; **58**: 2133-2143 [PMID: [26058503](https://pubmed.ncbi.nlm.nih.gov/26058503/) DOI: [10.1007/s00125-015-3656-y](https://doi.org/10.1007/s00125-015-3656-y)]
  - 50 **Candi E**, Tesaro M, Cardillo C, Lena AM, Schinzari F, Rodia G, Sica G, Gentileschi P, Rovella V, Annicchiarico-Petruzzelli M, Di Daniele N, Melino G. Metabolic profiling of visceral adipose tissue from obese subjects with or without metabolic syndrome. *Biochem J* 2018; **475**: 1019-1035 [PMID: [29437994](https://pubmed.ncbi.nlm.nih.gov/29437994/) DOI: [10.1042/bcj20170604](https://doi.org/10.1042/bcj20170604)]
  - 51 **Obici S**, Feng Z, Morgan K, Stein D, Karkanias G, Rossetti L. Central administration of oleic acid inhibits glucose production and food intake. *Diabetes* 2002; **51**: 271-275 [PMID: [11812732](https://pubmed.ncbi.nlm.nih.gov/11812732/) DOI: [10.2337/diabetes.51.2.271](https://doi.org/10.2337/diabetes.51.2.271)]
  - 52 **Voelker R**. Oleic Acid Can Make Heart Claim Without Hard Evidence. *JAMA* 2019; **321**: 23 [PMID: [30620358](https://pubmed.ncbi.nlm.nih.gov/30620358/) DOI: [10.1001/jama.2018.19747](https://doi.org/10.1001/jama.2018.19747)]
  - 53 **Kingsbury KJ**, Paul S, Crossley A, Morgan DM. The fatty acid composition of human depot fat. *Biochem J* 1961; **78**: 541-550 [PMID: [13756126](https://pubmed.ncbi.nlm.nih.gov/13756126/) DOI: [10.1042/bj0780541](https://doi.org/10.1042/bj0780541)]
  - 54 **Wolk A**, Vessby B, Ljung H, Barrefors P. Evaluation of a biological marker of dairy fat intake. *Am J Clin Nutr* 1998; **68**: 291-295 [PMID: [9701185](https://pubmed.ncbi.nlm.nih.gov/9701185/) DOI: [10.1093/ajcn/68.2.291](https://doi.org/10.1093/ajcn/68.2.291)]
  - 55 **Shen MC**, Zhao X, Siegal GP, Desmond R, Hardy RW. Dietary stearic acid leads to a reduction of visceral adipose tissue in athymic nude mice. *PLoS One* 2014; **9**: e104083 [PMID: [25222131](https://pubmed.ncbi.nlm.nih.gov/25222131/) DOI: [10.1371/journal.pone.0104083](https://doi.org/10.1371/journal.pone.0104083)]
  - 56 **Evans LM**, Toline EC, Desmond R, Siegal GP, Hashim AI, Hardy RW. Dietary stearate reduces human breast cancer metastasis burden in athymic nude mice. *Clin Exp Metastasis* 2009; **26**: 415-424 [PMID: [19267249](https://pubmed.ncbi.nlm.nih.gov/19267249/) DOI: [10.1007/s10585-009-9239-x](https://doi.org/10.1007/s10585-009-9239-x)]
  - 57 **Tallima H**, El Ridi R. Arachidonic acid: Physiological roles and potential health benefits - A review. *J Adv Res* 2018; **11**: 33-41 [PMID: [30034874](https://pubmed.ncbi.nlm.nih.gov/30034874/) DOI: [10.1016/j.jare.2017.11.004](https://doi.org/10.1016/j.jare.2017.11.004)]



## Programmed cell death-1 inhibitor-related sclerosing cholangitis: A systematic review

Takumi Onoyama, Yohei Takeda, Taro Yamashita, Wataru Hamamoto, Yuri Sakamoto, Hiroki Koda, Soichiro Kawata, Kazuya Matsumoto, Hajime Isomoto

**ORCID number:** Takumi Onoyama (0000-0003-0310-0720); Yohei Takeda (0000-0003-1096-5909); Taro Yamashita (0000-0003-2726-3356); Wataru Hamamoto (0000-0003-2220-9916); Yuri Sakamoto (0000-0001-9682-6410); Hiroki Koda (0000-0003-4000-6899); Soichiro Kawata (0000-0002-2194-0582); Kazuya Matsumoto (0000-0002-5680-4791); Hajime Isomoto (0000-0001-8998-7865).

**Author contributions:** Onoyama T and Takeda Y contributed equally to the work; Matsumoto K and Isomoto H conceptualized and designed the review together with Onoyama T; Onoyama T, Yamashita T, Koda H, Hamamoto W, Sakamoto Y and Kawata S carried out the analysis; Onoyama T drafted the initial manuscript; all authors reviewed and approved the final manuscript as submitted.

**Conflict-of-interest statement:** All the authors declare that they have no competing interests.

**PRISMA 2009 Checklist statement:** The authors have read the PRISMA 2009 Checklist, and the manuscript was prepared and revised according to the PRISMA 2009 Checklist.

**Open-Access:** This article is an open-access article that was selected by an in-house editor and fully peer-reviewed by external reviewers. It is distributed in accordance with the Creative Commons Attribution NonCommercial (CC BY-NC 4.0) license, which permits others to

**Takumi Onoyama, Yohei Takeda, Taro Yamashita, Wataru Hamamoto, Yuri Sakamoto, Hiroki Koda, Soichiro Kawata, Hajime Isomoto,** Division of Medicine and Clinical Science, Department of Multidisciplinary Internal Medicine, Faculty of Medicine, Tottori University, Tottori prefecture 683-8504, Japan

**Kazuya Matsumoto,** Internal Medicine, Irisawa Medical Clinic, Shimane prefecture 690-0025, Japan

**Corresponding author:** Takumi Onoyama, MD, PhD, Doctor, Division of Medicine and Clinical Science, Department of Multidisciplinary Internal Medicine, Faculty of Medicine, Tottori University, 36-1 Nishi-cho, Yonago, Tottori prefecture 683-8504, Japan. [golf4to@yahoo.co.jp](mailto:golf4to@yahoo.co.jp)

### Abstract

#### BACKGROUND

Programmed cell death-1 (PD-1) inhibitor has been indicated for many types of malignancies. However, these inhibitors also cause immune-related adverse events. Hepatobiliary disorder is a phenotype of immune-related adverse event affecting 0%–4.5% of patients treated with PD-1 inhibitors. Recent studies have reported PD-1 inhibitor-related sclerosing cholangitis (SC); however, the associated clinical and pathological features are unclear.

#### AIM

To evaluate the clinical and pathological features of PD-1 inhibitor-related SC through a systematic review of the literature.

#### METHODS

The review, conducted using electronic databases in PubMed, was restricted to the period from January 2014 to September 2019 and focused on case reports/series on PD-1 inhibitor-related SC published in English. We scanned the references of the selected literature to identify any further relevant studies. Six cases previously studied by us, including three that have not yet been published, were included in this review.

#### RESULTS

Thirty-one PD-1 inhibitor-related SC cases were evaluated. Median age of patients was 67 years (range, 43–89), with a male to female ratio of 21:10. The main disease requiring PD-1 inhibitor treatment was non-small cell lung cancer. Agents that caused PD-1 inhibitor-related SC were nivolumab (19 cases),



distribute, remix, adapt, build upon this work non-commercially, and license their derivative works on different terms, provided the original work is properly cited and the use is non-commercial. See: <http://creativecommons.org/licenses/by-nc/4.0/>

**Manuscript source:** Invited manuscript

**Received:** November 23, 2019

**Peer-review started:** November 23, 2019

**First decision:** December 23, 2019

**Revised:** January 7, 2020

**Accepted:** January 11, 2020

**Article in press:** January 11, 2020

**Published online:** January 21, 2020

**P-Reviewer:** Uhlmann D, Yang L

**S-Editor:** Zhang L

**L-Editor:** A

**E-Editor:** Xing YX



pembrolizumab (10 cases), avelumab (1 case), and durvalumab (1 case). The median number of cycles until PD-1 inhibitor-related SC onset was 5.5 (range, 1–27). Abdominal pain or discomfort (35.5%, 11/31) was the most frequent symptom. Blood serum tests identified liver dysfunction with a notable increase in biliary tract enzymes relative to hepatic enzymes, and a normal level of serum immunoglobulin G4. Biliary dilation without obstruction (76.9%, 20/26), diffuse hypertrophy of the extrahepatic biliary tract (90.5%, 19/21), and multiple strictures of the intrahepatic biliary tract (30.4%, 7/23) were noted. In 11/23 (47.8%) cases, pathological examination indicated that CD8+ T cells were the dominant inflammatory cells in the bile duct or peribiliary tract. Although corticosteroids were mainly used for PD inhibitor-related SC treatment, the response rate was 11.5% (3/26).

## CONCLUSION

Some clinical and pathological features of PD-1 inhibitor-related SC were revealed. To establish diagnostic criteria for PD-1 inhibitor-related SC, more cases need to be evaluated.

**Key words:** Nivolumab; Pembrolizumab; Avelumab; Durvalumab; Atezolizumab; Programmed cell death-1 inhibitor; Immune-related adverse events; Cholangitis

©The Author(s) 2020. Published by Baishideng Publishing Group Inc. All rights reserved.

**Core tip:** This study systematically reviewed the literature on the programmed cell death-1 inhibitor-related sclerosing cholangitis. Biliary dilation without obstruction, diffuse hypertrophy of the extrahepatic biliary tract and/or multiple strictures of intrahepatic biliary tract, liver dysfunction with a notable increase in biliary tract enzymes relative to hepatic enzymes, normal level of the serum immunoglobulin G4, and a moderate to poor response to steroid therapy, and CD8+ T cell infiltration in the biliary tract were clinical and pathological features of programmed cell death-1 inhibitor-related sclerosing cholangitis.

**Citation:** Onoyama T, Takeda Y, Yamashita T, Hamamoto W, Sakamoto Y, Koda H, Kawata S, Matsumoto K, Isomoto H. Programmed cell death-1 inhibitor-related sclerosing cholangitis: A systematic review. *World J Gastroenterol* 2020; 26(3): 353-365

**URL:** <https://www.wjgnet.com/1007-9327/full/v26/i3/353.htm>

**DOI:** <https://dx.doi.org/10.3748/wjg.v26.i3.353>

## INTRODUCTION

The programmed cell death-1 (PD-1) receptor is expressed on activated T cells, whereas the programmed cell death-ligand 1 (PD-L1) is overexpressed on specific types of cancer cells. When bound by PD-L1, PD-1 causes the suppression of T cell cytotoxic immune responses. This repression pathway is an essential immune prevention mechanism from host immunity and is upregulated in many malignant tumors and their surrounding microenvironment<sup>[1]</sup>. Recently, developments in immunotherapy have demonstrated efficacy for the treatment of various malignancies. PD-1 inhibitors were also indicated for many types of malignancies, such as non-small cell lung cancer, melanoma, Hodgkin lymphoma, renal cell cancer, bladder cancer, gastric cancer, and esophageal cancer<sup>[2-12]</sup>. Moreover, pembrolizumab has been indicated for solid carcinoma with mismatch repair deficiency<sup>[13,14]</sup>. Therefore, many patients with malignant disease will be treated with a PD-1 inhibitor. Although PD-1 inhibitors are beneficial for the treatment of malignancies, it has been noted that immune-related adverse events (irAEs) result from dysregulation of the host immune system<sup>[15]</sup>. Hepatobiliary disorders are irAEs that affect 0%–4.5% of patients treated with PD-1 inhibitors<sup>[16-18]</sup>. Recently, PD-1 inhibitor-related sclerosing cholangitis (SC) and its clinical features have been reported<sup>[19,20]</sup>. However, the diagnostic criteria for PD-1 inhibitor-related SC have not been clarified. We also have experience of six cases of suspected of PD-1 inhibitor-related SC.

The objective of this work was to perform a systematic review of cases of PD-1 inhibitor-related SC, and to evaluate the clinical and imaging features of PD-1

inhibitor-related SC.

## MATERIALS AND METHODS

### Literature search strategy

We identified relevant studies in the literature by searching the databases of PubMed. The review was restricted to the period from January 2014 to September 2019 and focused on case reports or case series with PD-1 inhibitor-related SC that were published in English. The search terms consisted of the words ["Programmed cell death 1" (All Fields) and "cholangitis" (All Fields)], ["Programmed cell death ligand 1" [All Fields] AND "cholangitis" (All Fields)], ["Nivolumab" (All Fields) and "cholangitis" (All Fields)], ["Pembrolizumab" (All Fields) and "cholangitis" (All Fields)], ["Cemiplimab" (All Fields) and "cholangitis" (All Fields)], ["Atezolizumab" (All Fields) and "cholangitis" (All Fields)], ["Avelumab" (All Fields) and "cholangitis" (All Fields)], and ["Durvalumab" (All Fields) and "cholangitis" (All Fields)]. We also read the reference lists of the selected studies to manually identify further relevant studies.

Articles were excluded from this review if: (1) The article was a review, basic research, commentary, or clinical study; (2) The study had insufficient information and descriptions; and (3) The full text was unavailable.

We have also investigated six cases of PD-1 inhibitor-related SC, three of which have not yet been published. We have included these three cases in this case review.

## RESULTS

The process of the literature selection is presented in [Figure 1](#). The literature search of the databases of PubMed identified 70 studies that met the search terms. We found an additional three relevant articles in the references of those studies. After the removal of duplicate studies, we evaluated 56 studies by screening the titles and abstracts to check that they met the search criteria. Consequently, we excluded 20 basic research studies, 3 review articles, 3 editorial letters, and 10 clinical studies. Moreover, two studies were case reports about same patient with PD-1 inhibitor-related SC; therefore, one of these studies was excluded. Finally, 19 studies, which included 5 case series and 14 case reports, were assessed in this review<sup>[19-37]</sup>. One case series reported 10 patients with hepatobiliary disorder caused by PD-1 inhibitors, which included two patients with PD-1 inhibitor-related SC<sup>[37]</sup>. With the inclusion of our three cases, a total of 31 cases of PD-1 inhibitor-related SC were evaluated.

The characteristics of patients with PD-1 inhibitor-related SC are shown in [Tables 1-3](#). The median age at the onset of PD-1 inhibitor-related SC was 67 years (range, 43-89). PD-1 inhibitor-related SC appeared to be more prevalent in men, with a male-to-female ratio of 21:10. The patients' primary diseases that were an adaptation disease for the treatment of PD-1 inhibitor were non-small cell lung cancer (20 cases), melanoma (4 cases), gastric cancer (3 cases), bladder cancer (2 cases), small cell lung cancer (1 case), and epithelioid mesothelioma (1 case). The agents that caused PD-1 inhibitor-related SC were nivolumab (19 cases), pembrolizumab (10 cases), avelumab (1 case), and durvalumab (1 case). The median number of cycles until onset of PD-1 inhibitor-related SC was 5.5 (range, 1-27). Abdominal pain or discomfort (35.5%, 11/31) was the most frequent symptom, followed by fever (19.4%, 6/31) and jaundice (12.9%, 4/31). Eight patients did not have any symptoms, but did have liver dysfunction (25.8%, 8/31). The median levels of total bilirubin, aspartate aminotransferase, alanine aminotransferase, alkaline phosphatase (ALP), and gamma-glutamyl transpeptidase were 0.75 mg/dL (range, 0.3-15.9), 129.0 U/L (range, 49-961), 125.0 U/L (range, 31-1536), 1543.0 U/L (range, 237-5066), and 452.0 U/L (range, 114-2094), respectively. Of the 13 patients tested for immunoglobulin G4 (IgG4), almost all patients were negative (92.3%, 12/13).

Biliary stenosis occurred in 8 patients (34.8%, 8/23); 7 had stenosis in the intrahepatic biliary tract, which included 4 patients with multiple strictures in the biliary tract. Biliary dilation was observed in 20 patients (76.9%, 20/26). Twenty patients had hypertrophy of the biliary tract (95.2%, 20/21), of which 19 cases were diffuse ([Figure 2](#)).

Peroral cholangioscopy was performed in only 5 cases<sup>[26,33,38]</sup>. Multiple scarred lesions and band-like narrowing were found in 4 patients, and 2 patients with PD-1 inhibitor-related SC showed diverticulum-like outpouching<sup>[33,38]</sup>. Ulcerative lesions with many black spots (*e.g.*, "burned-out" epithelium) and yellow plaque were found in 1 patient<sup>[26]</sup>.

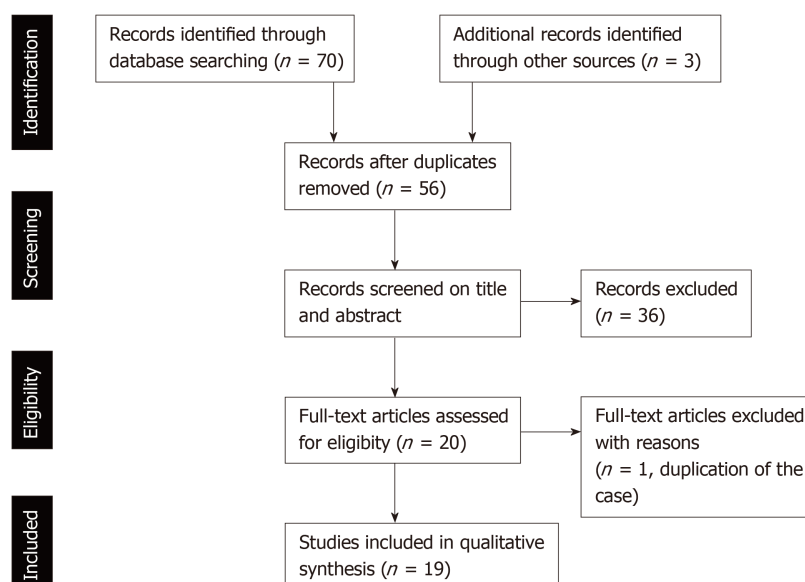


**Figure 1** PRISMA 2009 Flow diagram describing the selection of the studies reporting programmed cell death-1 inhibitor-related cholangitis for our review.

In total, 23 patients underwent pathological evaluation; of these, 15 patients underwent liver biopsy. Fourteen patients had inflammatory changes in the bile duct and/or peribiliary tract, and CD8+ T cells were dominant in the inflammatory cells in 8 of these patients (53.3%, 8/15). Lobular hepatitis was found in 2 patients (13.3%, 2/15).

Transpapillary biopsy of the biliary tract with biopsy forceps was performed for 8 patients, and these pathological findings revealed inflammatory cells infiltration in the bile duct. In 2 patients, CD8+ T cells were the dominant inflammatory cells in the bile duct.

Of the 6 patients that underwent biliary drainage, 5 did not respond.

Corticosteroids were the main treatment for PD inhibitor-related SC (83.8%, 26/31). Only 3 patients who the levels of liver and biliary enzymes were improved to normal level with steroid therapy, so that the response rate to corticosteroids was 11.5% (3/26). Eight patients with PD-1 inhibitor-related SC had poor response, no improvement of liver and biliary enzymes, to steroid therapy. In 15 patients who received steroid therapy, the levels of liver and biliary enzymes were improved, although normalization of enzyme activities was not achieved (*i.e.* only a moderate response occurred).

## DISCUSSION

PD-1/PD-L1 inhibitors are used widely for the treatment of many types of malignancies. However, irAEs, including cardiac, respiratory, endocrine, gastrointestinal, musculoskeletal, skin, and, importantly, hepatobiliary disorders, were also reported<sup>[15-18]</sup>. However, the reasons for the occurrence of irAEs, including cholangitis, are unclear, although it may involve the T cell, antibody, and cytokine responses<sup>[39]</sup>.

Gelsomino *et al*<sup>[20,21]</sup> reported the first case of PD-1 inhibitor-related SC; subsequently, this group and Kawakami *et al*<sup>[19]</sup> suggested the clinical features of PD-1 inhibitor-related SC. However, PD-1 inhibitor-related SC is still not well known. Kawakami *et al*<sup>[19]</sup> reported SC related to the PD-1 inhibitor nivolumab was characterized by: (1) Localized extrahepatic bile duct dilation without obstruction; (2) Diffuse hypertrophy of the extrahepatic bile duct wall; (3) A dominant increase in the biliary tract enzymes alkaline phosphatase and gamma-glutamyl transpeptidase relative to hepatic enzymes aspartate aminotransferase and alanine aminotransferase; (4) Normal or reduced levels of the serum immunological markers, such as antinuclear antibody, antimitochondrial antibody, smooth muscle antibody, and IgG4; (5) The pathological finding of biliary tract CD8+ T cell infiltration from liver biopsy; and (6) A moderate to poor response to steroid therapy. In our study, some clinical features, such as biliary dilation without obstruction, diffuse hypertrophy of the

**Table 1** Demographic characteristics of patients with programmed cell death-1 inhibitor-related sclerosing cholangitis

Patient characteristics	Value
Age, median (range, yr)	67.0 (43–89)
Sex, male/female	21/10
Primary disease	
NSCLC	20
Melanoma	4
GC	3
BC	2
SCLC	1
Epithelioid mesothelioma	1
Drugs	
Nivolumab	19
Pembrolizumab	10
Avelumab	1
Durvalumab	1
Atezolizumab	0
Treatment cycles until onset	5.5 (1–27)
Symptoms	
Abdominal pain or discomfort	11
Fever	6
Jaundice	4
Vomiting	2
Appetite loss	2
Diarrhea or soft stool	2
Skin disorder	2
General fatigue	1
Backache	1
None (liver dysfunction)	8
Liver functional test	
T-Bil, median (range, mg/dL)	0.75 (0.3–15.9)
AST, median (range, U/L)	129.0 (49–961)
ALT, median (range, U/L)	125.0 (31–1536)
ALP, median (range, U/L)	1543.0 (237–5066)
GGT, median (range, U/L)	452.0 (114–2094)
Serological test	
IgG, median (range, U/L)	1230.0 (1050–1789)
IgA, median (range, U/L)	297.5 (199–474.4)
IgM, median (range, U/L)	64.0 (38–94)
IgG4, $\geq 135$ U/L / $< 135$ U/L	1/12
Antinuclear antibody, $\geq 40$ / $< 40$	7/12
Imaging findings	
Biliary stenosis	8
Intrahepatic bile duct	3
Extrahepatic bile duct	1
Multiple	4
Absence	15
Biliary dilation	
Presence/Absence	20 / 6
Hypertrophy of the biliary tract	20
Diffuse	19
Gallbladder	1
Absence	1
Pathological findings	

Liver	15
Inflammation	15
Biliary or peribiliary tract	14
-CD 8+ T cells dominant	8
Lobular hepatitis	2
Bile duct	8
Inflammation	8
-CD 8+ T cells dominant	2
Gallbladder	2
Inflammation	2
-CD 8+ T cells dominant	1
Therapy	
Corticosteroid	26
UDCA	13
MMF	6
Tacrolimus	1
Bezafibrate	1
Response to steroid therapy	
Good	3
Moderate	15
Poor	8

NSCLC: Non-small cell lung cancer; SCLC: Small cell lung cancer; GC: Gastric cancer; BC: Bladder cancer; MCC: Merkel cell carcinoma; RPC: Renal pelvis cancer; T-Bil: Total bilirubin; AST: Aspartate aminotransferase; ALT: Alanine aminotransferase; ALP: Alkaline phosphatase; GGT: Gamma-glutamyl transpeptidase; IgG: Immunoglobulin G; IgA: Immunoglobulin A; IgM: Immunoglobulin M; IgG4: Immunoglobulin G4; Mpsl: Methylprednisolone; PSL: Prednisolone; UDCA: Ursodeoxycholic acid; MMF: Mycophenolate mofetil.

extrahepatic biliary tract, liver dysfunction with a dominant increase in the biliary tract enzymes relative to hepatic enzymes, normal level of serum IgG4, and a moderate to poor response to steroid therapy, were similar to those reported by Kawakami *et al*<sup>[19]</sup>. In contrast, Gelsomino *et al*<sup>[20]</sup> suggested that there were different types of PD-1 inhibitor-related SC, such as large duct cholangitis and small ducts cholangitis, and that those types have different clinical presentation and biochemical evolution and were associated with various outcomes. Indeed, in our case review, 15 patients had diffuse extrahepatic biliary hypertrophy without biliary stenosis (extrahepatic type). Three patients had multiple stenoses, especially in the intrahepatic bile duct, without extrahepatic biliary hypertrophy (intrahepatic type). Moreover, four patients had diffuse biliary tract hypertrophy with multiple stenoses of the intrahepatic and extrahepatic bile ducts (diffuse type). The clinical implications of these types of PD-1 inhibitor-SC is uncertain, but may be clarified by more cases in the future.

Zen *et al*<sup>[40]</sup> reported that CD8+ T lymphocytes were the predominant infiltrates in the bile duct of patients with PD-1 inhibitor-related SC, similar to hepatic irAEs. Moreover, they reported the clinical features and detailed pathological findings of 10 cases of hepatobiliary disorders caused by PD-1 inhibitors. In that study, the ratio of CD8+ to CD4+ cells was significantly higher than that in autoimmune hepatitis or idiosyncratic drug-induced liver injury<sup>[37]</sup>. Although CD8+ T cell infiltration is one of the clinical features of irAEs, in the pathological findings of PD-1 inhibitor-related SC, CD8+ T cells were not necessarily dominant, especially in the bile duct biopsy. Other inflammatory cells, such as eosinophils, neutrophils, plasma cells, and macrophages, were also observed in the biliary tract. Although this finding may be used for auxiliary diagnosis for PD-1 inhibitor-SC, it may not always be observable.

In general, steroid therapy was recommended for the treatment of irAEs<sup>[41,42]</sup>, however, corticosteroids were not useful for the treatment of PD-1 inhibitor-related SC. Although four patients received high-dose steroid therapy (methylprednisolone, 500–1000 mg/d), a good response was not shown. Therefore, at least in our study, steroid therapy was not recommended for the treatment of PD-1 inhibitor-related SC. However, the response to steroid therapy may be dependent on the type of PD-1 inhibitor-related SC, as described above. Although 15 patients with extrahepatic and diffuse type PD-1 inhibitor-related SC received steroid therapy in our case review, a good response occurred only in one case (6.7%, 1/15). Meanwhile, only two patients



**Table 2** Baseline characteristics of cases of programmed cell death-1 inhibitor-related sclerosing cholangitis

Case	Ref.	Age	Sex	Primary disease	Drug	Cycles until onset	Symptoms
1	Gelsomino <i>et al</i> <sup>[21]</sup>	79	M	NSCLC	Nivolumab	4	Itching, jaundice
2	Kawakami <i>et al</i> <sup>[19]</sup>	64	M	NSCLC	Nivolumab	9	Fever, abdominal discomfort
3	Kawakami <i>et al</i> <sup>[19]</sup>	73	F	NSCLC	Nivolumab	6	Fever, vomiting, abdominal discomfort, diarrhea
4	Kawakami <i>et al</i> <sup>[19]</sup>	82	F	NSCLC	Nivolumab	12	Fever, general fatigue
5	Kashima <i>et al</i> <sup>[22]</sup>	63	M	NSCLC	Nivolumab	24	Epigastric pain, soft stool
6	Doherty <i>et al</i> <sup>[23]</sup>	49	F	Melanoma	Pembrolizumab	1	Jaundice
7	Doherty <i>et al</i> <sup>[23]</sup>	59	F	Melanoma	Nivolumab	3	None (liver dysfunction)
8	Doherty <i>et al</i> <sup>[23]</sup>	76	M	epithelioid mesothelioma	Pembrolizumab	1	Jaundice
9	Cho <i>et al</i> <sup>[24]</sup>	69	M	NSCLC	Avelumab	21	Right upper abdominal discomfort
10	Hamoir <i>et al</i> <sup>[25]</sup>	71	M	NSCLC	Nivolumab	NA (11 mo)	None (liver dysfunction)
11	Kuraoka <i>et al</i> <sup>[26]</sup>	69	M	NSCLC	Nivolumab	3	Pruritic rash, liver dysfunction
12	Ogawa <i>et al</i> <sup>[27]</sup>	73	M	Melanoma	Pembrolizumab	NA (3 mo)	None (liver dysfunction)
13	Kono <i>et al</i> <sup>[28]</sup>	69	F	GC	Nivolumab	2	Jaundice
14	Noda-Narita <i>et al</i> <sup>[29]</sup>	57	F	NSCLC	Nivolumab	NA (12 mo)	Abdominal pain
15	Sawada <i>et al</i> <sup>[30]</sup>	76	M	GC	Nivolumab	4	None (liver dysfunction)
16	Taltec <i>et al</i> <sup>[31]</sup>	56	F	NSCLC	Nivolumab	16 (9 mo)	Myalgia, skin thickening
17	Oda <i>et al</i> <sup>[32]</sup>	43	M	GC	Nivolumab	1	Fever, tachycardia, appetite loss, malaise
18	Koya <i>et al</i> <sup>[33]</sup>	66	M	SCLC	Pembrolizumab	5	Epigastric pain
19	Fouchard <i>et al</i> <sup>[34]</sup>	52	M	NSCLC	Nivolumab	8	Abdominal pain
20	Fouchard <i>et al</i> <sup>[34]</sup>	NA	M	NSCLC	Durvalumab (+ tremelimumab)	4	Fever, abdominal pain
21	Fouchard <i>et al</i> <sup>[34]</sup>	61	M	NSCLC	Pembrolizumab	17	None (liver dysfunction)
22	Clugreanu <i>et al</i> <sup>[35]</sup>	43	F	Melanoma	Nivolumab	27	Epigastralgia, anorexia,
23	Anderson <i>et al</i> <sup>[36]</sup>	67	M	NSCLC	Nivolumab	8	Right upper abdominal pain
24	Zen <i>et al</i> <sup>[37]</sup>	68	M	NSCLC	Pembrolizumab	NA (5.5 mo)	Abdominal pain, vomiting
25	Zen <i>et al</i> <sup>[40]</sup>	67	M	NSCLC	Pembrolizumab	NA (1 mo)	Fever, malaise
26	Our case	61	M	BC	Pembrolizumab	5	Fever
27	Our case	89	M	BC	Pembrolizumab	4	None (liver dysfunction)
28	Our case	63	M	NSCLC	Pembrolizumab	7	None (liver dysfunction)
29	Our case	55	M	NSCLC	Nivolumab	11	Abdominal pain
30	Our case	81	F	NSCLC	Nivolumab	25	Backache
31	Our case	82	F	NSCLC	Nivolumab	2	None (liver dysfunction)

NSCLC: Non-small cell lung cancer; SCLC: Small cell lung cancer; GC: Gastric cancer; BC: Bladder cancer; NA: Not available.

**Table 3 Clinical, imaging, and pathological findings of cases of programmed cell death-1 inhibitor-related sclerosing cholangitis**

Case	T-Bil/AST/ALT/ALP/GGT/IgG4	Biliary stenosis/dilation	Hypertrophy of biliary tract	Pathological findings	Treatment (Dosage)	Steroid response
1	Grade 4/NA/Grade 3; Grade 3/Grade 4/NA	NA	NA	Liver: CD8+ T cells infiltration in bile duct	mPSL (1 mg/kg), + UDCA (15 mg/kg)	Moderate
2	0.7/142/144; 1769/902/normal	-/+	Diffuse	Liver: CD8+ and CD4+ T cells infiltration in Glisson's capsule	PSL (0.5 mg/kg)	Poor
3	3.8/89/101; 1947/804/normal	-/+	Diffuse	NA	PSL (0.5 mg/kg), Biliary drainage	Moderate
4	0.8/108/70; 2996/813/normal	-/+	Diffuse	Liver: CD8+ and CD4+ T cells infiltration in Glisson's capsule	Biliary drainage	-
5	NA/88/92; 1543/NA/NA	Distal bile duct/+	Diffuse	Bile duct: Interstitial fibrosis, neutrophils infiltration in mucosa	PSL (2 mg/kg) Biliary drainage	Moderate
6	NA/961/1536; 237/2094/NA	NA/-	NA	Liver: Severe steatohepatitis, absence of bile ducts	1 <sup>st</sup> PSL (1 mg/kg), 2 <sup>nd</sup> PSL + UDCA (NA) + MMF (2 g)	Poor
7	NA/NA/>300; >1000/NA/NA	NA	NA	Liver: Degenerative bile duct atypia and periductal fibrosis	1 <sup>st</sup> PSL (1 mg/kg), 2 <sup>nd</sup> PSL + UDCA (NA)	Poor
8	NA/NA/>500; >700/NA/NA	NA	NA	Liver: Attenuated bile duct, cellular and canalicular cholestasis in parenchyma	mPSL (2 mg/kg) + cholestyramine (NA) + MMF (1 g) + UDCA (NA)	Poor
9	0.6/Grade 1/Grade 1; Grade 2/Grade 2/NA	-/+	Diffuse	NA	mPSL (1 mg/kg)	Moderate
10	Normal/129/135; 558/984/NA	Multiple/-	None	Liver: CD8+ T cell infiltration in the periportal zone and cholangitis	mPSL (0.5 mg/kg), + UDCA (10 mg/kg)	Good
11	NA/NA/NA; NA/NA/NA	-/+	Diffuse	Bile duct: Inflammatory cells and lymphocytes infiltration in epithelium	1 <sup>st</sup> PSL (60 mg), 2 <sup>nd</sup> mPSL (500 mg)	Poor
12	NA/58/77; 1111/461/NA	Multiple/+	Diffuse	Bile duct: Destruction of epithelium, fibrosis with CD8+ T cell infiltration in submucosa	Discontinuation of Pembrolizumab	-
13	15.9/454/NA; 5066/NA/20.2	Intrahepatic bile duct/-	Gall bladder	NA	Biliary drainage	-
14	NA/NA/NA; 1065/304/normal	-/+	Diffuse	NA	UDCA (300 mg)	-
15	0.8/69/68; 2427/252/41.0	-/+	NA	Liver: Eosinophil, CD8+, and CD4+ T cell infiltration in the portal tract. Eosinophil infiltration in the epithelial linings of the bile duct	PSL (0.5 mg/kg), + UDCA (NA)	Good
16	Normal/272/516; 615/442/NA	NA	Diffuse	NA	Corticosteroid (NA)	Good
17	3.7/49/31; 598/151/90	-/-	NA	Liver: CD8+ T cells and macrophage infiltration in bile duct	1 <sup>st</sup> PSL (1 mg/kg), 2 <sup>nd</sup> m PSL (1 g), 3 <sup>rd</sup> PSL + MMF (2 g)	Poor

18	1.1/313/296; 2241/868/normal	Intrahepatic bile duct/+	Diffuse	Liver: CD8+ T cell and eosinophil infiltration in the periportal zones, Bile duct: CD8+ T cell infiltration and fibrosis in submucosa	1 <sup>st</sup> UDCA (900 mg) + bezafibrate (400 mg), 2 <sup>nd</sup> m PSL (0.5 g) followed by PSL (1 mg/kg), Biliary drainage	Poor
19	Normal/>100/>100; >900/>500/NA	-/+	NA	Gall bladder: Inflammatory cell infiltration	PSL (0.5 mg/kg) + UDCA (NA), Cholecystectomy	Moderate
20	NA/>100/>300; >800/>1700/normal	-/+	NA	Gall bladder: CD8+ T cell infiltration	PSL (120 mg) + UDCA (NA), Cholecystectomy	Moderate
21	Normal/NA/>100; >400/>1400/NA	NA	NA	NA	PSL (1 mg/kg)	Moderate
22	Normal/52/126; 545/1007/NA	Multiple/+	NA	Liver: CD3+ and CD8 T cell infiltration in the bile duct	PSL (1 mg/kg)	Moderate
23	NA/>300/NA; 793/NA/NA	Multiple/+	Diffuse	Liver: Fibrosis and inflammation in the portal tract, lobular inflammation, mild macrovesicular steatosis	mPSL (NA) following PSL (50 mg), MMF (NA), Tacrolimu (NA)s	Poor
24	0.5/67/68; 2107/279/59	NA/-	Diffuse	Liver: Cholangiopathologic change, CD8/CD4 ratio 12:7, Bile duct: Lymphocyte, eosinophil and plasma cell infiltration	PSL (50 mg)	Moderate
25	1.2/198/233; 1540/332/78	NA/-	Diffuse	Liver: Lobular hepatitis with cholangiopathic change, CD8/CD4 ratio 17:2	PSL (40 mg)	Moderate
26	0.3/91/65; 1683/159/80.4	-/+	Diffuse	Bile duct: Inflammatory cell infiltration	PSL (1 mg/kg) + UDCA (600 mg)	Moderate
27	0.4/245/124; 1245/114/352	-/+	Diffuse	Bile duct: Neutrophil and lymphocyte infiltration	UDCA (600 mg)	-
28	0.6/184/254; 1783/452/128	-/+	Diffuse	Bile duct: Inflammatory cell infiltration	PSL (1 mg/kg) + UDCA (600 mg)	Moderate
29	0.3/64/245; 1328/448/67.3	Intrahepatic bile duct/+	Diffuse	NA	mPSL (2 mg/kg) + MMF (2 g)	Moderate
30	1.3/284/248; 3029/1070/NA	-/+	Diffuse	NA	mPSL (2 mg/kg) + MMF (2 g), Biliary drainage	Moderate
31	0.7/294/85; 4635/829/NA	-/+	Diffuse	Liver: Lymphocyte infiltration in Glisson's capsule, hydropic degeneration of hepatocytes	mPSL (1.6 mg/kg)	Moderate

T-Bil: Total bilirubin; AST: Aspartate aminotransferase; ALT: Alanine aminotransferase; ALP: Alkaline phosphatase; GGT: Gamma-glutamyl transpeptidase; IgG4: Immunoglobulin G4; mPSL: Methylprednisolone; PSL: Prednisolone; UDCA: Ursodeoxycholic acid; MMF: Mycophenolate mofetil; AZA: Azathioprine; NA: Not available.

with intrahepatic type PD-1 inhibitor-related SC received steroid therapy: One patient's liver function was improved and the other had a moderate response, with a response ratio of 1:1. This finding is still uncertain in a few cases.

Ursodeoxycholic acid (UDCA) was used for treatment of PD-1 inhibitor-related SC in 13 patients. Two patients received only UDCA, with discontinuation of nivolumab, and displayed a moderate response. In contrast, no response was found in the single

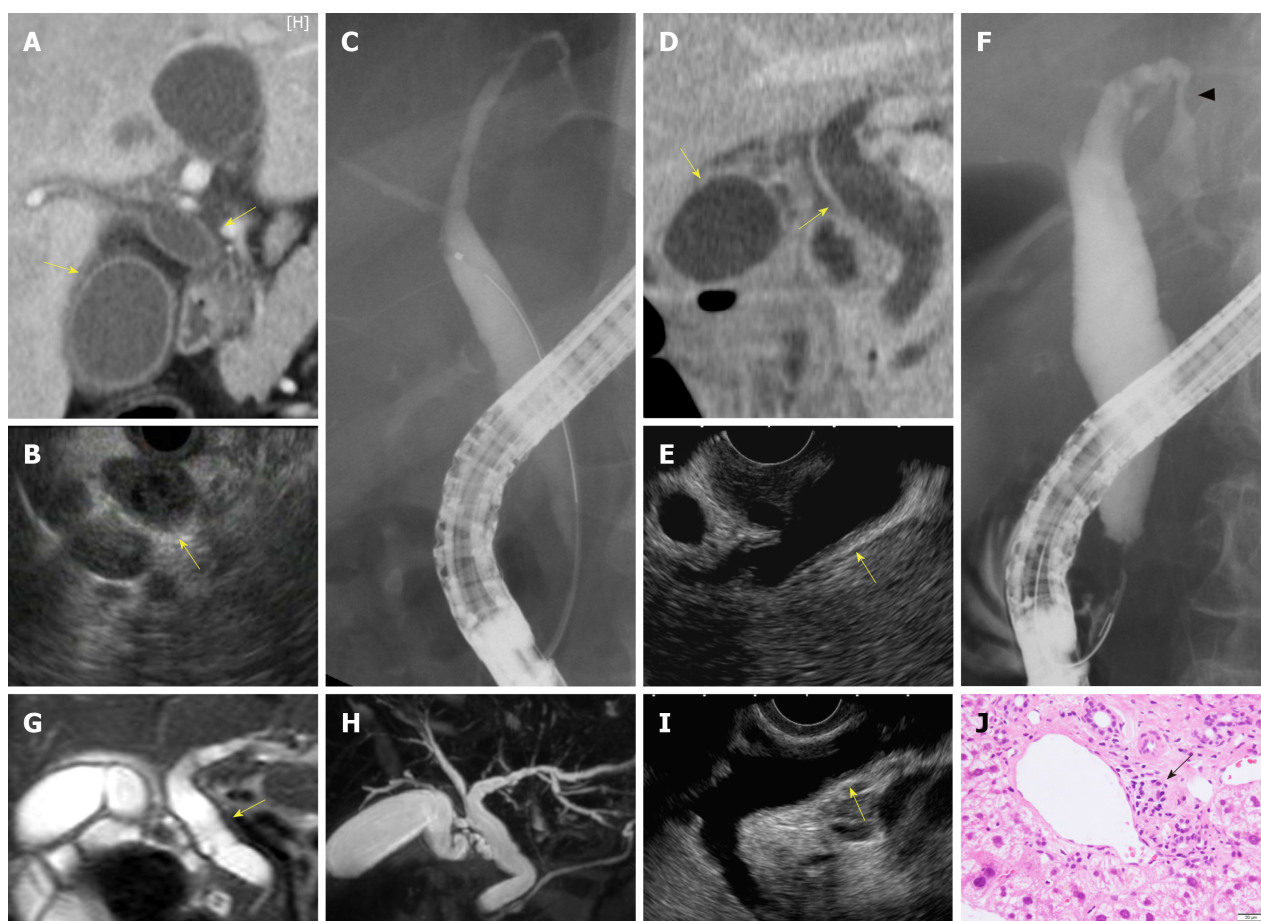


**Figure 2** Our cases with sclerosing cholangitis caused by nivolumab (Case 29, A–C; Case 30, D–F; Case 31, G–J). A, D: Computed tomography; G, H: Magnetic resonance imaging; B, E, I: Endoscopic ultrasonography. Revealed diffuse hypertrophy of biliary tract (yellow allows) in all cases. C, F: Endoscopic retrograde cholangiopancreatography revealed biliary stenosis of the intrahepatic bile duct (arrow-head) in Case 30. J: In Case 31, liver biopsy showed lymphocyte infiltration in Glisson's capsule (black arrow).

patient who received UDCA with bezafibrate. Seven patients received combination therapy of steroids and UDCA. The response rate to that therapy was 28.6% (2/7). Three patients received steroid therapy first; when no improvement was observed, UDCA was added and a moderate response was observed in these patients. Although the efficacy was insufficient, UDCA was considered a treatment for PD-1 inhibitor-related SC owing to the low rate of adverse events<sup>[43]</sup>.

Other anti-inflammatory agents, including immunomodulators or infliximab were sometimes considered to using for treatment of irAEs<sup>[44]</sup>. Tacrolimus, an immunomodulator, was also used for one case of PD-1 inhibitor-related SC; however, the response was insufficient. Infliximab was used for some irAEs, such as colitis and pneumonitis. In our case review, infliximab was not used for the treatment of PD-1 inhibitor-related SC. More cases may be needed to evaluate the usefulness of these drugs for PD-1 inhibitor-related SC.

This study had some limitations. First, there are no current diagnostic criteria for PD-1 inhibitor-related SC. Second, some clinical cases, for which blood test data, image findings, and pathological evaluation were not presented, were included in this study. Therefore, our study may include different diseases that cause sclerosing cholangitis.

In conclusion, some clinical features of PD-1 inhibitor-related SC, such as biliary dilation without obstruction, diffuse hypertrophy of the extrahepatic biliary tract and/or multiple strictures of intrahepatic biliary tract, liver dysfunction with a dominant increase in biliary tract enzymes relative to hepatic enzymes, normal level of serum IgG4, and a moderate-to-poor response to steroid therapy, were revealed, although there were many unsolved questions in our study. To establish the diagnostic criteria for PD-1 inhibitor-related SC, more cases, for which clinical data including hepatobiliary enzymes, immunological marker, image findings, and pathological evaluation were presented clearly, need to be evaluated. Although CD8+ T cell infiltration is one of the pathological features of PD-1 inhibitor-related SC, it is not enough to exclude different diseases that cause sclerosing cholangitis. We will

have to find more specific features of PD-1 inhibitor-related SC.

## ARTICLE HIGHLIGHTS

### Research background

Programmed cell death-1 (PD-1) inhibitor has been indicated for many types of malignancies. On the other hands, these inhibitors cause immune-related adverse events (irAEs). Hepatobiliary disorder is a phenotype of irAEs that affect 0%–4.5% of patients treated with PD-1 inhibitors.

### Research motivation

Recently, PD-1 inhibitor-related sclerosing cholangitis (SC), one of the irAEs, have been reported. However, the clinical and pathological features of PD-1 inhibitor-related SC are uncertain.

### Research objectives

The objective of this study to evaluate the clinical and pathological features of PD-1 inhibitor-related SC through a systematic review of the literature.

### Research methods

We conducted an electronic search through databases of PubMed. The review was restricted to the period from January 2014 to September 2019 and focused on case reports/series on PD-1 inhibitor-related SC published in English. The reference lists of the identified papers were also scanned to find out further relevant studies. Six cases previously studied by us, including three that have not yet been published, were included in this review.

### Research results

Thirty-one PD-1 inhibitor-related SC cases were evaluated. The median number of cycles until PD-1 inhibitor-related SC onset was 5.5 (range, 1–27). Abdominal pain or discomfort (35.5%, 11/31) was the most frequent symptom. Liver dysfunction with a notable increase in biliary tract enzymes relative to hepatic enzymes, and a normal level of serum IgG4 were shown in blood serum test. Biliary dilation without obstruction (76.9%, 20/26), diffuse hypertrophy of the extrahepatic biliary tract (90.5%, 19/21), and multiple strictures of the intrahepatic biliary tract (30.4%, 7/23) were noted. CD8+ T cells were the dominant inflammatory cells in the bile duct or peribiliary tract in 11/23 (47.8%) cases. The response rate of corticosteroids for PD inhibitor-related SC was 11.5% (3/26).

### Research conclusions

Some clinical features of PD-1 inhibitor-related SC, such as biliary dilation without obstruction, diffuse hypertrophy of the extrahepatic biliary tract and/or multiple strictures of intrahepatic biliary tract, liver dysfunction with a dominant increase in biliary tract enzymes relative to hepatic enzymes, normal level of serum IgG4, and a moderate-to-poor response to steroid therapy, were revealed.

### Research perspectives

To establish the diagnostic criteria for PD-1 inhibitor-related SC, more cases, for which clinical data including hepatobiliary enzymes, immunological marker, image findings, and pathological evaluation were presented clearly, need to be evaluated. We will have to find more specific features of PD-1 inhibitor-related SC.

## ACKNOWLEDGEMENTS

We wish to thank to our colleagues in the Departments of Gastroenterology and Hepatology, and Pathology at Tottori University Faculty of Medicine (Tottori, Japan).

## REFERENCES

- 1 Francisco LM, Sage PT, Sharpe AH. The PD-1 pathway in tolerance and autoimmunity. *Immunol Rev* 2010; **236**: 219–242 [PMID: 20636820 DOI: 10.1111/j.1600-065X.2010.00923.x]
- 2 Wolchok JD, Kluger H, Callahan MK, Postow MA, Rizvi NA, Lesokhin AM, Segal NH, Ariyan CE, Gordon RA, Reed K, Burke MM, Caldwell A, Kronenberg SA, Agunwamba BU, Zhang X, Lowy I, Inzunza HD, Feely W, Horak CE, Hong Q, Korman AJ, Wigginton JM, Gupta A, Sznol M. Nivolumab plus ipilimumab in advanced melanoma. *N Engl J Med* 2013; **369**: 122–133 [PMID: 23724867 DOI: 10.1056/NEJMoa1302369]
- 3 Postow MA, Chesney J, Pavlick AC, Robert C, Grossmann K, McDermott D, Linette GP, Meyer N, Giguere JK, Agarwala SS, Shaheen M, Ernstoff MS, Minor D, Salama AK, Taylor M, Ott PA, Rollin LM, Horak C, Gagnier P, Wolchok JD, Hodi FS. Nivolumab and ipilimumab versus ipilimumab in untreated melanoma. *N Engl J Med* 2015; **372**: 2006–2017 [PMID: 25891304 DOI: 10.1056/NEJMoa1414428]
- 4 Robert C, Long GV, Brady B, Dutriaux C, Maio M, Mortier L, Hassel JC, Rutkowski P, McNeil C, Kalinka-Warzocho E, Savage KJ, Hernberg MM, Lebbé C, Charles J, Mihalcioiu C, Chiarion-Sileni V, Mauch C, Cognetti F, Arance A, Schmidt H, Schadendorf D, Gogas H, Lundgren-Eriksson L, Horak C, Sharkey B, Waxman IM, Atkinson V, Ascierto PA. Nivolumab in previously untreated melanoma without



- BRAF mutation. *N Engl J Med* 2015; **372**: 320-330 [PMID: 25399552 DOI: 10.1056/NEJMoa1412082]
- 5 **Brahmer J**, Reckamp KL, Baas P, Crinò L, Eberhardt WE, Poddubskaya E, Antonia S, Pluzanski A, Vokes EE, Holgado E, Waterhouse D, Ready N, Gainor J, Arén Frontera O, Havel L, Steins M, Garassino MC, Aerts JG, Domine M, Paz-Ares L, Reck M, Baudelet C, Harbison CT, Lestini B, Spigel DR. Nivolumab versus Docetaxel in Advanced Squamous-Cell Non-Small-Cell Lung Cancer. *N Engl J Med* 2015; **373**: 123-135 [PMID: 26028407 DOI: 10.1056/NEJMoa1504627]
- 6 **Borghaei H**, Paz-Ares L, Horn L, Spigel DR, Steins M, Ready NE, Chow LQ, Vokes EE, Felip E, Holgado E, Barlesi F, Kohlhäufel M, Arrieta O, Burgio MA, Fayette J, Lena H, Poddubskaya E, Gerber DE, Gettinger SN, Rudin CM, Rizvi N, Crinò L, Blumenschein GR, Antonia SJ, Dorange C, Harbison CT, Graf Finckenstein F, Brahmer JR. Nivolumab versus Docetaxel in Advanced Nonsquamous Non-Small-Cell Lung Cancer. *N Engl J Med* 2015; **373**: 1627-1639 [PMID: 26412456 DOI: 10.1056/NEJMoa1507643]
- 7 **Ansell SM**, Lesokhin AM, Borrello I, Halwani A, Scott EC, Gutierrez M, Schuster SJ, Millenson MM, Cattray D, Freeman GJ, Rodig SJ, Chapuy B, Ligon AH, Zhu L, Grosso JF, Kim SY, Timmerman JM, Shipp MA, Armand P. PD-1 blockade with nivolumab in relapsed or refractory Hodgkin's lymphoma. *N Engl J Med* 2015; **372**: 311-319 [PMID: 25482239 DOI: 10.1056/NEJMoa1411087]
- 8 **Motzer RJ**, Escudier B, McDermott DF, George S, Hammers HJ, Srinivas S, Tykodi SS, Sosman JA, Procopio G, Plimack ER, Castellano D, Choueiri TK, Gurney H, Donskov F, Bono P, Wagstaff J, Gauder TC, Ueda T, Tomita Y, Schutz FA, Kollmannsberger C, Larkin J, Ravaud A, Simon JS, Xu LA, Waxman IM, Sharma P; CheckMate 025 Investigators. Nivolumab versus Everolimus in Advanced Renal-Cell Carcinoma. *N Engl J Med* 2015; **373**: 1803-1813 [PMID: 26406148 DOI: 10.1056/NEJMoa1510665]
- 9 **Powles T**, Eder JP, Fine GD, Braith F, Loriot Y, Cruz C, Bellmunt J, Burris HA, Petrylak DP, Teng SL, Shen X, Boyd Z, Hegde PS, Chen DS, Vogelzang NJ. MPDL3280A (anti-PD-L1) treatment leads to clinical activity in metastatic bladder cancer. *Nature* 2014; **515**: 558-562 [PMID: 25428503 DOI: 10.1038/nature13904]
- 10 **Kang YK**, Boku N, Satoh T, Ryu MH, Chao Y, Kato K, Chung HC, Chen JS, Muro K, Kang WK, Yeh KH, Yoshikawa T, Oh SC, Bai LY, Tamura T, Lee KW, Hamamoto Y, Kim JG, Chin K, Oh DY, Minashi K, Cho JY, Tsuda M, Chen LT. Nivolumab in patients with advanced gastric or gastro-oesophageal junction cancer refractory to, or intolerant of, at least two previous chemotherapy regimens (ONO-4538-12, ATTRACTION-2): a randomised, double-blind, placebo-controlled, phase 3 trial. *Lancet* 2017; **390**: 2461-2471 [PMID: 28993052 DOI: 10.1016/S0140-6736(17)31827-5]
- 11 **Kato K**, Cho BC, Takahashi M, Okada M, Lin CY, Chin K, Kadowaki S, Ahn MJ, Hamamoto Y, Doki Y, Yen CC, Kubota Y, Kim SB, Hsu CH, Holtved E, Xynos I, Kodani M, Kitagawa Y. Nivolumab versus chemotherapy in patients with advanced oesophageal squamous cell carcinoma refractory or intolerant to previous chemotherapy (ATTRACTION-3): a multicentre, randomised, open-label, phase 3 trial. *Lancet Oncol* 2019; **20**: 1506-1517 [PMID: 31582355 DOI: 10.1016/S1470-2045(19)30626-6]
- 12 **Robert C**, Schachter J, Long GV, Arance A, Grob JJ, Mortier L, Daud A, Carlino MS, McNeil C, Lotem M, Larkin J, Lorigan P, Neyns B, Blank CU, Hamid O, Mateus C, Shapira-Frommer R, Kosh M, Zhou H, Ibrahim N, Ebbinghaus S, Ribas A; KEYNOTE-006 investigators. Pembrolizumab versus Ipilimumab in Advanced Melanoma. *N Engl J Med* 2015; **372**: 2521-2532 [PMID: 25891173 DOI: 10.1056/NEJMoa1503093]
- 13 **Le DT**, Durham JN, Smith KN, Wang H, Bartlett BR, Aulakh LK, Lu S, Kemberling H, Wilt C, Luber BS, Wong F, Azad NS, Rucki AA, Laheru D, Donehower R, Zaheer A, Fisher GA, Crocenzi TS, Lee JJ, Greten TF, Duffy AG, Ciombor KK, Eyring AD, Lam BH, Joe A, Kang SP, Holdhoff M, Danilova L, Cope L, Meyer C, Zhou S, Goldberg RM, Armstrong DK, Bever KM, Fader AN, Taube J, Housseau F, Spetzler D, Xiao N, Pardoll DM, Papadopoulos N, Kinzler KW, Eshleman JR, Vogelstein B, Anders RA, Diaz LA. Mismatch repair deficiency predicts response of solid tumors to PD-1 blockade. *Science* 2017; **357**: 409-413 [PMID: 28596308 DOI: 10.1126/science.aan6733]
- 14 **Le DT**, Uram JN, Wang H, Bartlett BR, Kemberling H, Eyring AD, Skora AD, Luber BS, Azad NS, Laheru D, Biedrzycki B, Donehower RC, Zaheer A, Fisher GA, Crocenzi TS, Lee JJ, Duffy SM, Goldberg RM, de la Chapelle A, Koshiji M, Bhaijee F, Huebner T, Hruban RH, Wood LD, Cuka N, Pardoll DM, Papadopoulos N, Kinzler KW, Zhou S, Cornish TC, Taube JM, Anders RA, Eshleman JR, Vogelstein B, Diaz LA. PD-1 Blockade in Tumors with Mismatch-Repair Deficiency. *N Engl J Med* 2015; **372**: 2509-2520 [PMID: 26028255 DOI: 10.1056/NEJMoa1500596]
- 15 **Friedman CF**, Proverbs-Singh TA, Postow MA. Treatment of the Immune-Related Adverse Effects of Immune Checkpoint Inhibitors: A Review. *JAMA Oncol* 2016; **2**: 1346-1353 [PMID: 27367787 DOI: 10.1001/jamaoncol.2016.1051]
- 16 **Villadolid J**, Amin A. Immune checkpoint inhibitors in clinical practice: update on management of immune-related toxicities. *Transl Lung Cancer Res* 2015; **4**: 560-575 [PMID: 26629425 DOI: 10.3978/j.issn.2218-6751.2015.06.06]
- 17 **Spain L**, Diem S, Larkin J. Management of toxicities of immune checkpoint inhibitors. *Cancer Treat Rev* 2016; **44**: 51-60 [PMID: 26874776 DOI: 10.1016/j.ctrv.2016.02.001]
- 18 **Raschi E**, Mazzearella A, Antonazzo IC, Bendinelli N, Forcesi E, Tuccori M, Moretti U, Poluzzi E, De Ponti F. Toxicities with Immune Checkpoint Inhibitors: Emerging Priorities from Disproportionality Analysis of the FDA Adverse Event Reporting System. *Target Oncol* 2019; **14**: 205-221 [PMID: 30927173 DOI: 10.1007/s11523-019-00632-w]
- 19 **Kawakami H**, Tanizaki J, Tanaka K, Haratani K, Hayashi H, Takeda M, Kamata K, Takenaka M, Kimura M, Chikugo T, Sato T, Kudo M, Ito A, Nakagawa K. Imaging and clinicopathological features of nivolumab-related cholangitis in patients with non-small cell lung cancer. *Invest New Drugs* 2017; **35**: 529-536 [PMID: 28317087 DOI: 10.1007/s10637-017-0453-0]
- 20 **Gelsomino F**, Vitale G, Ardizzoni A. A case of nivolumab-related cholangitis and literature review: how to look for the right tools for a correct diagnosis of this rare immune-related adverse event. *Invest New Drugs* 2018; **36**: 144-146 [PMID: 28631096 DOI: 10.1007/s10637-017-0484-6]
- 21 **Gelsomino F**, Vitale G, D'Errico A, Bertuzzi C, Andreone P, Ardizzoni A. Nivolumab-induced cholangitic liver disease: a novel form of serious liver injury. *Ann Oncol* 2017; **28**: 671-672 [PMID: 27993797 DOI: 10.1093/annonc/mdw649]
- 22 **Kashima J**, Okuma Y, Shimizuguchi R, Chiba K. Bile duct obstruction in a patient treated with nivolumab as second-line chemotherapy for advanced non-small-cell lung cancer: a case report. *Cancer Immunol Immunother* 2018; **67**: 61-65 [PMID: 28913619 DOI: 10.1007/s00262-017-2062-3]
- 23 **Doherty GJ**, Duckworth AM, Davies SE, Mells GF, Brais R, Harden SV, Parkinson CA, Corrie PG. Severe steroid-resistant anti-PD1 T-cell checkpoint inhibitor-induced hepatotoxicity driven by biliary

- injury. *ESMO Open* 2017; **2**: e000268 [PMID: 29081991 DOI: 10.1136/esmoopen-2017-000268]
- 24 **Cho JH**, Sun JM, Lee SH, Ahn JS, Park K, Ahn MJ. Late-Onset Cholecystitis with Cholangitis after Avelumab Treatment in Non-Small Cell Lung Cancer. *J Thorac Oncol* 2018; **13**: e34-e36 [PMID: 29472055 DOI: 10.1016/j.jtho.2017.10.007]
- 25 **Hamoir C**, de Vos M, Clinckart F, Nicaise G, Komuta M, Lanthier N. Hepatobiliary and Pancreatic: Nivolumab-related cholangiopathy. *J Gastroenterol Hepatol* 2018; **33**: 1695 [PMID: 29707809 DOI: 10.1111/jgh.14136]
- 26 **Kuraoka N**, Hara K, Terai S, Yatabe Y, Horio Y. Peroral cholangioscopy of nivolumab-related (induced) ulcerative cholangitis in a patient with non-small cell lung cancer. *Endoscopy* 2018; **50**: E259-E261 [PMID: 29969801 DOI: 10.1055/a-0640-2392]
- 27 **Ogawa K**, Kamimura K, Terai S. Antiprogrammed Cell Death-1 Immunotherapy-Related Secondary Sclerosing Cholangitis. *Hepatology* 2019; **69**: 914-916 [PMID: 30033637 DOI: 10.1002/hep.30189]
- 28 **Kono M**, Sakurai T, Okamoto K, Masaki S, Nagai T, Komeda Y, Kamata K, Minaga K, Yamao K, Takenaka M, Watanabe T, Nishida N, Kudo M. Efficacy and Safety of Chemotherapy Following Anti-PD-1 Antibody Therapy for Gastric Cancer: A Case of Sclerosing Cholangitis. *Intern Med* 2019; **58**: 1263-1266 [PMID: 30626829 DOI: 10.2169/internalmedicine.1981-18]
- 29 **Noda-Narita S**, Mizuno S, Noguchi S, Watanabe K, Nakai Y, Koike K, Kage H, Nagase T. Development of mild drug-induced sclerosing cholangitis after discontinuation of nivolumab. *Eur J Cancer* 2019; **107**: 93-96 [PMID: 30554074 DOI: 10.1016/j.ejca.2018.11.021]
- 30 **Sawada K**, Shonaka T, Nishikawa Y, Hasegawa K, Hayashi H, Hasebe T, Nakajima S, Ikuta K, Fujiya M, Furukawa H, Okumura T. Successful Treatment of Nivolumab-related Cholangitis with Prednisolone: A Case Report and Review of the Literature. *Intern Med* 2019; **58**: 1747-1752 [PMID: 30799364 DOI: 10.2169/internalmedicine.2330-18]
- 31 **Le Tallec E**, Ricordel C, Triquet L, Deniel A, Marcorelles P, Lena H, Jegou P, Belhomme N. An Original Case of an Association of Eosinophilic Fasciitis with Cholangitis Induced by Nivolumab. *J Thorac Oncol* 2019; **14**: e13-e15 [PMID: 30579548 DOI: 10.1016/j.jtho.2018.09.016]
- 32 **Oda H**, Ishihara M, Miyahara Y, Nakamura J, Kozuka Y, Iwasa M, Tsunoda A, Yamashita Y, Saito K, Mizuno T, Shiku H, Katayama N. First Case of Cytokine Release Syndrome after Nivolumab for Gastric Cancer. *Case Rep Oncol* 2019; **12**: 147-156 [PMID: 31043953 DOI: 10.1159/000496933]
- 33 **Koya Y**, Shibata M, Shinohara N, Nebuya S, Oe S, Honma Y, Senju M, Sato N, Harada M. Secondary sclerosing cholangitis with hemobilia induced by pembrolizumab: Case report and review of published work. *Hepatol Res* 2019; **49**: 950-956 [PMID: 30861263 DOI: 10.1111/hepr.13329]
- 34 **Fouchard M**, Jantzen H, Quere G, Descourt R, Robinet G, Poureau PG. Three cases of immune cholangitis related to anti-programmed cell death and programmed cell death ligand agents for the treatment of non-small cell lung cancer. *Eur J Cancer* 2019; **115**: 107-110 [PMID: 31132740 DOI: 10.1016/j.ejca.2019.04.022]
- 35 **Călugăreanu A**, Romptaux P, Bohelay G, Goldfarb L, Barrau V, Cucherousset N, Heidelberger V, Nault JC, Ziol M, Caux F, Maubec E. Late onset of nivolumab-induced severe gastroduodenitis and cholangitis in a patient with stage IV melanoma. *Immunotherapy* 2019; **11**: 1005-1013 [PMID: 31304833 DOI: 10.2217/imt-2019-0077]
- 36 **Anderson B**, Dawe DE. Nivolumab-Induced Secondary Sclerosing Cholangitis with Deterioration Despite Immunosuppression. *J Thorac Oncol* 2019; **14**: e205-e206 [PMID: 31445738 DOI: 10.1016/j.jtho.2019.04.023]
- 37 **Zen Y**, Chen YY, Jeng YM, Tsai HW, Yeh MM. Immune-related adverse reactions in the hepatobiliary system: second-generation check-point inhibitors highlight diverse histological changes. *Histopathology* 2019 [PMID: 31550390 DOI: 10.1111/his.14000]
- 38 **Onoyama T**, Takeda Y, Kato M, Edano M, Tarumoto R, Matsumoto K, Isomoto H. Peroral cholangioscopy of programmed cell death-1 inhibitor-related sclerosing cholangitis: three case reports. *Endoscopy* 2019; **51**: E402-E403 [PMID: 31340390 DOI: 10.1055/a-0948-1271]
- 39 **Postow MA**, Sidlow R, Hellmann MD. Immune-Related Adverse Events Associated with Immune Checkpoint Blockade. *N Engl J Med* 2018; **378**: 158-168 [PMID: 29320654 DOI: 10.1056/NEJMr1703481]
- 40 **Zen Y**, Yeh MM. Checkpoint inhibitor-induced liver injury: A novel form of liver disease emerging in the era of cancer immunotherapy. *Semin Diagn Pathol* 2019; **36**: 434-440 [PMID: 31358424 DOI: 10.1053/j.semdp.2019.07.009]
- 41 **Haanen JBA**G, Carbonnel F, Robert C, Kerr KM, Peters S, Larkin J, Jordan K; ESMO Guidelines Committee. Management of toxicities from immunotherapy: ESMO Clinical Practice Guidelines for diagnosis, treatment and follow-up. *Ann Oncol* 2017; **28**: iv119-iv142 [PMID: 28881921 DOI: 10.1093/annonc/mdx225]
- 42 **Brahmer JR**, Lacchetti C, Thompson JA. Management of Immune-Related Adverse Events in Patients Treated with Immune Checkpoint Inhibitor Therapy: American Society of Clinical Oncology Clinical Practice Guideline Summary. *J Oncol Pract* 2018; **14**: 247-249 [PMID: 29517954 DOI: 10.1200/JOP.18.00005]
- 43 **Zhu GQ**, Shi KQ, Huang GQ, Wang LR, Lin YQ, Braddock M, Chen YP, Zhou MT, Zheng MH. A network meta-analysis of the efficacy and side effects of UDCA-based therapies for primary sclerosing cholangitis. *Oncotarget* 2015; **6**: 26757-26769 [PMID: 26378046 DOI: 10.18632/oncotarget.5610]
- 44 **Puzanov I**, Diab A, Abdallah K, Bingham CO, Brogdon C, Dadu R, Hamad L, Kim S, Lacouture ME, LeBoeuf NR, Lenihan D, Onofrei C, Shannon V, Sharma R, Silk AW, Skondra D, Suarez-Almazor ME, Wang Y, Wiley K, Kaufman HL, Ernstoff MS; Society for Immunotherapy of Cancer Toxicity Management Working Group. Managing toxicities associated with immune checkpoint inhibitors: consensus recommendations from the Society for Immunotherapy of Cancer (SITC) Toxicity Management Working Group. *J Immunother Cancer* 2017; **5**: 95 [PMID: 29162153 DOI: 10.1186/s40425-017-0300-z]



## Unexpected metastasis of intraductal papillary neoplasm of the bile duct without an invasive component to the brain and lungs: A case report

Nguyen Hai Nam, Kojiro Taura, Masashi Kanai, Keita Fukuyama, Norimitsu Uza, Hirona Maeda, Yojiro Yutaka, Toyofumi F Chen-Yoshikawa, Manabu Muto, Shinji Uemoto

**ORCID number:** Nguyen Hai Nam (0000-0001-5184-6936); Kojiro Taura (0000-0003-4164-3988); Masashi Kanai (0000-0002-6954-4474); Keita Fukuyama (0000-0001-8176-6961); Norimitsu Uza (0000-0002-1334-5740); Hirona Maeda (0000-0003-3406-1680); Yojiro Yutaka (0000-0003-4220-969X); Toyofumi F Chen-Yoshikawa (0000-0003-0494-7077); Manabu Muto (0000-0002-3127-8203); Shinji Uemoto (0000-0003-0126-9346).

**Author contributions:** Nam NH and Taura K designed this report, reviewed the literature and contributed to manuscript drafting; Taura K and Uemoto S were the patient's HPB surgeons; Maeda H performed the pathological examination; Yutaka Y and Chen-Yoshikawa TF were the patient's thoracic surgeons; Kanai M, Fukuyama K, Muto M performed the genomic profiling analysis using whole exome sequencing; Nam NH, Taura K and Uza N were responsible for the revision of the manuscript for important intellectual content; all authors issued final approval for the version to be submitted.

**Informed consent statement:** Informed written consent was obtained from the patient for publication of this report and any accompanying images.

**Conflict-of-interest statement:** The authors declare that they have no conflict of interest.

**Nguyen Hai Nam, Kojiro Taura, Shinji Uemoto,** Division of Hepato-Biliary-Pancreatic Surgery and Transplantation, Department of Surgery, Graduate School of Medicine, Kyoto University, Kyoto 606-8501, Japan

**Masashi Kanai, Keita Fukuyama,** Department of Clinical Oncology, Pharmacogenomics, and Palliative Medicine, Graduate School of Medicine, Kyoto University, Kyoto 606-8507, Japan

**Norimitsu Uza,** Department of Gastroenterology and Hepatology, Graduate School of Medicine, Kyoto University, Kyoto 606-8507, Japan

**Hirona Maeda,** Department of Diagnostic Pathology, Kyoto University Hospital, Kyoto 606-8507, Japan

**Yojiro Yutaka, Toyofumi F Chen-Yoshikawa,** Department of Thoracic Surgery, Graduate School of Medicine, Kyoto University, Kyoto 606-8507, Japan

**Manabu Muto,** Department of Therapeutic Oncology, Graduate School of Medicine, Kyoto University, Kyoto 606-8507, Japan

**Corresponding author:** Kojiro Taura, MD, PhD, Associate Professor, Doctor, Surgeon, Surgical Oncologist, Division of Hepato-Biliary-Pancreatic Surgery and Transplantation, Department of Surgery, Graduate School of Medicine, Kyoto University, 54 Kawahara-cho, Shogoin, Sakyo-ku, Kyoto 606-8507, Japan. [ktaura@kuhp.kyoto-u.ac.jp](mailto:ktaura@kuhp.kyoto-u.ac.jp)

### Abstract

#### BACKGROUND

Despite an expanding number of studies on intraductal papillary neoplasm of the bile duct (IPNB), distant metastasis remains unexplained especially in cases of carcinoma *in situ*. In the present study, we report a rare and interesting case of IPNB without invasive components that later metastasized to lungs and brain.

#### CASE SUMMARY

A 69-year-old male was referred to our hospital due to suspected cholangiocarcinoma. Laboratory tests on admission reported a mild elevation of alkaline phosphatase,  $\gamma$ -glutamyl transpeptidase, and total bilirubin in serum. Endoscopic retrograde cholangiography revealed a filling defect in the common bile duct (CBD) extending to the left hepatic duct. Peroral cholangioscopy delineated a tumor in the CBD that had a papillary pattern. Multidetector

# CARE Checklist (2016) statement:

The authors have read the CARE Checklist (2016), and the manuscript was prepared and revised according to the CARE Checklist (2016).

**Open-Access:** This article is an open-access article that was selected by an in-house editor and fully peer-reviewed by external reviewers. It is distributed in accordance with the Creative Commons Attribution NonCommercial (CC BY-NC 4.0) license, which permits others to distribute, remix, adapt, build upon this work non-commercially, and license their derivative works on different terms, provided the original work is properly cited and the use is non-commercial. See: <http://creativecommons.org/licenses/by-nc/4.0/>

**Received:** October 13, 2019

**Peer-review started:** October 13, 2019

**First decision:** December 5, 2019

**Revised:** December 13, 2019

**Accepted:** December 22, 2019

**Article in press:** December 22, 2019

**Published online:** January 21, 2020

**P-Reviewer:** Viswanath Y

**S-Editor:** Tang JZ

**L-Editor:** A

**E-Editor:** Ma YJ



computed tomography and magnetic resonance cholangiopancreatography detected partial blockage of interlode in the CBD leading to cholestasis without evidence of metastasis. Therefore, a diagnosis of IPNB cT1N0M0 was established. Left hepatectomy with bile duct reconstruction was performed. Pathological examination confirmed an intraepithelial neoplasia pattern without an invasive component and an R0 resection achievement. The patient was monitored carefully by regular examinations. However, at 32 mo after the operation, a 26 mm tumor in the lungs and a 12 mm lesion in the brain were detected following a suspicious elevated CA 19-9 level. Video-assisted thoracoscopic surgery of left upper lobectomy and stereotactic radiotherapy are indicated. In addition to histopathological results, a genomic profiling analysis using whole exome sequencing subsequently confirmed lung metastasis originating from bile duct cancer.

## CONCLUSION

This case highlights the important role of genomic profiling analysis using whole exome sequencing in identifying the origin of metastasis in patients with IPNB.

**Key words:** Intraductal papillary neoplasm of the bile duct; Distant metastasis; Invasive component; Whole exome sequencing; CA 19-9; Case report

©The Author(s) 2020. Published by Baishideng Publishing Group Inc. All rights reserved.

**Core tip:** An intraductal papillary neoplasm of the bile duct without an invasive component has unexpectedly metastasized to the brain and lungs. In addition to histopathological results, a genomic profiling analysis using whole exome sequencing subsequently confirmed lung metastasis originating from bile duct cancer by detecting 100 single nucleotide variants and 168 insertion/deletions.

**Citation:** Nam NH, Taura K, Kanai M, Fukuyama K, Uza N, Maeda H, Yutaka Y, Chen-Yoshikawa TF, Muto M, Uemoto S. Unexpected metastasis of intraductal papillary neoplasm of the bile duct without an invasive component to the brain and lungs: A case report. *World J Gastroenterol* 2020; 26(3): 366-374

**URL:** <https://www.wjgnet.com/1007-9327/full/v26/i3/366.htm>

**DOI:** <https://dx.doi.org/10.3748/wjg.v26.i3.366>

## INTRODUCTION

Intraductal papillary neoplasm of the bile duct (IPNB) has recently obtained interest in the field of hepato-biliary-pancreatic surgery. This rare lesion is predominant in Asian countries, such as Japan, Taiwan and Korea, where hepatolithiasis and clonorchiasis are endemic<sup>[1]</sup>. Since IPNB was recognized as a distinct pathological entity by the World Health Organization in the 2010 Classification of Tumors of the Digestive System<sup>[2]</sup>, this condition has been identified by the predominance of biliary neoplasms accompanied by papillary or villous proliferation inside a dilated bile duct, with or without macroscopically visible mucin secretion. In reference to histomorphology and the immunophenotypical profile, four phenotypes of epithelium have been categorized, including pancreaticobiliary, intestinal, gastric and oncocytic types<sup>[3]</sup>. From a systematic review and meta-analysis, Gordon *et al*<sup>[4]</sup> identified an invasive component in 43% of 476 patients, suggesting a high potential for malignancy. Despite an expanding number of studies on IPNB, distant metastasis remains a mysterious question, especially in cases of carcinoma *in situ*. In the present study, we report a rare and interesting case of IPNB without invasive components that metastasized to the lungs and brain.

## CASE PRESENTATION

### Chief complaints

A 69-year-old male with a body mass index of 21.5 kg/m<sup>2</sup> was referred to our hospital



due to jaundice for a suspected cholangiocarcinoma.

### **History of present illness**

His past medical and surgical history was unremarkable, except for diabetes type 2 and hypertension; both conditions were controlled with medications, including metformin 500 mg twice a day, glimepiride 1 mg twice a day, nifedipine CR 20 mg daily, valsartan 80 mg daily and enalapril 5 mg daily.

### **History of past illness**

His social history was significant for smoking 20 cigarettes per day for 46 years and the frequent intake of alcohol at approximately 360-540 mL a day.

### **Family history**

Family history was notable for a father diagnosed with esophageal cancer, a mother with uterine cancer and an elderly brother with duodenal cancer and leukemia.

### **Physical examination upon admission**

On examination, the patient had icteric sclera and pale conjunctiva. His vital signs were stable, and physical examination did not reveal any extraordinary signs.

### **Laboratory examinations**

Laboratory tests on admission were within the normal range, except for a mild elevation in the levels of alkaline phosphatase (507 IU/L; normal range, < 359 IU/L),  $\gamma$ -glutamyl transpeptidase (199 IU/L; normal range, < 47 IU/L) and total serum bilirubin (1.4 mg/dL normal range, < 1 mg/dL). Carcinoembryonic antigen and CA 19-9 were within the normal range (2.7 ng/mL, 13.6 U/mL, respectively). Serology was negative for hepatitis B and C infections.

### **Imaging examinations**

Endoscopic ultrasonography detected a solid lesion filling the intrapancreatic CBD to the main biliary. There was no evidence of extension outside of the bile duct wall, and invasion into the right hepatic artery was not observed. In addition, multilobar and unilateral cystic lesions of the pancreas, which had a maximum diameter of 13.1 mm, were found. Endoscopic retrograde cholangiography revealed bilateral intrahepatic biliary tree dilatation with a filling defect in the upper and middle bile duct, which extended partly to the left hepatic duct. Intraductal ultrasonography confirmed that there was no extended lesion in the right bile duct. Tumor and adjacent tissue biopsies were performed, and a 5 Fr endoscopic nasobiliary drainage ENBD was placed to facilitate biliary drainage. Pathological results endorsed IPNB with high grade and intestinal type neoplasia. In addition, images obtained from peroral cholangioscopy POCS delineated a tumor with a papillary pattern located at the CBD to the left hepatic duct (Figure 1). Multidetector computed tomography detected an interruption for a long segment of CBD causing biliary occlusion, which resulted in bilateral intrahepatic biliary tree dilatation with no intrahepatic lesion. The tumor was predominantly extended into the left hepatic duct. An enlargement of the pancreatic duct suggested the extension of injury into the intrapancreatic CBD. Traces of metastasis, such as lymph node growth, ascites, lung mass or pleural effusion, have not been reported. Three-dimensional liver surgery simulation demonstrated that the right hepatic artery and right portal vein were not in contact with the tumor. Magnetic resonance cholangiopancreatography confirmed these findings (Figure 2).

### **Initial diagnosis**

Therefore, an initial diagnosis of IPNB cT1N0M0 was established with good prognosis.

---

## **FINAL DIAGNOSIS**

The final diagnosis of the presented case is metastasis of IPNB without an invasive component to the brain and lungs.

---

## **TREATMENT**

The remnant liver was estimated at 63.1% of its original size after left hemihepatectomy, including the caudate lobe, extrahepatic bile duct resection with Roux-en-Y hepaticojejunostomy and regional lymph node dissection. During the operation, the tumor was not exposed to the serosa, and severe diffuse liver steatosis,



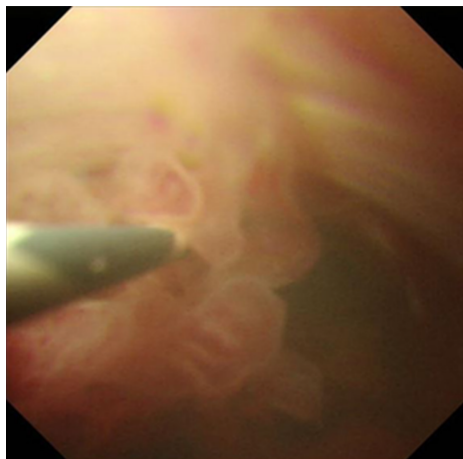


Figure 1 Peroral cholangioscopy findings: Biliary papillomatosis in the common bile duct.

including a small amount of ascites, was reported. Rapid ascites cytology, para aortic lymph node, and stumps of bile duct in frozen section were intraoperatively negative for cancer. The duration of the operation was 647 min, with blood loss amounting to 360 g without blood transfusion. Intraoperative cholangiography confirmed no evidence of bile leakage.

## OUTCOME AND FOLLOW-UP

Macroscopic examination of the resected specimen revealed a papillary tumor measuring 22 mm × 10 mm expanding the CBD and the left hepatic bile duct (Figure 3). Microscopic findings showed the papillary neoplasm confined within the bile duct. The intraductal neoplastic growth was a cribriform and tubular pattern and showed no infiltration into the basal ductal wall. The neoplastic epithelial cells revealed nuclear atypia and stratification. Histological examination confirmed the diagnosis of IPNB with high-grade intraepithelial neoplasia (carcinoma *in situ*) and no regional lymph node metastases (pTis pN0) (Figure 4). Immunohistochemical staining showed that the tumor cells were positive for CK7, CK20 and CDX2. The surgical margin was negative, and no malignant findings were observed in the gallbladder.

The postoperative course showed a high-grade fever caused by acute cholangitis, which was successfully treated by the intravenous administration of teicoplanin and piperacillin/tazobactam for 6 d and was classified as Clavien-Dindo complication grade II. Glycemia and blood pressure were effectively controlled during the perioperative time by insulin therapy and antihypertensive drugs. The patient was discharged at 31 d after surgery. The patient did not receive further supportive treatment and was monitored at regular intervals through clinical examination, biochemical investigations and imaging diagnosis. Unfortunately, at 32 mo after the operation, a 26 mm tumor in the left upper lobe lung field was detected following a suspicious elevation of CA 19-9 (Figure 5), and a suspected metastasis 12 mm brain tumor in the right frontal lobe was determined (Figure 6). The initial diagnosis was confidently proposed as primary lung cancer with brain metastasis (cT1bN0M1b). Lung tumor markers, such as squamous cell carcinoma antigen, neuron-specific enolase, sialyl stage-specific embryonic antigen-I and cytokeratin 19 fragment (CYFRA 21-1), were within the normal range.

Video-assisted thoracoscopic surgery of the left upper lobectomy and stereotactic radiotherapy for brain tumor given as dose of 44.2 Gy in 13 fractions are indicated. The postoperative course was uneventful, and he was discharged on postoperative day 10. The gross findings of the lung tumor revealed well-circumscribed yellowish-white nodules located in the peripheral lung (Figure 7). Histopathological examination showed a well-demarcated nodule with marked necrosis in the center of the tumor (Figure 8). At the high power field, the tumor exhibited a cribriform pattern consisting of eosinophilic, tall, columnar cells with nuclear pseudostratification. Immunohistological staining showed that the tumor cells were positive for CK7, CK20 and CDX2 and negative for TTF-1, which was the same profile as the primary bile duct lesion. The lung tumor was diagnosed as metastatic adenocarcinoma of a bile duct origin. Subsequently, a genomic profiling analysis using whole exome sequencing (WES) with paired tissue and blood samples was performed (Riken



**Figure 2** Magnetic resonance imaging revealed extensively dilated bile ducts due to an intraluminal lesion located in the common bile duct.

Genesis Co., LTD., Tokyo, Japan) to investigate common variants between two specimens. We obtained informed consent from the patient for undergoing WES tests. A comparison between primary and lung metastatic tumors revealed 100 somatic single nucleotide variants (SNVs) and 168 insertion/deletions (InDels) that were common in the two tumors (Supplementary table 1). We annotated the variants detected by WES using SnpEff (<http://snpeff.sourceforge.net/SnpEff.html>)<sup>[5]</sup>. This result confirmed lung metastasis originating from bile duct cancer. The patient currently remains in a stable condition without recurrence and continues to receive treatment with S-1.

## DISCUSSION

Distant metastasis after an antecedent diagnosis of high grade intraepithelial neoplasm is extraordinarily illogical and infrequent IPNB is a rare tumor characterized by a lesion protruding into the biliary lumen, which might cause cholestasis. According to the degree of dysplasia and depth of invasion, IPNB is classified into four stages: (stage 1) IPNB with low-to-intermediate grade dysplasia, (stage 2) IPNB with high-grade dysplasia, (stage 3) intraductal growth-type cholangiocarcinoma, American Joint Committee on Cancer stage T1 and (stage 4) intraductal growth-type cholangiocarcinoma, American Joint Committee on Cancer stage T2 or higher<sup>[1]</sup>. As without an invasive component and evidence of metastasis, our present case was defined as an early stage of IPNB, which has a good prognostic value through radical resection. Regrettably, after more than two years of careful follow-up, distant metastasis was revealed without primary site recurrence and accompanied by an incomprehensible malignancy mechanism. Thus, two potential hypotheses were proposed: (1) Pulmonary enteric adenocarcinoma, a very rare type of primary lung cancer that shares some identical components with colorectal carcinoma and is difficult to discriminate from the metastasis of intestinal adenocarcinoma, even with immunohistochemical staining; and (2) Escape of the invasive components from the observation of the pathologist due to intervals between the adjacent slices. In the second supposition, even if it occurs, the dimension of the lesion should be restricted and smaller than the intervals between the adjacent slices (usually 3-4 mm). Another situation that could have happened is that a skip lesion escaping from our observation metastasized to the lungs and brain. However, this scenario also appears unlikely as the skip lesion should have developed unobtrusively in small dimension enough to escape from our observation and should have rarely metastasized.

This study is a very rare report of IPNB without locoregional lymph node metastasis and extension to distant organs. In retrieving the current literature, a unique case report by Yoshida *et al*<sup>[6]</sup> delineated an advanced stage of IPNB with metastases to the ovary and lymph nodes. Basically, IPNB was considered less malignant than conventional bile duct cholangiocarcinoma<sup>[1]</sup>. Far fewer lymph node metastases were identified in patients with IPNB than in those with cholangiocarcinoma<sup>[7]</sup>. Strikingly, a single center retrospective study over 16 years by Wu *et al*<sup>[8]</sup> revealed only three metastatic lymph nodes in one patient among 88 harvested lymph nodes in a series of 28 patients with IPNB. Fundamentally, the

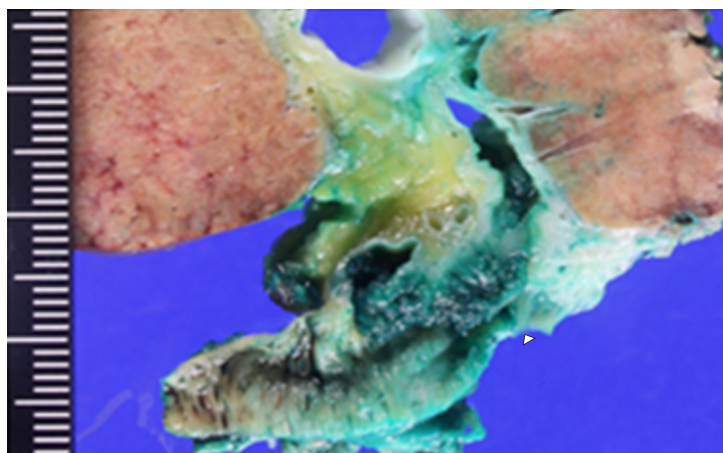


**Figure 3** Macroscopic findings showed a papillary tumor of the bile duct (arrowhead).

detention of neoplastic cells by the entire basal lamina layer prevents the risk of metastasis. Despite a favorable prognosis, such as R0 resection achievement, an intraepithelial neoplasia pattern without an invasive component, no evidence of extended metastasis, negative metastatic lymph node and ascites cytology, our patient suffered from an unpredictable metastasis to the lungs and brain. This phenomenon seems to imply a complex mechanism that defies a simple explanation. Lymphatic permeation, blood circulation, perineural invasion and intestinal subtype may somehow suggest an answer. Using WES, the detection of shared 100 somatic SNVs and 168 InDels confirmed the diagnosis of metastatic lung tumor from IPNB. Thus, all physicians are forewarned to engage in extensive research toward cancer metastasis.

Another important clinical implication of this study was the association between variations in the CA 19-9 level and metastasis. At the time of lung and brain metastasis detection, the CA 19-9 level was four-fold higher than the baseline value. Subsequently, in performing VATS lobectomy and SRT, CA 19-9 level returned to the normal range. Luvira V *et al*<sup>[9]</sup> found that the serum CA 19-9 level was a significant prognostic factor for malignant IPNB. In addition, Yeh *et al*<sup>[10]</sup> observed an enhanced serum CA 19-9 level in 35% of benign lesions, whereas that in malignant lesions was 61%. Furthermore, Lee *et al*<sup>[11]</sup> demonstrated a higher mean CA 19-9 level in IPNB with mucin hypersecretion. Thus, CA 19-9 screening during follow-up should be valuable for the detection of extended lesions.

## CONCLUSION

In conclusion, we report a distant and simultaneous metastasis (brain and lungs) of an extrahepatic IPNB case, which was diagnosed as high grade intraepithelial neoplasia (T1N0M0) and was rigorously treated with curative resection (R0 resection without malignant lymph node). Regardless of the rarity of this lesion, our case report raises the following question: What is the actual mechanism of distant metastasis in the early stage of IPNB without an invasive component? Further studies should be performed to elucidate this unusual phenomenon.



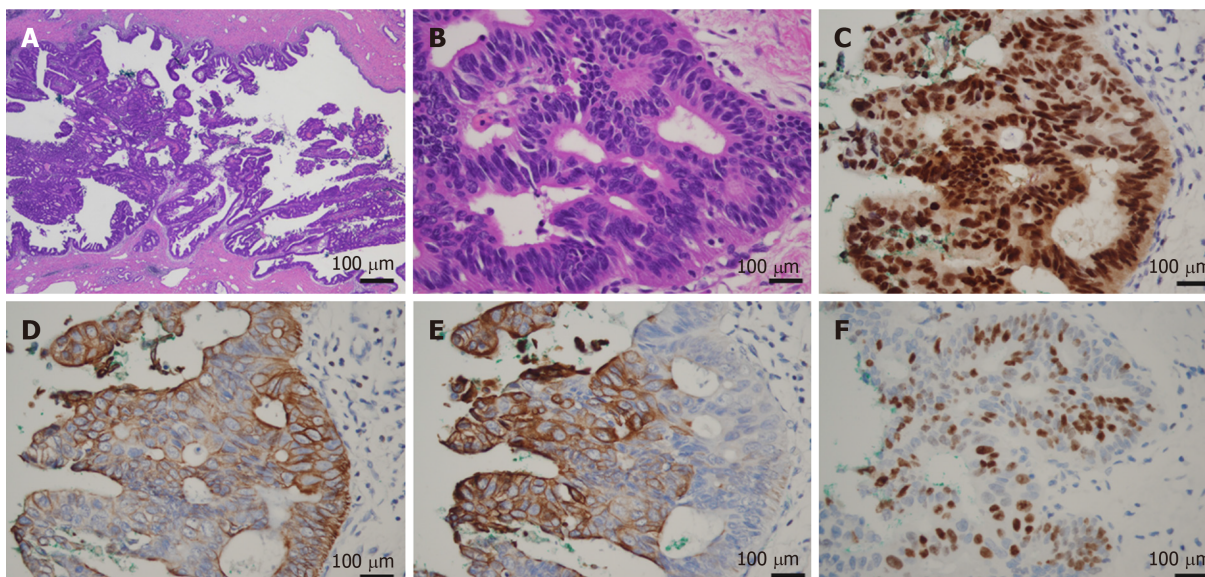


**Figure 4 Microscopic findings of the bile duct tumor.** A: The tumor showed the intraductal papillary proliferation of columnar cells with a high nuclear/cytoplasmic ratio; B: These neoplastic cells were entirely confined within the duct, and no invasion was identified (A: magnification  $\times 20$ , B: magnification  $\times 400$ ); C-F: Immunohistological staining showed that the tumor cells were positive for CDX2, CK7, CK20, and Ki67.

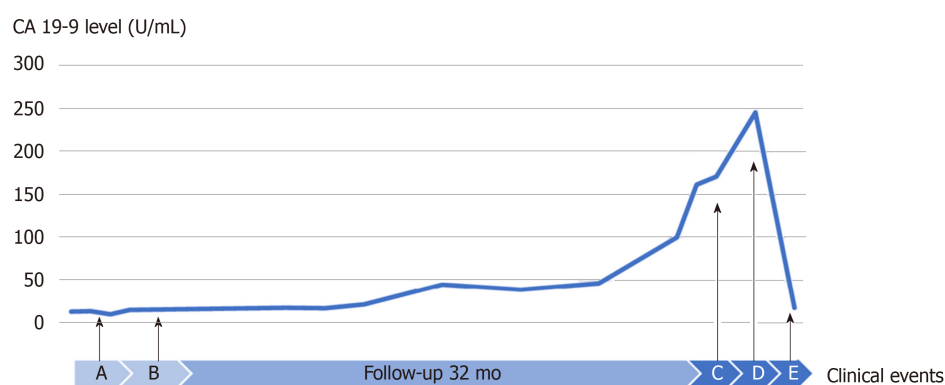


**Figure 5 Variation in the CA 19-9 level in correlation with clinical events.** Time A (2015 December): Diagnosis of intraductal papillary neoplasm of the bile duct T1N0M0; Time B (2016 January): Good prognosis with satisfactory postoperative pathological findings, such as high-grade intraepithelial neoplasia pattern without an invasive component, R0 resection, no extended metastasis, lymph node (-) and ascites cytology (-); Time C (2018 September): Detection of suspected metastatic adenocarcinoma of bile duct origin with a 26 mm lung tumor, a 12 mm brain tumor and a 4-fold higher level of CA 19-9; Time D (2018 November): VATS lobectomy and SRT for brain tumor; and Time E (2019 January): Stable condition with normal level of CA 19-9.

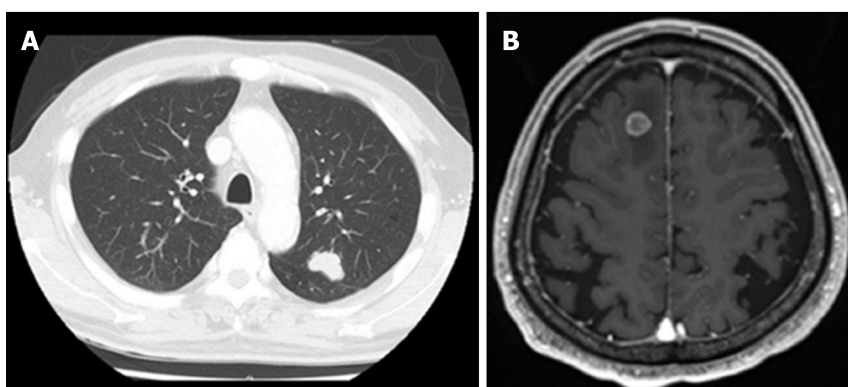


**Figure 6 Magnetic resonance imaging of a metastatic lung tumor in the left upper lobe (A) and suspected metastatic brain tumor on the right frontal lobe (B).**

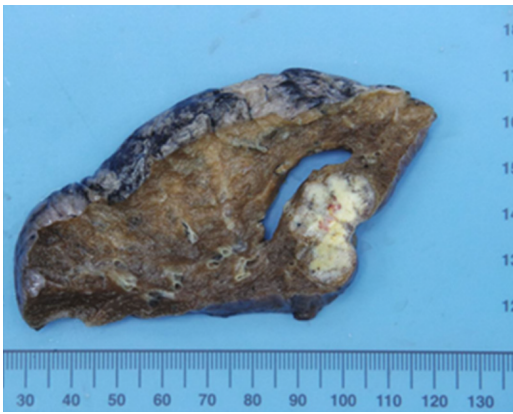


**Figure 7** Macroscopic findings of lung-resected specimens.

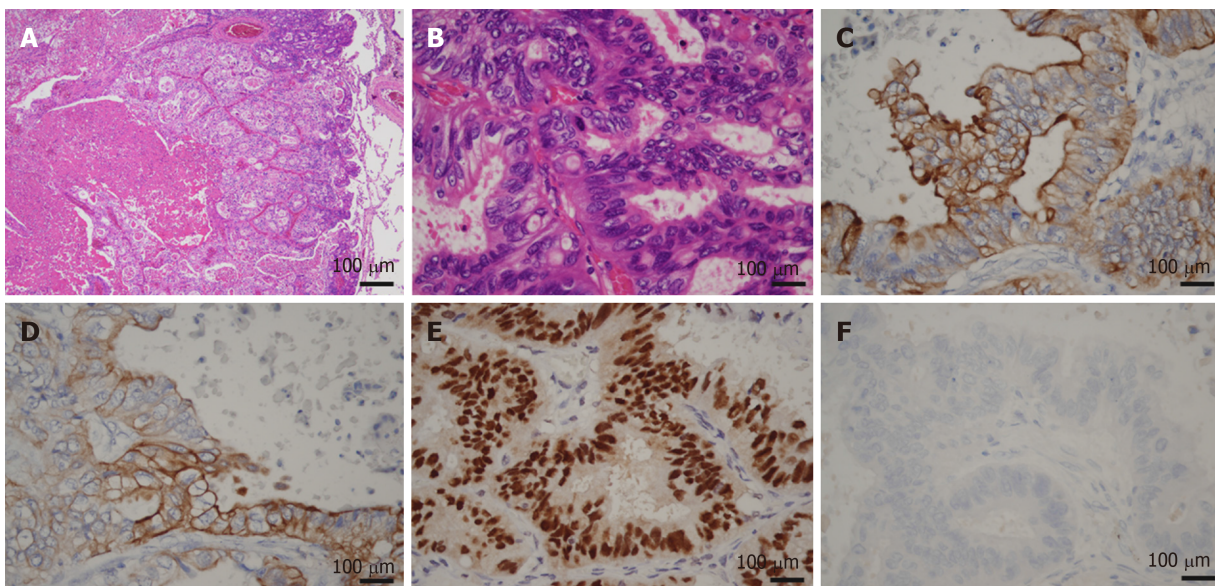


**Figure 8** Microscopic images of lung metastasis. A and B: Histologic appearance showed a well-demarcated nodule with marked necrosis in the center of the tumor (A: magnification  $\times 20$ , B: magnification  $\times 400$ ). At high power magnification, there were eosinophilic, tall, columnar cells with nuclear pseudostratification. C-E: Immunohistological staining showed that the tumor cells were positive for CK7 (Panel C), CK20 (Panel D) and CDX2 (Panel E); F: Immunohistological staining showed that the tumor cells were negative for TTF-1.

## REFERENCES

- Wan XS, Xu YY, Qian JY, Yang XB, Wang AQ, He L, Zhao HT, Sang XT. Intraductal papillary neoplasm of the bile duct. *World J Gastroenterol* 2013; **19**: 8595-8604 [PMID: [24379576](#) DOI: [10.3748/wjg.v19.i46.8595](#)]
- Bosman FT, Carneiro F, Hruban RH, Theise ND. WHO Classification of Tumours of the Digestive System. Lyon: IARC Press 2010; 417
- Choi SC, Lee JK, Jung JH, Lee JS, Lee KH, Lee KT, Rhee JC, Jang KT, Choi SH, Heo JS, Choi DW, Lim JH. The clinicopathological features of biliary intraductal papillary neoplasms according to the location of tumors. *J Gastroenterol Hepatol* 2010; **25**: 725-730 [PMID: [20492329](#) DOI: [10.1111/j.1440-1746.2009.06104.x](#)]
- Gordon-Weeks AN, Jones K, Harriss E, Smith A, Silva M. Systematic Review and Meta-analysis of Current Experience in Treating IPNB: Clinical and Pathological Correlates. *Ann Surg* 2016; **263**: 656-663 [PMID: [26501712](#) DOI: [10.1097/SLA.0000000000001426](#)]
- Cingolani P, Platts A, Wang le L, Coon M, Nguyen T, Wang L, Land SJ, Lu X, Ruden DM. A program for annotating and predicting the effects of single nucleotide polymorphisms, SnpEff: SNPs in the genome of *Drosophila melanogaster* strain w1118; iso-2; iso-3. *Fly (Austin)* 2012; **6**: 80-92 [PMID: [22728672](#) DOI: [10.4161/fly.19695](#)]
- Yoshida Y, Ajiki T, Ueno K, Ohtsubo I, Murakami S, Shinozaki K. Advanced Intraductal Papillary Neoplasm of Bile Duct (IPNB) in a young female with metastases to lymph nodes and ovary. *Tando*. 2012; 231-236 [DOI: [10.11210/tando.26.231](#)]
- Yeh TS, Tseng JH, Chiu CT, Liu NJ, Chen TC, Jan YY, Chen MF. Cholangiographic spectrum of intraductal papillary mucinous neoplasm of the bile ducts. *Ann Surg* 2006; **244**: 248-253 [PMID: [16858187](#) DOI: [10.1097/01.sla.0000217636.40050.54](#)]



- 8 **Wu X**, Li B, Zheng C, Chang X, Zhang T, He X, Zhao Y. Intraductal papillary neoplasm of the bile duct: a single-center retrospective study. *J Int Med Res* 2018; **46**: 4258-4268 [PMID: [30111208](#) DOI: [10.1177/0300060518792800](#)]
- 9 **Luvira V**, Pugkhem A, Bhudhisawasdi V, Pairojkul C, Sathitkarnmanee E, Luvira V, Kamsa-Ard S. Long-term outcome of surgical resection for intraductal papillary neoplasm of the bile duct. *J Gastroenterol Hepatol* 2017; **32**: 527-533 [PMID: [27356284](#) DOI: [10.1111/jgh.13481](#)]
- 10 **Yeh TS**, Tseng JH, Chen TC, Liu NJ, Chiu CT, Jan YY, Chen MF. Characterization of intrahepatic cholangiocarcinoma of the intraductal growth-type and its precursor lesions. *Hepatology* 2005; **42**: 657-664 [PMID: [16116640](#) DOI: [10.1002/hep.20837](#)]
- 11 **Lee SS**, Kim MH, Lee SK, Jang SJ, Song MH, Kim KP, Kim HJ, Seo DW, Song DE, Yu E, Lee SG, Min YI. Clinicopathologic review of 58 patients with biliary papillomatosis. *Cancer* 2004; **100**: 783-793 [PMID: [14770435](#) DOI: [10.1002/cncr.20031](#)]



Published By Baishideng Publishing Group Inc  
7041 Koll Center Parkway, Suite 160, Pleasanton, CA 94566, USA  
Telephone: +1-925-3991568  
E-mail: [bpgoffice@wjgnet.com](mailto:bpgoffice@wjgnet.com)  
Help Desk: <http://www.f6publishing.com/helpdesk>  
<http://www.wjgnet.com>

